PERVIOUS CONCRETE:

INVESTIGATION INTO STRUCTURAL PERFORMANCE AND EVALUATION OF THE APPLICABILITY OF EXISTING THICKNESS DESIGN METHODS

By

WILLIAM GUNTER GOEDE

A thesis submitted in partial fulfillment of
the requirements for the degree of

MASTER OF SCIENCE IN CIVIL ENGINEERING

WASHINGTON STATE UNIVERSITY
Department of Civil and Environmental Engineering

DECEMBER 2009

To the Faculty of Washington State University:

The members of the Committee appointed to examine the thesis of WILLIAM GUNTER GOEDE find it satisfactory and recommend that it be accepted.

_____

Liv Haselbach, Ph.D., Chair

_____

David McLean, Ph.D.

_____

Haifang Wen, Ph.D.

ACKNOWLEDGEMENT

The completion of this thesis was made possible by the help of many different individuals. First, I would like to thank my advisor, Dr. Liv Haselbach, for her guidance, enthusiasm and proactive attitude. Thank you for giving me the opportunity to work on such a unique and innovative project, and for providing the financial support for my research. Without your direction, this thesis could not possibly have been completed in such an organized and timely manner. I would also like to thank my committee members, Dr. David McLean and Dr. Haifang Wen, for their assistance and for contributing their expertise to this project. Lastly, I would like to thank both Jon Thomle and Camille Reneaux for their assistance with the many hours of experimental testing required to complete this thesis. I greatly appreciate the time and effort contributed by all of you.

PERVIOUS CONCRETE: INVESTIGATION INTO STRUCTURAL PERFORMANCE AND EVALUATION OF THE APPLICABILITY OF EXISTING THICKNESS DESIGN METHODS

ABSTRACT

By William Gunter Goede, M.S.
Washington State University
December 2009

Chair: Liv Haselbach

In order to expand the applications of pervious concrete, additional research and testing must be done into its structural performance. Distress surveys were performed on two field installations of pervious concrete subjected to equivalent stresses as a "Collector" street in use for approximately 20 years. The results of the distress survey were then used to calculate the Pavement Condition Index (PCI) using the procedure from ASTM D 6433 (2007). The PCI rating was considered to be a quantification of structural performance. The high PCI ratings of the thicker pervious concrete sections indicated that pervious concrete, when properly designed, is capable of being used for most "Residential" streets and many "Collector" streets for typical design life durations (20-30 years) while exhibiting satisfactory structural performance.

Currently, there is no accepted thickness design method for pervious concrete pavements. This thesis evaluates the two most commonly used concrete thickness design methods, AASHTO (1993) and PCA (1984), for their applicability to pervious concrete. The observed performance of a pervious concrete field installation was used to assess each thickness design method for use with pervious concrete. Both methods yielded results having a higher variation for pervious concrete than for regular concrete. The lower percent of thicknesses under designed and closer correlation between actual and predicted thicknesses of the AASTHO (1993) method implies that this may be the preferred method for the design of pervious concrete pavements. However, since both models showed a very poor goodness-of-fit to actual thicknesses, additional research into alternative thickness design methods or the creation of a new thickness design method may be needed.

TABLE OF CONTENTS

LIST OF FIGURES

LIST OF TABLES

1. INTRODUCTION

This thesis attempts to accomplish two main purposes. The first purpose of this thesis is to examine the structural performance of pervious concrete. This structural performance examination is performed with the goal of showing that pervious concrete may be successfully used as a roadway paving material. After the structural performance characteristics of pervious concrete have been thoroughly investigated, the second purpose of this thesis is to evaluate current thickness design methods for their applicability to pervious concrete. The objectives of this thesis are discussed in more detail in Section 1.3.

1.1 FORMAT OF THESIS

In Section 1.2, this thesis begins with a brief literature review of pervious concrete research. The review of the research of others gives special attention to the strength, porosity, durability and structural performance of pervious concrete, as well as the current uses of pervious concrete.

Following this literature review, the objectives of this research are presented in Section 1.3. The objectives are presented in an outline format and are referenced throughout the rest of this thesis to eliminate confusion as to why something is being done.

In order to complete this research, two pervious concrete field placement sites were visited. Section 2 of this thesis gives a background for each of the sites visited, and discusses the pervious concrete placed at each site.

As is discussed later in this thesis, the strength and structural performance of pervious concrete is dependent on its material characteristics. Before an investigation into the structural performance and the evaluation of thickness design methods for pervious concrete can begin, it is necessary to perform the applicable tests to determine the material characteristics of the pervious concrete being analyzed. This material characterization is summarized in Section 3 of this thesis.

Section 4 covers the procedure and results of the investigation into the structural performance of the pervious concrete at the two sites discussed.

In Section 5, two widely used thickness design methods for concrete pavements are evaluated for their applicability to pervious concrete. The goal of this section is to begin the discussion as to the applicability of current thickness design methods for the design of pervious concrete pavements.

In Section 6, this paper ends with conclusions drawn from the research performed for this thesis. There is some future research which could be done to strengthen and support the conclusions found from this research. Some recommendations for this future research are also presented in Section 6.

At the end of this thesis, Section 7 summarizes the references used to complete this research and Section 8 is a notation guide, providing definitions of all variables used throughout this thesis. Lastly, Section 9 contains the appendices.

1.2 LITERATURE REVIEW

1.2.1 BENEFITS OF PERVIOUS CONCRETE

Pervious concrete is a relatively new paving material valued for its use as a stormwater best management practice. It has environmental benefits such as water pollution removal and maintaining ground water levels. According to Tennis et al. (2004), pervious concrete collects automobile fluids such as oil and anti-freeze and prevents them from being washed into nearby streams or lakes during a rainstorm. Tennis et al. (2004) also presents the results of two studies that showed very high water pollutant removal rates for pervious concrete. The tests performed in Virginia and Maryland showed 82 and 95% total suspended solids removal for pervious concrete, respectively.

Pervious concrete also has other benefits. It may increase driver safety by preventing standing water on road surfaces which will decrease hydroplaning and glare (Wanielista & Chopra, 2007). Pervious concrete may also improve land utilization by decreasing the need for detention basins (ACI Committee 522, 2006). Some cities are now charging property owners impact fees based on the amount

of impervious surface area on their property. Pervious concrete may help property owners avoid these impact fees (Tennis et al., 2004).

According to Hendrickx (1998) pervious concrete also reduces road noise. This is because the pore structure allows the air between the tire and the pavement to escape, producing a lower frequency road noise. The results of an experiment conducted in Belgium, taken directly from Hendrickx (1998), are depicted in Figure 1.1 which shows that pervious concrete produced the lowest decibel levels of all the pavements at all four traffic speeds tested.

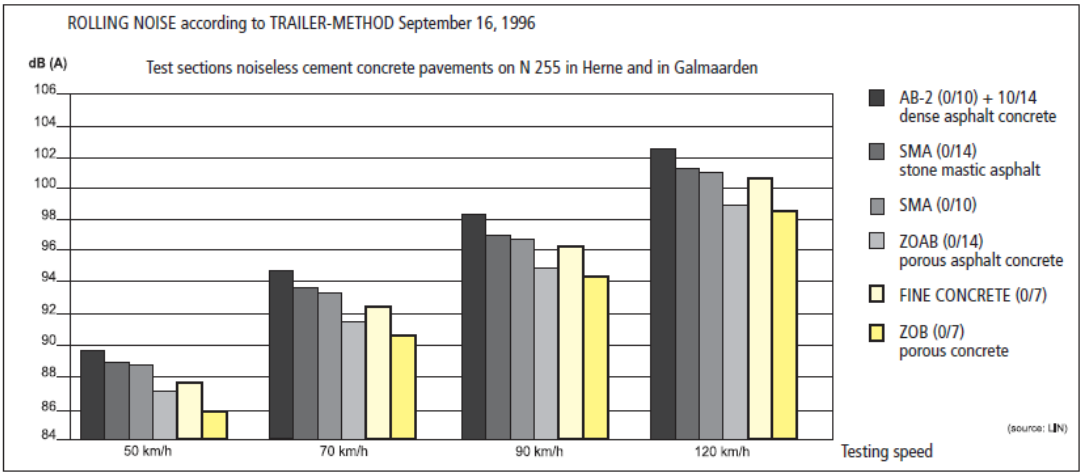

Figure 1.1: Road Noise of Different Pavements (Hendrickx, 1998)

1.2.2 POROSITY

The strength and structural performance of pervious concrete is more variable than traditional concrete, and depends primarily on the porosity (Crouch et al., 2003). Greater porosities (also called void contents and void ratios) will allow for increased infiltration rates, but will greatly decrease the compressive strength. This must be taken into account during the mix design and placement of pervious concrete. Recommended porosities range from 15 to 25% (Tennis et al., 2004). The porosity is dependent on both the water-to-cement ratio, and the compaction effort. ACI Committee 522 recommends a minimum of 10 psi of vertical force for compaction. Tennis et al. (2004) report that water-to-cement ratios between 0.27 and 0.30 are most commonly used.

Haselbach and Freeman (2006) report that porosity not only varies with changing water-to-cement ratios and compaction effort, but also varies with depth of the pavement. This vertical porosity distribution is caused by the surface compaction of the pervious concrete compacting the top of the pavement more than the bottom. Haselbach and Freeman (2006) assumed that the vertical porosity distribution is linear throughout the depth of the sample. The vertical porosity distribution could make maintenance actions such as vacuuming more effective because decreased porosity at the top of the pavement will trap solids in runoff near the surface. Since greater porosities may result in lower strengths, the vertical porosity distribution may decrease the tensile strength at the bottom of the pavement. Since pavements often fail due to the formation of tensile cracks at the bottom of the pavement, the vertical porosity distribution should be considered in the design of pervious concrete pavements.

The porosity is the ratio of the volume of voids to the total volume of the specimen. Even though porosity is a commonly reported property of pervious concrete, there is still some confusion as to its definition. Some of the voids in pervious concrete are not effective in transporting water through the material. The voids that are active in transporting water through the material are frequently called the "effective voids". Some methods for finding the porosity of pervious concrete only calculate the effective voids. According to Montes et al. (2005) both the definition of effective void ratio, and the results produced vary when different methods are used. In order to avoid the confusion created by discrepancies in the definition of "effective voids", Montes et al. (2005) recommend finding the total porosity of pervious concrete using a water displacement method. The water displacement method is based on Archimedes' principle of buoyancy which states that the buoyancy force is equal to the weight of the fluid displaced. All that must be known to calculate the porosity using this method is the dry mass, the submerged mass, and the total volume. The total porosity should be more directly correlated to the compressive strength because all the voids, regardless if they are "effective", will affect strength. This is the method that was used in this research.

1.2.3 STRENGTH PROPERTIES

Pervious concrete is not usually as strong as traditional concrete for similar mixes and depths. The matrix of pores that allow water to flow through the material also decreases its strength. While traditional concrete has compressive strengths ranging from 3500 to 5000 psi and tensile strength ranging from 350 to 600 psi (Wang et al., 2007), pervious concrete has compressive strengths ranging typically from 500 to 4000 psi and tensile strengths ranging from 150 to 550 psi (Tennis et al., 2004). However, higher pervious concrete strengths are possible. Yang and Jiang report that pervious compressive strengths and tensile strengths as high as 7200 psi and 870 psi, respectively, can be reached by including 2 admixtures: silica fume and superplasticizer (Yang & Jiang, 2003).

While the compressive strength of pervious concrete does depend primarily on the porosity, it is also affected by aggregate size, shape and gradation. According to Crouch et al. (2007), a uniformly graded aggregate will result in a higher compressive strength, as well as a higher void ratio. A uniformly graded aggregate is also beneficial for field installations because it is harder to over-compact. Crouch et al. (2007) also reports that smaller aggregates will produce a higher compressive strength than larger aggregates, and will result in similar porosities. Even though it is intuitive that increasing aggregate size would produce a higher porosity, this is not the case. Larger aggregate will produce larger voids, but since the aggregate has less surface area per volume for the cement paste to stick to, excess paste will partially fill in the voids (Crouch et al., 2007). According to the authors of this paper, a uniformly graded small aggregate will produce the best results.

Yang et al. (2008) found that increasing the fine aggregate content increases strength, but decreases permeability. For this reason many pervious concrete companies use small amounts of fine materials in their pervious concrete mixes. Aggregate shape may also affect the properties of pervious concrete. According to Scott Erickson (2007), president of the pervious concrete company Evolution Paving, pervious concrete containing crushed aggregate shows superior performance to pervious concrete containing round aggregate.

1.2.4 STRUCTURAL PERFORMANCE

In an investigation into the structural performance of field placed pervious concrete, Delatte et al. (2007) performed testing on samples obtained from Indiana, Kentucky, and Ohio. The uses of the pervious concrete investigated include driveways, parking lots, storage pads, sidewalks, patios, and bike paths. Delatte et al. (2007) summarize qualitatively distresses observed at each of the test sites, (cracking, raveling, etc.). Compressive strengths between 500 and 5000 psi and tensile strengths ranging from 100 to 500 psi were found for samples with a reported porosity ranging from approximately 40 to 10%, respectively. Due to the differing definitions of porosity as previously discussed, clarification is needed about what type of porosity Delatte et al. (2007) found. Delatte et al. (2007) calculated the total porosity of the samples using the same water displacement method similar to that which was used in this research.

Delatte et al. (2007) report good freeze-thaw performance. The good freeze-thaw performance is attributed to the fact that the sites were adequately drained and the pervious concrete was not saturated during freezing. Most of the installations observed showed either minimal or moderate clogging. Relatively small amounts of damage to the field installations were observed. Of the 18 field installation observed, 15 only showed minimal raveling, and 12 did not show any cracking. However, because pervious concrete is a relatively new material, all the samples viewed by Delatte et al. (2007) were less than four years old. Large amounts of pavement distress are not expected to be evident after only four years, since a common design life for a jointed concrete pavement is usually from 20 to 30 years (ACI Committee 325, 2002). In the conclusion, Delatte et al. (2007) recommend that the study be repeated at a later date, when the field pervious installations have been in use for a longer duration.

1.2.5 DURABILITY

A laboratory test has been proposed for assessing the surface durability of pervious concrete. Offenberg (2009) summarizes the development of this test method in his article, "Proving Pervious Concrete's Durability." In his article, Offenberg (2009) recognizes surface durability as an existing concern among specifiers of pervious concrete. He points out that for traditional concrete, raveling issues

are usually caused by improper batching, handling, or curing. However, for pervious concrete raveling can occur even with proper batching, handling, and curing. Several existing ASTM test methods were investigated for their applicability to testing the surface durability of pervious concrete. All test methods investigated were discounted for various reasons, except ASTM C131 (2006), more commonly known as the LA Abrasion Test.

The LA Abrasion Test measures the abrasion resistance of aggregates by placing aggregate in a rotating steel chamber with 12 steel balls. However, Offenberg (2009) reports that the research team thought a similar, but less aggressive procedure could be used to measure the surface durability of pervious concrete. After many variations of the ASTM C131 (2006) test procedure, the research team proposed the following procedure: a 4 inch high, 4 inch diameter cylinder must be subject to 50 revolutions in the ASTM C131 (2006) steel chamber without any steel balls. The mass before and after the revolutions should be recorded in order to calculate the mass loss.

Offenberg (2009) concludes that the test effectively measures the raveling of pervious concrete, but admits that there is some additional research needed. During the development of the test, only 3/8 in. aggregate was used. He suggests that the results of the test should be evaluated for additional aggregate sizes. Also, the test was not performed on any samples cored from field placements. In order to better understand the relationship between the results of this test, and actual field performance, Offenberg (2009) recommends that the results of this test be evaluated for cored samples.

1.2.6 PERVIOUS CONCRETE USES

The importance of strength for pervious concrete design is still undecided, so the primary applications of pervious concrete have been limited to walkways, sidewalks, bike lanes and parking lots. In these applications the pervious concrete is usually subjected to relatively light and low frequency loading. Although pervious concrete has been used for some low-traffic roads and shoulders, it is not widely used as a street paving material. This could be due to its decrease in strength from traditional concrete, concerns over surface durability, or simply because pervious concrete is a relatively new

product and has not yet had time to prove itself. ACI Committee 522 states that "Little field data exists on the long-term durability of pervious concrete in northern climates." For expanded applications, additional research and testing must be done to determine how to incorporate the different strength and durability aspects of pervious concrete into successful pavement designs. There is currently no accepted thickness design method for pervious concrete. Without an accepted thickness design method, engineers may be hesitant to design pervious concrete pavements for road applications. This could be limiting its uses.

Even though pervious concrete is not a common road paving material, it is being used around the world as a top layer on roads. In Europe, it is used as a top layer to reduce traffic noise, increase skid resistance, and prevent water pooling on the surface of the road. However, in this application freeze-thaw damage is a large concern because of the higher likelihood that the pervious top layer will remain saturated (Van Gemert et al., 2003).

1.2.7 COST OF PERVIOUS CONCRETE

Regardless of the numerous environmental benefits of pervious concrete, if the cost of pervious concrete is not comparable to that of traditional pavements, the use of pervious concrete will most likely be limited. According to Wanielista and Chopra (2007), the initial cost of pervious concrete can be up to 1.5 times the initial cost of other conventional paving methods. They attribute this increased cost to the requirement for more skilled workers during the placement of pervious concrete, and to the increased thickness of pervious required due to its weaker strength.

In a report prepared for the president of Bellevue Community College, McMillan (2007) reports very comparable costs for the installation of traditional and pervious concretes in the Seattle area. After personally contacting many of the traditional and pervious concrete installers in her area, McMillan (2007) generated cost installation estimates ranging from $3 to $11.24 per square foot for traditional concrete, and ranging from $4 to $9 per square foot for pervious concrete. On their website, the EPA

(2008) also reports comparable costs for traditional and pervious concretes. The EPA (2008) lists both the cost of traditional concrete and the cost of pervious concrete as $2 to $6 per square foot.

However, to fully understand the cost of pervious concrete one must look further than just the installation cost. Pervious concrete may have many potential cost benefits such as eliminating the need for traditional curb and gutter systems, underground piping, retention basins, and site grading requirements to prevent water ponding. The use of pervious concrete may improve land utilization by eliminating the need for retention basins. Pervious concrete does not add water to existing sewer systems. This may save cities money that would otherwise be spent increasing the capacity of sewer systems, or may save businesses money by avoiding stormwater impact fees.

Another cost issue for pervious concrete is the maintenance. In order to keep the pervious concrete functioning properly, and prevent clogging, many pervious concrete pavements must be cleaned occasionally. Common ways of cleaning pervious concrete include pressure washing and vacuum sweeping. Wanielista and Chopra (2007) concluded that both methods were equally effective, and typically increased infiltration rates by 200% or more. Pervious concrete may also require a thicker layer of base material than is needed for traditional concrete to allow for increased water storage. This will also affect the overall pavement cost.

1.3 OBJECTIVES OF THIS RESEARCH

As is explained in the literature review section of this paper, since pervious concrete is a relatively new paving material, further research needs to be done into its structural performance to allow the use of pervious concrete as a roadway paving material. This research investigates two different pervious concrete test sites which have been subjected to heavy truck loading and high levels of clogging sediments for extended periods of time. The resulting surface damage was recorded and analyzed and conclusions were drawn about the structural performance of pervious concrete.

In order to design a regular concrete pavement, the design engineer can choose from several different widely used thickness design methods that can then be used to calculate the required pavement

thickness based on the stress it will be subjected to. However, for pervious concrete there are currently no established thickness design methods. This paper evaluates two of the most common methods for the thickness design of concrete pavements for their applicability to pervious concrete. The distress results found from the two test sites inspected will be used to assess the two thickness design methods.

In summary, the objectives of this thesis are:

1) Objective 1: Investigate the structural performance of pervious concrete subjected to heavy truck loading based on various design parameters.
    a) Objective 1a: Determine material characteristics and structural properties of representative pervious concrete samples from the field sites.
    b) Objective 1b: Perform a surface distress survey on the pervious concrete pavements at the field sites.
    c) Objective 1c: Use the results from the surface distress survey to quantify the structural performance of the pervious concrete at each field site.
2) Objective 2: Evaluate two common thickness design methods for their applicability to the design of pervious concrete pavements.
    a) Objective 2a: Determine material characteristics and structural properties for representative pervious concrete samples from field sites.
    b) Objective 2b: Evaluate AASHTO (1993) thickness design method for its applicability to pervious concrete.
    c) Objective 2c: Evaluate PCA (1984) thickness design method for its applicability to pervious concrete.

2. SITE VISITS

In order to complete this research, two pervious concrete field placement sites were visited. Both field sites were pervious concrete driveways located at concrete/aggregate plants. Sections of the pervious concrete analyzed were subjected to the loads produced by full concrete trucks, while other

sections were subjected to the loads produced by empty concrete trucks. The first site, Evolution Paving's concrete/aggregate plant near Salem, Oregon was visited on May 19, 2009. The second site, Miles Sand & Gravel's concrete/aggregate plant in Kent, Washington was visited on August 17, 2009. Sections 2.1 and 2.2 of this thesis give more detailed descriptions of each test site.

2.1 PERVIOUS CONCRETE DRIVEWAY AT EVOLUTION PAVING

2.1.1 BACKGROUND

A good way to determine if pervious concrete is able to stand up to heavy traffic loading is to subject it to heavy traffic loading and observe the results. This is exactly what Scott Erickson, president of Evolution Paving has done. Sixteen panels of pervious concrete were placed as a section of the driveway leading to his aggregate plant near Salem, Oregon, half on the egress, and half on the ingress side. The pervious panels, totaling approximately 4000 square feet, are shown in Figure 2.1 and are numbered for reference. The panels on the ingress side received loading from predominantly empty concrete trucks, while the panels on the egress side received loading from full concrete trucks. Contrary to standard practice in the US, the trucks always drove on the left side of the driveway. Over the 6 years of testing, Evolution Paving recorded every load that the pervious panels were subjected to, and took extensive photographic documentation of the surface distress of each of the panels. The testing was conducted in one of the worst environments for pervious to be used because of the heavy loads and large amounts of sediments and cements in the vicinity which might clog the pores of the pervious concrete.

Figure 2.1: Evolution Paving Test Site (Picture taken 5/29/2009)

2.1.2 PERVIOUS CONCRETE MIX DESIGN PARAMETERS

The testing began in 2003 when Evolution Paving began Phase I of the testing by placing 16 different panels of pervious concrete in the driveway. The panels varied in depth, aggregate size, and aggregate shape. In 2004, six panels were replaced, and the new panels were referred to as Phase II. The panels replaced were panels 2, 4, 6, 8, 10, and 12 in Figure 2.1. In May of 2009, a distress survey was performed on the pervious concrete panels, of which six had been placed in 2004 (Phase II) and ten placed in 2003 (Phase I). This survey was then used to calculate a pavement condition index, which would allow the pervious panels to be compared to other pavements. After the distress survey was completed, all of the Phase I and II panels were removed and selected specimens were collected for additional laboratory analysis.

A list of the various individual design properties of each panel from the Salem, OR site is compiled in Table 2.1. The maximum aggregate size is listed, as well as the aggregate shape: round rock (RR) or crushed rock (CR). The 3/8 in. round rock (pea gravel) did not contain any other size of rock.

The 5/8 in. crushed rock contained 75% 5/8 in. to 1/4 in. and also had 25% 3/8 in. blended in. The 1/2 in. crushed rock was 75% 1/2 in. to 1/4 in. crushed rock with 25% quarter-ten rock blended in.

Table 2.1: Evolution Paving Pervious Concrete Panel Design Properties

Evolution Paving Pervious Concrete Panel Summary					
Panel #	Depth (in)	Loaded Trucks?	Aggregate*	Age (yrs)	Compaction
1	7.5	no	3/8 in. RR	6	1/2 in. heavy roller
2	10	yes	5/8 in. CR	5	Heavy weighted Fresno
3	10	no	5/8 in. CR	6	1/2 in. heavy roller
4	7	yes	5/8 in. CR	5	Heavy weighted Fresno
5	8	no	5/8 in. CR	6	1/2 in. heavy roller
6	5	yes	1/2 in. CR	5	Heavy weighted Fresno
7	6	no	5/8 in. CR	6	1/2 in. heavy roller
8	5	yes	3/8 in. RR	5	Heavy weighted Fresno
9	4	no	5/8 in. CR	6	1/2 in. heavy roller
10	4	yes	3/8 in. RR	5	Heavy weighted Fresno
11	4	no	3/8 in. RR	6	None
12	4	yes	3/8 in. RR	5	Heavy rolled from 4.5 to 4 in.
13	6	no	3/8 in. RR	6	None
14	6	yes	3/8 in. RR	6	None
15	8	no	3/8 in. RR	6	None
16	8	yes	3/8 in. RR	6	None

*Maximum aggregate sizes are reported, RR = Round Rock, CR = Crushed Rock

For compaction, "1/2 in. heavy roller" means that a roller was used to compact the pervious concrete 1/2 in. "Heavy weighted Fresno" refers to the use of a Fresno float: a hand tool for surface compaction and leveling. Extra weight was also added to the back of the blade of the Fresno float to increase compaction. The pervious concrete panels contained various admixtures to increase workability and hardness, however the specific admixtures are not included in this thesis as requested by Evolution Paving. None of these pervious concrete panels contained any fiber reinforced polymer (FRP).

The panels were placed with a 12 in. thickened edge. The thickened edge extended approximately one foot from the outside parameter of the pervious concrete. The depths of the panels at

all other locations besides within one foot of the outside parameter are approximately equal to the depths shown in Table 2.1. Joints were saw cut between each panel as interior forms were not used. One inch minus rock, containing aggregate ranging in size from 1 in. to 0 in. was compacted to form the subgrade. The compaction of subgrade material is typically not recommended underneath pervious concrete because it decreases the infiltration rate of the subgrade. On top of the subgrade, a subbase of 1.5 in. to 3/4 in. crushed rock with approximately 37% voids was placed. The depth of the subbase varied from 4-10 in. based on the depth of the panel. The subbase for the pervious concrete acted as a recharge bed. The purpose of the recharge bed is to store water until it is able to infiltrate into the soil below. A typical cross section of the pervious concrete panels is depicted in Figure 2.2.

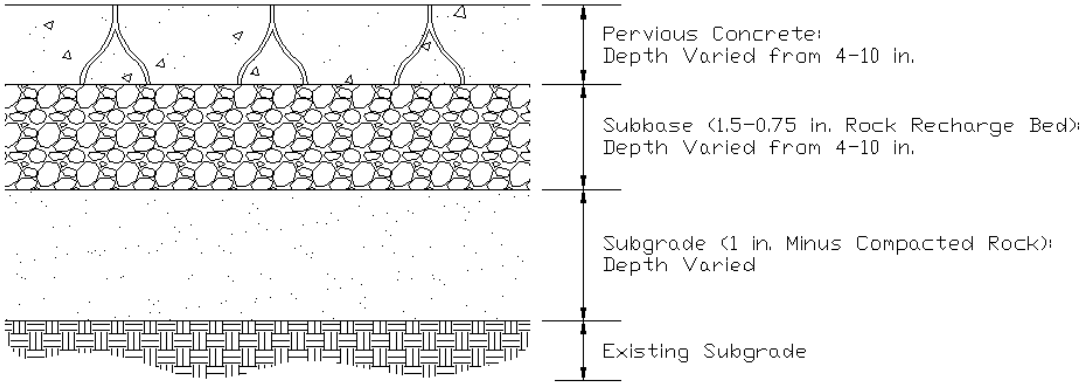

Figure 2.2: Typical Cross Section for Evolution Paving Pervious Concrete Panels

To better understand the depths of the pervious concrete panels at Evolution Paving, the panel depths were compared to typical concrete pavement street design depths. Typical concrete pavements with unsupported edges (no curb and gutter or shoulder) when being used for a "Residential" street typically would have a thickness ranging from about 5 inches to about 8 inches depending on the type of subgrade soil and the structural properties of the concrete. Concrete pavements with unsupported edges are typically between 7 and 12 inches thick for "Industrial" streets (ACI 325, 2002). The pervious concrete panels at Evolution Paving range from 4 to 10 inches thick, as shown in Table 2.1. The driveway to a concrete/aggregate plant would most likely be classified as an "Industrial" street. Since many of the pervious concrete panels at Evolution Paving are below or at the lower end of typical

"Industrial" concrete road thicknesses, the panels were intended and expected to fail. In this context, fail means to show significant distress such as cracking or surface raveling. Roadways that have failed can still be driven on, but the distress may decrease the smoothness of the road's surface and cause some discomfort to drivers.

2.1.3 LOADING CONDITIONS

The pervious concrete panels at Evolution Paving were subjected to approximately 40 truck loads a day in each direction. Over the entire life of the pervious concrete panels, panels in Phase I and II were subjected to a total of approximately 85,000 and 70,000 truck loads, respectively. The average concrete truck used at Evolution Paving had five axles, two of which were booster axles that were only lowered when the drum was filled, and weighed approximately 65,000 lbs when filled, and 30,000 lbs when empty. The average concrete truck was similar to the one shown in Figure 2.3.

Figure 2.3: Miles Sand & Gravel Concrete Truck: Similar to Typical Truck used at Evolution Paving

Concrete truck loads can be converted into an equivalent number of 18,000 lb single axle loads (ESAL) using the American Association of State Highway and Transportation Official's (AASHTO) published equivalent axle load factors (EALFs). Huang (2004) presents the EALFs for rigid pavements. For the full concrete trucks, assuming that the center tridem axle holds 45,000 lb, and both the front axle and back booster axle hold 10,000 lb, and using the EALF values from Huang (2004), the ESAL for one average concrete truck at Evolution Paving was calculated to be 2.1. Raymond (2004), a principal

engineer working for the City of Spokane, confirmed this value in his report "Pavement Performance Considerations for Heavy Traffic Loads." He calculated the ESAL for one fully loaded concrete truck to be approximately two. This means that one concrete truck produces the same pavement stress as two 18 kip single axle loads, or that the pervious concrete panels at Evolution Paving were subjected to 80 ESALs per day. Raymond (2004) reported that one loaded concrete truck produces stresses equivalent to that of about 5000 passenger cars. This shows the relative unimportance of pavement stresses produced by typical passenger cars. For this reason, Section 3.2 of ACI 325.12R-02 (2002) states that passenger cars may be ignored during the pavement thickness design.

According to ACI 325.12R-02 (2002) an average "Residential" street only has an average daily truck traffic (ADTT) of 5-25 trucks per day in one direction, while a "Collector" street has an ADTT of 25 to 250 trucks per day, and a "Minor Arterial" has an ADTT of 300 to 600 trucks per day (See Table 2.2). (ACI 325.12R-02 only accounts for 2-axle, 6-tire and heavier trucks.) For comparison with the pervious concrete panels, these ADTT values needed to be converted into ESALs using Tables 6.9 and 6.10 from Huang (2004). Table 6.9 from Huang's (2004) text reports the distribution of different truck types on different classes of streets. For example, approximately 11% of the trucks driving on a "Collector" street are 2-axle, 6-tire, single-unit trucks. Table 6.10 from Huang's (2004) text reports the equivalent axle load factor (EALF) of different truck types for each street classification. For example, the EALF for a 2-axle, 6-tire, single unit truck driving on a "Collector" is approximately 0.13. Using Tables 6.9 and 6.10 from Huang (2004), an average EALF for all trucks (2-axle, 6-tire and heavier) could be found for each street classification. These average EALF values are shown in Table 2.2. The EALF values were then multiplied by the number of trucks per day to yield the approximate ESALs per day (shown in Table 2.2). Since Tables 6.9 and 6.10 from Huang (2004) did not report values for "Light Residential" and "Residential" classifications, the number of ESALs per day for these classifications could not be calculated.

The predicted ESALs per day based on street classification could then be compared to the actual ESALs per day that the pervious concrete panels at Evolution Paving were subjected to. Since the

pervious concrete panels at Evolution Paving were subjected to 80 ESALs per day for approximately 6 years (totaling approximately 175,000 ESALS), the panels were exposed to an equivalent amount of stress as a "Collector" street in use for between 8 and 80 years. Even though the number of ESALs per day for "Light Residential" and "Residential" streets were not calculated, since they both are expected to be subjected to less trucks per day than "Collector" streets, it can be assumed that the pervious concrete at Evolution Paving was exposed to an equivalent amount of stress as a "Light Residential" or "Residential" street in use for more than 20 years.

Table 2.2: ESALs per Day for Different Street Classifications

ACI 325.12R-11 Street Classification	ACI 325.12R -11 Trucks per day in one direction (2-axle, 6 tire and heavier)	Average EALF for all Trucks (2-axle, 6 tire and heavier) (Tables 6.9 & 6.10 of Huang, 2004)	ESALs per day
Light Residentidal	1 - 2	-	-
Residential	5 - 25	-	-
Collector	25 - 250	0.24	6 - 60
Minor Arterial	150 - 300	0.43	65 - 130

The 30,000 lb load produced by an empty concrete truck was also converted into ESALs. Since concrete trucks only lower their booster axles when they are loaded, the load of an empty concrete truck is only supported on three axles. It was assumed that the back tandem axle supported 22,000 lb and the front axle supported 8,000 lb. Based on this an EALF of 0.34 was calculate for an unloaded concrete truck, resulting in the unloaded truck lane at Evolution Paving being subjected to approximately 14 ESALs per day. This totals to approximately 30,000 ESALs over its life, significantly less than the number of ESALs seen by the loaded truck lane at Evolution Paving.

2.2 Pervious Concrete Driveway at Miles Sand & Gravel

2.2.1 Background

Miles Sand & Gravel used pervious concrete for the entire driveway area of approximately 25,000 square feet leading out of their concrete and aggregate plant in Kent, Washington. This egress driveway at Miles Sand & Gravel is made up of a 180 degree turn, followed by a long straight-away, then

a large pad at the exit of the concrete/aggregate plant (Figure 2.4). The lines dividing the pervious concrete driveway represent joints between individual panels. Most joints were saw cut after the pervious concrete had cured. The 180 degree turn is made up of approximately 30 individual panels, the long straight-away is made up of 26 panels, and the large exit pad is made up of about 32 panels. The individual panels are of various shapes and sizes. Any panel less than 40 square feet in area was ignored for this research.

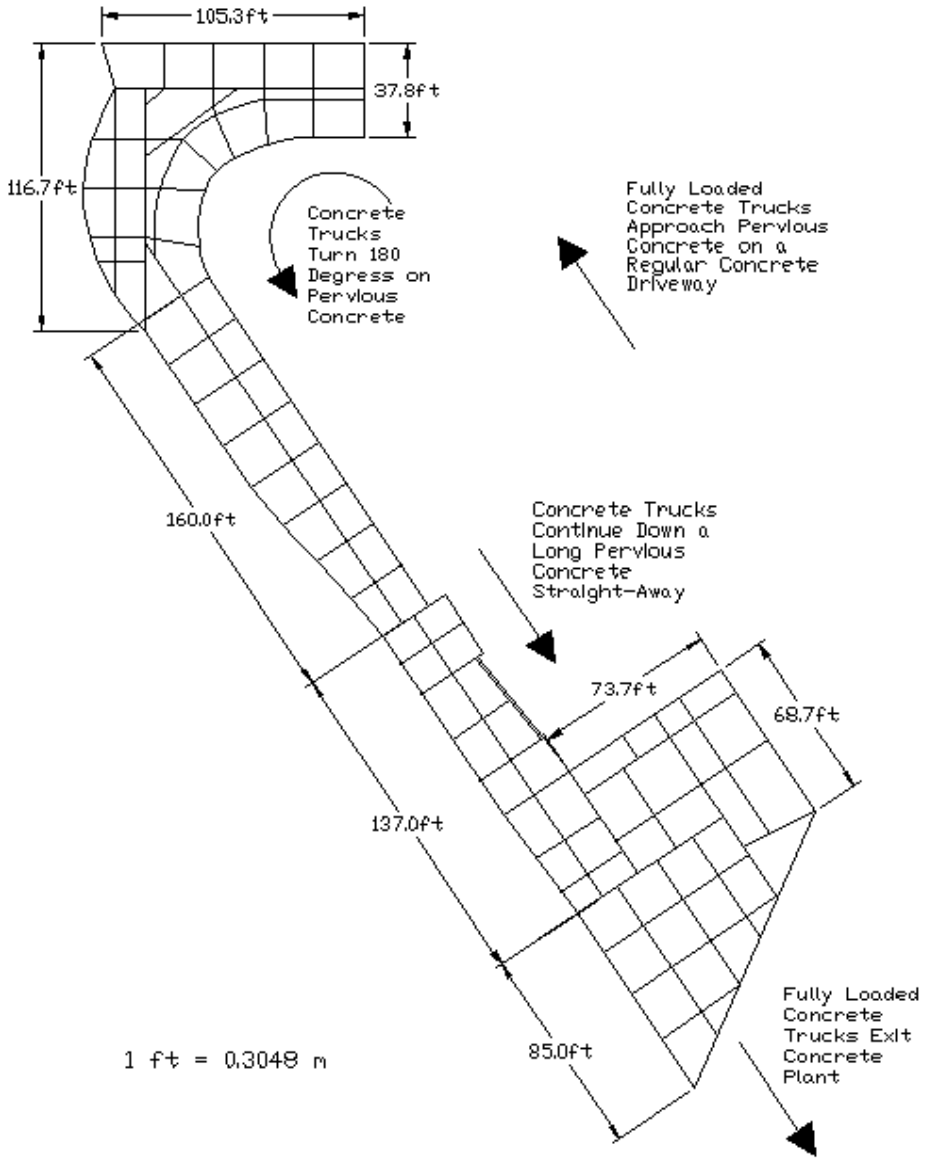

Figure 2.4: Pervious Concrete Driveway Layout at Miles Sand & Gravel in Kent, WA

More than two thirds of the 180 degree turn is made of pervious concrete (Figure 2.5). Having fully loaded concrete trucks turning a sharp corner could produce different distresses than those of fully loaded concrete trucks traveling on a straight portion of the driveway. Also, the distress produced by the acceleration and deceleration of concrete trucks as they exit the plant may differ from distresses at other locations of the driveway. A surface distress survey was performed on the entire driveway, and then the results for the 180 degree corner, the straight portion of the driveway, and the exit pad were compared.

Figure 2.5: 180 Degree Turn on Pervious Concrete at Miles Sand & Gravel

The long straight-away at Miles Sand & Gravel is shown in Figure 2.6. The figure shows the straight-away looking towards the exit of the concrete/aggregate plant. For reference, the 180 degree turn connects to the straight-away at the bottom of the picture.

Figure 2.6: Pervious Concrete Straight-Away at Miles Sand & Gravel

2.2.2 PERVIOUS CONCRETE MIX DESIGN PARAMETERS

At the Miles Sand & Gravel site all the pervious concrete panels have the following design parameters; 12 in. depth, uniformly-graded 3/8 in. round rock aggregate, no fine aggregate, and two water-reducing admixtures (not reported in this thesis). A hydraulic roller compacter was used to slightly compact and smooth the surface of the pervious concrete after it was placed.

2.2.3 LOADING CONDITIONS

The driveway at Miles Sand & Gravel was installed in April 2008 and had been subjected to approximately 30 full concrete truck loads a day. The full concrete trucks weigh an average of 80,000 lb and are usually supported on 5 or 6 axles. According to the plant manager, approximately half of the concrete truck drivers do not lower the booster axles until they have exited the concrete plant. For these trucks, the 80,000 lb load was supported by only 3 axles while it was on the pervious concrete, which would produce much larger stresses. In Figure 2.7, a fully-loaded 5 axle concrete truck is shown preparing to exit Miles Sand & Gravel's concrete/aggregate plant. As shown in the figure, the concrete truck has not lowered its two booster axles yet.

Figure 2.7: Fully Loaded Concrete Truck at Miles Sand & Gravel with Booster Axles Up

The concrete truck loads at Miles Sand & Gravel were also converted to an equivalent number of 18,000 lb single axle loads (ESAL). It was assumed that 15 trucks per day, weighing 80,000 lb, were only supported by one single axle and one tandem axle (3 axles total). The remaining 15 trucks per day were supported by between 5 and 6 axles. For the trucks without booster axles lowered, assuming that the back tandem axle holds 60,000 lb, and the front axle holds 20,000 lb, the ESAL was calculated to be

about 20. For the trucks with booster axles lowered, assuming that the center tridem axle holds 55,000 lb, and both the front axle and back booster axle hold 12,500 lb, the ESAL was calculated to be about 4.5. So lowering the booster axles on a concrete truck will cause the ESAL to drop from 20 ESALs to 4.5 ESALs. Multiplying these ESAL values by the estimated corresponding number of trucks per day and adding them together results in the pervious concrete pavement being subjected to about 370 ESALs each day at this site.

The distress survey was performed on August 17, 2009. At this time the pervious concrete at Miles Sand & Gravel had been subjected to approximately 370 ESALs per day for 1.5 years, totaling approximately 200,000 ESALS. The pervious concrete at Miles Sand & Gravel had been exposed to an equivalent amount of loads as a "Collector" street in use for between 9 and 90 years according to the number of ESALs per day calculated in Table 2.2.

3. MATERIAL CHARACTERIZATION

Some of the material characteristics of the pervious concrete were investigated. This material characterization completes Objectives 1a and 2a stated in Section 1.3 of this thesis, and is complementary to both the investigation into the structural performance of pervious concrete and the development of a thickness design method. The properties investigated were porosity, exfiltration rate, flexural strength, modulus of elasticity, Poisson's ratio, and compressive strength. Each property is defined and further discussed individually in the properties section of this paper that follow. Since no samples were obtained from the Miles Sand & Gravel pervious concrete driveway, the necessary tests could not be performed to characterize the pervious concrete at this site. The testing was only performed on the samples from Evolution Paving and some laboratory prepared samples. The reason for making laboratory samples is discussed in Section 3.1.2.1 of this thesis. The Evolution Paving samples and the laboratory prepared samples were given alphanumeric labels beginning with the letters EG (E for Evolution Paving) and WE (W for Washington State University), respectively. These labels will be referenced throughout this thesis to clarify which samples are being discussed.

3.1 MATERIAL CHARACTERIZATION PROCEDURE

This section summarizes the procedures used during all tests performed for the material characterization of the pervious concrete samples. The procedures are discussed in detail so the reader can better understand the reported test results, and even repeat the test if desired.

3.1.1 FLEXURAL STRENGTH

The flexural strengths of twelve samples from Evolution Paving were found using the Third-Point Loading Test as described in ASTM C 78 (2002). The test was performed in the Composite Materials Engineering Center at Washington State University on August 21, 2009. The purpose of this testing was to find the modulus of rupture of the pervious concrete samples obtained from Evolution Paving. The modulus of rupture will allow for the comparison of the strength of these pervious concrete samples with other reported pervious concrete strengths and traditional concrete strengths, and also aid in the evaluation of a thickness design method.

3.1.1.1 Cutting Beams from Evolution Paving (EG) Samples

The samples obtained from Evolution Paving had to be cut to the proper dimension in preparation for the flexural strength test (ASTM C 78, 2002). This test requires beam samples to have a test span approximately equal to three times the depth of the sample, and for the sides of the samples to be at right angles with the top and bottom. Since the samples obtained from Evolution Paving were 6 to 8 in. deep, the beams were cut to approximately 18 to 22.5 in. lengths. ASTM C 78 (2002) also requires all surfaces to be smooth and free of any indentations. The flexural strength test has no requirements for the width of the beam samples, so the samples were cut so that their width would be approximately equal to their depth.

The twelve beam samples were cut on June 23, 2009 using a hand held wet-cutting concrete saw that could cut to a maximum depth of approximately 4.5 inches. Because all of the samples exceeded a depth of 4.5 inches, it was necessary to cut from both the top and bottom faces. This made it difficult to

obtain sides that were flush and exactly 90 degrees to the top and bottom faces, but the requirements of ASTM C 78 (2002) were adhered to as closely as possible. The bottom face of the samples was not smooth because the cement adhered to the top layer of the subbase when it was originally placed in the field.

ASTM C 78 (2002) also requires that sawn beams conform to the requirements of ASTM C 42. The beam samples were cut in accordance with ASTM C 42 with the following two exceptions to the required moisture conditions:

1) The specimens were not covered with wet burlap after they were sawed.
2) The test specimens were not submerged in lime-saturated water for 40 hours prior to performing the flexural strength test.

The exceptions were made in order to more accurately replicate the in-situ conditions of pervious concrete. Unlike traditional concrete, pervious concrete is exposed to air throughout its entire depth by pores so covering it in wet burlap or submerging it in lime-saturated water does not necessarily represent in-situ conditions.

3.1.1.2 Third-Point Loading Test

The flexural strength test using a simple beam subjected to third-point loading was performed according to ASTM C 78 (2002). The purpose of this test was to determine the modulus of rupture of the samples. The modulus of rupture is the measured flexural strength, and these terms are used interchangeably in this thesis. This test is called the Third-Point Loading Test because the load is applied at two locations on the top of the beam, each location 1/3 of the length from the supports. This loading configuration results in the middle third of the beam having a constant moment, which simplifies the calculations to find the modulus of rupture. A picture of the test set up was taken during testing, and is shown in Figure 3.1.

Figure 3.1: Third-Point Loading Test Set-up

The Third-Point Loading Test was completed on twelve samples that were brought back from Evolution Paving and cut into beams. The testing was completed at the Composite Materials and Engineering Center at Washington State University on August 21st, 2009.

In accordance with ASTM C 78 (2002), the unsupported test span for each beam was approximately equal to three times the depth of the beam. Also, the horizontal distance between the support and the load application point was approximately equal to the depth of the beam. Since the samples obtained from Evolution Paving had varying depths, to meet the requirements of ASTM C 78 (2002) both the span and the load application points had to be adjusted based on the sample depth.

Both the supports and the loading points on the testing apparatus were allowed to rotate. This allowed the beams to act as simply-supported members. Extra care was taken during testing to ensure that the tension face during testing corresponded to the bottom face of the concrete as it existed in the field. This was done to simulate actual field conditions.

The pervious concrete panels at Evolution Paving had been placed directly on 1.5 in. to 3/4 in. aggregate subbase in the field. When the pervious concrete cured, some of the subbase aggregate had bonded to the pervious concrete. This large aggregate resulted in a very uneven surface on the bottom of the samples. In order to allow good contact between the bottom of the beam and the supports, prior to

testing a hammer was used to dislodge any large rocks at the location of the supports. Also, leather shims were used as needed between the beam samples and the supports to increase beam stability.

ASTM C 78 (2002) requires that the load be applied at a rate that will constantly increase the extreme fiber stress between 125 and 175 psi/min. The loading rate of the apparatus used was controlled by deflection, so the trial-and-error approach was used during the testing of the first beam (Beam EG11306R01) to provide the required loading rate. A deflection rate was chosen, and then the beam was loaded. The recorded load was monitored over durations of ten seconds and the corresponding rate of increase in extreme fiber stress was calculated. After several attempts, the deflection rate of the loading apparatus was set to 0.05 in/min for all beams having spans of between 18 in. and 19.5 in. All beams having spans larger than this were tested at a deflection rate of 0.07 in/min. The calculated rate of increase in extreme fiber stress for each beam tested can be seen in the summary of the Third-Point Loading Test, located in Appendix A.

The beam specimens were loaded until a tension crack caused them to break into two pieces (see Figure 3.2). After the beam specimens failed, the dimensions of the specimen at the failure plane were measured. The measurements were performed using digital calipers. The width and depth of the specimen at the failure plane were both measured three times: once at the center, and once at each end. The three measurements were then averaged, and used to find the modulus of rupture.

Figure 3.2: Failure of Beam Specimen during Third-Point Loading Test

All the failures occurred in the middle third of the specimen (see Figure 3.2). The equation used to calculate the modulus of rupture is shown below:

$$MOR = PL / (bd^2) \quad (3.1)$$

In this equation, MOR is the modulus of rupture reported in units of psi. P is the maximum applied load in pounds, L is the unsupported span length in inches, b is the average width of the specimen at the fracture in inches, and similarly d is the average depth of the specimen at the fracture in inches.

The results of the Third-Point Loading Test are presented in Section 3.2 of this thesis.

3.1.2 MODULUS OF ELASTICITY AND POISSON'S RATIO

While the definition of some of the other structural properties mentioned, such as compressive or flexural strength, are somewhat intuitive, this is not the case for the modulus of elasticity and Poisson's ratio. For this reason brief definitions are required. The modulus of elasticity is a measure of an object's resistance to deformation. It is the ratio of the applied stress to the resulting strain with both the applied stress and the resulting strain acting on the same axis. In case the reader is not familiar with the terms stress and strain, stress is a force per unit area and strain is the ratio of the total deformation (change in linear dimension) to the original dimension.

Poisson's ratio is the ratio of the strain perpendicular to the axis of the applied stress, to the strain parallel to the axis of the applied stress. For further clarification, a simple example will be presented. When you pull on two ends of a rubber band, the rubber band stretches creating a strain in the direction that you pull, parallel to the applied stress. The cross sectional area of the rubber band gets smaller in the middle, creating a strain perpendicular to the axis of the applied stress.

The modulus of elasticity and Poisson's ratio tests were performed on September 16, 2009 in the Sloan building at Washington State University. This section discusses the procedure used to complete these tests.

3.1.2.1 Preparation of Laboratory Samples (WE) for Modulus of Elasticity Testing

ASTM C 469 was followed in order to calculate the modulus of elasticity and Poisson's ratio of pervious concrete samples. ASTM C 469 requires the use of both a compressometer and an extensometer to calculate these variables. The only compressometer and extensometer that could be used at Washington State University were made for 6 in. by 12 in. cylinders. Since the samples obtained from Evolution Paving were not large enough to yield a 6 in. by 12 in. cylinder, 6 in. by 12 in. samples were prepared in the WSU laboratory on 7/7/09. The modulus of elasticity, Poisson's ratio, and compressive strength were found for the constructed samples. A relationship between the compressive strength and modulus of elasticity was then developed. This information was later used to estimate the modulus of elasticity and Poisson's ratio for the samples of pervious concrete obtained from Evolution Paving.

The WE pervious concrete samples were prepared using an approximate mass ratio of 1 lb cement, to 4 lb aggregate, to ¼ lb water. The aggregate that was used was a uniformly graded 3/8 in. round rock. Five 6 in. by 11 in. cylinders were made in one batch, and five 6 in. by 12 in. cylinders were made in a second batch. The pervious concrete cylinders were prepared according to the following procedure:

1) Wet all surfaces of the concrete mixer by using approximately 2 lb of water and 2 lb of cement. After all surfaces are wet, dump out excess liquid.
2) Put all the aggregates into the mixer and mix for 30 seconds.
3) Put all cementitious materials and ½ of the water into the mixer and mix for about 4 minutes.
4) Add ½ of the remaining water (1/4 of original water) and mix for another 4 minutes. After 4 minutes, turn of the mixer and scrape off any concrete that is sticking to the sides or bottom of the mixer.
5) Do the "Ball Test". Pick up a large handful of the concrete and pack it into a ball. If the concrete is able to maintain the shape of a ball without crumbling, then the concrete has sufficient water and is finished. Skip to step 7. If the concrete is not able to maintain the ball shape, then the concrete needs more water, proceed to step 6.

6) Add ½ of the remaining water and mix for another 3 minutes. After the 3 minutes, turn of the mixer and scrape off any concrete that is sticking to the sides or bottom of the mixer. Repeat the "Ball Test" described in step 5. Repeat steps 5 and 6 until the concrete is able maintain the shape of a ball.
7) Fill 6 in. by 12 in. plastic forms with pervious concrete (these forms did not have any holes in the bottom). In order to prevent very large voids in the sample, pick up and drop the forms 4 times from a height of about 3 in. Scrape off the top with a masonry knife. Record the mass of each sample. Set a minimum mass for each sample to ensure the void content is not too high.
8) Place a 6 in. by 12 in. cylinder of traditional concrete on top of the pervious concrete sample and hit the top of the traditional concrete cylinder with a rubber mallet until the pervious concrete is compacted approximately 9-10% (1.1 in.-1.2 in.). This step simulates field surface compaction techniques.
9) Immediately cover the pervious concrete samples with plastic caps.
10) Allow the samples to cure for 7 days. After 7 days, remove the pervious samples from the forms.

The first five samples were made from the first batch of pervious concrete prepared. The 6 in. by 12 in. plastic forms were filled to 12 in. then compacted down to approximately 11 in. (To ensure that the samples did not contain any large voids, if the mass of any sample was less than 9800g additional concrete was added as in step 7. This minimum mass was based on previously made pervious concrete samples here at Washington State University. The previously made samples were 4 in. by 8 in. cylinders. After these samples were removed from their forms it was observed that samples weighing less than 2900g contained large voids. The minimum mass for the samples prepared was roughly estimated based on this past observation, with a modification for the different sample size. It is recommended that future testing re-estimate this minimum mass to avoid high porosities.)

Samples 6-10 were made from the second batch of pervious concrete. The plastic forms were filled and then a collar was put on the top of the form to allow an extra 1 inch of concrete to be piled on

top of the form. The concrete was then compacted from 13 in. high, down to about 12 in. high. Similarly to the first batch, the samples had a minimum allowed mass of 10500 g.

3.1.2.2 Modulus of Elasticity and Poisson's Ratio

The modulus of elasticity and Poisson's ratio were found following the procedure described in ASTM C 469 (2002). The test was performed on the 10 laboratory prepared (WE) pervious concrete cylinders. The cylinders were all six inches in diameter, and ranged from about 11 to 12 inches in height. The modulus of elasticity and Poisson's ratio tests were performed simultaneously.

During each test, first a compressometer and an extensometer were attached to the test specimen. The compressometer was used to measure axial deformation, and the extensometer was used to measure deformations perpendicular to the axis of the specimen. The compressometer was made up of two separate pieces. One piece was attached to the top of the specimen, and the other attached to the bottom of the specimen with screws that were hand tightened until they were in contact with the pervious concrete surface. The extensometer was fastened similarly around the middle of the test specimen. The compressometer had a dial gauge that measured the change in the distance between the top and bottom pieces. The extensometer had a hinge in the back which allowed the ring to open as the specimen expanded in the middle. The extensometer also had a dial gauge to measure the amount of expansion in the middle of the specimen. Figure 3.3 depicts a test specimen with compressometer and extensometer attached prior to loading.

A test specimen was then placed in a compression loading machine. The compacted surface was on the top to simulate conditions for field placements of pervious concrete. The specimen was loaded at a constant rate up to approximately 20% of its ultimate load (about 10,000 lb) and then unloaded. This process was repeated. During these first two loadings, no data were recorded. The purpose of these loadings was to allow the seating of the gauges and to ensure that the compressometer and extensometer were functioning correctly.

Figure 3.3: Modulus of Elasticity and Poisson's Ratio Test Set-up (9/16/09, Sloan Building, WSU)

After the seating process was complete, the test was started. A compression load was applied at a constant rate up to approximately 40% of the ultimate load of the specimen (20,000 lb). The deformations indicated by the dial gauges on both the compressometer and extensometer were recorded at the following loads: 0 lb, 5000 lb, 10000 lb, 15000 lb, and 20000 lb. This process was repeated twice for each specimen and the resulting measured deformations were averaged.

ASTM C 469 (2002) requires the load to be applied at a rate that will cause a stress increase in the specimen of between 30 and 40 psi/sec. Since the machine was displacement controlled, it was difficult to maintain this loading rate. The actual loading rates were calculated, and are reported in the summary of the Modulus of Elasticity test located in Appendix A of this thesis.

The displacements recorded using the compressometer and extensometer were then used to calculate the longitudinal and transverse strain in the specimen. A stress vs. longitudinal strain curve was created for each specimen to verify the expected linear relationship between these two variables.

As previously discussed, the modulus of elasticity is equal to the change in stress divided by the change in longitudinal strain. The change in stress was found by subtracting the stress at 5,000 lb from the stress at 20,000 lb. Similarly, the change in strain was found by subtracting the strain record at 5,000 lb from the strain recorded at 20,000 lb.

Poisson's ratio is equal to the change in transverse strain, divided by the change in longitudinal strain. The change in both transverse and longitudinal strains was found by calculating the difference in strain readings taken at 20,000 and 5,000 lb. The modulus of elasticity and Poisson's ratio test results are presented in Section 3.2 of this thesis.

After the completion of this test, the compressometer and extensometer were removed from the specimen and a compression test was performed (see Section 3.1.3.3).

3.1.3 COMPRESSIVE STRENGTH

The compressive strength test was performed on September 16, 2009 at Washington State University. The test was performed on both the laboratory prepared (WE) samples discussed in Section 3.1.2.1 of this thesis, as well as cores drilled from samples obtained from Evolution Paving (EG) (discussed in Section 3.1.3.1).

3.1.3.1 Drilling Cores

In order to find the compressive strength of the samples that were obtained from Evolution Paving (EG), cores were drilled from the samples that were brought back from the site visit to Evolution Paving's concrete plant in Salem, Oregon. The cores were drilled on September 1, 2009 in the Albrook Laboratory at Washington State University using a Milwaukee brand, 20 amp, electric coring machine. The coring machine was attached to pallets to provide stability.

As discussed in Section 3.1.1.1, beams were cut from the Evolution Paving (EG) samples so the Third-Point Loading Test could be performed. After the completion of the Third-Point Loading Test, two 4 inch diameter cores were drilled from each beam. Since there were 12 beams in all, this resulted in 24 cores. The depths of the cores varied according to the thickness of the pervious concrete when it was installed in the field. There were also five samples brought back from Evolution Paving that were not big enough to be cut for beam samples. Two cores were taken from each of these five samples as well. Eight of these ten cores were 4 inch diameter cores, while 2 of the cores were 3 inch diameter. The cores were

from samples taken from 12 different panels at Evolution Paving. Samples were not obtained from four of the sixteen panels at Evolution Paving, so there were no cores representing these four panels.

3.1.3.2 Capping of Compression Test Specimens

The compression test was performed on both Evolution Paving (EG) cores and laboratory prepared (WE) cylinders according to ASTM C 39 (2005) which has several requirements regarding the shape of the test cylinders used for the compression test. First, each specimen is required to have uniform diameter throughout its length. Any specimens having a diameter varying more than 2% of any other diameter are not allowed to be used. All the pervious concrete cylinders met this requirement. Secondly, the ends of the specimen are required to be within 0.5^{o} of perpendicular to the axis, and must be plane. None of the pervious concrete cylinders met this requirement; therefore capping the ends of the specimens was required.

Three different capping options were considered for the compression test. The three different options were sulfur caps, gypsum plaster caps, and neoprene pad caps. John Kevern, an assistant professor at the University of Missouri-Kansas City who has experience with performing the compression test on pervious concrete samples, recommended the use of sulfur caps (Kevern, 2009). The sulfur cap molds to the irregular surface of pervious concrete and provide better support leading to higher compressive strength results.

Trejo, Folliard and Du also recommend the use of sulfur caps for controlled low-strength material, stating that they produce the largest compressive strength of the capping options (Trejo et al., 2003). Controlled low-strength material, as defined by ACI committee 229, is self-compacted, cementitious material used primarily as backfill. While this is not the same as pervious concrete, it is similar in that it is low-strength concrete that undergoes low compactive effort. Trejo reports that neoprene caps yield a compressive strength of more than 80% of sulfur caps, and gypsum plaster caps yield a compressive strength of more than 92% of sulfur caps.

Creating sulfur caps requires a mold of the proper size to shape the sulfur liquid while it cools. Since the proper sized mold was not available at Washington State University, gypsum plaster caps were made instead. The advantage to gypsum plaster caps is that no mold is required. All that is required is a flat, smooth surface to form the cap on and the rest of the shaping of the cap is done by hand. As stated above, gypsum plaster caps still mold to the irregular surface of the pervious concrete and are expected to yield concrete compressive strengths only slightly less than those that would be obtained using sulfur caps.

The gypsum plaster capping material that was used to make the caps was Hydro-stone (http://www.plaster.com/HYDROSTONE.html). Hydro-stone has a dry strength of 10,000 psi, much higher than the expected compressive strength of the pervious concrete. In total, 44 samples had to be capped: 34 drilled cores from Evolution Paving (EG) samples, and 10 laboratory prepared (WE) cylinders. The Hydro-stone was mixed with water by hand in a small bowl until it achieved the desired consistency. The plaster paste was then poured onto a piece of Plexiglas and the cylinder was placed on top of the paste. The excess Hydro-stone was then removed and the cap was allowed to dry for approximately 20 minutes before the sample was removed. The fast setting time of the Hydro-stone only allowed two samples to be capped at one time. A carpenter's level was used to ensure that after capping, the ends of the specimen were perpendicular to the axis, as required by ASTM C 39 (2005).

The very non-uniform bottoms of the cored pervious concrete cylinders required the use of a large amount of the Hydro-stone on the bottom of the samples, as can be seen in Figure 3.4. The more uniform ends of the laboratory prepared (WE) cylinders required much less of the capping material (Figure 3.5).

Figure 3.4: Gypsum Plaster Capping of Cored Pervious Concrete Samples (9/8/09, Sloan Building, WSU)

Figure 3.5: Gypsum Plaster Capping of Laboratory Prepared Pervious Concrete Samples (9/8/09, Sloan Building, WSU)

3.1.3.3 Compressive Strength

A compression test was performed on both the drilled cores from Evolution Paving, and the laboratory prepared (WE) samples. This section summarizes the procedure used during the testing of the samples. As previously mentioned, the procedure set forth in ASTM C 39 (2005) was followed.

The test machine used was hydraulically powered. The lower bearing block was stationary, while the upper bearing block moved down to compress the specimen. The upper bearing block was capable of tilting if the top of the specimen was not completely horizontal.

Prior to testing, the surfaces of the testing machine were wiped clean. The test cylinder was then placed on the lower bearing block with compacted surface oriented up, and centered. The load was

applied at a rate corresponding to a stress increase of between 28 psi/sec and 42 psi/sec. The actual rate of stress increase for each specimen can be seen in the results section, Section 3.2.3, of this thesis.

Each specimen was loaded until the load began to decrease rapidly, and a fracture was clearly evident. The maximum load applied and the types of fracture were then recorded. As defined in ASTM C 39 (2005), typical fracture patterns are shown in Figure 3.6.

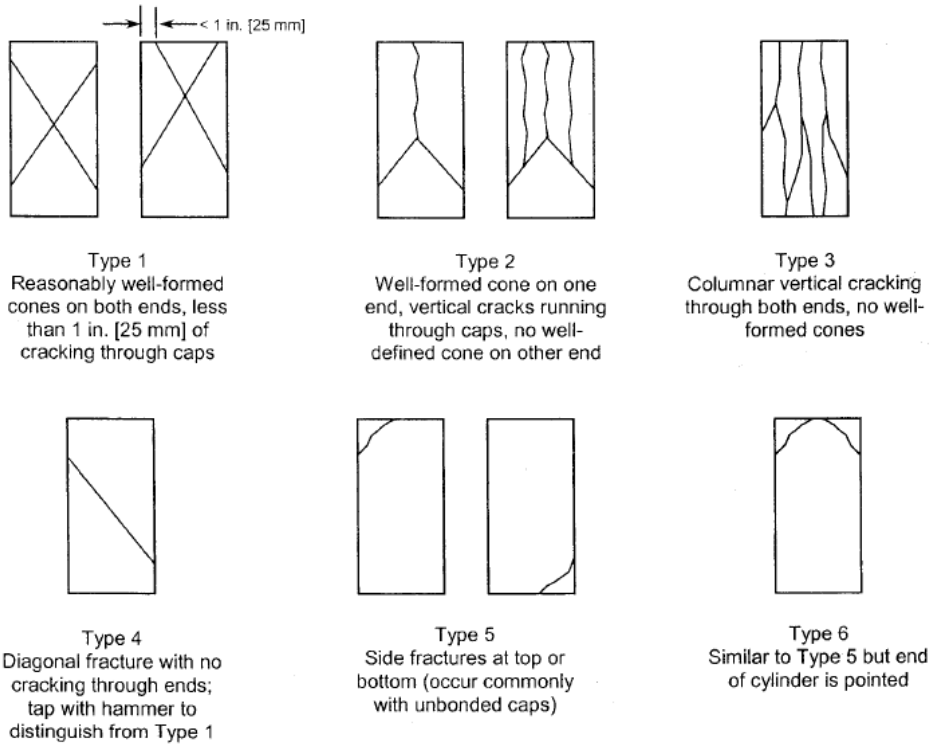

Figure 3.6: Typical Fracture Patterns for Compression Test (ASTM C 39, 2005 Figure 2)

The compressive strength of each specimen was then calculated by dividing the maximum load applied by the cross-sectional area of the specimen. The typical ratio of specimen length to diameter (L/D) of specimens used for the compression test is approximately 2. However, if the length L/D is less than 1.75, the calculated compressive strength must be multiplied by a correction factor. The correction factors are shown in Table 3.1. These correction factors are applicable to concretes having densities from 100 pcf up to about 150 pcf. The densities of all pervious concrete samples tested fall within this range (see Tables 3.2 and 3.3) therefore the correction factors may be used. When the L/D ratio was between the values listed in Table 3.1, interpolation was used to find the appropriate correction factor.

Table 3.1: Compressive Strength L/D Correction Factors (ASTM C39, 2005)

L/D	1.75	1.5	1.25	1
Factor	0.98	0.96	0.93	0.87

The results of the compression test are presented in Section 3.2.

3.1.4 POROSITY AND EXFILTRATION RATE

The main property that makes pervious concrete unique is its enhanced porosity which allows water to flow through the material. Different installations of pervious concrete, and even different sections within the same installation, may have highly variable porosities which will lead to highly variable infiltration and exfiltration rates. Due to the highly variable nature of these properties, tests were performed to quantify their values for the pervious concrete samples analyzed.

3.1.4.1 Porosity

It is well documented that the strength of pervious concrete is dependent on the porosity. For this reason, the porosity was found for all samples that underwent structural testing. The porosity was found using a test method developed by Montes et al. (2005) at the University of South Carolina. Their water displacement method was published in the Journal of ASTM international. This test method is designed to find the total porosity of a pervious concrete sample. Total porosity (P) is defined as the volume of all voids (V_{voids}) divided by the total volume (V_T) of the test specimen.

$$P = V_{voids}/V_T \tag{3.2}$$

The water displacement method is based on Archimedes principle of buoyancy which states that the buoyancy force is equal to the weight of the fluid displaced. All that must be known to calculate the porosity using this method is the dry mass, the submerged mass, and the total volume.

As previously mentioned, the total porosity is equal to the voids volume divided by the total volume. The total volume was found by measuring height and diameter of the sample at 3 locations and using an average to calculate the volume.

The volume of voids can be found using both the dry and submerged mass of the sample. The volume of voids is equal to the total volume minus the volume of solids (V_{sol}).

$$V_{voids} = V_T - V_{sol} \tag{3.3}$$

Since we already know the total volume, we only need to find the volume of the solids. According to Archimedes principle, the buoyancy force ($F_{buo)}$ is equal to the volume of the fluid displaced multiplied by the density of the fluid. In this case, the fluid being used is water. The volume of the water displaced is equal to the volume of the solids of the test specimen.

$$F_{buo} = V_{sol} \times \rho_w \tag{3.4}$$

From a simple summation of forces, the buoyancy force can be found by subtracting the submerged mass (M_{sub}) from the dry mass (M_{dry}).

$$F_{buo} = M_{dry} - M_{sub} \tag{3.5}$$

By substituting Equation 3.4 into Equation 3.5, an equation for the volume of solids is obtained.

$$V_{sol} = (M_{dry} - M_{sub})/ \rho_w \tag{3.6}$$

By substituting Equation 3.6 into Equation 3.3, and Equation 3.3 into Equation 3.2 a formula for porosity based on the dry and submerged mass and total volume of our sample is found.

$$P = [1- (M_{dry} - M_{sub})/ \rho_w]/ V_T \tag{3.7}$$

The submerged mass of the sample was found by submerging the sample in water for at least 30 minutes to allow water to penetrate nearly all pores in the specimen. After 30 minutes, while still submerged, each specimen was tapped against the side of the tank approximately five times to allow any air bubbles trapped in the pores to escape. The mass of the submerged sample was then measured using a wire basket connected to a digital scale. One exception to the test procedure presented by Montes et al.. (2005) was taken: the samples were not oven dried, rather the dry mass was taken at room temperature and humidity.

For drilled cores, a correction was needed to relate the measured porosity to the actual in-situ porosity because material was knocked off the surface of the core during the coring process. According to Haselbach and Freeman (2007), the corrected porosity (P_c) is a function of the sample's in-situ porosity

(P_i), the core diameter (D_c), and the maximum aggregate size (D_a). The corrected porosity can be calculated using the following equation:

$$P_c = P_i + \left(1 - P_i\right) \cdot \left[\frac{D_a}{D_c} - \left(\frac{D_a}{2 \cdot D_c}\right)^2\right] \cdot \left(\frac{P_i - P_{min}}{P_{max} - P_{min}}\right) \tag{3.8}$$

Where P_{min} is the minimum porosity and P_{max} is the maximum porosity. For this research, a max and min porosity of 0.05 and 0.45, respectively, were assumed.

3.1.4.2 Exfiltration Rate

To ensure that the pervious concrete would be able to effectively control runoff in a high intensity rainfall event, the exfiltration rate was found. The exfiltration rate is similar to the infiltration rate, except it measures the flow of water coming out of the bottom of the sample rather than the flow of water going into the top of the sample.

The samples were wrapped in plastic wrap prior to performing the exfiltration test. The plastic wrap not only prevents the water from flowing out the sides of the sample, it also provides a lip on top of the sample so that a sufficient head can be maintained. The plastic wrap was taped tightly around the top the test specimen to ensure that all water had to flow through the pore system of the specimen and could not flow between the plastic and the specimen.

The sample was placed in a funnel, which was positioned above a graduated cylinder (see Figure 3.7). Water was then poured into the top of the sample. The water was poured at a rate that maintained approximately 2 cm of head on top of the sample. The time was started when the first drop fell from the bottom of the sample, and was stopped when the graduate cylinder was filled to 2000 mL. The exfiltration was then found by dividing 2000 mL by the recorded time. The exfiltration test was performed twice on each sample.

Figure 3.7: Exfiltration Rate Test Setup (7/7/09, Albrook Building, WSU)

3.2 MATERIAL CHARACTERIZATION RESULTS

This section summarizes the results from all testing performed for the purpose of material characterization. The results of all testing performed on samples retrieved from Evolution Paving (EG) are shown in Table 3.2, and the results of all testing performed on samples prepared in the WSU laboratory (WE) are shown in Table 3.3. The material characterization results are discussed in Section 3.3. The coefficient of variation was calculated for the results of each test, and is also shown in Tables 3.2 and 3.3. The coefficient of variation is a normalized measure of the dispersion of data points, and is equal to the standard deviation divided by the mean. Since the different panels at Evolution Paving had different mix design parameters, the coefficient of variation is expected to be high for these samples.

Detailed individual results for all experimental tests performed are located in Appendix A of this thesis.

Table 3.2: Material Characterization Results for Evolution Paving (EG) Samples

Material Characterization Results for Evolution Paving Samples										
Panel #	Panel Depth (in)	Loaded Trucks?	# of Cores Tested	# of Beams Tested	Unit Weight (pcf)	Flexural Strength (psi)	Compressive Strength (psi)	Measured Core Porosity	Estimated In-Situ Porosity	Exfiltration Rate (in/hr)
1	7.5	no	2	1	122	297	3520	15%	14%	5.3
2	10	yes	2	0	111		1780	27%	21%	8.9
3	10	no	2	0	127		5030	13%	11%	14
4	7	yes	2	1	117	284	2940	22%	18%	
5	8	no	4	2	118	329	2900	21%	17%	16
6	5	yes	4	2	112	206	2260	26%	22%	29
7	6	no	0	0						
8	5	yes	8	4	113	275	2840	24%	21%	35
9	4	no	0	0						
10	4	yes	0	0						
11	4	no	2	0	109		2520	32%	27%	124
12	4	yes	2	0	116		2730	23%	20%	
13	6	no	2	1	120	260	2880	22%	19%	
14	6	yes	2	0	122		4200	15%	13%	
15	8	no	0	0						
16	8	yes	2	1	124	407	3470	13%	12%	
Mean					118	294	3089	21%	18%	33
Standard Deviation					6	62	871	6%	5%	41
Coefficient of Variation					4.7%	21%	28%	28%	27%	125%

Table 3.3: Material Characterization Results for Laboratory Prepared (WE) Samples

Material Characterization Results for Laboratory Prepared Samples						
Sample ID	Unit Weight (pcf)	Avg Compressive Strength (psi)	Modulus of Elasticity (psi)	Poisson's Ratio	Measured Porosity	Average Exfiltration Rate (in/hr)
WE1	116	1650	1886000	0.237	27%	1570
WE2	114	1340	1866000	0.337	28%	1680
WE3	117	1660	2205000	0.225	26%	1460
WE4	116	1670	1951000	0.169	27%	1760
WE5	115	1400	1750000	0.165	28%	1970
WE6	117	1650	1825000	0.129	26%	1290
WE7	115	1420	1415000*	0.644*	28%	1700
WE8	116	1620	2176000	0.239	27%	1830
WE9	118	1550	1886000	0.222	26%	1230
WE10	115	1440	1768000	0.236	28%	1860
Mean	116	1540	1923667	0.22	27%	1635
Standard Deviation	1.31	127	163500	0.06	0.9%	245
Coefficient of Variation	1.1%	8.3%	8.5%	27%	3.2%	15%

*OUTLIER: RESULTS WERE IGNORED

3.3 DISCUSSION OF MATERIAL CHARACTERIZATION RESULTS

This section provides a discussion of the results presented in Section 3.2 of this thesis. The results obtained are compared to test results reported by others to verify their validity. As shown in Table 3.2, the number of specimens tested varied for the different panels at Evolution Paving. The number of cores tested ranged from zero to eight for the different panels. The cores were used to find the unit weight, compressive strength, porosity, and exfiltration rate. The beams were used to find the flexural strength, and the number of beams tested for each panel ranged from zero to four. The laboratory test results shown in Table 3.3 are all for one test specimen only.

3.3.1 FLEXURAL STRENGTH

The average flexural strength results for each panel at Evolution Paving (EG) are shown in Table 3.2, and are the average of between 1 and 4 tests. The average width and depth used to calculate the flexural strength (aka modulus of rupture) were an average of measurements taken at three different locations as required by ASTM C78 (2008). The peak loads reported are not exact, but should be accurate within 20 lb. This is because the load apparatus was lowered until it made contact with the beam before the test was started. When the load apparatus came into contact with the beam often a small load was applied to the beam. However, 20 lb is less than 1% of the peak load for all tests, and therefore is not significant.

ASTM C78 (2008) requires that the fracture of the beams occurs within 5% of the middle third of the span length; otherwise the test results must be discarded. All the samples tested failed within the middle third of the span length.

The modulus of rupture (MOR) values ranged from approximately 150 to 410 psi (see Appendix A for individual test results). As discussed in the literature review section of this thesis, Tennis et al. (2004) report typical MOR values for pervious concrete ranging from 150 to 550 psi. The MOR results obtained during this testing fall within this typical range. Typical MOR values for traditional concrete are usually slightly higher, ranging from 350 to 600 psi (Wang et al., 2007).

Because results of the Third-Point Loading Test are typically highly variable, Marks (2008) recommends finding the modulus of rupture by equating it to the square root of the compressive strength (f'_c). In his paper, Marks (2008) uses the following equation to equate these values:

$$MOR = k_c \times (f'_c)^{1/2} \tag{3.9}$$

In Equation 3.9, k_c is defined as a constant with a value between 8 and 10. For traditional concrete the constant, k_c, is equal to 7.5 (Wang et al., 2007). For pervious concrete, k_c has been experimentally found to equal 8.72 (Ghafoori & Dutta, 1995).

This relationship was also developed for the samples tested in this research. The k_c factor was found to be 5.3 for the samples tested, significantly lower than the results reported by Ghaforri & Dutta (1995). This difference could have been caused in part by the irregular surfaces of the samples' tension faces. The base course loosely bonded to the bottom of the samples may not have increased the bending strength of the member significantly, but it certainly increased the depth of the sample. As shown in Equation 3.1, the MOR is found by dividing by the square of the depth, therefore increasing the depth will greatly decrease the calculated MOR. So if the base course did not increase strength, but only increased depth, it would be expected to decrease the calculated MOR values.

The developed relationship between MOR and compressive strength is shown in Equation 3.10.

$$MOR = 5.3 \times (f'_c)^{1/2} \tag{3.10}$$

Figure 3.8 shows the MOR values calculated from the Third-Point Loading Test, as well as a line showing MOR values calculated using Equation 3.10.

The MOR values found were later used during the evaluation of existing thickness design methods to determine their applicability to pervious concrete. Since samples large enough to perform the Third-Point Loading Test were unable to be obtained from all the pervious concrete panels at Evolution Paving, Equation 3.10 was used to calculate the MOR when test results were unavailable.

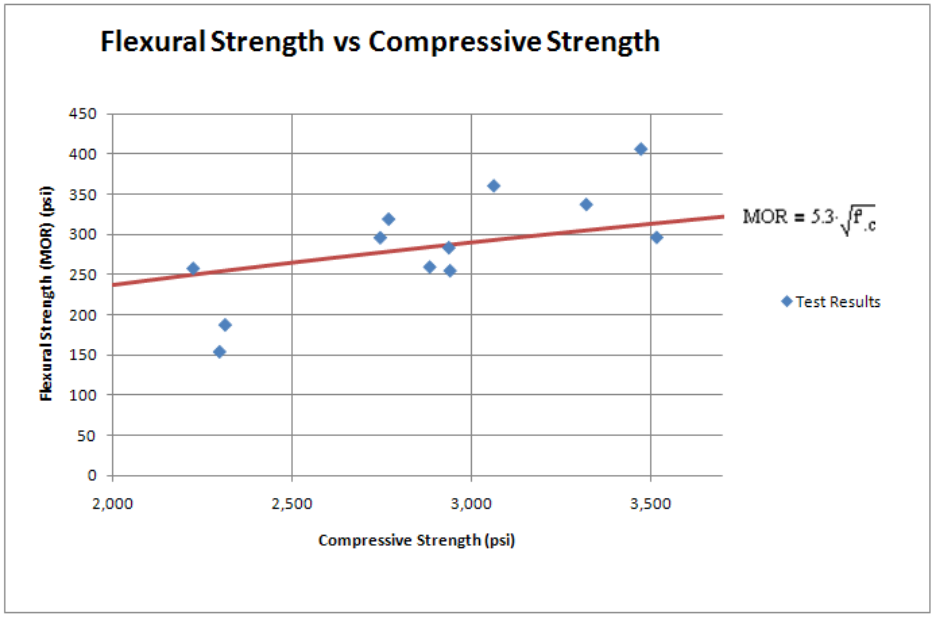

Figure 3.8: Relationship between Modulus of Rupture and Compressive Strength for Evolution Paving Beam Samples

The coefficient of determination (R^2) is a measure of how well a model predicts the actual results (also known as goodness-of-fit), and ranges from 0 to 1. An R^2 value of 1 indicates that the model perfectly predicts all results. The standard error ratio (S_E/S_y) was also used to determine goodness-of-fit. The standard error ratio is equal to the standard error of the estimate (S_E) divided by the standard deviation of the original variable (S_y), and represents the error expected from the prediction model. Both goodness-of-fit parameters were used to assess the models analyzed in this thesis. The subjective classifications used to describe the goodness-of-fit parameters are from Table 7 of Witczak et al., (2002) are summarized in Table 3.4 in this thesis.

Table 3.4: Subjective Classifications of Goodness-of-Fit (Witczak et al., 2002 Table 7)

CRITERIA	*R^2*	*Se/Sy*
Excellent	> 0.90	< 0.350
Good	0.70–0.89	0.36–0.55
Fair	0.40–0.69	0.56–0.75
Poor	0.20–0.39	0.76–0.90
Very Poor	< 0.19	> 0.90

These subjective classifications are used throughout this thesis. Witczak et al., (2002) state that R^2 is dependent on the linear separation of variation, and therefore is not always a good measure of accuracy for non-linear models. For this reason, in this thesis the goodness-of-fit of non-linear models will only be determined with S_E/S_y.

The S_E/S_y value for Equation 3.10 is 0.75, indicating a fair goodness-of-fit of the equation. Since the MOR has a relationship with the square root of the compressive strength, and the compressive strength has an approximately linear relationship with total porosity (P) for the range of values in these experiments (discussed in Section 3.3.3 of this thesis) it is logical that the MOR would also have a relationship with the square root of the total porosity. For the Evolution Paving pervious concrete samples, the MOR is compared to the total porosity (P) in Figure 3.9. Equation 3.11 was developed to calculate the modulus of rupture (MOR) based on the total porosity (P) of the sample.

$$MOR = -1105 \cdot \sqrt{P} + 800 \tag{3.11}$$

For this equation S_E/S_y is 0.67, indicating that this equation provides a fair approximation of the MOR. The MOR could have also been affected by other design parameters; however, no clear correlations between the MOR and the other design parameters could be made for the samples evaluated.

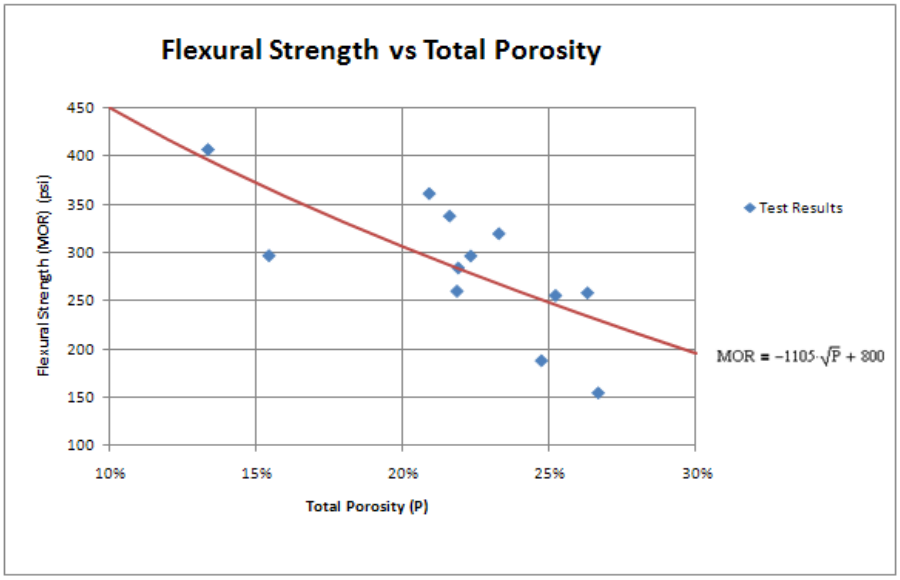

Figure 3.9: Flexural Strength versus Total Porosity for Evolution Paving Pervious Concrete Samples

Since the samples obtained from Evolution Paving all underwent surface compaction, it is expected that they have a linear vertical porosity distribution. As discussed in Section 1.2.2 of this thesis, the vertical porosity distribution of pervious concrete will result in higher porosities at the bottom of the sample, and consequently lower tensile strengths at the bottom of the sample (Haselbach & Freeman, 2006). Because of this, care was taken during testing to ensure that the surface that underwent compaction was facing up. Figure 3.9 compares the flexural strength to the total porosity of pervious concrete samples, however there may be a higher correlation between the flexural strength and the porosity at the bottom of the sample. It is recommended that future research be done to further investigate the effect of the vertical porosity distribution on flexural strength.

3.3.2 MODULUS OF ELASTICITY AND POISSON'S RATIO

This section discusses the results of the modulus of elasticity and Poisson's ratio tests. The results of these tests are presented in Table 3.3 of this thesis.

3.3.2.1 Preparation of Laboratory Samples (WE) for Modulus of Elasticity Testing

The first batch of pervious concrete was formed into five 6 in. by 11 in. cylinders, and the second batch of concrete was formed into five 6 in. by 12 in. cylinders. Both batches of cylinders were compacted approximately one inch. As discussed in the mix design procedure used for making these samples (Section 3.1.2.1), a design water-to-cement ratio of 0.25 was used. However, in order to pass the "Ball Test" (Step 5 of the mix design procedure, Section 3.1.2.1) it was necessary to increase the water-to-cement ratio. The first and second batches of pervious concrete had actual water-to-cement ratios of approximately 0.29 and 0.28, respectively. These water-to-cement ratios fall within the typical values of 0.27 to 0.30 reported by Tennis et al. (2004).

To determine the volume of these specimens, the diameter and height dimensions were measured at three different locations on the cylinder. The wet mass was taken immediately after the pervious concrete was put into the cylinder forms, before any hardening occurred. The dry mass was taken on 9/3/09; about 60 days after the samples were prepared, prior to compression strength testing. The dry unit

weight shown in Table 3.3 was found by dividing the dry mass, by the volume. Tennis et al. (2004) report that in-place pervious concrete unit weights between 100 and 125 pcf are common. As shown in Table 3.3, the unit weights of the pervious concrete cylinders range from approximately 114 to 118 pcf, falling within this acceptable range. Other details of the mix design, as well as individual cylinder's wet and dry masses can be viewed in Appendix A.

3.3.2.2 Modulus of Elasticity

The results from the modulus of elasticity test are summarized in Table 3.3. The full test results including all displacement gauge readings and stress vs. strain curves for each sample can be seen in Appendix A. Wang et al. (2007) report typical modulus of elasticity values for traditional concrete of between 3 and 4 million psi. The modulus of elasticity test on the laboratory prepared (WE) pervious concrete cylinders varied from approximately 1.75 to 2.2 million psi, somewhat lower than traditional concrete values. Since modulus of elasticity is correlated to compressive strength (ACI 318, 2008), it is logical that the modulus of elasticity would be lower for pervious concrete than traditional concrete because its compressive strength is typically lower for similar mixes. As noted in Table 3.3, the modulus of elasticity and Poisson's ratio results for test specimen WE7 were ignored since the results were outliers. The cause of the outlier was attributed to human error in recording data during the testing.

For traditional concrete, ACI 318 (2008) allows the static modulus of elasticity (E) to be found using the following equation:

$$E = 33 \times w_c^{1.5} \times (f'_c)^{1/2} \tag{3.12}$$

The variable, w_c, is the unit weight of the concrete, ranging from 90 to 160 pcf for traditional concrete (ACI 318, 2008). The modulus of elasticity is a function of the square root of the compressive strength (f'_c). For pervious concrete, Ghafoori and Dutta (1995) experimentally developed a similar equation to find the modulus of elasticity.

$$E = 32.88 \times w_{pc}^{1.5} \times (f'_c)^{1/2} \tag{3.13}$$

To find this equation, Ghafoori and Dutta (1995) experimentally found the static modulus of elasticity (E), unit weight (w_{pc}), and compressive strength (f'_c) for many pervious concrete samples, then used these results to calculate the constant 32.88, which is nearly identical to the value published in ACI 318 (2008) to be used for traditional concrete.

The results of the modulus of elasticity and compressive strength tests performed on the laboratory prepared pervious concrete samples were used to develop a similar relationship. The test results yielded the following equation:

$$E = 39.1 \times w_{pc}^{1.5} \times (f'_c)^{1/2} \quad (3.14)$$

The constant value of 39.1 is larger than the constant, 32.88, calculated by Ghafoori and Dutta (1995) and the constant, 33, recommended by ACI 318 (2008) for traditional concrete.

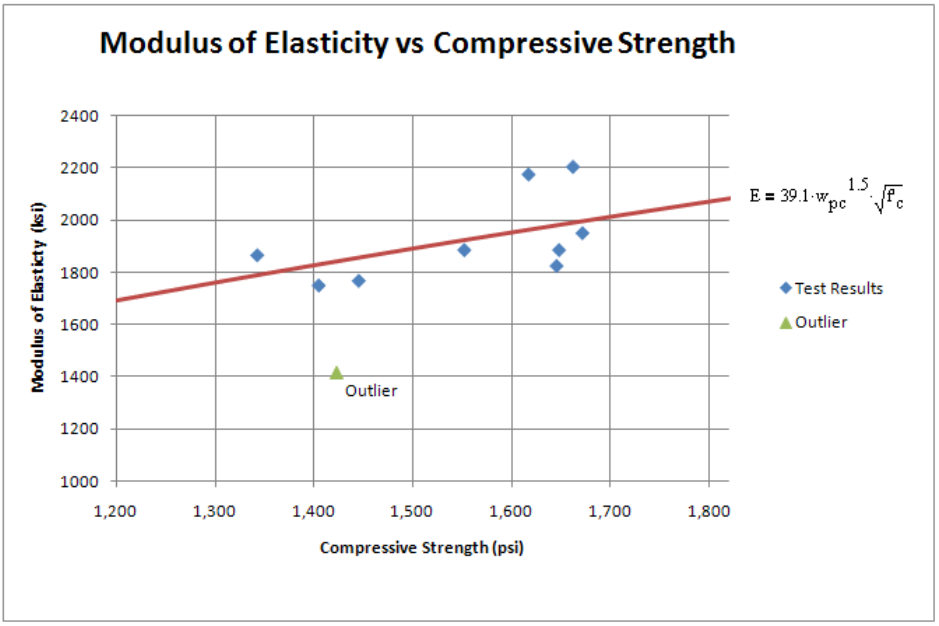

Figure 3.10: Comparison of Modulus of Elasticity and Compressive Strength for Laboratory Prepared (WE) Samples

Figure 3.10 show the modulus of elasticity test results plotted against the compressive strength test results for the laboratory prepared (WE) samples. The equation yielded from these results, Equation 3.14, is also shown on the plot. The modulus of elasticity for sample WE7 is shown in the figure, but is labeled "Outlier". As shown in the figure, Equation 3.14 seems to provide a reasonable estimate of the

modulus of elasticity based on the unit weight and compressive strength of the pervious concrete. For Equation 3.14, S_E/S_y is 0.79 indicating a poor goodness-of-fit of this model.

Since the Evolution Paving (EG) samples were not large enough to produce the 6 x 12 in. cylinders required for the modulus of elasticity test, Equation 3.14 was used to estimate the modulus of elasticity of these samples. These estimated moduli of elasticity were used to evaluate the two existing thickness design methods applicability to pervious concrete.

3.3.2.3 Poisson's Ratio

The Poisson's ratio test was performed at the same time as the modulus of elasticity test. The results from the Poisson's ratio test are shown with the modulus of elasticity results, in Table 3.3. Poisson's ratio for the laboratory prepared (WE) samples was found to be between 0.13 and 0.34 (again ignoring sample WE7), with an average value of 0.22. These results are similar but somewhat more variable than the findings of Ghafoori and Dutta (1995), who concluded that Poisson's for pervious concrete is similar to that of traditional concrete, varying between 0.15 and 0.20 (Huang, 2004).

3.3.3 COMPRESSIVE STRENGTH

The compressive strength test was performed on both the cores drilled from the Evolution Paving beam samples, and the laboratory prepared cylinders. The results of the compression test performed on the drilled cores from Evolution Paving (EG) and the laboratory prepared (WE) samples are shown in Tables 3.2 and 3.3, respectively.

The compressive strength values for Evolution Paving (EG) samples shown in Table 3.2 are the average results from between 2 and 8 tests. These samples had compressive strengths ranging from 1600 to 5100 psi (see Appendix A for individual results); higher than typical values reported by Tennis et al. (2004), which were 500 to 4000 psi. These results show that it is possible to obtain pervious concrete compressive strengths that are as high as traditional concrete compressive strengths. Wang et al. (2007) reports typical compressive strengths of 3500 to 5000 psi for traditional concretes. Some of the pervious concrete tested showed results at the top of this typical range for traditional concrete. The high variability

in these compressive strength results is attributed to the fact that all the pervious concrete panels at Evolution Paving had different mix design and placement parameters (see Table 2.1).

Since all the laboratory prepared cylinders were made with identical mix design parameters, the variability in the compressive strength results was very low, varying from 1350 to 1650 psi. The average compressive strengths for the laboratory prepared (WE) samples were significantly lower than those of the Evolution Paving (EG) samples. The lower strength was probably caused primarily by the higher porosity of these samples. Other factors such as aggregate size, aggregate shape (crushed vs. round), admixtures, and compaction may have also contributed. The relationship between compressive strength and porosity for both the laboratory prepared and the Evolution Paving (EG) samples is shown in Figure 3.11.

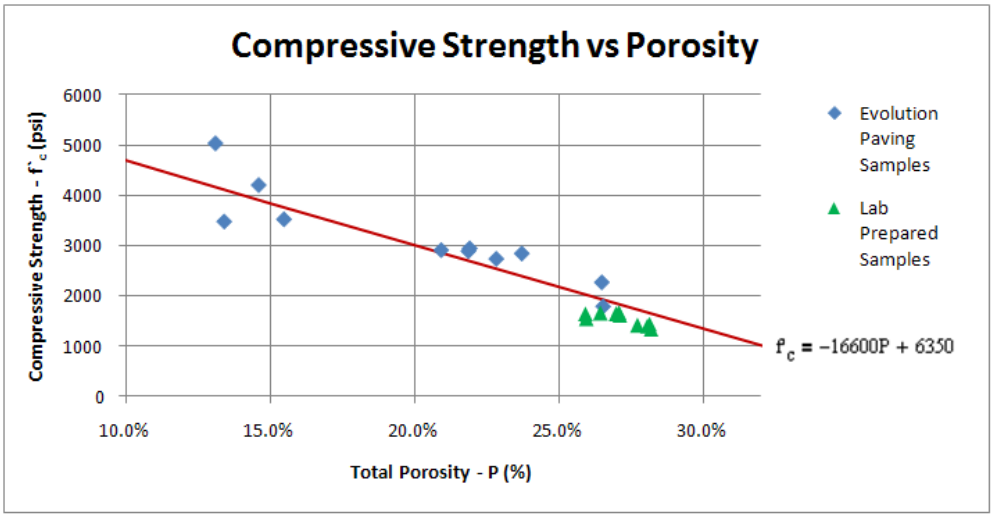

Figure 3.11: Relationship between Compressive Strength and Porosity

Clearly this figure shows that increasing porosity decreases compressive strength. The following linear equation was developed from this data to predict the compressive strength of pervious concrete based on the measured total porosity:

$$f'_c = -16600P + 6350 \quad (3.15)$$

Where compressive strength (f'_c) has units of psi, and P is the measured total porosity of the sample in decimal form. The predicted values obtained from this equation are shown in Figure 3.11. The

coefficient of determination (R^2) for Equation 3.15 is 0.77, and the value of S_E/S_y is 0.47, both indicating that the equation provides a good approximation of the actual test results. This R^2 value is representative of the reasonably strong correlation between these two variables. Despite the unique mix design and placement parameters of different samples tested, the compressive strength remains primarily dependent on the porosity.

Zouaghi et al. (2000) developed a very similar equation to the one found in this research:

$$f'_c = -16000P + 6200 \quad (3.16)$$

The variables in Equation 3.16 have the same units as the variables in Equations 3.15. They also found a high correlation between compressive strength and porosity, calculating a coefficient of determination (R^2) of 0.96 for Equation 3.16.

3.3.4 POROSITY AND EXFILTRATION RATE

This section discusses the results of both the porosity test and the exfiltration rate tests that were performed in the Albrook Laboratory at Washington State University. The results of these tests are presented in Table 3.2 for Evolution Paving (EG) samples and in Table 3.3 for laboratory prepared (WE) samples. The porosity and exfiltration tests were performed at two separate times. First, on July 14, 2009 the tests were performed on the 10 laboratory prepared (WE) samples. Then on September 4, 2009 the tests were repeated on the cores that were taken from the samples obtained from Evolution Paving (EG).

3.3.4.1 Porosity

The porosity of pervious concrete is very important, not only for stormwater management, but also for strength. As previously discussed, the compressive strength and flexural strength are both dependent on the porosity. The modulus of elasticity was found to increase with the square root of the compressive strength, and since the compressive strength is dependent on porosity, the modulus of elasticity is also dependent on the porosity. After equations relating these structural properties to porosity (such as Equations 3.11 and 3.15 developed in this research) have been established for a particular mix of pervious concrete, these structural properties can be reasonably estimated from the porosity. However, it

is important that equations relating these structural properties to porosity are developed based on the particular mix design parameters, as different mix design parameters, such as the addition of admixtures, fly ash, or fiber reinforcement, could have an effect on the equations.

The measured core porosities for the Evolution Paving (EG) samples, shown in Table 3.2, are the average results from tests performed on between 2 and 8 samples. The measured results for individual samples ranged from 12 to 32% (see Appendix A for individual test results), a slightly wider range than the typical values of 15 to 25% reported by Tennis et al. (2004). The wide range of porosities could have been caused by either the unique mix design and placement parameters for the different pervious concrete panels at Evolution Paving, or by variable amounts of clogging caused by the high level of sediment at the location of the pervious concrete driveway. The measured porosities were used to calculate estimated in-situ porosity. As shown in Table 3.2, the average in-situ porosities for Evolution Paving panels ranged from 11 to 27%.

Table 3.3 shows the porosity test results for the laboratory prepared (WE) samples, which range from approximately 26 to 28%. Since all these samples were made using the same mix design, were subjected to similar compactive effort, and were cured in the same conditions, the low variability in porosities was expected. These porosities are higher than the typical porosities of 15 to 25% reported by Tennis et al. (2004). The high porosity of the WE samples resulted in a low compressive strength. To achieve lower porosities, and consequently higher compressive strengths, either the water-to-cement ratio or the compaction effort can be increased.

3.3.4.2 Exfiltration Rate

The results of the exfiltration test performed on the laboratory prepared (WE) samples are reported in Table 3.3. The results from the exfiltration test performed on cores drilled from Evolution Paving (EG) samples are shown in Table 3.2. The exfiltration rate test was only performed on 10 of the 34 cores taken from Evolution Paving (EG).

Cleary the calculated exfiltration rates for the laboratory prepared (WE) samples, ranging from approximately 1300 to 2000 in/hr, are sufficient to handle even the worst of storms. It is important to note that field installations will most likely have much lower exfiltration rates due to the clogging effects of sediments and other small particles, which can decrease the exfiltration rate by an order of magnitude or greater. Since these laboratory prepared (WE) samples were never subjected to clogging sediments, the exfiltration rates were extremely high. The high porosity of these WE samples also contributed to the high exfiltration rates.

The Evolution Paving (EG) cores tested had exfiltration rates between approximately 5 and 120 in/hr, much lower than the exfiltration rates of the laboratory prepared (WE) samples. This is most likely due to excessive clogging in the field, expected because of the large amounts of cement and debris in the area. Scott Erickson (2007) tested the in-situ infiltration rates for both the loaded and unloaded truck lanes after they had been in use for two years. He reports infiltration rates of approximately 2 in/hr for the loaded truck lane, and 150 in/hr for the unloaded truck lane.

However, even with these low exfiltration rates, Scott Erickson reports that the pervious concrete still drains during heavy storms. The rainfall intensity for a 60 minute duration 10 year design storm in Salem, Oregon is only approximately 0.6 in/hr (City of Salem Public Works Dept, 2007). Even the cores showing the lowest exfiltration rates should still be capable of handling the rainfall from such a storm.

4. STRUCTURAL PERFORMANCE INVESTIGATION

Since pervious concrete is a relatively new paving material, contractors and engineers are hesitant to use it for applications where it will be subjected to heavy loads. This has limited the primary uses of pervious concrete to sidewalks, bike paths, and parking lots, not because pervious concrete is not capable of standing up to heavier loading, but because there has not been adequate research into the structural performance of pervious concrete. Section 4 of this thesis will present the results from two pavement distress surveys performed on pervious concrete pavements subjected to loads from fully-loaded concrete trucks for as long as six years. The pavement distress surveys were then used to calculate the Pavement

Condition Index (PCI) using ASTM D6433-07, which allowed the performance of the pervious concrete pavement to be quantified and compared to the performance of pavements made of more traditional materials.

As stated in Section 1.3 of this thesis, Objective 1 is to investigate structural performance of pervious concrete subjected to heavy truck loading based on various design parameters. This section completes this objective.

4.1 STRUCTURAL PERFORMANCE INVESTIGATION PROCEDURE

This section completes Objective 1b from Section 1.3 of this report. Objective 1b was to perform a surface distress survey on the pervious concrete pavements at the field sites.

4.1.1 DISTRESS IDENTIFICATION

In order to determine the performance of the pervious concrete panels at both the Evolution Paving and the Miles Sand & Gravel field sites, site visits were made to both sites in order to perform surface distress surveys. This section summarizes the procedure used to perform the surface distress survey at both test sites. Since the procedures used at the two test sites had some differences, the distress survey procedures for Evolution Paving (Section 4.1.1.1) and for Miles Sand & Gravel (Section 4.1.1.2) are discussed individually.

4.1.1.1 Evolution Paving

During the May 19th, 2009 site visit to Evolution Paving's concrete plant near Salem, OR, the pervious concrete panels were viewed prior to their excavation. The FHWA Distress Identification Manual (FHWA, 2003) was used to quantify the type, quantity, and severity of distress for each of the panels. In this context, distress is used to refer to any type of visible damage on the surface of the pervious concrete, such as cracking or surface raveling. A more detailed list of types of distress is discussed below. The second section of the manual, "Distress for Pavements with Jointed Portland Cement Concrete Surfaces" was used to identify the surface stresses. This section was considered the

most applicable since the other sections of the manual were for asphalts and for reinforced concretes. Clearly the asphalt section of the manual could not be used because asphalt is a flexible pavement, while concrete is a rigid pavement, and the two materials will experience different failures.

The FHWA (2003) manual gives clear descriptions of the different types of distress and severity levels. The 16 different types of distress included in this manual are shown in Table 4.1. Severity levels of distress ranged from low, to moderate, to high. FHWA (2003) defines the severity level of each type of distress individually. For example, low severity longitudinal cracking is defined as cracks having widths less than 3 mm (0.12 in.) with no spalling or faulting. While moderate severity longitudinal cracking includes cracks with widths between 3 and 13 mm (0.12 and 0.52 in.) or cracks with spalling less than 75 mm (3.0 in.) or faulting less than 13 mm (0.52 in.).

Some of the panels of pervious concrete were made using larger aggregates than others. The larger aggregate resulted in a rough surface, which made it difficult to identify surface deformations and identify the start and end of cracks. Because of this, extra care was taken to identify all distresses. Each panel had to be closely examined to ensure that no distress was missed.

Pictures summarizing the crack pattern, type and severity for each panel were drawn according to FHWA (2003). Also, extensive photographic documentation of each panel was taken to use for later reference.

The purpose of performing the distress survey was to use the data to calculate a pavement condition index. ASTM D 6433-07 (2007) "Standard Practice for Roads and Parking Lots Pavement Condition Index Surveys" was chosen as the method to be used to calculate the pavement condition index. In order to use the results of the distress survey to calculate the pavement condition index as defined in ASTM D 6433 (2007), the results from the previously mentioned FHWA distress survey had to be converted to match the distress definitions in ASTM D 6433 (2007). Most of the types of distress observed were the same for both the FHWA (2003) survey and the ASTM (2007) survey. A complete list of all distress types included in each survey can be seen in Table 4.1. The distress types for the FHWA

(2003) method were not listed in order in this table; rather they were placed next to the corresponding distress type for the ASTM D 6433 (2007) method.

Table 4.1: Comparison of Types of Distress as Defined by ASTM D 6433 (2007) and the FHWA Distress Identification Manual (2003)

ASTM D 6433-07: Roads and Parking Lots Pavement Condition Index Surveys	FHWA Distress Identification Manual (2003)
21. Blow up/Buckling	11. Blowups
22. Corner Break	1. Corner Breaks
23. Divided Slab	
24. Durability Cracking	2. Durability Cracking
25. Faulting	12. Faulting
26. Joint Seal	5a. Transverse Joint Seal Damage
	5b. Longitudinal Joint Seal Damage
27. Lane/Shoulder Drop-off	13. Lane-to-Shoulder Dropoff
28. Linear Cracking	3. Longitudinal Cracking
	4. Transverse Cracking
29. Patching (Large)	15. Patch/Patch Deterioration
30. Patching (Small	
31. Polished Aggregate	9. Polished Aggregate
32. Popouts	10. Popouts
33. Pumping	16. Water Bleeding and Pumping
34. Punchout	
35. Railroad Crossing	
36. Scaling	8a. Map Cracking
	8b. Scaling
37. Shrinkage Cracks	
38. Spalling Corner	
39. Spalling Joint	6. Spalling of Longitudinal Joints
	7. Spalling of Transverse Joints
	14. Lane-to-Shoulder Separation

Similar to the FHWA (2003) method, ASTM D 6433(2007) defines three different distress severity levels: low, medium, and high. However, the distress severities were defined differently for each distress survey. For example, the FHWA Distress Identification Manual (2003) defines a low severity longitudinal crack as a crack having a width of less than 3 mm. However, ASTM D 6433 (2007) defines a low severity longitudinal crack for unreinforced concrete as a crack having a width of less than 13 mm. In general, the FHWA Distress Identification Manual (2003) was more conservative on severity level than ASTM D 6433(2007). This difference was taken into account when the distress survey results were converted from the FHWA (2003) method, to the ASTM (2007) method. Examples of Low, Medium, and High severity linear cracking as defined by ASTM D 6433 (2007) are shown in Figure 4.1.

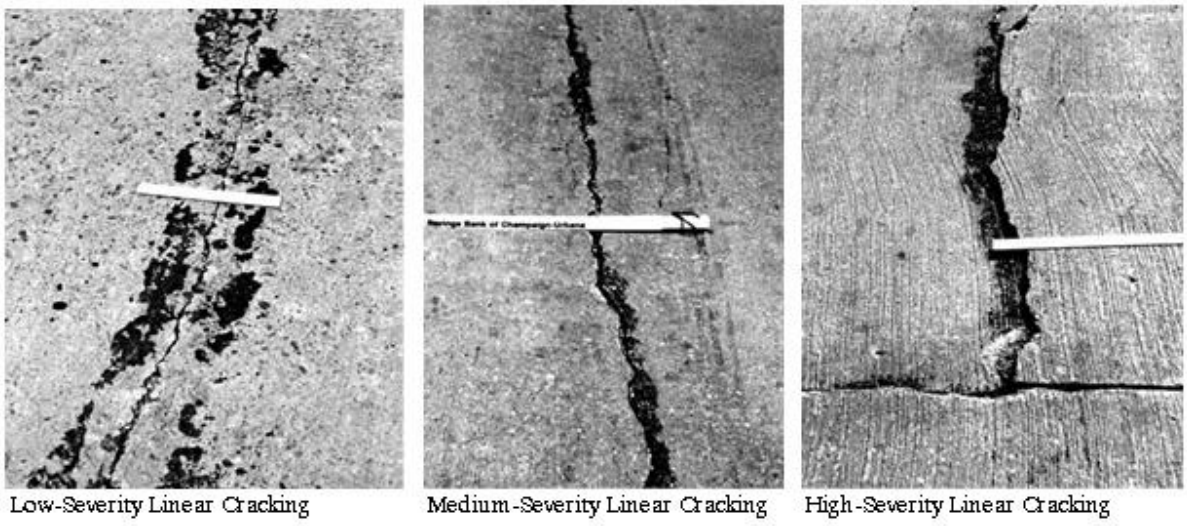

Figure 4.1: Severity of Linear Cracking (ASTM D6433, 2007 Figures X2.22-X2.24)

4.1.1.2 Miles Sand & Gravel

A distress survey was done on the pervious concrete driveway at Miles Sand & Gravel concrete/aggregate plant on August 17th, 2009. This distress survey was performed similarly to the distress survey that was performed at Evolution Paving discussed in Section 4.1.1.1, except that the survey was performed using ASTM D 6433 (2007). (The distress survey performed at Evolution Paving was originally done using the FHWA (2003) method and then converted to the ASTM D 6433 (2007) method.) Since the distress survey done at Miles Sand & Gravel was originally done using the ASTM D 6433 (2007) method, no conversion of the results was necessary.

4.1.2 PAVEMENT CONDITION INDEX

The results from the ASTM D 6433(2007) distress survey for both test sites were then used to calculate the pavement condition index using the procedure specified in ASTM D 6433-07 (2007). The pavement condition index (PCI) is a numerical value that represents the surface condition of the pavement and in this study was used to measure the structural performance of pervious concrete. Even though it is not a direct measure of structural integrity, the surface distress is a good indicator of the structural

integrity of the pavement being evaluated. The PCI can range from 0-100, with 0 being the worst score (failed), and 100 being the best score (good). The rating scale for the PCI is shown in Table 4.2.

In 2007, ASTM published an updated version of ASTM D6433. The new version included a different PCI rating scale from the previous 2003 version. Both PCI ratings are shown in Table 4.2 because many documents report the PCI rating using the 2003 rating scale. As can be seen in Table 4.2, the 2003 rating scale is more generous than the 2007 rating scale.

Table 4.2: ASTM D6433 Pavement Condition Index (PCI) Rating Scale for 2003 and 2007 versions

Rating	ASTM D6433 - 2003	ASTM D6433 - 2007
100	Excellent	Good
85	Very Good	Satisfactory
70	Good	Fair
55	Fair	Poor
40	Poor	Very Poor
25	Very Poor	Serious
10	Failed	Failed
0		

The first step in calculating the PCI is the identification of the type and severity of distress shown by a slab. These values were found from the previously mentioned distress survey. Then the total quantity of distress at each distress level and severity were summed. Next, the percent density of each distress type must be calculated. The percent density is equal to the number of slabs showing a particular distress type, divided by the total number of slabs surveyed. Each individual panel at Evolution Paving was unique in regards to at least one design parameter (depth, aggregate size, admixtures, etc…). Because of this, each panel had to be evaluated individually. This meant that for the pervious concrete panels at Evolution Paving, the percent density for all distress types would be 100%. Since the entire

pervious concrete driveway at Miles Sand & Gravel had the same design parameters, the percent density of distress types could be calculated for the entire test site.

Based on the distress type, severity, and percent density, the deduct value (DV) for each distress type could be found using the distress deduct curves located in Appendix X3 of ASTM D6433. An example deduct curve for linear cracking distresses can be seen in Figure 4.2.

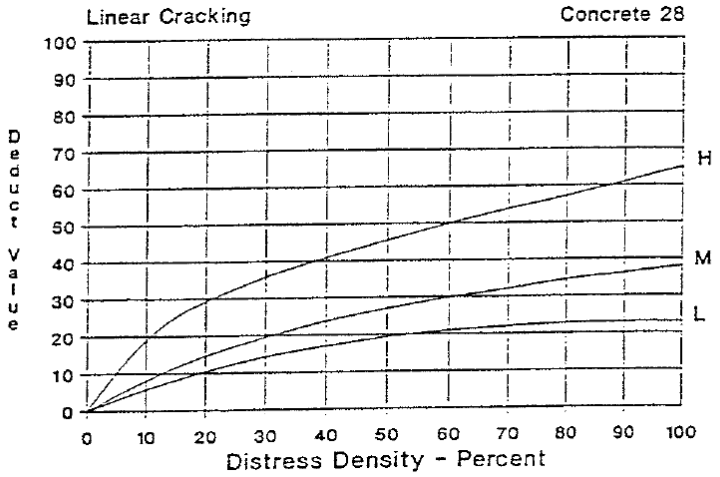

Figure 4.2: Linear Cracking Deduct Value Chart (ASTM D6433, 2007 Figure X4.8)

The individual DVs were then used to find the maximum corrected deduct value (CDV). First the individual DVs were listed in descending order. The sum of these values, called the total deduct value (TDV), and the number of DVs greater than 2.0, q, could then be used to find the first CDV using Figure X4.20 of ASTM D6433 (2007) shown in Figure 4.3. The smallest individual DV was then reduced to 2.0, and the process was repeated. Note that with each repetition, q is reduced by 1. The process should be repeated until q is equal to 1. Then the maximum CDV is found as the largest of all the CDVs. The pavement condition index (PCI) is then found by subtracting the maximum CDV from 100. The rating scale shown in Table 4.2 can then be used to rate the surface distress of the pervious concrete. An example set of PCI calculations can be found in ASTM D6433 (2007) if further clarification on the calculations performed is needed.

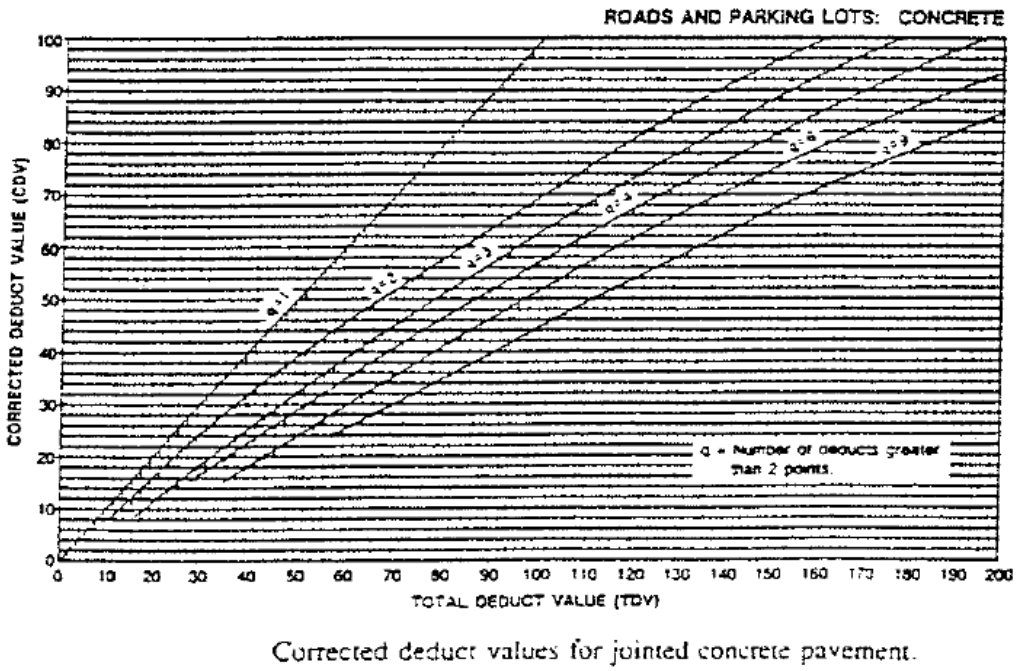

Figure 4.3: Corrected Deduct Values for Jointed Concrete Pavements (ASTM D6433, 2007 Figure X4.20)

4.2 STRUCTURAL PERFORMANCE INVESTIGATION RESULTS

This section of the thesis completes Objective 1c: Use the results from the surface distress survey to quantify the structural performance of the pervious concrete at each field site, as stated in Section 1.3.

4.2.1 DISTRESS IDENTIFICATION

The results of the ASTM D6433 (2007) distress survey for both test sites can be found in Appendix B. The variability in the amount of distress in the slabs at the Evolution Paving test site, as well as the unique design parameters of each pervious concrete panel made it necessary to report the results of the distress survey for each panel individually. However, since the Miles Sand & Gravel test site showed much less distress and had uniform design parameters, the results for the entire site were reported together on one page. In the distress surveys, each number corresponds to a type of distress. A list of all the types of distress and their corresponding number are shown in Table 4.1. The letter following the number indicates the severity level of distress. The distress severity can be either low-severity (L), medium-severity (M), or high-severity (H).

Not all distress types were found in the pervious concrete panels, and not all distress types were considered relevant to pervious concrete. Particularly, polished aggregate was not included as a distress type. Traditional concrete and asphalt pavements have a layer of binder above the top layer of aggregate that vehicles drive on. Pervious concrete, however, only has a very thin layer of binder on the aggregate, making polished aggregate an expected occurrence.

To further explain the distress survey results, the results of the distress survey for one of the panels at Evolution Paving are shown below in Figure 4.5. In Figure 4.5, 28L represents low severity linear cracking, 39L represents low severity joint spalling, and 22L represents a low severity corner break. The rest of the distress survey results can be found in Appendix B, and are discussed in Section 4.3.1.

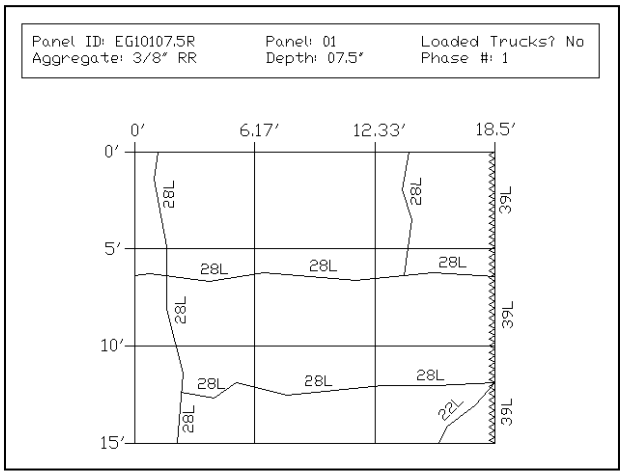

Figure 4.4: Example Distress Survey Results

4.2.2 PAVEMENT CONDITION INDEX (PCI)

The distress survey results were used to find the pavement condition index using ASTM D 6433 (2008). The results of the pavement condition index calculations can be seen in Appendix B, and are summarized in Table 4.3 for the Evolution Paving test site and in Table 4.4 for the Miles Sand & Gravel test site. These results are discussed in Section 4.3.2 of this thesis.

In both Tables 4.3 and 4.4, the design properties of the pervious concrete are shown along with the PCI so that conclusions may be drawn as to which factors had the greatest effect on distress. Both the 2003 and the 2007 PCI rating scales are shown in the tables to allow comparison of the two different

rating scales. Table 4.3 lists PCI values for each panel at Evolution Paving individually so that comparisons can be made based on the different design parameters. Since the entire driveway at Miles Sand & Gravel had the same design properties, it was not necessary to report a PCI value for each individual panel. Table 4.4 lists the PCI value for the entire driveway at Miles Sand & Gravel, then lists PCI values for individual regions of the driveway so that comparisons can be made based on different truck behaviors.

Table 4.3: Pavement Condition Index (PCI) Summary for Evolution Paving's Pervious Concrete

Evolution Paving Panel Design Properties						Evolution Paving PCI Summary		
Panel #	Depth (in)	Loaded Trucks?	Aggregate	Age (yrs)	Compaction	PCI	2007 ASTM Rating	2003 ASTM Rating
1	7.5	no	3/8 in. RR	6	1/2 in. heavy roller	48	Poor	Fair
2	10	yes	5/8 in. CR	5	Heavy weighted Fresno	87	Good	Excellent
3	10	no	5/8 in. CR	6	1/2 in. heavy roller	89	Good	Excellent
4	7	yes	5/8 in. CR	5	Heavy weighted Fresno	86	Good	Excellent
5	8	no	5/8 in. CR	6	1/2 in. heavy roller	87	Good	Excellent
6	5	yes	1/2 in. CR	5	Heavy weighted Fresno	77	Satisfactory	Very Good
7	6	no	5/8 in. CR	6	1/2 in. heavy roller	26	Very Poor	Poor
8	5	yes	3/8 in. RR	5	Heavy weighted Fresno	8	Failed	Failed
9	4	no	5/8 in. CR	6	1/2 in. heavy roller	27	Very Poor	Poor
10	4	yes	3/8 in. RR	5	Heavy weighted Fresno	8	Failed	Failed
11	4	no	3/8 in. RR	6	None	8	Failed	Failed
12	4	yes	3/8 in. RR	5	Heavy rolled from 4.5 to 4 in.	8	Failed	Failed
13	6	no	3/8 in. RR	6	None	8	Failed	Failed
14	6	yes	3/8 in. RR	6	None	8	Failed	Failed
15	8	no	3/8 in. RR	6	None	60	Fair	Good
16	8	yes	3/8 in. RR	6	None	50	Poor	Fair

Table 4.4: Pavement Condition Index (PCI) Summary for Miles Sand & Gravel's Pervious Concrete

Miles Sand & Gravel Design Properties							Miles Sand & Gravel PCI Summary		
Region	Depth (in)	Loaded Trucks?	Applied ESALs	Aggregate	Age (yrs)	Compaction	PCI	2007 ASTM Rating	2003 ASTM Rating
Entire Driveway	12	yes	200,000	3/8 in. RR	1.5	Hydraulic roller	94	Good	Excellent
180 degree	12	yes	200,000	3/8 in. RR	1.5	Hydraulic roller	88	Good	Excellent
straight-away	12	yes	200,000	3/8 in. RR	1.5	Hydraulic roller	100	Good	Excellent
exit pad	12	yes	200,000	3/8 in. RR	1.5	Hydraulic roller	92	Good	Excellent

4.3 DISCUSSION OF STRUCTURAL PERFORMANCE INVESTIGATION RESULTS

This section of the thesis completes Objective 1c: Use the results from the surface distress survey to quantify the structural performance of the pervious concrete at each field site, as stated in Section 1.3.

4.3.1 DISTRESS IDENTIFICATION

Every slab showed at least one type of distress at the Evolution Paving test site. However, most of the panels at Miles Sand & Gravel did not show any distress. This is most likely because the pervious concrete driveway at Miles Sand & Gravel was thicker than the thickest panels at Evolution Paving. As will be discussed later, thicker panels showed less surface distress and therefore showed better structural performance. Also as expected, the panels that were subjected to the heavier loaded trucks showed higher levels of distress than those subjected to the lighter unloaded trucks. The most commonly occurring type of distress was linear cracking.

4.3.2 PAVEMENT CONDITION INDEX (PCI)

4.3.2.1 PCI Relationship with Design Variables

The loaded truck lane at Evolution Paving and the entire driveway at Miles Sand & Gravel had seen similar stresses over their life (≈175,000 ESALS for the loaded lane at Evolution Paving, and ≈200,000 ESALS at Miles Sand & Gravel). However, the unloaded lane at Evolution Paving, only having been subjected to empty concrete trucks, was only subjected to approximately 30,000 ESALs over its life. Figure 4.5 shows that without holding depth constant there is no significant correlation between PCI and the number of applied ESALs. However, the PCI is compared to the applied ESALs for similar pavement depths in Figure 4.6 and the pavement subjected to less ESALs showed higher PCI values in four out of five cases. This implies that PCI has an inverse relationship to stress, although further research is needed to confirm this. In the one case where the panel subjected to higher ESALs (panel #4) outperformed the panel subjected to lower ESALs (panel #1), the panel subjected to lower ESALs (panel #1) was the last panel on the ingress side of the driveway. The interaction between this pervious concrete

panel and the adjacent regular concrete panel could have created unique loading conditions that contributed to the lower PCI value.

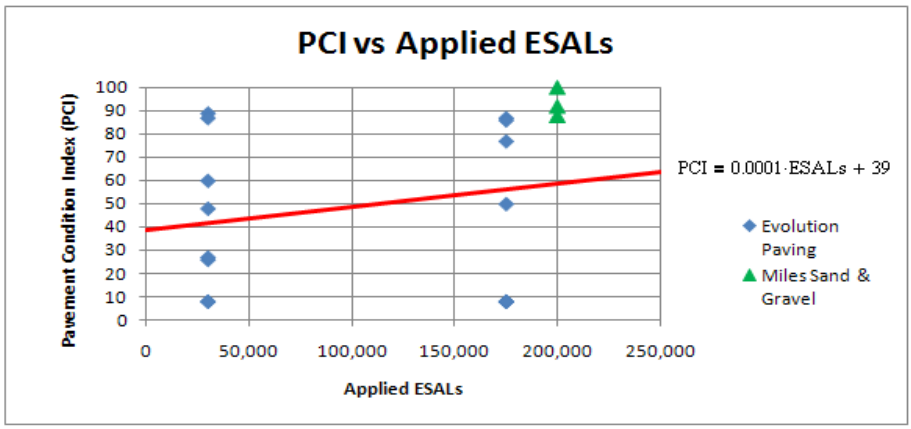

Figure 4.5: Pavement Condition Index (PCI) versus Applied Equivalent 18 kip Single Axle Loads (ESALs)

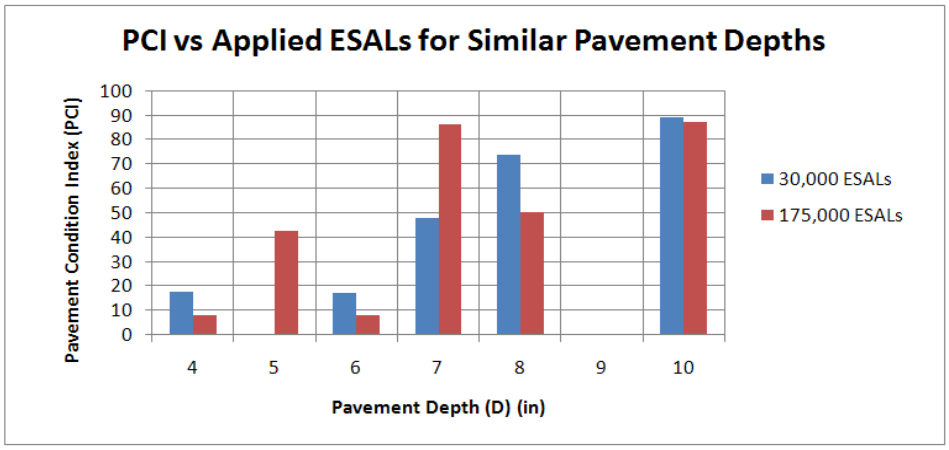

Figure 4.6: PCI versus Applied ESALs for Similar Depths

All the 4 in. panels failed at Evolution Paving, while the 10 and 12 in. panels at both field sites remained in good condition (or excellent condition depending on the rating scale used), indicating a correlation between PCI and pavement depth. Figure 4.7 shows PCI versus pavement depth for the pervious concrete at Evolution Paving and Miles Sand & Gravel. First a linear correlation was examined. For the linear trendline shown, R^2 is 0.67 and S_E/S_y is 0.56, indicating a fair goodness-of-fit of this model. Regardless of the variability of other variables, the relationship between increasing depth and an increasing PCI rating is clear. Since PCI has an inverse relationship to stress, and stress is a function of

one divided by the square of the depth, the PCI is expected to be a function of the depth squared. The dotted trendline shown in Figure 4.7 makes PCI a function of the depth squared. The S_E/S_y value for this trendline is 0.62, again indicating a fair goodness-of-fit.

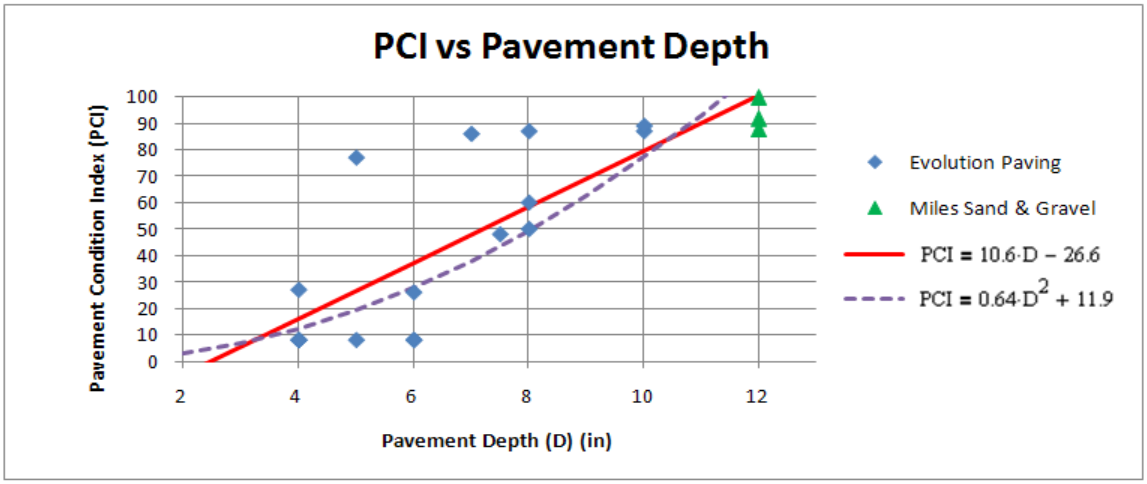

Figure 4.7: Pavement Condition Index versus Pavement Depth

The PCI results were also compared to the modulus of rupture. This comparison could only be done for pervious concrete panels at Evolution Paving for which either the modulus of rupture or compressive strength were found experimentally. If the modulus of rupture was not found experimentally for a panel, but the compressive strength was found, Equation 3.10 was used to estimate the modulus of rupture. The results of this comparison are shown in Figure 4.8.

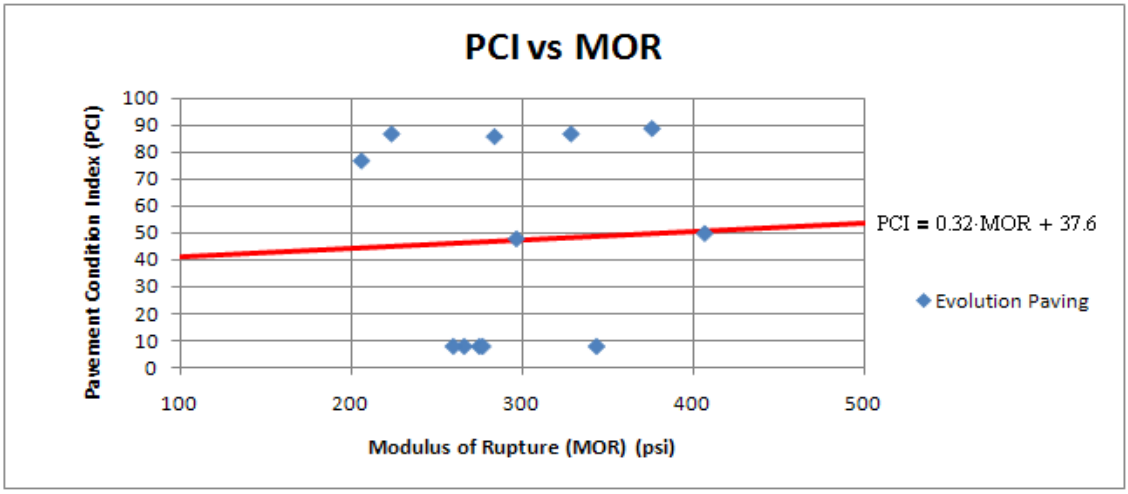

Figure 4.8: Pavement Condition Index (PCI) versus Modulus of Rupture (MOR)

Without holding depth constant, no clear trend between PCI and modulus of rupture (MOR) was evident. This was expected since the PCI is expected to be a function of depth squared, but only have a linear relationship with the stress (MOR). Variations in depth have a much greater affect on the PCI value than variations in MOR.

The effects other design variables had on the PCI are unclear. Since the test panels have so many changing variables, it is hard to attribute the higher or lower PCI rating to one individual variable. More test panels would be required to determine the affects of variables such as admixtures, compaction effort, aggregate size and aggregate shape. If this test were repeated in the future, it is recommended that some of the variables be eliminated so variability in PCI ratings can be attributed to one variable.

4.3.2.2 PCI Relationship with Traffic Behavior

The driveway at Miles Sand & Gravel was divided into three regions: 180 degree turn, straight-away, and exit pad. The driveway was divided to allow the comparison of the PCI between regions of the driveway that saw different traffic behavior. At the start of the pervious concrete driveway, fully loaded concrete trucks must make a 180 degree turn. This region showed increased surface wear, and cracking. As shown in Table 4.4, this region had the lowest PCI rating (88) of the three regions at Miles Sand & Gravel, suggesting that vehicles turning cause more distress to the pervious concrete than other vehicles. The second region consists of a long straight-away which connects the 180 degree turn and the exit pad. While driving this straight-away, the concrete trucks usually maintain a constant speed. This region did not show any distress, and had the highest PCI rating (100) of the regions at Miles Sand & Gravel. The last region of the pervious concrete driveway is a large exit pad. The concrete trucks often slow down when preparing to exit the concrete plant, so this region is subjected to the acceleration and deceleration of fully-loaded concrete trucks. The PCI rating of this region (92) was higher than the PCI of the 180 degree turn (88), but lower than that of the straight-away (100).

4.3.2.3 Comparison of PCI Values for Pervious Concrete and Other Pavements

In order to better understand the PCI results, the results were compared to the PCI of pavements in multiple cities across the US. The average PCI of the San Francisco Bay Area's local streets in 2007 was 64 (Local Streets & Roads Group of San Francisco Bay Area Partnership, 2007). In 2008, the city of Los Angeles reported similar results, with an average PCI of 62 (Stroup-Gardiner, 2008). Smaller California regions including Mendocino County, Lake County, and the City of Clearlake reported average PCI values of 50, 51, and 38 respectively in 2003 (Stroup-Gardiner, 2008). The mayor of Oregon City, OR reported an average PCI of about 55 in her 2007 State of the City Address. The City of Minneapolis, Minnesota (2009) reports a 2008 average PCI of 73 for all city streets. While the majority of the pervious concrete panels having pavement thicknesses between 4 and 7 in. performed well below the average of these cities, most of the panels having thicknesses between 7 and 12 in. showed higher PCI values. This indicates that the thicker panels of pervious concrete showed adequate structural performance to be considered as a street paving material.

Figure 4.9 shows the PCI values versus thickness for both the Evolution Paving panels, and the Miles Sand & Gravel regions. It is important to understand that each point for Evolution Paving in table only represents one pervious concrete panel, while each point for Miles Sand & Gravel represents a region which is made up of approximately 30 individual panels. Each panel at Evolution Paving was unique and therefore had to be treated individually, but all the pervious concrete placed at Miles Sand & Gravel was uniform and was only divided into three separate regions.

Also in Figure 4.9, the average PCI values for all road types in Minneapolis, San Francisco, and Los Angeles are shown as horizontal lines across the entire graph for comparison with the PCI values from the two field sites. While the PCI values for the pervious concrete obtained from the two test sites cannot be directly compared to the average PCI values for these major cities, due to different pavement ages, loading, and design parameters, the average PCI values from these major cities can help to better understand the PCI results for the pervious concrete.

The typical thicknesses for concrete car parking lots and concrete "Industrial" streets, also shown in Figure 4.9, were taken from thickness design tables in ACI 330 (2008) and ACI 325 (2002) respectively. The driveway leaving a concrete plant, classified as an "Industrial" street, would therefore be 7 to 12 inches thick if it is made of regular concrete. Based on this, clearly the thinner pervious concrete panels at the Evolution Paving field site were expected to fail. The intention for evaluating these thinner panels was to aid in determining the lower limits of design depths.

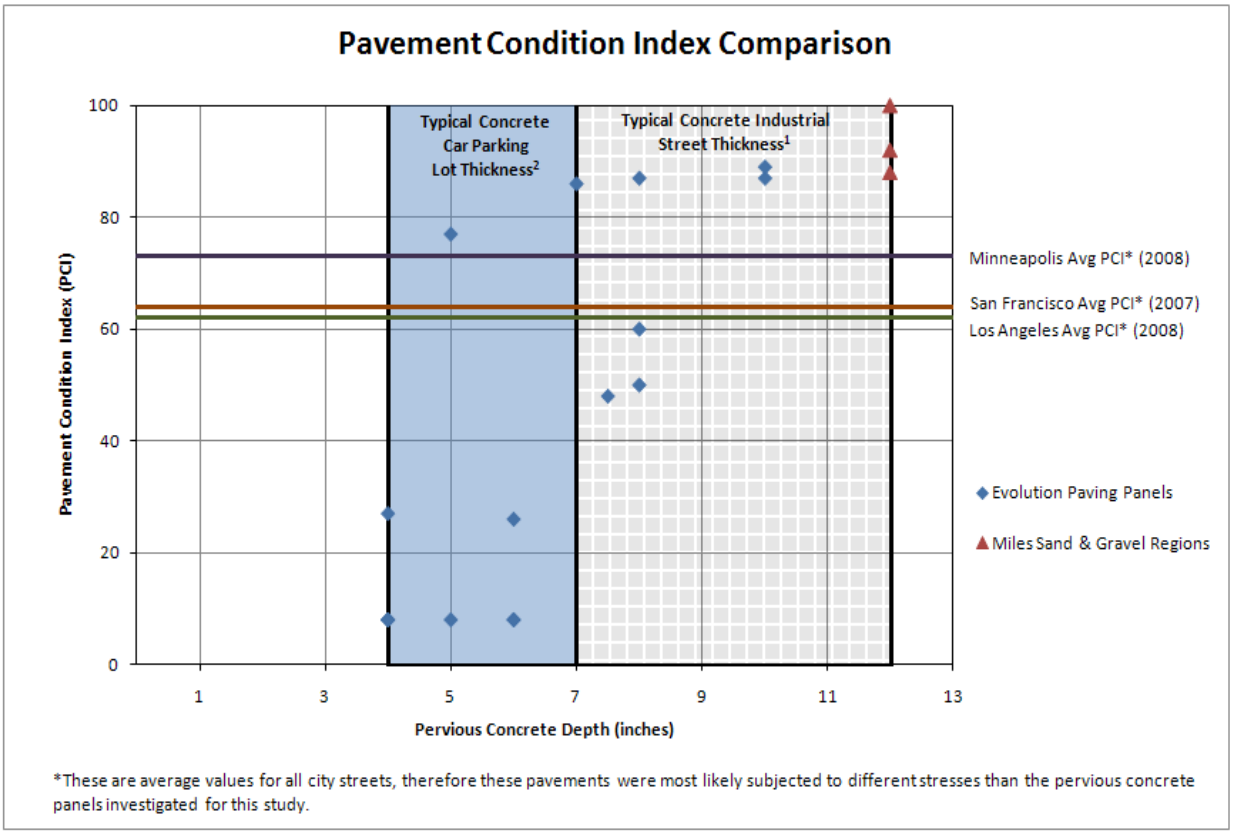

Figure 4.9: Pavement Condition Index (PCI) Comparison

As discussed in Section 2.1.3, the pervious concrete panels at Evolution Paving and at Miles Sand & Gravel were exposed to an equivalent amount of stress as a "Collector" street in use for between approximately 8 and 80 years. The high PCI ratings of the thicker pervious concrete sections indicate that pervious concrete, when properly designed, is capable of being used for many "Collector" streets and most "Residential" streets for typical design life durations (20-30 years) while exhibiting satisfactory structural performance.

5. THICKNESS DESIGN METHOD EVALUATION

This section completes Objective 2, from Section 1.3 of this thesis. There are currently no accepted thickness design methods for the design of pervious concrete pavements. For this reason, thickness design methods used for traditional concretes were evaluated for their applicability to the design of pervious concrete. The most commonly used thickness design methods for traditional concrete are the AASHTO (1993) design guide and the Portland Cement Association's (PCA) (1984) design procedure (ACI 325.12R, 2002). A survey conducted in 1994 and 1995 by Jiang et al. (1996) reported that approximately 84% of state highway agencies use either the 1972 or the 1986/1993 AASHTO design guide, 4% use the PCA design procedure, and the remaining 12% use their own design procedures.

The purpose of this section is to evaluate these two thickness design methods for their applicability to pervious concrete design. Evolution Paving personnel performed regular inspections of the pervious concrete panels and dates were recorded when cracking was first observed in some of the panels. These dates could then be correlated to the number of truck loads using truck manifests. The number of concrete truck loads to first cracking for these panels (shown in Table 5.1) was used to assess the accuracy of the two thickness design methods. The number of loads to first cracking was only recorded for panels in the egress lane (subject to full concrete trucks) at Evolution Paving.

Table 5.1: Number of Full Concrete Truck Loads to First Cracking for Pervious Concrete Panels at Evolution Paving

Number of Concrete Truck Loads to 1st Cracking for Pervious Concrete Panels at			
Panel #	Depth (in)	Loaded Trucks?	Number of Loads to 1st Cracking (N_{1c})
2	10	yes	65,000
4	7	yes	50,780
6	5	yes	27,000
8	5	yes	10,000
12	4	yes	375
14	6	yes	12,500
16	8	yes	13,990

5.1 THICKNESS DESIGN METHOD PROCEDURE

5.1.1 AASHTO (1993) THICKNESS DESIGN METHOD

The American Association of State Highway and Transportation Officials (AASHTO) developed thickness design methods for both flexible (asphalt) and rigid (concrete) pavements based on the results of the AASHO (American Association of State Highway Officials – AASTHO's former name) Road Test. The AASHO Road Test involved subjecting both asphalt and concrete pavements to specified loading conditions and observing their performance. To complete this test, six pavement loops were constructed in Ottawa, Illinois, each having both asphalt and concrete sections of various thicknesses. The loops were then subjected to 1,114,000 axle loads of different magnitudes and configuration between October 15, 195-8 and November 30, 1960. The results of this $27,000,000 test were then used to derive empirically based thickness design formulas (Huang, 2004).

Since the first AASHTO design guide was published in 1961, it has undergone multiple revisions in order to accommodate other regions in the United States. The most current revision of the AASHTO design guide was published in 1993 and is widely used by state highway agencies today (Huang, 2004). The final design equation for rigid (concrete) pavements as presented in AASHTO (1993) is shown as Equation 5.1.

$$\log(W_{18}) = Z_R \cdot S_o + 7.35\log(D+1) - 0.06 + \frac{\log\left(\frac{\Delta PSI}{4.5-1.5}\right)}{1+\frac{1.624\cdot 10^7}{(D+1)^{8.46}}} + (4.22-0.32p_t)\cdot\log\left[\frac{MOR\cdot C_d\cdot\left(D^{0.75}-1.132\right)}{215.63J\cdot\left[D^{0.75}-\frac{18.42}{\left(\frac{E}{k}\right)^{0.25}}\right]}\right] \quad (5.1)$$

Since Equation 5.1 was developed based on test results for traditional Portland Cement Concrete, further investigation was required to evaluate its applicability to pervious concrete. To evaluate its applicability to pervious concrete, Equation 5.1 was used to determine the slab thickness of each pervious concrete panel at Evolution Paving. The actual loading conditions and material characteristics for each panel at Evolution Paving were used as input values. The slab thickness calculated using Equation 5.1

was then compared to the actual slab thickness used at Evolution Paving to assess the accuracy of using this method for the design of pervious concrete pavements.

In Equation 5.1, W_{18} is the number of equivalent 18 kip single axle load applications (ESALs). As discussed in Section 2.1.3 of this thesis, one full concrete truck at Evolution Paving is equal to approximately 2.1 ESALs. The value used for W_{18} in this research was the number of full concrete truck loads to first cracking recorded for each panel multiplied by 2.1 to convert to ESALs. This means the design life of the pervious concrete panels is assumed to end when first cracking occurs.

Z_R is the standard normal deviate for a given reliability. AASHTO (1986) recommends levels of reliability based on the functional classification of the street, shown in Table 5.2. For this research a reliability of 85% was used. The standard normal deviate corresponding to a reliability of 90% is -1.037 (Huang, 2004 Table 11.15). S_o is the standard deviation, and was assumed to be 0.39 as recommended by Huang (2004) for rigid pavements.

Table 5.2: AASHTO (1986) Recommended Level of Reliability Based on Roadway Functional Classification

Functional Classification	Recommended Level of Reliability	
	Urban Streets	Rural Streets
Interstate and other freeways	85-99.9	80-99.9
Principal arterials	80-99	75-95
Collectors	80-95	75-95
Local	50-80	50-80

D is the slab thickness in inches, and is the desired output from Equation 5.1. It is important to note that since Equation 5.1 was empirically derived, the units of the variables in this equation are not consistent. Special care should be taken to ensure that the input value has the correct units, as required by AASHTO (1993).

Equation 5.1 incorporates the present serviceability index (PSI) into the design of rigid pavements. The PSI is a subjective measure of pavement condition developed by having a panel of raters ride in a vehicle driving on the pavements constructed for the AASHO Road test. The panel personnel then assign a rating to the level of service provided by each pavement. An equation was later developed

to calculate the PSI in a more objective manner. However, the equation is primarily dependent on the slope variance (or roughness) which is difficult to calculate. The PSI ranges from 5, a 'perfect road', down to 0, an 'impossible road'. Approximately 50% of people agree that a roadway having a PSI rating of 2.5 is unacceptable (AASHTO, 1993).

The initial serviceability index is the serviceability index immediately after construction, and is typically taken to be equal to 4.5 for rigid pavements. The terminal serviceability index (p_t) is the serviceability index at the end of the pavements design life, suggested to be 2.5 or 3.0 for design of major highways, and 2.0 for highways with lesser traffic volumes (AASHTO, 1993). Since the design life of each pervious concrete panel at Evolution Paving was considered to be over when the first visible crack occurred, the highest recommended p_t value (3.0) was used since it was assumed that one crack is not enough to significantly increase roughness. ΔPSI is the change in serviceability index, and is equal to $(4.5 - p_t)$ in Equation 5.1, therefore 1.5 was used for ΔPSI.

The modulus of rupture (MOR) found from the Third-Point Loading Test was used for the thickness design calculations when it was available. The MOR test results for the Evolution Paving samples are shown in Table 3.2. Since the Third-Point Loading Test was unable to be performed on samples from every panel, the relationship between MOR and compressive strength (f'_c) developed using Evolution Paving samples and discussed in Section 3.3.1 (Equation 5.1) had to be used to calculate the MOR when no test results were available. In Equation 5.1, the MOR value must be in units of psi.

As discussed in Section 3.1.2.1, the modulus of elasticity (E) test was unable to be performed on any of the samples from Evolution Paving. However, as was done for the MOR, a relationship was developed in Section 3.3.2.2 between E and f'_c. The E value calculated using this relationship was used as an input into Equation 5.1, and had units of psi.

In order to determine the drainage coefficient (C_d), Table 2.4 in AASHTO (1993) can be referenced. The pervious concrete at Evolution Paving was assumed to be exposed to moisture levels approaching saturation between 5 and 25% of the time. Also, good quality drainage was assumed, meaning that the pervious concrete structure will not be exposed to water for more than one day. These

assumptions should be conservative as long as the hydrological design of the pervious concrete pavement is adequate. Based on these assumptions, C_d was set equal to 1.1.

Table 2.6 in AASHTO (1993) recommends a load transfer coefficient (J) of between 3.6 and 4.2 for jointed concretes with no load transfer devices. Since the pervious concrete panels at Evolution Paving did not have any load transfer devices, the average value (3.9) of the recommended range was used.

A geotechnical investigation of the soil under the pervious concrete panels at Evolution Paving was performed by Willamette Engineering and Earth Sciences in October of 2004. They performed dynamic cone penetration tests at six different locations under the panels. The resulting average penetration index (PI) was calculated for each location. The PI for the six locations was then averaged to find the average PI of the subgrade soil, which was 0.36 in. This value was then converted into a resilient modulus (M_r) value using the following relationship developed by Salgado & Yoon (2003):

$$M_r = -3279*PI + 114100 \quad (5.2)$$

Where the resilient modulus (M_r) has units of kPa, and the penetration index (PI) has units of mm/blow. Converting Salgado & Yoon's (2003) equation into US customary units yields:

$$M_r = -12080*PI + 16550 \quad (5.3)$$

Where M_r has units of psi, and the penetration index (PI) has units of in/blow. Salgado & Yoon (2003) do caution that this relationship should be used with caution because it was derived from a weak correlation. However, without performing another geotechnical investigation at Evolution Paving, this is the best estimate of the resilient modulus.

WSDOT reports typical elastic modulus values for crushed stone ranging from 20,000 to 40,000 psi (Muench et al.). For this research, the subbase elastic modulus was assumed to be 20,000 psi. The resilient modulus, the assumed subbase elastic modulus, and the subbase thickness were then used as input into Figure 3.3 in AASHTO (1993) to calculate the composite modulus of subgrade reaction. (This AASHTO (1993) Figure 3.3 is shown as Figure 5.1 in this thesis.) Despite varying subbase thicknesses, the composite modulus of subgrade reaction was calculated to be 600 pci for all panels. Figure 3.6 of

AASTHO (1993) was used to correct the composite modulus of subgrade reaction for the potential loss of subbase support assuming a loss of support (LS) factor of 2.5. (This AASTHO (1993) Figure 3.6 is shown as Figure 5.2 in this thesis). Table 2.7 of AASHTO (1993) recommends the loss of support (LS) factor for unbound granular subbase material to be between 1 and 3. The slightly conservative value of 2.5 was used because the water infiltrating through the pervious concrete and through the base material was assumed to increase the chance of loss of support. The corrected modulus of subgrade reaction (k) was calculated to be 28 pci for all panels.

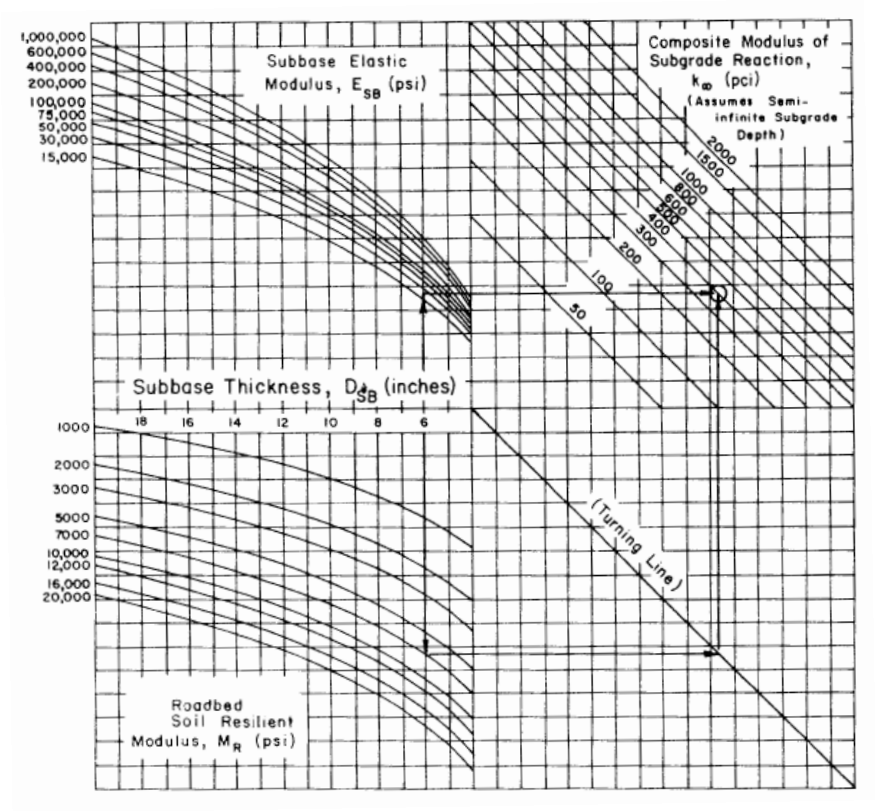

Figure 5.1: Chart for Estimating Composite Modulus of Subgrade Reaction (AASHTO, 1993 Figure 3.3)

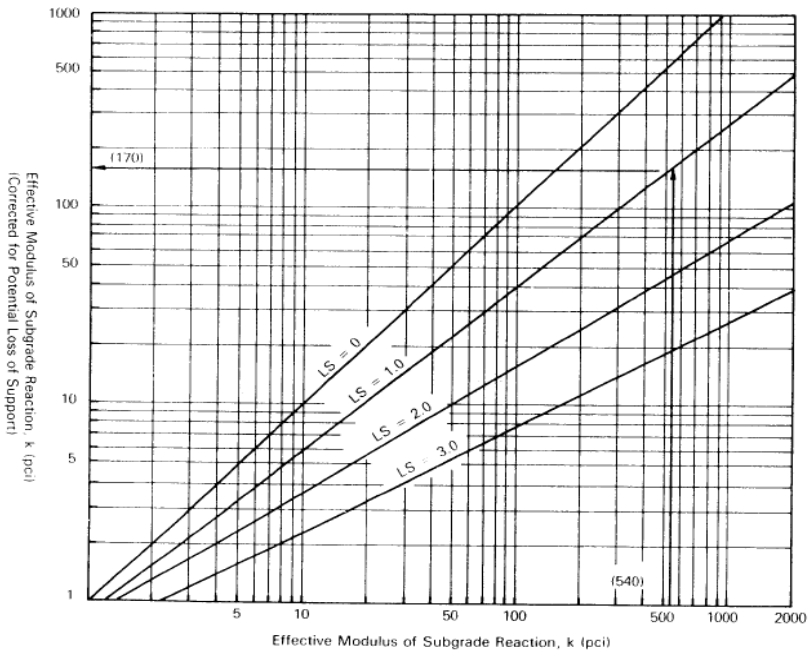

Figure 5.2: Correction of Effective Modulus of Subgrade Reaction for Potential Loss of Subbase Support (AASHTO, 1993 Figure 3.6)

5.1.2 PCA (1984) THICKNESS DESIGN METHOD

The Portland Cement Association (PCA) Method consists of both a fatigue analysis and an erosion analysis. The erosion analysis was not in the original 1966 method, but was added in the PCA (1984) thickness design procedure. The fatigue analysis is based on the edge stress produced by a load placed near the longitudinal joint of a pavement. The erosion analysis accounts for pumping, erosion of the foundation, and joint faulting. A computer program called JSLAB was used in the PCA method to calculate the pavement stresses and deflections, these results were then used to develop tables used in the PCA thickness design procedure (Huang, 2004).

Both a fatigue analysis and an erosion analysis were performed on the pervious concrete panels at Evolution Paving in order to calculate the required slab thickness using the PCA (1984) method. These calculated thicknesses were then compared to the actual slab thicknesses to assess the accuracy of this design method for use with pervious concrete. It was assumed that when the total percent fatigue, was equal to 100%, the first visible fatigue cracking would occur. Similarly, it was assumed that when the total percent erosion damage was equal to 100%, the first visible erosion cracking would occur. Because

of these assumptions, the recorded number of loads to first cracking could be used to calculate the required slab thickness.

Unlike the AASHTO (1993) design, for the PCA (1984) method, the loads produced by a full concrete truck are not converted into an equivalent number of 18 kip single axle loads (ESALs). Rather each axle load is considered individually. As was done for the AASHTO (1993) design, the tridem axle of the full concrete truck was assumed to support 45 kip, while the front axle and the back booster axle were both assumed to support 10 kip. The number of loads to first cracking was multiplied by a load magnification factor as recommended by PCA (1984). PCA (1984) recommends using a load safety factor of 1.2 for high volume of truck traffic (interstates), 1.1 for moderate volumes of truck traffic (highways), and 1.0 for low volumes of truck traffic (residential). For this research a load safety factor of 1.1 was used.

Similarly to the AASHTO (1993) design, the penetration index reported in the geotechnical report performed by Willamette Engineering and Earth Sciences was converted into an equivalent resilient modulus (M_r) using the relationship developed by Salgado & Yoon (2003) (Reference Equation 5.3). In order to convert the M_r into an equivalent modulus of subgrade reaction both Figures 7.10 and 7.36 in Huang's (2004) text were used. Figure 7.10 was used first to convert the M_r into an equivalent California Bearing Ratio (CBR), and then Figure 7.36 was used to convert the CBR into an equivalent modulus of subgrade reaction, which was 230 pci for all panels. Table 1 in PCA (1984) was used to account for the effect of subbase on the modulus of subgrade reaction, and is shown as Table 5.3 in this thesis. Since the subbase depth varied for different pervious concrete panels at Evolution Paving, the corrected modulus of subgrade reaction (k) also varied, ranging from approximately 250 to 320 pci. Corrected modulus of subgrade reaction values are reported for each panel in Appendix C of this thesis.

As was done for the AASHTO (1993) design, the MOR found from test results was used when available, and was calculated using Equation 3.10 when test results were not available.

Table 5.3: Effect of Untreated Subbase on Modulus of Subgrade Reaction (PCA, 1984 Table 1)

Subgrade *k* value, *pci*	Subbase *k* value, pci			
	4 in.	6 in.	9 in.	12 in.
50	65	75	85	110
100	130	140	160	190
200	220	230	270	320
300	320	330	370	430

5.1.2.1 Fatigue Analysis

For the fatigue analysis, equivalent stresses were found using Table 6a in PCA (1984) for single axles, and Table C1 in PCA (1984) for tridem axles (shown as Tables 5.4 & 5.5 in this thesis). Since the pervious concrete panels at Evolution Paving were not connected to concrete shoulders, the equivalent stresses for pavements without concrete shoulders were used. As shown in Tables 5.4 and 5.5, the equivalent stress is dependent on the corrected modulus of subgrade reaction (k), and the slab thickness (D). The equivalent stress values used for this analysis ranged from approximately 200 to 410 psi for single axles and 130 to 260 psi for tridem axles. The equivalent stress for individual panels can be found in Appendix C.

Table 5.4: Equivalent Stress for Single/Tandem Axle Loads (Without Concrete Shoulder) (PCA, 1984 Table 6a)

Slab thickness, in.	*k* of subgrade-subbase, pci						
	50	100	150	200	300	500	700
4	825/679	726/585	671/542	634/516	584/486	523/457	484/443
4.5	699/586	616/500	571/460	540/435	498/406	448/378	417/363
5	602/516	531/436	493/399	467/376	432/349	390/321	363/307
5.5	526/461	464/387	431/353	409/331	379/305	343/278	320/264
6	465/416	411/348	382/316	362/296	336/271	304/246	285/232
6.5	417/380	367/317	341/286	324/267	300/244	273/220	256/207
7	375/349	331/290	307/262	292/244	271/222	246/199	231/186
7.5	340/323	300/268	279/241	265/224	246/203	224/181	210/169
8	311/300	274/249	255/223	242/208	225/188	205/167	192/155
8.5	285/281	252/232	234/208	222/193	206/174	188/154	177/143
9	264/264	232/218	216/195	205/181	190/163	174/144	163/133
9.5	245/248	215/205	200/183	190/170	176/153	161/134	151/124
10	228/235	200/193	186/173	177/160	164/144	150/126	141/117
10.5	213/222	187/183	174/164	165/151	153/136	140/119	132/110
11	200/211	175/174	163/155	154/143	144/129	131/113	123/104
11.5	188/201	165/165	153/148	145/136	135/122	123/107	116/98
12	177/192	155/158	144/141	137/130	127/116	116/102	109/93
12.5	168/183	147/151	136/135	129/124	120/111	109/97	103/89
13	159/176	139/144	129/129	122/119	113/106	103/93	97/85
13.5	152/168	132/138	122/123	116/114	107/102	98/89	92/81
14	144/162	125/133	116/118	110/109	102/98	93/85	88/78

Table 5.5: Equivalent Stress for Tridem Axle Loads (Without/With Concrete Shoulder) (PCA, 1984 Table C1)

Slab thickness, in.	*k* of subgrade-subbase, pci						
	50	100	150	200	300	500	700
4	510/431	456/392	437/377	428/369	419/362	414/360	412/359
4.5	439/365	380/328	359/313	349/305	339/297	331/292	328/291
5	387/317	328/281	305/266	293/258	282/250	272/244	269/242
5.5	347/279	290/246	266/231	253/223	240/214	230/208	226/206
6	315/249	261/218	237/204	223/196	209/187	198/180	193/178
6.5	289/225	238/196	214/183	201/175	186/166	173/159	168/156
7	267/204	219/178	196/165	183/158	167/149	154/142	148/138
7.5	247/187	203/162	181/151	168/143	153/135	139/127	132/124
8	230/172	189/149	168/138	156/131	141/123	126/116	120/112
8.5	215/159	177/138	158/128	145/121	131/113	116/106	109/102
9	200/147	166/128	148/119	136/112	122/105	108/98	101/94
9.5	187/137	157/120	140/111	129/105	115/98	101/91	93/87
10	174/127	148/112	132/104	122/98	108/91	95/84	87/81
10.5	163/119	140/105	125/97	115/92	103/86	89/79	82/76
11	153/111	132/99	119/92	110/87	98/81	85/74	78/71
11.5	142/104	125/93	113/86	104/82	93/76	80/70	74/67
12	133/97	119/88	108/82	100/78	89/72	77/66	70/63
12.5	123/91	113/83	103/78	95/74	85/68	73/63	67/60
13	114/85	107/79	98/74	91/70	81/65	70/60	64/57
13.5	105/80	101/75	93/70	87/67	78/62	67/57	61/54
14	97/75	96/71	89/67	83/63	75/59	65/54	59/51

The stress ratio factor was then found by dividing the equivalent stress by the modulus of rupture. The stress ratio factor and the axle load could then be used as inputs into Figure 5 in PCA (1984) (shown as Figure 5.3 in this thesis) to calculate the allowable number of load repetitions. To find the allowable load repetitions for tridem axles, the scale for single axles in Figure 5.3 was used, and the tridem axle load was divided by 3 (Haung, 2004). The allowable load repetitions ranged from 900 to 160,000 for single axle loads, and 3200 to 1,000,000 for tridem axles. Allowable load repetitions are reported for individual panels in Appendix C.

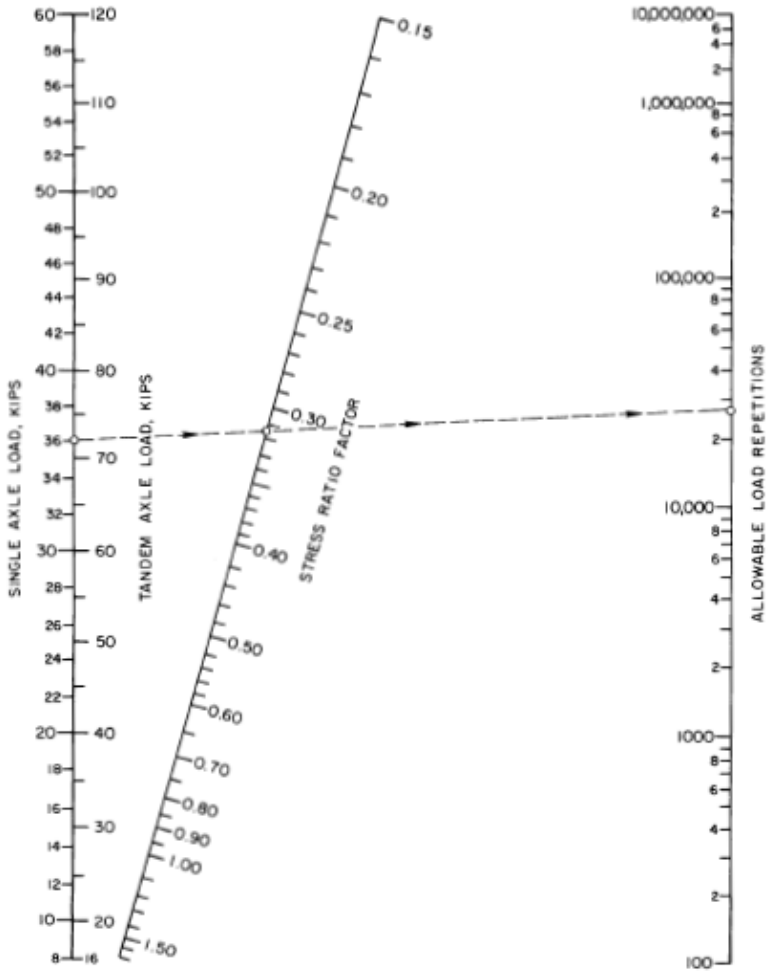

Figure 5.3: Fatigue Analysis - Allowable Load Repetitions Based on Stress Ratio Factor (PCA, 1984 Figure 5)

Once the allowable load repetitions were calculated for both single and tridem axles, the total percent fatigue was calculated by dividing the actual load repetitions by the allowable repetitions for both single and tridem axles, and summing these values. The actual load repetitions used to calculate the percent fatigue was the observed number of loads to first cracking as reported by Evolution Paving. Since it was assumed that the first visible fatigue cracking would occur when the total percent fatigue was equal to 100%, design slab thicknesses were iteratively calculated to result in a total percent fatigue equal to approximately 100% using Tables 5.4 and 5.5 as well as Figure 5.3.

In order to develop the equivalent stress tables used for the fatigue analysis (Tables 5.4 & 5.5), the PCA (1984) method uses the fatigue relationship shown in Figure 5.4. According to the PCA curve

shown in Figure 5.4, if a load is applied to a concrete specimen that creates a maximum tensile stress that is 80% of the modulus of rupture (Stress Ratio = 0.8), it must be applied approximately100 times to cause the concrete specimen to fail. Or, if a load is applied to a concrete specimen that creates a maximum tensile stress that is 60% of the modulus of rupture (Stress Ratio = 0.6), it must be applied approximately 30,000 times to cause the concrete specimen to fail. PCA (1984) states that this fatigue relationship is based conservatively on the fatigue research of others.

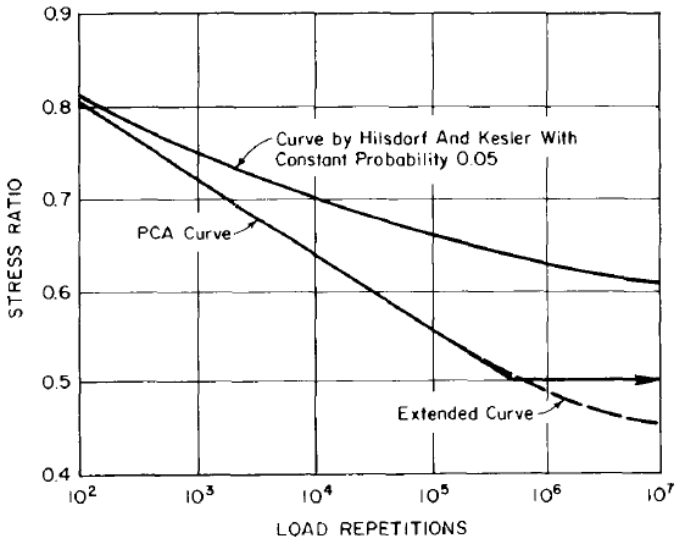

Figure 5.4: Fatigue Relationship for Concrete Used for the PCA (1984) Fatigue Analysis (PCA, 1984 Figure A.3)

This fatigue relationship is for regular concrete, and the question of whether it can apply to pervious concrete must be answered. Pindado et al. (1999) experimentally created a fatigue relationship for four different mixes of pervious concrete, shown in Figure 5.5. The four mixes had different design parameters, and mixes 2 and 3 contained a polymer additive. All four of the pervious concrete mixes showed better fatigue performance than the conservative results used by PCA (1984). For the pervious concrete mixes without the polymer additive (mixes 1 and 4), a load that creates a stress ratio of 0.8 must be applied approximately 300 times to fail the specimen; approximately 3 times the number of load repetitions taken to fail a concrete specimen subjected to the same stress ratio according to the PCA curve (Figure 5.4). For a stress ratio of 0.6, 2 million load repetitions will cause failure for the pervious

concrete (Pindado et al., 1999), while only 30,000 load repetitions will cause failure for the traditional concrete (PCA, 1984). Since the fatigue relationship developed for pervious concrete by Pindado et al. (1999) showed better fatigue performance than the fatigue relationship for regular concrete used in the PCA (1984) method, the PCA (1984) fatigue analysis should be applicable for use with pervious concrete pavements.

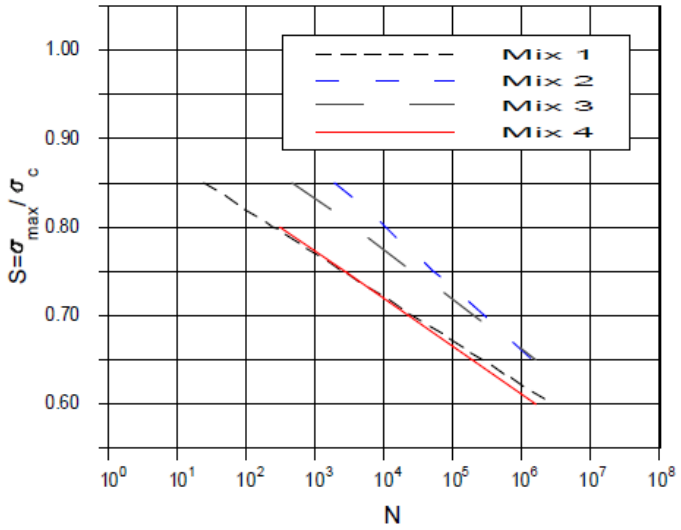

Figure 5.5: Fatigue Relationship Developed for Pervious Concrete (Pindado et al., 1999 Figure 4)

5.1.2.2 Erosion Analysis

An erosion analysis was also performed using the PCA (1984) method. Table 5.6 was used to find the erosion factor for single axle loads, and Table 5.7 was used to find the erosion factors for tridem axle loads. The erosion factors found ranged from approximately 3.8 to 3.9 psi for singles axles, and were approximately equal to 3.8 psi for tridem axles. Individual panel erosion factors can be found in Appendix C.

Table 5.6: Erosion Factors for Single/Tandem Axle Loads (Without Dowelled Joints or Concrete Shoulder) (PCA, 1984 Table 7b)

Slab thickness, in.	*k* of subgrade-subbase, pci					
	50	100	200	300	500	700
4	3.94/4.03	3.91/3.95	3.88/3.89	3.86/3.86	3.82/3.83	3.77/3.80
4.5	3.79/3.91	3.76/3.82	3.73/3.75	3.71/3.72	3.68/3.68	3.64/3.65
5	3.66/3.81	3.63/3.72	3.60/3.64	3.58/3.60	3.55/3.55	3.52/3.52
5.5	3.54/3.72	3.51/3.62	3.48/3.53	3.46/3.49	3.43/3.44	3.41/3.40
6	3.44/3.64	3.40/3.53	3.37/3.44	3.35/3.40	3.32/3.34	3.30/3.30
6.5	3.34/3.56	3.30/3.46	3.26/3.36	3.25/3.31	3.22/3.25	3.20/3.21
7	3.26/3.49	3.21/3.39	3.17/3.29	3.15/3.24	3.13/3.17	3.11/3.13
7.5	3.18/3.43	3.13/3.32	3.09/3.22	3.07/3.17	3.04/3.10	3.02/3.06
8	3.11/3.37	3.05/3.26	3.01/3.16	2.99/3.10	2.96/3.03	2.94/2.99
8.5	3.04/3.32	2.98/3.21	2.93/3.10	2.91/3.04	2.88/2.97	2.87/2.93
9	2.98/3.27	2.91/3.16	2.86/3.05	2.84/2.99	2.81/2.92	2.79/2.87
9.5	2.92/3.22	2.85/3.11	2.80/3.00	2.77/2.94	2.75/2.86	2.73/2.81
10	2.86/3.18	2.79/3.06	2.74/2.95	2.71/2.89	2.68/2.81	2.66/2.76
10.5	2.81/3.14	2.74/3.02	2.68/2.91	2.65/2.84	2.62/2.76	2.60/2.72
11	2.77/3.10	2.69/2.98	2.63/2.86	2.60/2.80	2.57/2.72	2.54/2.67
11.5	2.72/3.06	2.64/2.94	2.58/2.82	2.55/2.76	2.51/2.68	2.49/2.63
12	2.68/3.03	2.60/2.90	2.53/2.78	2.50/2.72	2.46/2.64	2.44/2.59
12.5	2.64/2.99	2.55/2.87	2.48/2.75	2.45/2.68	2.41/2.60	2.39/2.55
13	2.60/2.96	2.51/2.83	2.44/2.71	2.40/2.65	2.36/2.56	2.34/2.51
13.5	2.56/2.93	2.47/2.80	2.40/2.68	2.36/2.61	2.32/2.53	2.30/2.48
14	2.53/2.90	2.44/2.77	2.36/2.65	2.32/2.58	2.28/2.50	2.25/2.44

Table 5.7: Erosion Factors for Tridem Axle Loads (Without Dowelled Joints, With/Without Concrete Shoulder) (PCA, 1984 Table C3)

Slab thickness, in.	*k* of subgrade-subbase, pci					
	50	100	200	300	500	700
4	4.06/3.50	3.97/3.38	3.88/3.30	3.82/3.25	3.74/3.21	3.67/3.16
4.5	3.95/3.40	3.85/3.28	3.76/3.18	3.70/3.13	3.63/3.08	3.56/3.04
5	3.85/3.32	3.75/3.19	3.66/3.08	3.60/3.03	3.52/2.97	3.46/2.93
5.5	3.76/3.26	3.66/3.11	3.56/3.00	3.51/2.94	3.43/2.87	3.37/2.83
6	3.68/3.20	3.58/3.05	3.48/2.92	3.42/2.86	3.35/2.79	3.29/2.74
6.5	3.61/3.14	3.50/2.99	3.40/2.86	3.34/2.79	3.27/2.72	3.21/2.67
7	3.54/3.09	3.43/2.94	3.33/2.80	3.27/2.73	3.20/2.65	3.14/2.60
7.5	3.48/3.05	3.37/2.89	3.26/2.75	3.20/2.67	3.13/2.59	3.08/2.54
8	3.42/3.01	3.31/2.84	3.20/2.70	3.14/2.62	3.07/2.54	3.01/2.48
8.5	3.37/2.97	3.25/2.80	3.15/2.65	3.09/2.58	3.01/2.49	2.96/2.43
9	3.32/2.94	3.20/2.77	3.09/2.61	3.03/2.53	2.95/2.44	2.90/2.38
9.5	3.27/2.91	3.15/2.73	3.04/2.58	2.98/2.49	2.90/2.40	2.85/2.34
10	3.22/2.88	3.11/2.70	3.00/2.54	2.93/2.46	2.85/2.36	2.80/2.29
10.5	3.18/2.85	3.06/2.67	2.95/2.51	2.89/2.42	2.81/2.32	2.76/2.26
11	3.14/2.83	3.02/2.65	2.91/2.48	2.84/2.39	2.77/2.29	2.71/2.22
11.5	3.10/2.80	2.98/2.62	2.87/2.45	2.80/2.36	2.72/2.26	2.67/2.19
12	3.07/2.78	2.95/2.59	2.83/2.43	2.76/2.33	2.68/2.23	2.63/2.16
12.5	3.03/2.76	2.91/2.57	2.79/2.40	2.73/2.31	2.65/2.20	2.59/2.13
13	3.00/2.74	2.88/2.55	2.76/2.38	2.69/2.28	2.61/2.17	2.56/2.10
13.5	2.97/2.72	2.84/2.53	2.73/2.35	2.66/2.26	2.58/2.15	2.52/2.07
14	2.94/2.70	2.81/2.51	2.69/2.33	2.63/2.24	2.54/2.12	2.49/2.05

Then the erosion factors and axle loads for both single and tridem axles were both used as input into Figure 5.6 to determine the number of allowable load repetitions. The number of allowable loads ranged from 450,000 to 650,000 for single axles, and 60,000 to 80,000 for tridem axles (Individual panel values can be found in Appendix C).

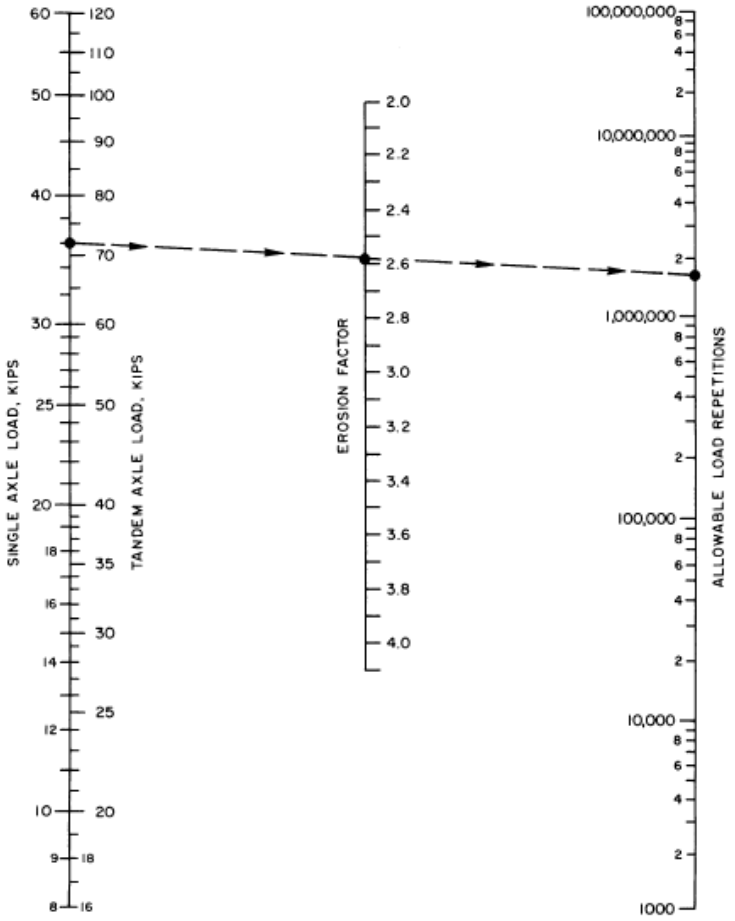

Figure 5.6: Erosion Analysis - Allowable Load Repetitions Based on Erosion Factor (Without Concrete Shoulder) (PCA, 1984 Figure 6a)

The observed load repetitions to first cracking for the pervious concrete panels at Evolution Paving were then divided by the number of allowable load repetitions to calculate the percent erosion damage. The total percent erosion damage was calculated by summing the percent erosion damage for the single and tridem axles. Similarly to the fatigue analysis, a slab thickness was iteratively chosen that would make the total percent erosion damage approximately equal to 100 percent. However, the total percent erosion damage could not always equal 100% because for some panels the required slab thickness

was less than the minimum slab thickness shown in Tables 5.6 and 5.7 (4 in.). When this occurred, the minimum slab thickness of 4 in. was used.

The larger of the two slab thicknesses calculated using the fatigue analysis and the erosion analysis controls the pavements design. The fatigue analysis controlled the design of all pervious concrete panels at Evolution Paving. The slab thicknesses calculated for the fatigue analysis ranged from approximately 5 to 9 in., while thicknesses calculated for the erosion analysis only ranged from 4 to 4.2 in. Individual slab thicknesses for both the fatigue and erosion analysis can be found in Appendix C. The controlling thicknesses calculated for the fatigue analysis are reported in Table 5.8.

5.2 THICKNESS DESIGN METHOD RESULTS

The results of the thickness design calculations using both the AASHTO (1993) and the PCA (1984) methods are shown in Table 5.8. These results are discussed in Section 6.3 of this thesis. Also in Table 5.8, the actual pervious concrete panel thicknesses used at Evolution Paving are shown for comparison. The recorded number of loads to first cracking and the modulus of rupture measured for each panel are also shown so that correlations between slab thickness and these variables may be discussed. The actual and predicted pavement depths are shown in Figure 5.7 to allow for comparison.

Table 5.8: Thickness Design Method Evaluation Results for Pervious Concrete Panels at Evolution Paving

Thickness Design Method Evaluation					
Panel #	Number of Loads to 1st Cracking (N_{1c})	Modulus of Rupture (psi)	Actual Panel Thickness (in)	Thickness calculated using AASHTO (1993) (in)	Thickness calculated using PCA (1984) (in)
2	65,000	224*	10	9.8	8.8
4	50,780	284	7	8.4	7.2
6	27,000	206	5	8.9	8.7
8	10,000	275	5	6.4	6.7
12	375	277*	4	3.6	5.8
14	12,500	344*	6	6.0	5.8
16	13,990	407	8	5.5	5.3

* Since the flexural test was unable to be performed on any samples from this panel, relationship between MOR and f'_c developed from experiemental results was used to calculate MOR

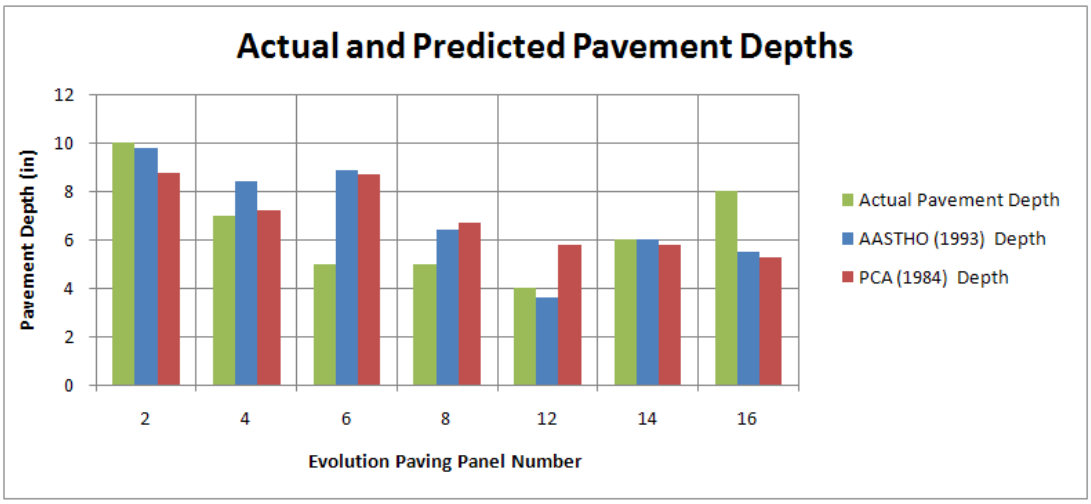

Figure 5.7: Comparison of Actual Pavement Depth at Evolution Paving with Pavement Depths Calculated with AASTHO (1993) and PCA (1984) design methods

5.3 Discussion of Thickness Design Method Results

This section completes Objective 2b and 2c as stated in Section 1.3 of this thesis, and discusses the results shown in Table 5.8. The goal of a pavement thickness design method is to design a pavement that is thick enough to stand up to the expected stresses without being excessively thick because this will increase the cost of the pavement. Both the AASHTO (1993) and the PCA (1984) thickness design methods will be evaluated to see how effective they are in meeting this goal.

5.3.1 Pervious Concrete Results

Figures 5.8 and 5.9 show both the AASTHO (1993) and PCA (1984) predicted pavement thickness versus actual thickness for the pervious concrete panels at Evolution Paving. The diagonal line in each figure represents the ideal outcome, where the predicted thickness equals the actual thickness. Since both thickness design equations are non-linear equations, the standard error ratio was used to assess the goodness-of-fit of each model. For the AASTHO (1993) method S_E/S_y for the predicted versus actual thickness is equal to 0.92, indicating a very poor goodness-of-fit. For the PCA (1984) method S_E/S_y is 0.98, also indicating a very poor goodness-of-fit, even worse than that of the AASTHO (1993) method. This indicates that the AASTHO (1993) method may be more accurate for the thickness design of

pervious concrete than the PCA (1984) method, but neither method provides a good prediction of the actual thicknesses.

Figure 5.8 shows AASHTO (1993) thicknesses calculated using a reliability level of 85%. This means that the AASTHO (1993) method should over design the pavement thickness 85% of the time, or that it should only under design the pavement thickness 15% of the time. The AASTHO (1993) method actually under designs the thicknesses of three out of the seven panels analyzed. However, as shown in Figure 5.8, two of these under designed thicknesses are very close to the actual thickness, and only one is significantly thickness is significantly under designed. This means that the AASTHO (1993) method only significantly under designed the thickness of 1/7, or 14%, of the panels, almost exactly the expected percent of under designed thicknesses.

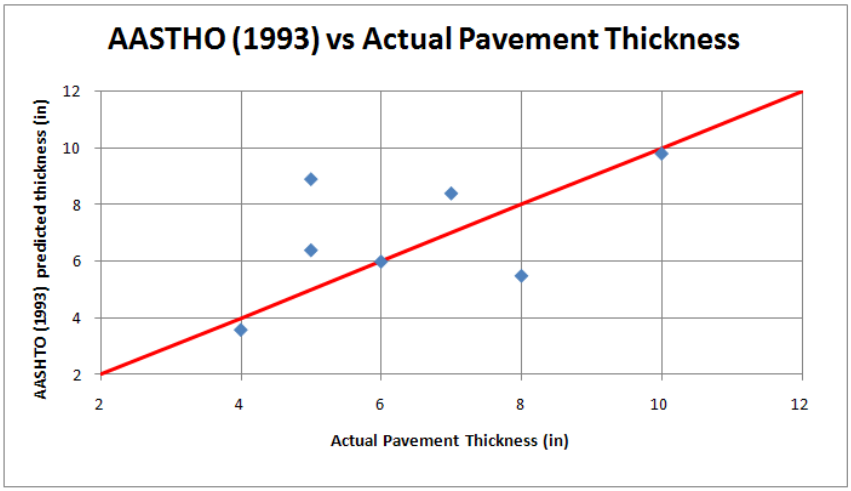

Figure 5.8: Predicted Pavement Thickness Based on AASHTO (1993) versus Actual Thickness for Pervious Concrete Panels at Evolution Paving

The PCA (1984) method does not directly use a level of reliability like the AASTHO (1993) method, but rather recommends the use of a load safety factor. Also, PCA (1984) uses some conservative assumptions in the development of their design tables. For the pervious concrete panels analyzed, the PCA (1984) method under designs the thicknesses of 3 of the 7 panels, but only under designs 2 of the thicknesses by a significant amount (See Figure 5.9). The weaker correlation of the PCA (1984) predicted thicknesses and the actual thicknesses, along with the significant underestimation of 2/7 (29%)

of the panels indicates that the AASTHO (1993) method may be preferred over the PCA (1984) method for the thickness design of pervious concrete pavements. However, future research should be done to confirm this conclusion.

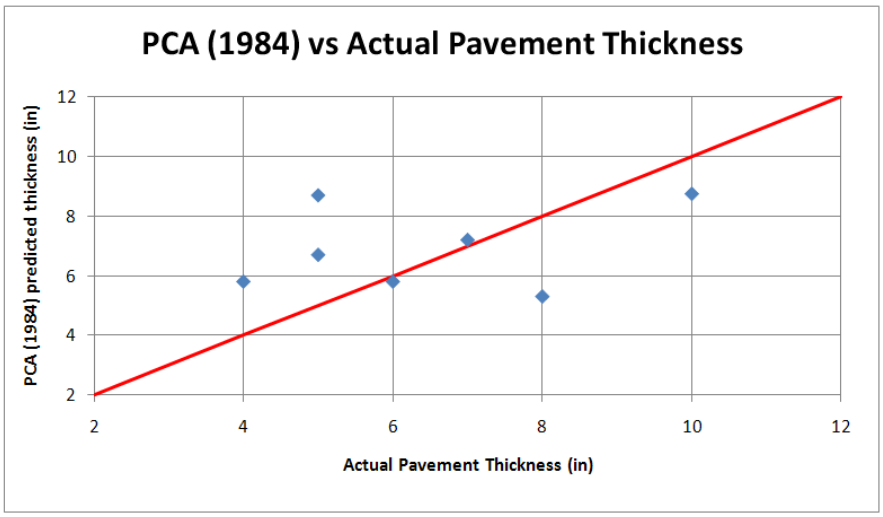

Figure 5.9: Predicted Pavement Thickness Based on PCA (1984) versus Actual Thickness for Pervious Concrete Panels at Evolution Paving

5.3.2 PERVIOUS CONCRETES RESULTS VS. REGULAR CONCRETES RESULTS

In order to better understand the variation in predicted thicknesses of each design method for pervious concrete, the variation in predicted thicknesses of these design methods for the design of traditional concrete must be discussed. Delatte et al., (2000) evaluated both the AASHTO (1993) and PCA (1984) methods for traditional concrete pavements. To do this, they used data from the Long Term Pavement Performance (LTPP) Program's database. The LTPP Program is a study of in-service pavements across North America established under the Strategic Highway Research Program and managed by the Federal Highway Administration (FHWA). Similarly to this research, Delatte et al., (2000) used the actual number of loads seen by ten different jointed plane concrete pavements (JPCP) to calculate the pavement thickness using the PCA (1984), AASTHO (1998), and AASTHO (1993) methods. The ten concrete pavements analyzed were located in Alabama, Florida, Georgia, North Carolina, and South Carolina. Delatte et al., (2000) used a reliability of 85% for the AASHTO (1993) thickness design, the same level of reliability that was used for this research. The calculated thicknesses

are shown in Table 5.9 as a ratio of the actual pavement thickness. In Table 5.9, minimum and maximum thickness values were calculated when the modulus of subgrade reaction (k_s) for a pavement was unknown and the AASHTO soil classification had to be used.

Table 5.9: Delatte et al. Concrete Comparison of Actual Pavement Thickness with PCA (1984), AASHTO (1998), and AASHTO (1993) Predicted Thicknesses (Delatte et al., 2000 Table 4-3)

	PCA		AASHTO 98		AASHTO 93	
Section	min	max	Min	max	min	max
AL 1-3028	0.85	0.85	0.96	0.96	0.97	0.97
FL 12-3811	0.84	0.95	1.22	1.32	0.96	1.02
FL 12-4057	0.47	0.51	0.88	0.98	0.59	0.65
FL 12-4138	0.81	0.88	1.26	1.30	1.16	1.20
GA 13-3016	0.64	0.78	1.06	1.16	0.86	0.91
GA 13-3017	0.95	1.20	0.98	1.12	1.00	1.05
GA 13-3018	0.90	1.05	1.13	1.25	1.04	1.09
NC 37-3011	0.90	1.10	0.70	1.48	0.83	1.14
NC 37-3044	0.83	1.00	1.46	1.73	1.29	1.35
SC 45-3012	0.65	0.75	1.16	1.44	0.97	1.08
Averages:	0.79	0.91	1.08	1.27	0.97	1.05
Standard Deviation:	0.14	0.19	0.20	0.22	0.18	0.18

Table 5.9 shows that in the Delatte et al. (2000) study, the thicknesses calculated using the PCA (1984) method ranged from approximately 50% to 120% of the actual concrete pavement thicknesses and had an average standard deviation of approximately 0.17. The thicknesses calculated using the AASTHO (1993) method ranged from approximately 60% to 135% of the actual concrete pavement thicknesses and had a standard deviation of 0.18. Using the Dellate et al. results, the average coefficients of variation of the PCA (1984) and the AASTHO (1993) were calculated to be 0.20 and 0.18, respectively. These results show that even for regular concrete, the accuracy of both thickness design methods is variable. Delatte et al. (2000) conclude that for JPCP the PCA (1984) method tends to under design the required pavement thickness, the AASHTO (1998) method tends to over design the required pavement thickness, and AASHTO (1993) appears to provide a good prediction of required pavement thickness. Table 5.9 shows the relatively high variability of thickness results produced by both the PCA (1984) method and the AASTHO (1993) method for the design of concrete pavements.

To allow comparison with the results presented in Table 5.9, Table 5.10 shows the pervious concrete thicknesses calculated for the panels at Evolution Paving as a ratio of the actual panel thickness.

Both thickness design methods tend to over design the required thickness of the pervious concrete. On average, AASHTO (1993) and PCA (1984) over designed the required pavement thickness by 12% and 15%, respectively. As shown in Tables 5.9 and 5.10, the standard deviations of the calculated to actual thickness ratios are greater for pervious concrete than for regular concrete for both methods. Also, the coefficients of variation are greater for pervious concrete. AASTHO (1993) thickness ratios had a coefficient of variation of 0.31 for pervious concrete and of 0.18 for regular concrete. Similarly, the PCA (1984) thickness ratios had a coefficient of variation of 0.32 for pervious concrete and 0.20 for regular concrete. The higher coefficients of variation for pervious concrete indicate that the accuracy of both thickness design methods is more variable for pervious concrete, than for regular concrete. However, if the thickness results of panel #6 at Evolution Paving are ignored, the coefficient of variation drops to 0.21 for the AASHTO (1993) method, and to 0.28 for the PCA (1984) method (values more comparable to those calculated for regular concrete). The outstanding performance of Panel #6 greatly increased the standard deviation for both methods. The high coefficient of variation could also have been caused by the small area of pervious concrete analyzed. To obtain more reliable results, the comparison of calculated and actual thicknesses should be performed on more samples, each made up of multiple individual panels.

Table 5.10: Pervious Concrete Comparison of Actual Thickness with PCA (1984) and AASHTO (1993) Predicted Thickness

Panel #	Actual Panel Thickness (in)	Thickness calculated using AASHTO (1993) (in)	AASHTO (1993) to Actual Ratio	Thickness calculated using PCA (1984) (in)	PCA (1984) to Actual Ratio
2	10	9.8	0.98	8.8	0.88
4	7	8.4	1.20	7.2	1.03
6	5	8.9	1.78	8.7	1.74
8	5	6.4	1.28	6.7	1.34
12	4	3.6	0.90	5.8	1.45
14	6	6.0	1.00	5.8	0.97
16	8	5.5	0.69	5.3	0.66
Average		-	1.12	-	1.15
Standard Deviation		-	0.35	-	0.37
Coefficient of Variation		-	0.31	-	0.32

So far, the results of this research have shown that the AASTHO (1993) design guide yields more accurate pervious concrete pavement predictions than the PCA (1984) thickness design method. To

further assess the accuracy of the AASTHO (1993) thickness design method, results were compared with the findings of Rauhut et al. (1994) in their report prepared for the Strategic Highway Research Program (SHRP). Using the 126 projects in the Long-Term Pavement Performance (LTPP) General Pavement Studies database, Rauhut et al. (1994) evaluated the accuracy of the AASTHO (1993) design guide for jointed plane concrete pavements (JPCP). Instead of using the actual number of loads applied to the pavement to calculate a thickness as has been done in this research, they used the actual thickness of the pavement to calculate allowable number of loads. The calculated allowable number of loads was then compared to the actual number of loads. The number of loads was measured in terms of KESALs, which are 1000 equivalent 18 kip single axle loads (ESALs). The results of their evaluation are shown in Figure 5.10. If the AASTHO (1993) equation was a perfect model, the predicted KESALs would always equal the actual KESALs, and the diagonal line in Figure 5.10 would be obtained. Figure 5.10 shows that the results produced by the AASHTO (1993) method are variable even for traditional concrete. Rauhut et al. (1994) used a reliability of 50% for their analysis, meaning that the AASTHO (1993) method should over design the number of KESALs 50% of the time, or that 50% of the data should be expected to fall on each side of the diagonal line.

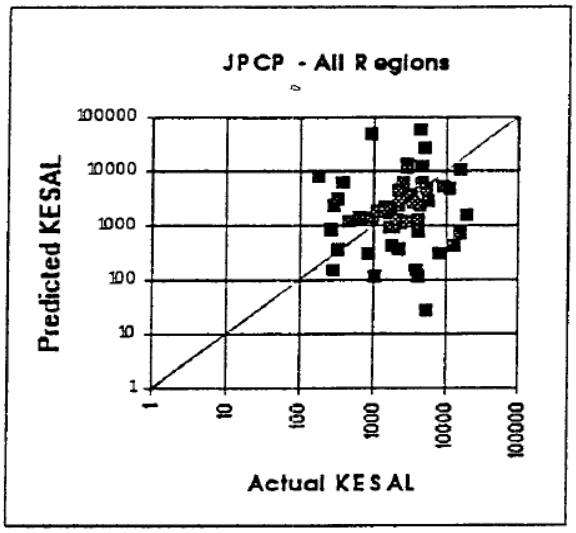

Figure 5.10: Rauhut et al. Results: AASHTO (1993) Predicted ESALs versus Actual ESALs for Concrete (50% Reliability) (Rauhut et al., 1994 Figure 2.11)

A similar graph is presented comparing the predicted KESALs calculated using the AASHTO (1993) design guide, to the actual KESALs the pervious concrete panels at Evolution Paving were subjected to (Figure 5.11). The predicted KESALs were calculated using a reliability of 50%, the same value used by Rauhut et al. (1994), to allow comparison of the accuracy of the AASHTO (1993) equation for pervious and regular concrete. Consistent with the reliability of 50%, AASTHO (1993) overe designed approximately half of the KESALs, shown in Figure 5.11 because approximately 50% of the data fell on each side of the diagonal line.

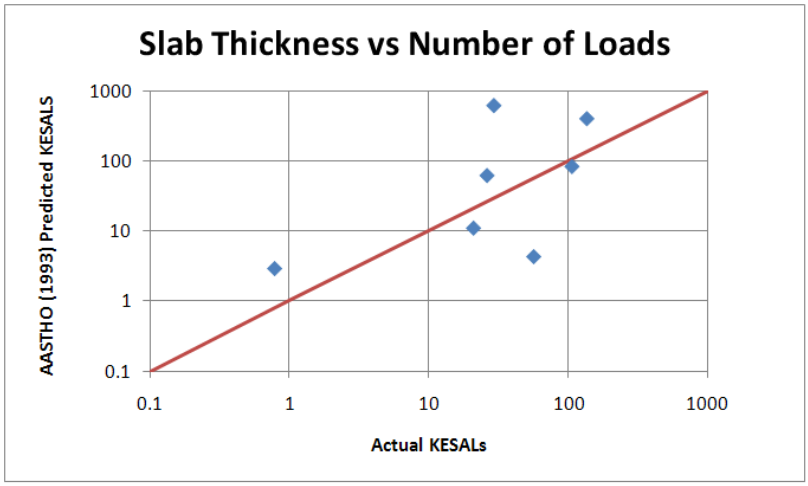

Figure 5.11: AASHTO (1993) Predicted ESALs versus Actual ESALs for Pervious Concrete at Evolution Paving (50% Reliability)

The difference in magnitude of KESALs is most likely due to the difference in depth and strength of the pavements analyzed, although this is not fully known because Rauhut et al. (1994) did not report these values for the pavement sections they analyzed. The scatter of both Figures 5.10 and 5.11 appears to be similar, however further statistical analysis may be required to develop any firm conclusions from Figures 5.10 and 5.11, and without access to the data used to create Figure 5.10, this is not possible.

5.3.3 Number of Loads to First Cracking Correlation to Design Variables

Both the AASTHO (1993) and PCA (1984) design methods use pavement thickness, modulus of rupture, and modulus of subgrade reaction as input values to calculate the desired number of load repetitions. In this research, the desired number of loads was set equal to the observed number of loads to

first cracking at Evolution Paving, and this was used to back-calculate the pavement thickness. Even though the creation of a new thickness design method is outside the scope of this research, if a new thickness design method were to be developed for pervious concrete pavements the correlation between the number of allowable load repetitions and other design variables must be understood.

Figure 5.12 shows the observed number of loads to first cracking compared with the pavement thickness for the pervious concrete panels at Evolution Paving. A trend line was created to show the relationship between these variables. As shown in Figure 5.4, the logarithm of the number of load repetitions (N) appears to have an inverse linear relationship with the stress ratio between load repetitions of approximately 100 and 300,000 (This range contains the number of loads to first cracking for all panels at Evolution Paving). Based on this, and knowing that the stress ratio is the ratio of the applied stress (σ_{app}) to the modulus of rupture (MOR), Equation 5.4 is obtained, showing that the logarithm of the number of load repetitions is a function the σ_{app} divided by the MOR.

$$\log\left(N_f\right) = f\left(\frac{-\sigma_{app}}{MOR}\right) \tag{5.4}$$

From the principles of mechanics of materials, the applied bending stress is equal to the applied bending moment (M) divided by the elastic section modulus (S) (Beer et al., 2006 Equation 4.18). Where the elastic section modulus equals the width of the member (b) times the depth of the member (d) squared divided by six for members with a rectangular cross section (Beer et al., 2006 Equation 4.19). Combining these two relationships, the applied bending stress for a member of rectangular cross section is shown as Equation 5.5.

$$\sigma_{app} = \frac{6 \cdot M}{b \cdot d^2} \tag{5.5}$$

Combining Equations 5.4 and 5.5 yields Equation 5.6, which shows that the logarithm of the number of load repetitions (N) is a function of one divided by depth squared.

$$\log\left(N_f\right) = f\left(\frac{-6 \cdot M}{MOR \cdot b \cdot d^2}\right) \tag{5.6}$$

Equation 5.6 shows that the logarithm of N is a function of some number divided by depth squared. An equation relating the logarithm of observed load repetitions to first cracking at Evolution Paving to one divided by the actual pavement depth squared was created, and is shown as Equation 5.7. Equation 5.7 is shown in Figure 5.12 along with the observed number of loads to first cracking at Evolution Paving versus the actual pervious concrete panel depths.

$$\log(N_{1c}) = 5 - \frac{21.7}{D^2} \tag{5.7}$$

The standard error ratio (S_E/S_y) of Equation 5.7 is 0.62, indicating that this equation provides a fair prediction of the actual number of loads to first cracking. If a new thickness design method is developed for pervious concrete, it must depend heavily on the number of loads the pavement will be subjected to.

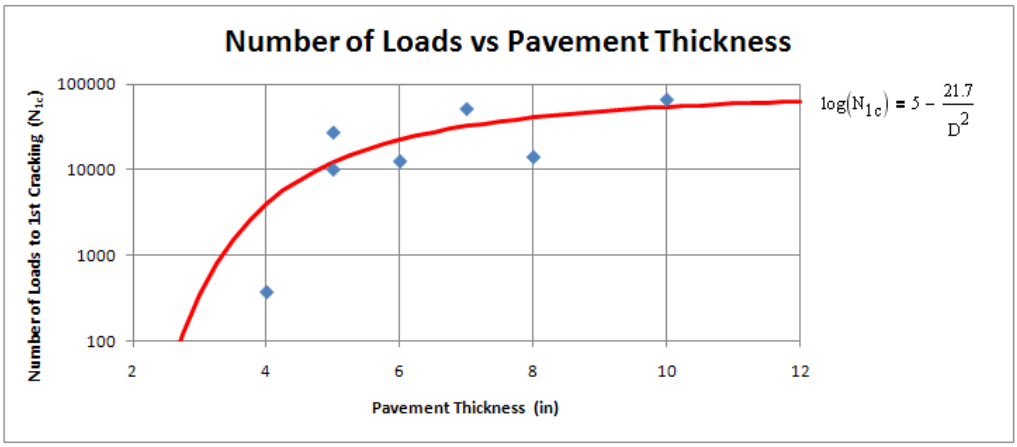

Figure 5.12: Number of Loads to 1st Cracking versus pavement thickness for Pervious Concrete Panels at Evolution Paving

Comparison of the standard error ratios (S_E/S_y) of Equation 5.7 ($S_E/S_y = 0.62$) with the results of the AASHTO (1993) ($S_E/S_y = 0.92$) and PCA (1984) ($S_E/S_y = 0.98$) design methods shows that Equation 5.7 provides a more accurate prediction of the actual performance of the pervious concrete at Evolution Paving than the other methods. This suggests that the required thickness for pervious concrete pavements may be able to be estimated using only the desired number of allowable load repetitions. However,

additional research is required to substantiate this claim since Equation 5.7 was developed using a relatively small population of data.

The allowable number of load repetitions is also dependent on the MOR in both the AASHTO (1993) and PCA (1984) design methods. According to Equation 5.6, the logarithm of the number of load repetitions (N) should be a function of some number divided by the MOR. Equation 5.8 was developed as the best fit for the observed number of load repetitions to first cracking and modulus of rupture for pervious concrete panels at Evolution Paving.

$$\log(N_{1C}) = 3.6 + \frac{208}{MOR} \tag{5.8}$$

Equation 5.8 not only has a very poor correlation to the data, but also produces results that are not logical. Increasing the MOR should not decrease the number of allowable load repetitions. This shows that the number of allowable loads is much more dependent on the pavement thickness than it is on the MOR of the pavement. The lack of correlation between slab thickness and MOR could also have been caused by the horizontal porosity distribution of the pervious concrete. The vertical porosity distribution of pervious concrete was discussed in Section 1.2.2 of this thesis, but porosity not only varies with depth, it also varies with horizontal location. As shown by Figure 3.9, the MOR is dependent on porosity and therefore the MOR must also vary with horizontal location. The MOR measured using the beam samples from Evolution Paving may not have been the same as the MOR at the location cracking occurred. Additional research should be done into the horizontal porosity distribution of pervious concrete and the effect this has on both strength, and thickness design. Also, the pervious concrete samples obtained from Evolution Paving could have been slightly damaged from the stresses created by concrete truck loads, causing the MOR test results to not be representative of the actual MOR of the rest of the pervious concrete panel.

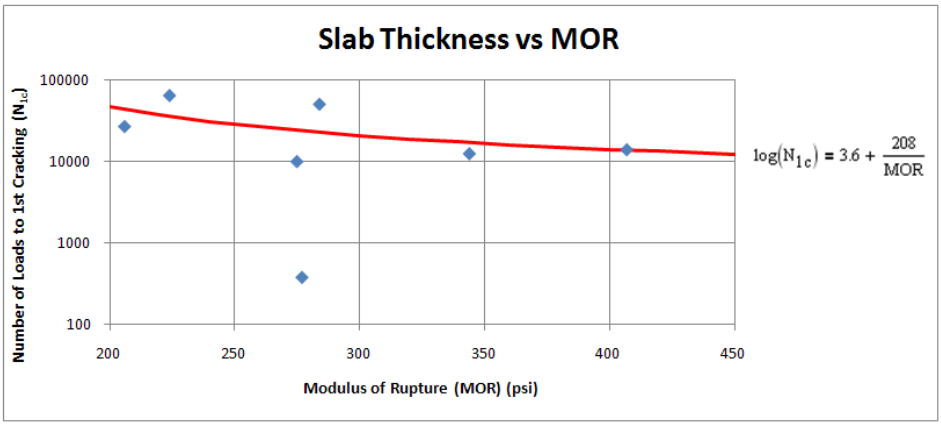

Figure 5.13: Number of Loads to 1st Cracking versus Modulus of Rupture for Pervious Concrete Panels at Evolution Paving

Even though the allowable number of load repetitions is also dependent on the modulus of subgrade reaction in both the AASHTO (1993) and PCA (1984) design methods, no correlations between these variables could be made because all the pervious concrete samples analyzed were at one location, and therefore were placed on the same type of soil. Future studies of the performance of pervious concrete pavements placed on different soil types should be done to establish this correlation.

6. CONCLUSIONS AND RECOMMENDED FUTURE RESEARCH

6.1 MATERIAL CHARACTERIZATION

The material characterization tests performed showed that pervious concrete strengths are typically more variable and slightly less than those of traditional concrete for similar mixes. However, it is possible to obtain both compressive and flexural strengths for pervious concrete that are as high as the strengths of traditional concrete. The Evolution Paving pervious concrete samples tested had compressive strengths ranging from 1600 to 5100 psi, while typical values for traditional concrete range from 3500 to 5000 psi. Similarly, pervious concrete flexural strengths ranged from 250 to 410 psi, compared to typical values for traditional concrete of 350 to 600 psi (Wang et al., 2007).

The increased variability of pervious concrete strength properties was attributed to the variability in porosities. There was a correlation between porosity and both flexural strength and compressive

strength. Equations were developed to represent the relationships between these variables (Equations 3.11 and 3.15).

The modulus of elasticity of traditional concrete can be calculated based on the unit weight and compressive strength (Equation 3.12). The modulus of rupture of the pervious concrete samples tested was found to have a relationship to unit weight and compressive strength (Equation 3.14) similar to that of traditional concrete.

Poisson's ratio was found to be similar but slightly more variable for pervious concrete than for traditional concrete. The average Poisson's ratio of the laboratory prepared samples tested was 0.22, while typical values for traditional concrete range from 0.15 to 0.2 (Huang, 2004).

6.2 STRUCTURAL PERFORMANCE INVESTIGATION

As can be seen in Figure 4.10, clearly thicker depths of pervious concrete showed better structural performance. While nearly all of the 4 to 7 in. depth panels received low PCI ratings (as expected since they were intentionally under designed), most of the 7 to 12 in. depth panels received PCI ratings well above the average PCI reported for streets in cities such as Minneapolis, San Francisco, and Los Angeles.

Both of the field sites visited were exposed to an equivalent amount of stress as a "Collector" street in use for between approximately 8 to 80 years. The high PCI ratings of the thicker pervious concrete sections indicate that pervious concrete, when properly designed, is capable of being used for many "Collector" streets and most "Residential" streets for typical design life durations (20-30 years) while exhibiting adequate structural performance. Even though the pervious concrete analyzed was subjected to an equivalent amount of stress from loading as a "Collector" street in use for between 8 and 80 years, it was only subject to weathering stresses during its actual life (approximately 6 years at Evolution Paving and 1.5 years at Miles Sand & Gravel). Additional research should be performed to study the long-term effects of weathering stresses on the structural performance of pervious concrete.

To support the findings of this paper, additional PCI calculations could be performed on field installations of pervious concrete that have been subjected to various levels of stress. Both the field

installations evaluated for this paper were subjected to stress equivalent to approximately 200,000 ESALs. Also, a testing environment with only one variable would allow a more reliable relationship to be developed between the variable of interest and the calculated PCI. The many unique mix design and placement parameters for each panel of pervious concrete make it difficult to distinguish the relationship of an individual parameter with the calculated PCI. Since the findings of this research indicate that depth has the greatest affect on PCI rating, a testing environment with identical mix design parameters and only varying depth is recommended to further analyze this conclusion.

6.3 THICKNESS DESIGN METHOD EVALUATION

The accuracy of the pervious concrete thicknesses calculated using both the AASTHO (1993) and PCA (1984) methods were variable. However, investigation into other research showed that the accuracy of these methods for use with traditional concrete is also quite variable. The variability in the thickness predictions of both methods does not mean these methods are not applicable for use with pervious concrete, but rather shows the difficulty and complexity of thickness design for any pavement material. Comparison between the accuracy of the thickness design methods for pervious concrete and regular concrete design, showed that the predicted thicknesses for pervious concrete were slightly less accurate than those for regular concrete.

The actual thicknesses had a higher correlation to the thicknesses predicted by the AASTHO (1993) method ($S_E/S_y = 0.92$) than those predicted with the PCA (1984) method ($S_E/S_y = 0.98$). The AASTHO (1993) method also proved to be more conservative than the PCA (1984) method. The AASTHO (1993) method only significantly under designed the thickness of 1 of the 7 panels analyzed, while the PCA (1984) significantly under designed the thickness of 2 of the 7 panels analyzed. Based on the results of this research, the AASTHO (1993) appears to be the preferred method for the design of pervious concrete pavements. However, since both models showed a very poor goodness-of-fit to actual thicknesses, additional research into alternative thickness design methods or the creation of a new thickness design method may be needed. It is recommended that additional research be done into the

applicability of the Mechanistic-Empirical Pavement Design Guide (MEPDG) for the design of pervious concrete pavements.

The better correlation between the number of allowable load repetitions and pavement thicknesses ($S_E/S_y = 0.62$) suggests that reasonable predictions of the required pervious concrete pavement thickness can be made using only the desired number of allowable load repetitions. The number of allowable load repetitions did not show a clear correlation to any of the other design variables investigated.

It is important to understand the limitations of this research. Since the pervious concrete studied was only subjected to an equivalent amount of stress as a "Collector" street, before the AASTHO (1993) method can be used for the design of streets subjected to higher stress levels (such as "Minor Arterials" or "Major Arterials") additional research must be done. Also, the pervious concrete samples from Evolution Paving ranged in measured porosity from 12 to 32%. The AASTHO (1993) method may not be applicable for pervious concrete with porosities outside of this range of porosities, and it is not recommended to use the AASTHO (1993) method for pervious concrete with porosities greater than 30% because porosities of this magnitude will greatly decrease strength.

To support the findings of this research, additional field installations of pervious concrete should be used to evaluate the predictions of the AASHTO (1993) and the PCA (1984) thickness design methods. The number of pervious concrete panels analyzed for this research is too small to produce firm conclusions. If a thickness design method specifically for pervious concrete is designed in the future, the method should make pavement thickness heavily dependent on the number of load repetitions, since these two variables were strongly correlated. Additional research should be done to better understand the horizontal porosity distribution of pervious concrete and the effect this has on strength and thickness design.

7. REFERENCES

AASHTO (1986). *AASHTO Guide for Design of Pavement Structures*, American Association of State Highway and Transportation Officials. Washington, D.C.

AASHTO (1993). *AASHTO Guide for Design of Pavement Structures*, American Association of State Highway and Transportation Officials. Washington, D.C.

ACI Committee 318 (2008). *ACI 318-08: Building code requirements for structural concrete*. American Concrete Institute.

ACI Committee 325 (2002). *ACI 325.12R-02: Guide for design of jointed concrete pavements for streets and local roads*. American Concrete Institute.

ACI Committee 330 (2008). *ACI 330R-08: Guide for design and construction of concrete parking lots*. American Concrete Institute.

ACI Committee 522 (2006). *ACI 522R-06: Pervious concrete*. American Concrete Institute.

ASTM Standard C39, (2005). "*Standard test method for compressive strength of cylindrical concrete specimens*," ASTM International, West Conshohocken, PA, 2005, DOI: 10.1520/C0039-05, www.astm.org.

ASTM Standard C78, (2002). "Standard test method for flexural strength of concrete (Using simple beam with third-point loading)," ASTM International, West Conshohocken, PA, 2002, DOI: 10.1520/C0078-02, www.astm.org.

ASTM Standard C131, (2006). "Standard Test Method for Resistance to Degradation of Small-Size Coarse Aggregate by Abrasion and Impact in the Los Angeles Machine," ASTM International, West Conshohocken, PA, 2006, DOI: 10.1520/C0131-06, www.astm.org.

ASTM Standard C469, 2002, "Standard test method for static modulus of elasticity and Poisson's ratio of concrete in compression," ASTM International, West Conshohocken, PA, 2002, DOI: 10.1520/C0469-02, www.astm.org.

ASTM Standard D6433, 2003, "Standard practice for roads and parking lots pavement condition index surveys," ASTM International, West Conshohocken, PA, 2003, DOI: 10.1520/D6433-03, www.astm.org.

ASTM Standard D6433, 2007, "Standard practice for roads and parking lots pavement condition index surveys," ASTM International, West Conshohocken, PA, 2003, DOI: 10.1520/D6433-07, www.astm.org.

Beer, F. P., Johnston, E. R., & DeWolf, J. T. (2006). *Mechanics of materials: 4th edition*. Boston, MA: McGraw-Hill.

City of Minneapolis, Minnesota (2009). Pavement Condition. Retrieved August 30, 2009, from Official Web Site of the City of Minneapolis, Minnesota Web site: http://www.ci.minneapolis.mn.us/results/pavement.asp

City of Salem Public Works Department, (2007). *Design Standards for Stormwater Management* Salem, OR: Retrieved from http://www.cityofsalem.net/Departments/PublicWorks/Engineering/Design%20Standards/ds_stormwater_management_2004.pdf

Crouch, L. K., Cates, M. A., Dotson, V. J., Honeycutt, K. R., & Badoe, D. (2003). Measuring the effective air void content of Portland cement pervious pavements. *Cement Concrete and Aggregates*, *25:1*, 16-20.

Crouch, L. K., Pitt, J., & Hewitt, R. (2007). Aggregate effects on pervious portland cement concrete static modulus of elasticity. *Journal of Materials in Civil Engineering , 19:7*, 561-567.

Delatte, N.J., Miller, D., & Mrkajic, A. (2007). Portland cement pervious concrete pavement: Field performance investigation on parking lot and roadway pavements. *RMC Research & Education Foundation*.

Delatte, N.J., Safarjalani, M., & Zinger, N.B. University Transportation Center for Alabama, (2000). *Concrete Pavement Performance in the Southeastern United States* (UTCA Report Number 99247). Birmingham, Alabama. Retrieved From http://utca.eng.ua.edu/projects/final_reports/99247report.pdf

Environmental Protection Agency (EPA), (2008). *Cool pavement product information: What kinds of cool paving products are currently available?* Retrieved from http://www.epa.gov/heatisld/images/extra/level3_pavingproducts.html

Erickson, S. (2007). Pervious Concrete Durability Testing. Retrieved from http://www.stoneycretenw.com/content/casestudy.asp?i=63

Federal Highway Adminstration (FHWA). (2003). *Distress identification manual for the long-term pavement performance program.* FHWA-RD-03-031.

Ghafoori, N., & Dutta, S. (1995). Pavement thickness design for no-fines concrete parking lots. *Journal of Transportation Engineering*, *121:6*, 476-484.

Haselbach, L. M., & Freeman, R. M. (2006). Vertical porosity distribution in pervious concrete pavement. *ACI Materials Journal*, 103(6), 452-458.

Haselbach, L. H., & Freeman R. M. (2007). Effectively estimating in situ porosity of pervious concrete from cores. *Journal of ASTM International*, 4(7).

Hendrickx, I. L. (1998). Noiseless concrete pavements. Retrieved from http://www.eupave.eu/documents/graphics/inventory-of-documents/febelcem-publicaties/noiseless-concrete-pavements.pdf

Huang, Y. H. (2004). *Pavement Analysis and Design: 2nd Edition*. Upper Saddle River, NJ: Pearson Prentice Hall.

Jiang, Y., Darter M. I., & Owusu-Antwi, E. (1996). "Analysis of current state rigid pavement design practices in the United States," Transportation Research Record 1525, pp. 72-82; Transportation Research Board

Kevern, John. Telephone Interview by Will Goede. 08 Jul 2009.

Local Streets & Roads Group of San Francisco Bay Area Partnership. (2007). *Saving our street: A strategic plan for maintaining the bay area's local streets and roads*. San Francisco, CA.

Marks, A. (2008).Pervious concrete pavement - How important is compressive strength?. *Journal of Green Building, 3(3),* 36-41.

McMillan, T. (2007). *Report: comparing traditional concrete to permeable concrete for a Community College pavement application*. Retrieved from http://www.eskimo.com/~tessmc/docs/Pervious_Report.pdf

Montes, F., Valavala, S., & Haselbach,, L. M. (2005). A new test method for porosity measurements of Portland cement pervious concrete. *Journal of ASTM International, 2:1,* 1-13.

Muench, S. T., Mahoney, J. P., & Pierce, L. M. Washington State Department of Transportation, (n.d.). *WSDOT pavement guide: design parameters - subgrade* Retrieved from http://training.ce.washington.edu/wsdot/modules/04_design_parameters/04-2_body.htm

Offenberg, M. (2009, January 1). Proving pervious concrete's durability: A proposed test method helps producers assess the surface durability of pervious pavement. *Concrete Producer Magazine,* Retrieved from http://www.theconcreteproducer.com/industry-news.asp?sectionID=1419&articleID=840824&artnum=1

Pindado, M. A., Aguado, A., & Josa, A. (1999). Fatigue behavior of polymer-modified porous concretes. *Cement and Concrete Research,* 29, 1077-1083.

Portland Cement Association (PCA), (1984) “Thickness design for concrete highway and stress pavements,” EB109.01P, Skokie, Ill.

Rauhut, J.B., Simpson, A.L., Daleiden, J.F., Darter, M.I., Owusu-Antwi, E., & Pendleton, O.J., National Research Council, Strategic Highway Research Program. (1994). *Early Analyses of Long-Term Pavement Performance General Pavement Studies Data* (SHRP-P-680). Washington, DC: National Academy of Sciences. Retrieved from http://onlinepubs.trb.org/onlinepubs/shrp/SHRP-P-680.pdf

Raymond, R. (2004). *Pavement performance considerations for heavy traffic loads*. City of Spokane, WA: Division of Public Works and Utilities.

Salgado, R., & Yoon, S. (2003). *Dynamic cone penetration test (DCPT) for subgrade assessment*. West Lafayette, IN: Purdue Libraries.

Stroup-Gardiner, M. (2008).State, municipal, county delegates get facts at California conference. *Pavement Preservation Journal, 2:1*, 22-25.

Tennis, P., Leming, M., & Akers, D. (2004). *Pervious Concrete Pavements*. Skokie, IL: Portland Cement Association.

Trejo, David, Folliard, Kevin, & Du, Lianxiang (2003). Alternative cap materials for evaluating the compressive strength of controlled low-strength materials. *Journal of Materials in Civil Engineering, 15:5*, 484-490.City of Ottawa Kansas. (2008). *2009 Transportation Master Plan*. Ottawa, KS.

Van Gemert, D., Beeldens, A., & Caestecker, C. (2003). Review on porous concrete in Europe. *Symposium on Design and Practical Method of Porous Concrete*. Tokyo, Japan.

Wang, C., Salmon, C., & Pincheira, J. (2007). *Reinforced Concrete Design*. Hoboken, NJ: John Wiley & Sons, Inc.

Wanielista, M., & Chopra, M. (2007). *Performance assessment of Portland Cement pervious pavements:Report 2 of 4: Construction and maintenance assessment of pervious concrete pavements*. Retrieved from http://www.stormwater.ucf.edu/research/Final%20Report%202%20of%204%20Construction%20and%20Maintenance%20Jan.pdf

Wanielista, M., & Chopra, M.(2007). *Performance assessment of Portland Cement pervious pavements: Report 4 of 4: Performance assessment of a pervious concrete pavement used as a shoulder for an interstate rest area parking lot*. Retrieved from http://www.dot.state.fl.us/research-center/Completed_Proj/Summary_RD/FDOT_BD521_02_rpt4.pdf

Witczak, M. W., Kaloush, K., Pellinen, T., El-Basyouny, M., & Von Quintus, H. (2002). NCHRP Report 465: *Simple performance test for superpave mix design*. Transportation Research Board.

Yang, J., & Jiang, G. (2003). Experimental study on properties of pervious concrete pavement materials. *Cement and Concrete Research, 33,* 381-386.

Yang, Z., Ma, W., Shen, W., & Zhou, M. (2008). The Aggregate Gradation for the Porous Concrete Pervious Road Base Material. *Journal of Wuhan University of Technology-Materials Science Edition, 23:3,* 391-394.

Zouaghi, A., Kumagai, M., & Nakazawa, T. (2000). Fundamental study on some properties of pervious concrete and its applicability to control stormwater run-off. *Transactions of the Japan Concrete Institute*, 22, 43-50.

8. NOTATION GUIDE

b	=	Width of Test Specimen	P_i	=	In-Situ Porosity
C_d	=	Drainage Coefficient	P_{min}	=	Minimum Porosity
CDV	=	Maximum Corrected Deduct Value	P_{max}	=	Maximum Porosity
CV	=	Coefficient of Variation	p_t	=	Terminal Serviceability Index
d	=	Depth of Test Specimen	PCI	=	Pavement Condition Index
D	=	Slab Thickness in Inches	PI	=	Penetration Index
D_c	=	Core Diameter	R^2	=	Coefficient of Determination
D_a	=	Maximum Aggregate Diameter	S_o	=	Standard Deviation
DV	=	Deduct Value	TDV	=	Total Deduct Value
E	=	Static Modulus of Elasticity	V_{sol}	=	Volume of Solids
ESAL	=	18 kip Equivalent Single Axle Load	V_T	=	Total Volume
F_{buo}	=	Buoyancy Force	V_{voids}	=	Volume of Voids
f'_c	=	Compressive Strength	W_{18}	=	Number of ESALs
J	=	Load Transfer Coefficient	w_c	=	Unit Weight of Concrete
k_c	=	Unknown Constant Value	w_{pc}	=	Unit Weight of Pervious Concrete
k	=	Corrected Modulus of Subgrade Reaction	Z_R	=	Standard Normal Deviate
L	=	Unsupported Span Length	ΔPSI	=	Change in Serviceability Index
M	=	Applied Bending Moment	ρ_w	=	Density of Water
M_{dry}	=	Dry Mass	σ_{app}	=	Applied Stress
M_{sub}	=	Submerged Mass			
M_r	=	Resilient Modulus			
MOR	=	Modulus of Rupture			
N_{1c}	=	Number of Loads to 1st Cracking			
N_f	=	Number of Allowable Load Repetitions			
P	=	Total Porosity			
P_c	=	Corrected Porosity			

9. APPENDICES

9.1 APPENDIX A – MATERIAL CHARACTERIZATION RESULTS

9.2 APPENDIX B – STRUCTURAL PERFORMANCE INVESTIGATION RESULTS

9.3 APPENDIX C – THICKNESS DESIGN CALCULATIONS

9.1 APPENDIX A – MATERIAL CHARACTERIZATION RESULTS

Flexure Test Results						
Sample ID	Avg Width (in)	Avg Depth (in)	Span Length (in)	Peak Load (lb)	Rate of Increase in Extreme Fiber Stress (psi/min)	Modulus of Rupture (psi)
EG11306R01	4.777	6.283	18	2721	256.6	259.8
EG10508C02	7.889	8.130	22.5	8364	160.3	360.9
EG10508C01	7.905	8.016	22.5	6688	149.9	296.3
EG20605C02	6.312	6.871	19.5	2356	113.6	154.2
EG20605C01	6.200	6.819	19.5	3814	139.5	258.0
EG11608R01	6.687	6.833	19.5	6511	200.0	406.7
EG20805R03	5.687	6.468	18	3373	141.9	255.2
EG20407C01	5.786	5.830	18	3101	180.0	283.8
EG20805R02	6.933	6.772	18	3315	110.3	187.7
EG20805R04	5.839	6.696	18	4645	124.0	319.4
EG20805R01	7.000	6.499	18	5546	174.1	337.6
EG10107.5R01	6.603	6.341	18	4375	149.5	296.7

	Summary of Pervious Concrete Cylinders Made on 7/7/09						
	Sample	Avg Diameter (in)	Avg Height (in)	Volume (in^3)	Wet Mass (g)	Dry Mass (g)	Dry Unit Weight (pcf)
Batch #1	WE1	6	11.2	317.2	10028	9674.1	116.2
	WE2	6	11.2	317.3	9902	9536	114.5
	WE3	6	11.2	316.5	10092	9750.9	117.4
	WE4	6	11.1	314.3	9907	9554.6	115.8
	WE5	6	11.3	318.7	9948	9597.2	114.7
Batch #2	WE6	6	12.0	338.5	10757	10406	117.1
	WE7	6	11.9	337.1	10525	10156.7	114.8
	WE8	6	12.0	339.2	10680	10320.7	115.9
	WE9	6	12.1	341.4	10941	10588.4	118.2
	WE10	6	12.0	340.5	10595	10236.2	114.5

Modulus of Elasticity & Poisson's Ratio Test Results for Laboratory Made Samples			
Sample ID	Avg Loading Rate (psi/s)	Modulus of Elasticity (psi)	Poisson's Ratio
WE1	27.9	1886000	0.2370
WE2	25.9	1866000	0.3370
WE3	26.6	2205000	0.2251
WE4	26.7	1951000	0.1686
WE5	23.6	1750000	0.1649
WE6	23.2	1825000	0.1290
WE7	25.3	1415000	0.6444
WE8	22.6	2176000	0.2393
WE9	25.8	1886000	0.2222
WE10	28.7	1768000	0.2361

Modulus of Elasticity & Poisson's Ratio Test Results

Sample Avg Diameter = 6 in Area = 28.3 in^2

Longitudinal Distance Meaasured = 8 in Average Loading Rate = 27.9 in

Sample ID	Load (lb)	Stress (psi)	Trial 1		Trial 2		Average Specimen Longitudinal Deformation	Average Specimen Transverse Deformation	Average Specimen Longitudinal Strain	Average Specimen Transverse Strain
			Longitudinal Gauge Reading	Transverse Gauge Reading	Longitudinal Gauge Reading	Transverse Gauge Reading				
WE1	0	0.0	0.0000	0.6000	0.0000	0.6000	0.00000	0.00000	0.00000	0.00000
	5000	176.8	0.0010	0.6000	0.0013	0.5998	0.00058	0.00005	0.00007	0.00001
	10000	353.7	0.0027	0.5998	0.0028	0.5995	0.00138	0.00017	0.00017	0.00003
	15000	530.5	0.0040	0.5995	0.0044	0.5992	0.00210	0.00032	0.00026	0.00005
	20000	707.4	0.0056	0.5992	0.0057	0.5990	0.00283	0.00045	0.00035	0.00008
	25000	884.2	0.0069	0.5990	0.0067	0.5988	0.00340	0.00055	0.00043	0.00009

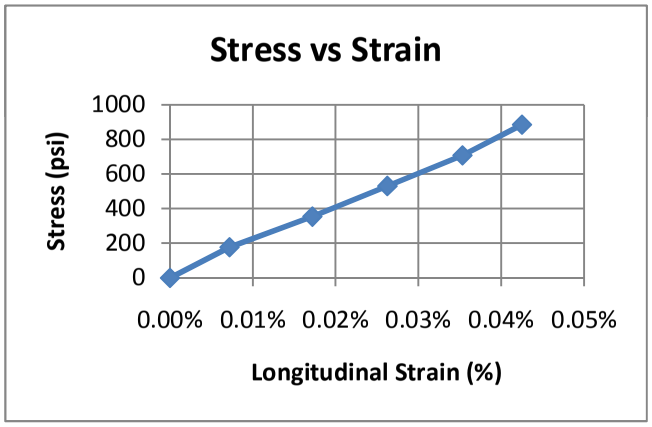

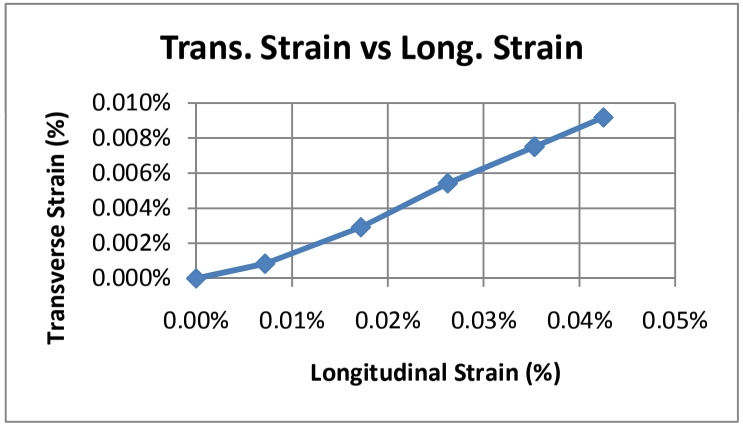

Modulus of Elasticity (psi)	1886000
Poisson's Ratio	0.237

NOTE: The modulus of elasticity and Poisson's ratio were calculated using stresses and strains corresponding to loads between 5,000lb and 20,000lb

Modulus of Elasticity & Poisson's Ratio Test Results

Sample Avg Diameter = 6 in
Longitudinal Distance Meaasured = 8 in
Area = 28.3 in^2
Average Loading Rate = 25.9 in

Sample ID	Load (lb)	Stress (psi)	Trial 1		Trial 2		Average Specimen Longitudinal Deformation	Average Specimen Transverse Deformation	Average Specimen Longitudinal Strain	Average Specimen Transverse Strain
			Longitudinal Gauge Reading	Transverse Gauge Reading	Longitudinal Gauge Reading	Transverse Gauge Reading				
WE2	0	0.0	0.0076	0.6000	0.0079	0.6000	0.00000	0.00000	0.00000	0.00000
	5000	176.8	0.0089	0.5998	0.0093	0.5995	0.00068	0.00017	0.00008	0.00003
	10000	353.7	0.0104	0.5995	0.0108	0.5990	0.00143	0.00037	0.00018	0.00006
	15000	530.5	0.0119	0.5990	0.0122	0.5989	0.00215	0.00052	0.00027	0.00009
	20000	707.4	0.0134	0.5985	0.0139	0.5985	0.00295	0.00075	0.00037	0.00012
	25000	884.2	0.0157	0.5980	0.0157	0.5980	0.00398	0.00100	0.00050	0.00017

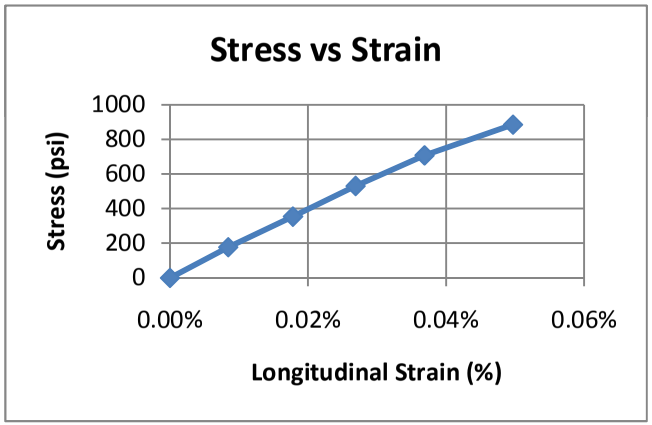

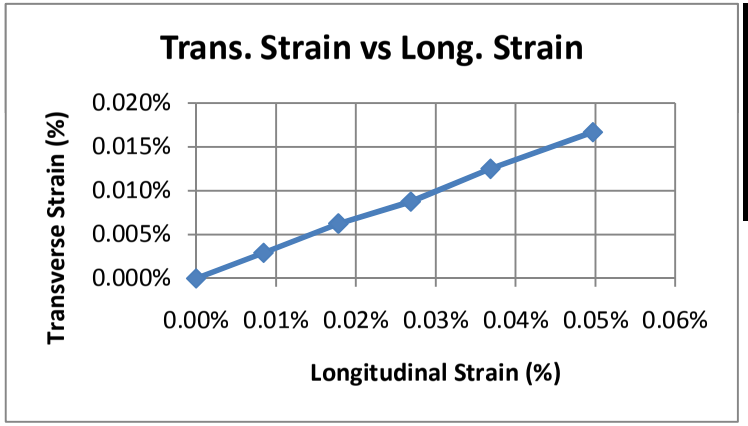

Modulus of Elasticity (psi)	1866000
Poisson's Ratio	0.337

NOTE: The modulus of elasticity and Poisson's ratio were calculated using stresses and strains corresponding to loads between 5,000lb and 20,000lb

Modulus of Elasticity & Poisson's Ratio Test Results

Sample Avg Diameter = 6 in Area = 28.3 in^2

Longitudinal Distance Meaasured = 8 in Average Loading Rate = 26.6 in

Sample ID	Load (lb)	Stress (psi)	Trial 1		Trial 2		Average Specimen Longitudinal Deformation	Average Specimen Transverse Deformation	Average Specimen Longitudinal Strain	Average Specimen Transverse Strain
			Longitudinal Gauge Reading	Transverse Gauge Reading	Longitudinal Gauge Reading	Transverse Gauge Reading				
WE3	0	0.0	0.0006	0.9000	0.0011	0.9000	0.00000	0.00000	0.00000	0.00000
	5000	176.8	0.0016	0.9000	0.0019	0.8998	0.00045	0.00005	0.00006	0.00001
	10000	353.7	0.0028	0.8999	0.0035	0.8996	0.00115	0.00013	0.00014	0.00002
	15000	530.5	0.0039	0.8998	0.0048	0.8994	0.00175	0.00020	0.00022	0.00003
	20000	707.4	0.0053	0.8994	0.0059	0.8991	0.00238	0.00038	0.00030	0.00006
	25000	884.2	0.0068	0.8990	0.0069	0.8990	0.00300	0.00050	0.00038	0.00008

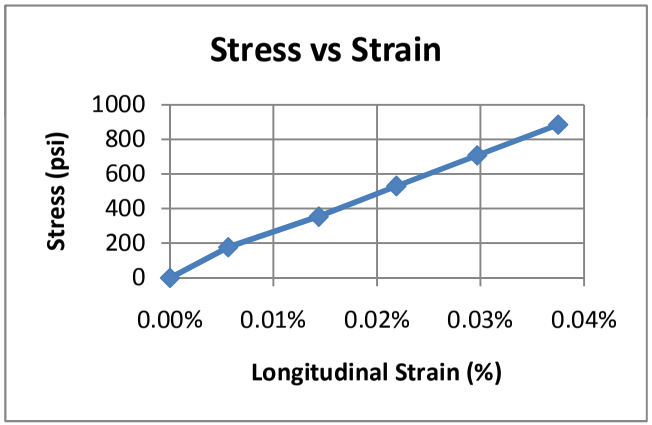

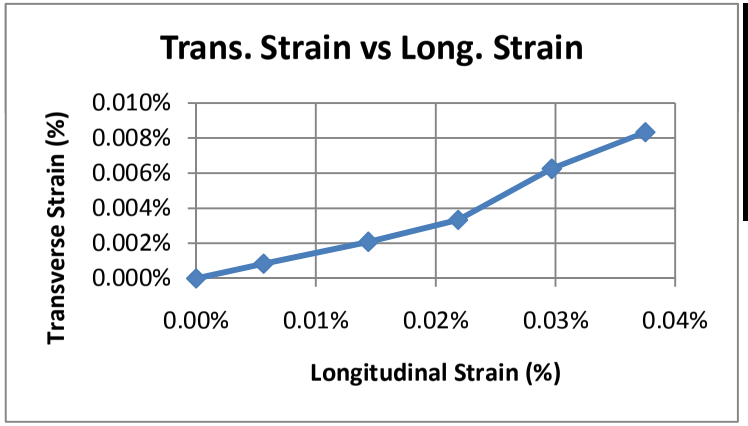

Modulus of Elasticity (psi)	2205000
Poisson's Ratio	0.225

NOTE: The modulus of elasticity and Poisson's ratio were calculated using stresses and strains corresponding to loads between 5,000lb and 20,000lb

Modulus of Elasticity & Poisson's Ratio Test Results

Sample Avg Diameter =	6	in	Area =	28.3	in^2	
Longitudinal Distance Meaasured =	8	in	Average Loading Rate =	26.7	in	

Sample ID	Load (lb)	Stress (psi)	Trial 1		Trial 2		Average Specimen Longitudinal Deformation	Average Specimen Transverse Deformation	Average Specimen Longitudinal Strain	Average Specimen Transverse Strain
			Longitudinal Gauge Reading	Transverse Gauge Reading	Longitudinal Gauge Reading	Transverse Gauge Reading				
WE4	0	0.0	0.0005	0.5000	0.0005	0.5000	0.00000	0.00000	0.00000	0.00000
	5000	176.8	0.0016	0.4999	0.0018	0.4994	0.00060	0.00017	0.00008	0.00003
	10000	353.7	0.0029	0.4998	0.0035	0.4993	0.00135	0.00022	0.00017	0.00004
	15000	530.5	0.0045	0.4996	0.0049	0.4992	0.00210	0.00030	0.00026	0.00005
	20000	707.4	0.0059	0.4992	0.0062	0.4990	0.00278	0.00045	0.00035	0.00008

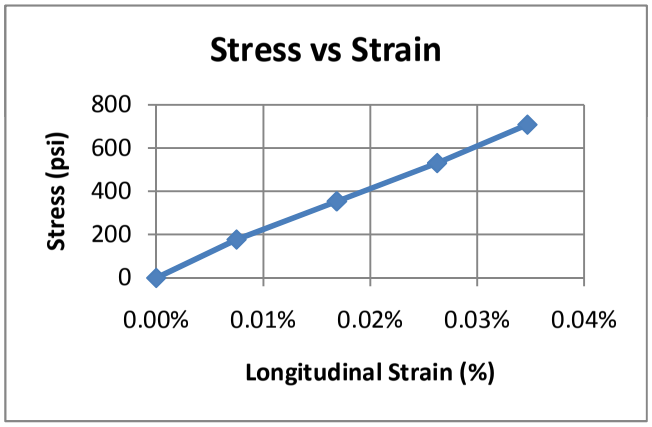

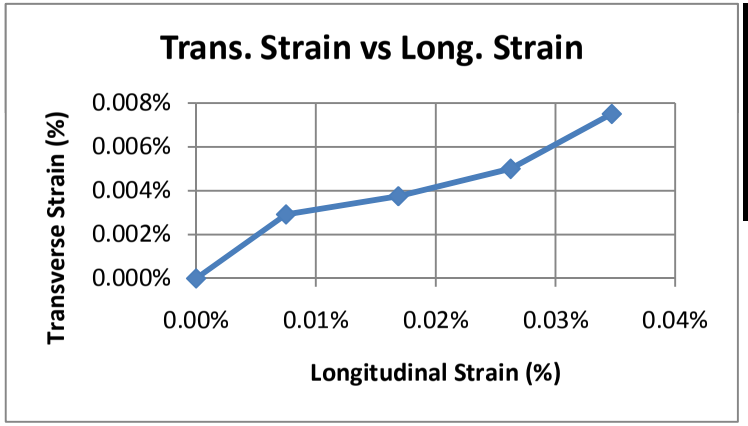

Modulus of Elasticity (psi)	1951000
Poisson's Ratio	0.169

NOTE: The modulus of elasticity and Poisson's ratio were calculated using stresses and strains corresponding to loads between 5,000lb and 20,000lb

Modulus of Elasticity & Poisson's Ratio Test Results

Sample Avg Diameter =	6	in	Area =	28.3	in^2	
Longitudinal Distance Meaasured =	8	in	Average Loading Rate =	23.6	in	

Sample ID	Load (lb)	Stress (psi)	Trial 1		Trial 2		Average Specimen Longitudinal Deformation	Average Specimen Transverse Deformation	Average Specimen Longitudinal Strain	Average Specimen Transverse Strain
			Longitudinal Gauge Reading	Transverse Gauge Reading	Longitudinal Gauge Reading	Transverse Gauge Reading				
WE5	0	0.0	0.0096	0.7388	0.0000	0.7385	0.00000	0.00000	0.00000	0.00000
	5000	176.8	0.0113	0.7387	0.0015	0.7382	0.00080	0.00010	0.00010	0.00002
	10000	353.7	0.0128	0.7383	0.0031	0.7381	0.00158	0.00023	0.00020	0.00004
	15000	530.5	0.0145	0.7381	0.0049	0.7379	0.00245	0.00033	0.00031	0.00005
	20000	707.4	0.0163	0.7379	0.0062	0.7378	0.00323	0.00040	0.00040	0.00007

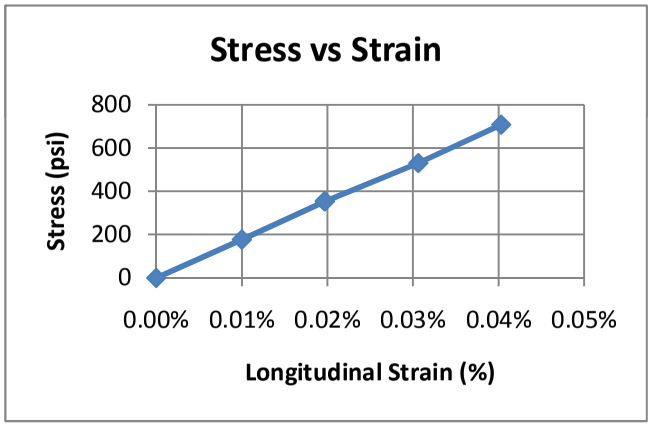

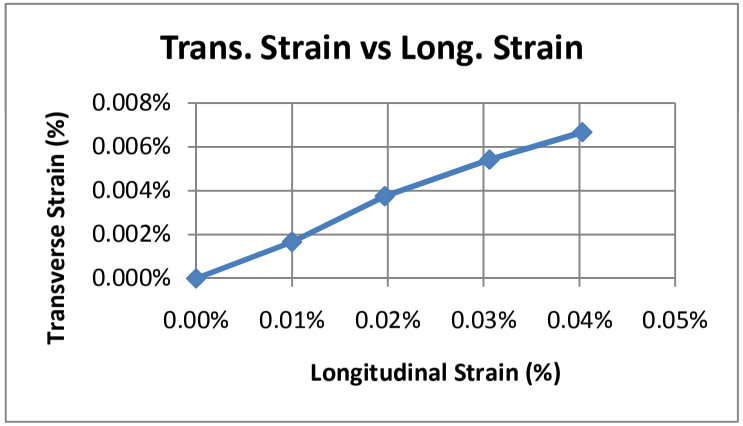

Modulus of Elasticity (psi)	1750000
Poisson's Ratio	0.165

NOTE: The modulus of elasticity and Poisson's ratio were calculated using stresses and strains corresponding to loads between 5,000lb and 20,000lb

Modulus of Elasticity & Poisson's Ratio Test Results

Sample Avg Diameter = 6 in
Longitudinal Distance Meaasured = 8 in
Area = 28.3 in^2
Average Loading Rate = 23.2 in

Sample ID	Load (lb)	Stress (psi)	Trial 1		Trial 2		Average Specimen Longitudinal Deformation	Average Specimen Transverse Deformation	Average Specimen Longitudinal Strain	Average Specimen Transverse Strain
			Longitudinal Gauge Reading	Transverse Gauge Reading	Longitudinal Gauge Reading	Transverse Gauge Reading				
WE6	0	0.0	0.0079	0.7891	0.0082	0.7890	0.00000	0.00000	0.00000	0.00000
	5000	176.8	0.0091	0.7890	0.0096	0.7889	0.00065	0.00005	0.00008	0.00001
	10000	353.7	0.0107	0.7889	0.0110	0.7888	0.00140	0.00010	0.00018	0.00002
	15000	530.5	0.0123	0.7887	0.0125	0.7888	0.00218	0.00015	0.00027	0.00003
	20000	707.4	0.0140	0.7884	0.0140	0.7886	0.00298	0.00028	0.00037	0.00005

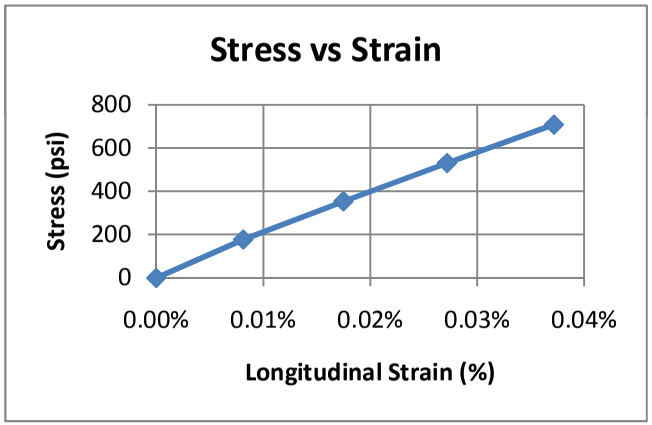

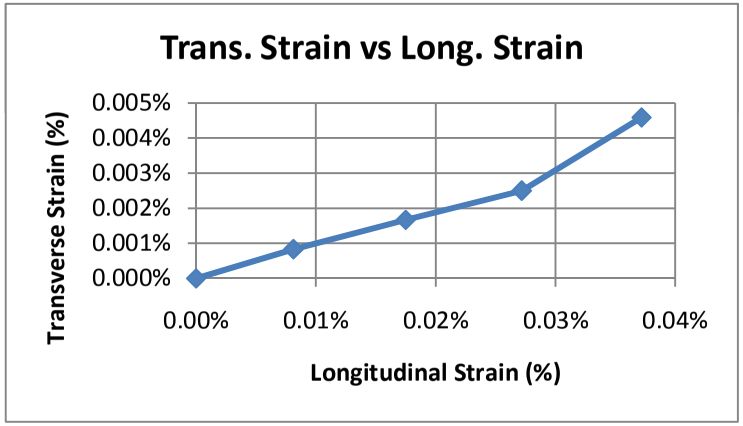

Modulus of Elasticity (psi)	1825000
Poisson's Ratio	0.129

NOTE: The modulus of elasticity and Poisson's ratio were calculated using stresses and strains corresponding to loads between 5,000lb and 20,000lb

Modulus of Elasticity & Poisson's Ratio Test Results

Sample Avg Diameter = 6 in
Longitudinal Distance Meaasured = 8 in
Area = 28.3 in^2
Average Loading Rate = 25.3 in

Sample ID	Load (lb)	Stress (psi)	Trial 1		Trial 2		Average Specimen Longitudinal Deformation	Average Specimen Transverse Deformation	Average Specimen Longitudinal Strain	Average Specimen Transverse Strain
			Longitudinal Gauge Reading	Transverse Gauge Reading	Longitudinal Gauge Reading	Transverse Gauge Reading				
WE7	0	0.0	0.0065	0.6900	0.0065	0.6900	0.00000	0.00000	0.00000	0.00000
	5000	176.8	0.0079	0.6899	0.0084	0.6899	0.00083	0.00005	0.00010	0.00001
	10000	353.7	0.0104	0.6890	0.0103	0.6890	0.00193	0.00050	0.00024	0.00008
	15000	530.5	0.0123	0.6880	0.0123	0.6880	0.00290	0.00100	0.00036	0.00017
	20000	707.4	0.0141	0.6870	0.0142	0.6870	0.00383	0.00150	0.00048	0.00025

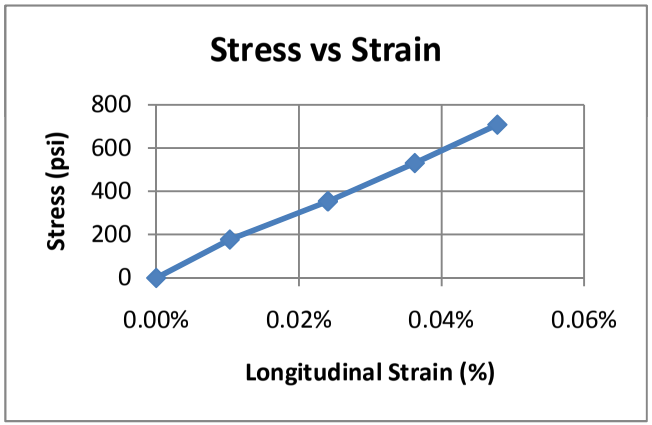

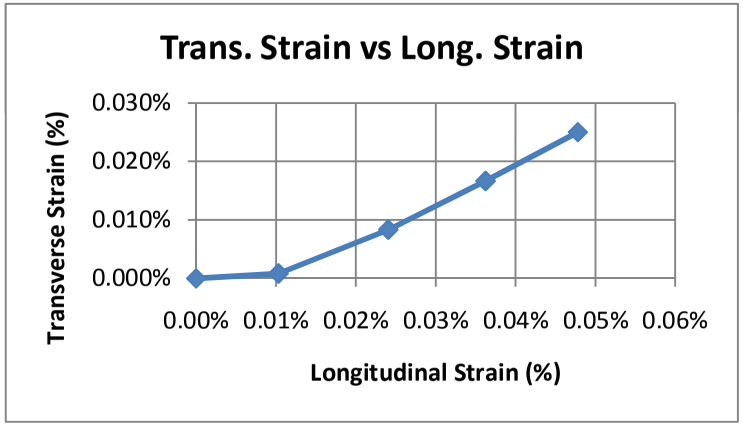

Modulus of Elasticity (psi)	1415000
Poisson's Ratio	0.644

OUTLIER: IGNORE THESE RESULTS

NOTE: The modulus of elasticity and Poisson's ratio were calculated using stresses and strains corresponding to loads between 5,000lb and 20,000lb

Modulus of Elasticity & Poisson's Ratio Test Results

Sample Avg Diameter =	6	in	Area =	28.3	in^2	
Longitudinal Distance Meaasured =	8	in	Average Loading Rate =	22.6	in	

Sample ID	Load (lb)	Stress (psi)	Trial 1		Trial 2		Average Specimen Longitudinal Deformation	Average Specimen Transverse Deformation	Average Specimen Longitudinal Strain	Average Specimen Transverse Strain
			Longitudinal Gauge Reading	Transverse Gauge Reading	Longitudinal Gauge Reading	Transverse Gauge Reading				
WE8	0	0.0	0.0056	0.6000	0.0056	0.6000	0.00000	0.00000	0.00000	0.00000
	5000	176.8	0.0066	0.5999	0.0068	0.5998	0.00055	0.00007	0.00007	0.00001
	10000	353.7	0.0079	0.5997	0.0079	0.5996	0.00115	0.00017	0.00014	0.00003
	15000	530.5	0.0089	0.5995	0.0093	0.5994	0.00175	0.00027	0.00022	0.00005
	20000	707.4	0.0106	0.5992	0.0106	0.5991	0.00250	0.00043	0.00031	0.00007

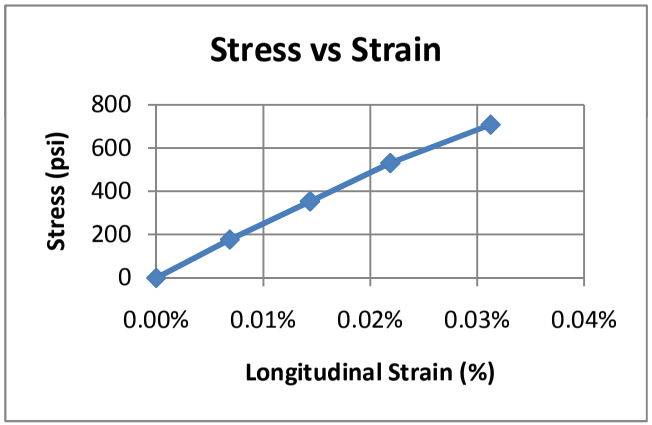

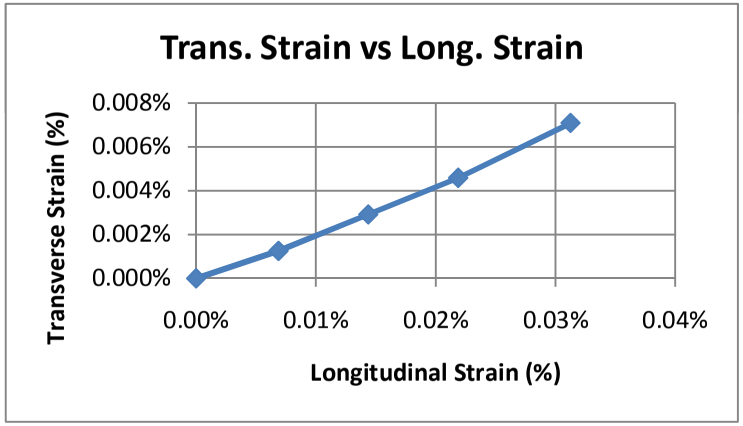

Modulus of Elasticity (psi)	2176000
Poisson's Ratio	0.239

NOTE: The modulus of elasticity and Poisson's ratio were calculated using stresses and strains corresponding to loads between 5,000lb and 20,000lb

Modulus of Elasticity & Poisson's Ratio Test Results

Sample Avg Diameter = 6 in
Longitudinal Distance Meaasured = 8 in
Area = 28.3 in^2
Average Loading Rate = 25.8 in

Sample ID	Load (lb)	Stress (psi)	Trial 1		Trial 2		Average Specimen Longitudinal Deformation	Average Specimen Transverse Deformation	Average Specimen Longitudinal Strain	Average Specimen Transverse Strain
			Longitudinal Gauge Reading	Transverse Gauge Reading	Longitudinal Gauge Reading	Transverse Gauge Reading				
WE9	0	0.0	0.0007	0.4980	0.0013	0.4980	0.00000	0.00000	0.00000	0.00000
	5000	176.8	0.0020	0.4980	0.0025	0.4979	0.00063	0.00002	0.00008	0.00000
	10000	353.7	0.0035	0.4979	0.0044	0.4977	0.00148	0.00010	0.00018	0.00002
	15000	530.5	0.0049	0.4976	0.0055	0.4975	0.00210	0.00023	0.00026	0.00004
	20000	707.4	0.0067	0.4972	0.0068	0.4972	0.00288	0.00040	0.00036	0.00007

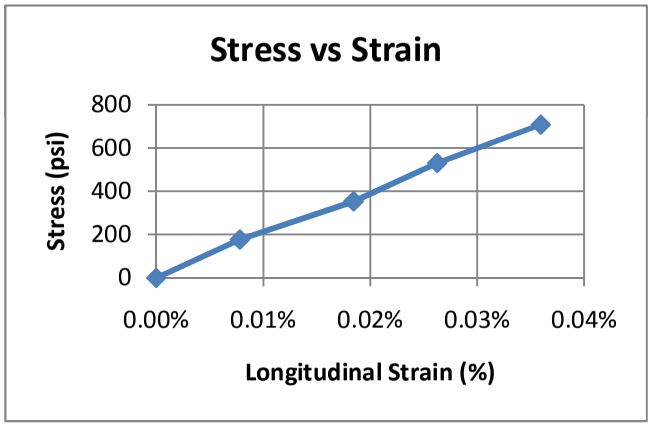

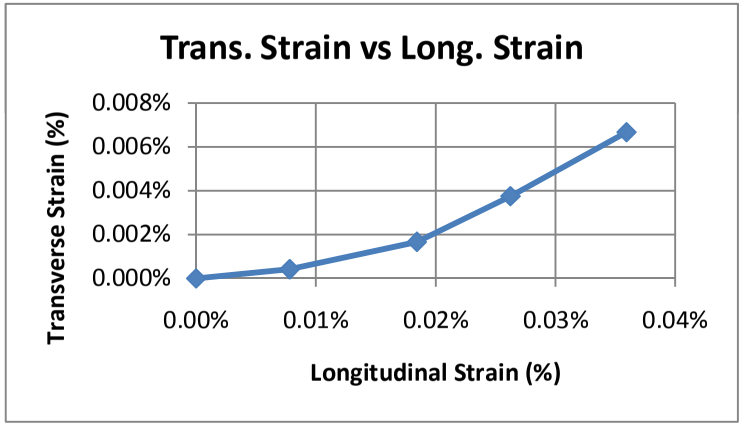

Modulus of Elasticity (psi)	1886000
Poisson's Ratio	0.222

NOTE: The modulus of elasticity and Poisson's ratio were calculated using stresses and strains corresponding to loads between 5,000lb and 20,000lb

Modulus of Elasticity & Poisson's Ratio Test Results

Sample Avg Diameter =	6	in	Area =	28.3	in^2	
Longitudinal Distance Meaasured =	8	in	Average Loading Rate =	28.7	in	

Sample ID	Load (lb)	Stress (psi)	Trial 1		Trial 2		Average Specimen Longitudinal Deformation	Average Specimen Transverse Deformation	Average Specimen Longitudinal Strain	Average Specimen Transverse Strain
			Longitudinal Gauge Reading	Transverse Gauge Reading	Longitudinal Gauge Reading	Transverse Gauge Reading				
WE10	0	0.0	0.0077	0.5000	0.0084	0.5000	0.00000	0.00000	0.00000	0.00000
	5000	176.8	0.0090	0.5000	0.0096	0.4999	0.00063	0.00002	0.00008	0.00000
	10000	353.7	0.0108	0.4999	0.0109	0.4996	0.00140	0.00013	0.00018	0.00002
	15000	530.5	0.0122	0.4995	0.0127	0.4993	0.00220	0.00030	0.00028	0.00005
	20000	707.4	0.0140	0.4991	0.0142	0.4991	0.00303	0.00045	0.00038	0.00008

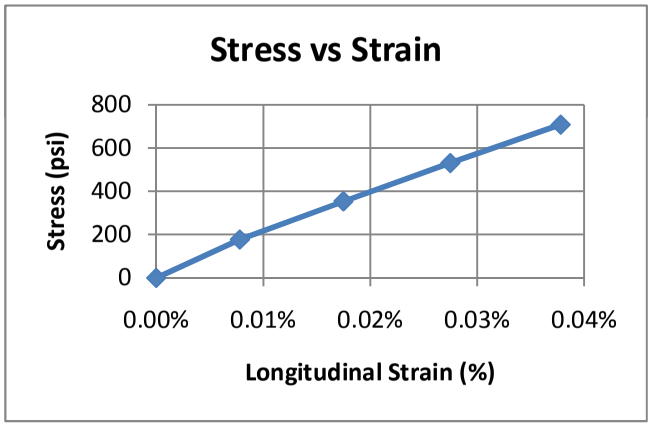

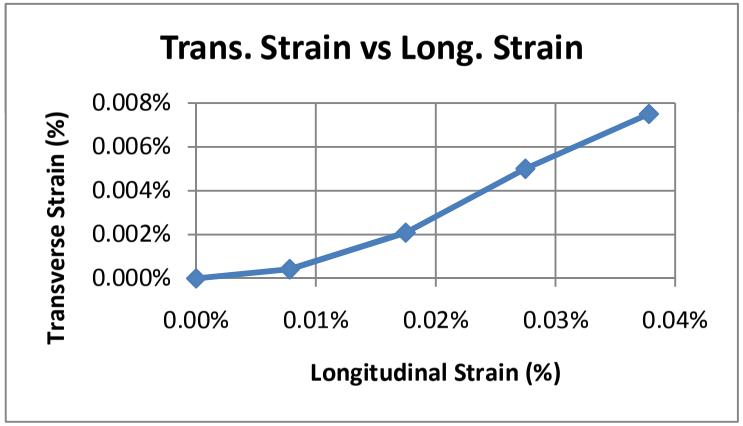

Modulus of Elasticity (psi)	1768000
Poisson's Ratio	0.236

NOTE: The modulus of elasticity and Poisson's ratio were calculated using stresses and strains corresponding to loads between 5,000lb and 20,000lb

Compression Test Results for Evolution Paving Samples								
Sample ID	Avg Diameter (in)	Avg Height (in)	L/D	L/D Factor	Max Applied Load (lb)	Loading Rate (psi/s)	Compressive Strength (psi)	Type of Fracture
EG11406R01a	3.780	6.3	1.67	0.97	57709	70.7	5005.3	4
EG11306R01a	3.780	6.6	1.75	0.98	38172	57.5	3332.4	4
EG10508C01a	3.780	7.8	2.06	1.00	34952	36.1	3114.6	4
EG11406R01b	3.780	6.67	1.76	0.98	38822	58.1	3394.3	4
EG10508C01b	3.780	8.2	2.17	1.00	26667	38.7	2376.3	1
EG20210C01a	3.780	8.74	2.31	1.00	17627	16.8	1570.7	4
EG20805R02a	3.780	6.7	1.77	0.98	26708	34.4	2336.6	1
EG20210C01b	3.780	7.32	1.94	0.99	22448	29.4	1990.2	4
EG20407C01a	3.780	6.15	1.63	0.97	35821	23.3	3096.8	1
EG10310C01b	3.780	10.77	2.85	1.00	57160	35.7	5093.5	1
EG10310C01a	3.780	10.97	2.90	1.000	55757	34.4	4968.5	1
EG20805R02b	3.780	6.8	1.80	0.98	26108	35.8	2289.1	4
EG21204R01b	3.780	6.41	1.70	0.98	25429	36.5	2210.8	1
EG20407C01b	3.780	5.85	1.55	0.96	32336	40.5	2777.2	4
EG11104R01b	2.790	4.35	1.56	0.96	15256	22.6	2407.4	1
EG11104R01a	2.790	4.68	1.68	0.97	16492	52.2	2628.0	1
EG20605C02b	3.780	7.01	1.85	0.99	30240	41.7	2663.3	1
EG20805R04a	3.780	6.98	1.85	0.99	31499	49.7	2772.4	4
EG11306R01b	3.780	6.95	1.84	0.99	27680	35.6	2434.7	1
EG20805R04b	3.780	7	1.85	0.99	31406	46.8	2765.4	1
EG20605C01a	3.780	7.04	1.86	0.99	21213	36.7	1869.5	1
EG20605C01b	3.780	6.96	1.84	0.99	29303	41.3	2578.0	1
EG20805R03a	3.780	7.14	1.89	0.99	33298	53.7	2940.8	1
EG20805R03b	3.780	6.82	1.80	0.98	33509	44.2	2939.2	1
EG20605C02a	3.780	6.85	1.81	0.98	22003	34.8	1931.2	1
EG20805R01a	3.780	6.71	1.78	0.98	39375	59.1	3445.6	4
EG20805R01b	3.780	6.73	1.78	0.98	36496	51.1	3195.0	4
EG21204R01a	3.780	6.2	1.64	0.97	37522	48.4	3247.4	1
EG11608R01b	3.780	6.57	1.74	0.98	33542	36.0	2926.3	4
EG11608R01a	3.780	7.02	1.86	0.99	45627	67.9	4019.4	1
EG10508C02a	3.780	8.88	2.35	1.000	30423	51.0	2711.0	4
EG10107.5R01a	3.780	6.57	1.74	0.98	41166	54.3	3591.4	4
EG10107.5R01b	3.780	6.62	1.75	0.98	39407	49.6	3441.7	1
EG10508C02b	3.780	8.6	2.28	1.000	38305	39.8	3413.4	1

Compression Test Results for Laboratory Made Samples											
Sample ID	Avg Diameter (in)	Avg Cross-sectional Area (in)	Avg Height (in)	L/D	L/D Factor	Loading Duration (s)	Load when Timer was Started (lb)	Max Applied Load (lb)	Loading Rate (psi/s)	Compressive Strength (psi)	Type of Fracture
WE1	6.000	28.3	11.35	1.892	0.99	50.2	5000	46999	29.6	1647.8	4
WE2	6.000	28.3	11.33	1.888	0.99	41.8	5000	38283	28.2	1341.9	4
WE3	6.000	28.3	11.32	1.887	0.99	68.2	6000	47419	21.5	1661.9	4
WE4	6.000	28.3	11.41	1.902	0.99	60.6	5000	47637	24.9	1671.6	4
WE5	6.000	28.3	11.45	1.908	0.99	60.9	5000	39996	20.3	1404.2	1
WE6	6.000	28.3	12.07	2.012	1.00	73.1	5000	46521	20.1	1645.3	4
WE7	6.000	28.3	12.07	2.012	1.00	44.8	5000	40236	27.8	1423.1	1
WE8	6.000	28.3	12.13	2.022	1.00	54.2	5000	45717	26.6	1616.9	4
WE9	6.000	28.3	12.25	2.042	1.00	47.9	5000	43876	28.7	1551.8	1
WE10	6.000	28.3	12.25	2.042	1.00	48.8	5000	40850	26.0	1444.8	1

Porosity Test Results for Evolution Paving Samples										
Sample ID	Volume							Submerged Mass (g)	Dry Mass (g)	Porosity
	Diameter (in)			Height (in)			Volume (in^3)			
	Top	Middle	Bottom	Top	Middle	Bottom				
EG20407C01a	3.78	3.78	3.70	6.01	5.91	6.24	66.91	1206	2068.7	21.3%
EG20407C01b	3.78	3.78	3.76	5.51	5.91	5.58	63.35	1137.6	1942.2	22.5%
EG20805R03a	3.78	3.76	3.79	7.29	6.96	7.30	80.39	1373	2371.2	24.2%
EG20805R03b	3.78	3.78	3.79	6.97	6.96	6.91	78.03	1296.2	2239.9	26.2%
EG20605C02a	3.78	3.76	3.76	6.87	6.89	6.83	76.48	1309.8	2225.2	27.0%
EG20605C02b	3.76	3.78	3.77	6.89	6.83	6.63	75.75	1295.2	2209.2	26.4%
EG20805R04a	3.78	3.78	3.78	6.66	6.76	6.65	75.08	1314	2267.1	22.5%
EG20805R04b	3.77	3.77	3.75	6.81	7.01	6.95	77.11	1317.5	2277.3	24.0%
EG20605C01a	3.78	3.78	3.78	6.90	7.14	7.00	78.66	1364.1	2288.4	28.3%
EG20605C01b	3.79	3.78	3.78	7.00	6.83	7.14	78.53	1403	2377	24.3%
EG10508C02b	3.79	3.78	3.79	8.63	8.70	8.64	97.27	1767.8	3052.9	19.4%
EG10508C02a	3.77	3.80	3.79	8.58	8.54	8.75	96.98	1741	2973.3	22.5%
EG20805R01a	3.78	3.79	3.79	6.35	6.51	6.65	73.27	1302	2245	21.5%
EG20805R01b	3.80	3.78	3.78	6.65	6.59	6.45	73.84	1319.4	2266.1	21.8%
EG10508C01a	3.78	3.78	3.78	7.71	7.67	7.62	85.96	1554.5	2661.5	21.4%
EG10508C01b	3.79	3.79	3.78	7.98	8.26	8.27	91.87	1628.4	2784	23.2%
EG11306R01a	3.79	3.78	3.78	6.48	6.42	6.31	71.90	1257.8	2194.1	20.5%
EG11306R01b	3.78	3.79	3.78	6.65	6.68	6.64	74.79	1355	2296.4	23.2%
EG20805R02a	3.78	3.78	3.77	6.39	6.29	6.46	71.59	1226.2	2100.8	25.5%
EG20805R02b	3.78	3.77	3.77	6.48	7.18	6.65	75.82	1312.2	2256.3	24.0%
EG10107.5R01a	3.78	3.78	3.79	6.30	6.29	6.24	70.54	1320.8	2329.5	12.7%
EG10107.5R01b	3.79	3.78	3.79	6.38	6.45	6.42	72.28	1279.8	2248.9	18.2%
EG11608R01a	3.80	3.79	3.78	6.89	6.84	6.74	76.97	1423.4	2532.3	12.1%
EG11608R01b	3.78	3.78	3.78	6.37	6.14	6.15	69.86	1259.6	2236.1	14.7%
EG10310C01a	3.82	3.79	3.78	10.71	10.68	10.86	121.73	2294.8	4023	13.4%
EG10310C01b	3.79	3.80	3.78	10.48	10.59	10.53	118.65	2277.8	3972.9	12.8%
EG11406R01a	3.79	3.79	3.79	6.21	6.12	6.05	69.03	1262.6	2245.7	13.1%
EG11406R01b	3.78	3.78	3.77	6.57	6.48	6.44	72.69	1302.6	2302.3	16.1%
EG21204R01a	3.80	3.80	3.80	6.10	5.92	6.02	68.09	1218.5	2081.4	22.7%
EG21204R01b	3.80	3.79	3.79	6.00	6.11	6.21	69.01	1239	2110	23.0%
EG20210C01a	3.82	3.81	3.80	8.22	8.07	8.17	92.94	1640.3	2794.3	24.2%
EG20210C01b	3.83	3.80	3.81	7.64	7.44	7.48	85.70	1415.2	2414.7	28.8%
EG11104R01a	2.79	2.79	2.78	4.78	4.91	4.80	29.49	508.4	835	32.4%
EG11104R01b	2.79	2.80	2.81	4.09	4.39	4.27	26.10	464.8	755.2	32.1%

Porosity Test Results for Laboratory Made Samples										
Sample ID	Volume							Submerged Mass (g)	Dry Mass (g)	Porosity
	Diameter (in)			Height (in)			Volume (in^3)			
	Top	Middle	Bottom	Top	Middle	Bottom				
WE1	5.97	6.00	6.03	11.19	11.20	11.27	317.19	5878.6	9674.1	27.0%
WE2	5.97	6.00	6.03	11.20	11.28	11.19	317.32	5802	9536	28.2%
WE3	5.98	6.00	6.03	11.20	11.23	11.14	317.01	5929.1	9750.9	26.4%
WE4	5.97	5.98	6.02	11.05	11.14	11.16	313.26	5811.1	9554.6	27.1%
WE5	5.98	6.00	6.03	11.26	11.31	11.24	319.29	5833.3	9597.2	28.1%
WE6	5.97	6.00	6.03	12.00	12.00	11.92	338.48	6296.6	10406	25.9%
WE7	5.97	6.00	6.03	11.91	11.93	11.93	337.12	6163.6	10156.7	27.7%
WE8	5.97	6.00	6.03	12.01	12.03	11.94	339.20	6269	10320.7	27.1%
WE9	5.98	6.00	6.05	12.07	12.07	12.07	342.55	6431.2	10588.4	25.9%
WE10	5.98	6.00	6.03	11.99	12.07	12.07	341.13	6219	10236.2	28.1%

Exfiltration Rate Test Results for Evolution Paving Samples							
Sample ID	Amount of water used		Trial Duration		Average Exfiltration Rate (mL/s)	Average Exfiltration Rate (in^3/hr)	Average Exfiltration Rate (in/hr)
	Trial 1 (mL)	Trial 2 (mL)	Trial 1 (s)	Trial 2 (s)			
EG20605C02a	50	50	97.5	105	0.5	108.6	9.7
EG20605C02b	100	100	32.2	37.7	2.9	632.5	56.7
EG20805R04b	100	100	51.6	62	1.8	390.0	34.9
EG20605C01a	100	100	70.9	78	1.3	295.8	26.4
EG20605C01b	50	50	41.1	44	1.2	258.4	23.0
EG10508C01b	50	50	65.1	59	0.8	177.5	15.8
EG10107.5R01b	200	50	658	212	0.3	59.3	5.3
EG10310C01a	200	50	287.4	72	0.7	152.7	13.5
EG20210C01a	50	50	115	103	0.5	101.1	8.9
EG11104R01a	100	100	29.1	29.1	3.4	754.9	123.5

Exfiltration Rate Test Results for Laboratory Made Samples

Sample Diameter = 6 in

Sample Surface Area = 28.3 in^2

Sample ID	Time for 2000mL of Water to Exfiltrate		Average Exfiltration Rate (mL/s)	Average Exfiltration Rate (in^3/hr)	Average Exfiltration Rate (in/hr)
	Trial 1 (s)	Trial 2 (s)			
WE1	9.97	9.8	202.3	44448.3	1572.0
WE2	9.44	9.02	216.7	47602.5	1683.6
WE3	10.7	10.54	188.3	41372.0	1463.2
WE4	8.76	8.93	226.1	49674.5	1756.9
WE5	7.48	8.28	253.8	55757.7	1972.0
WE6	12.22	11.91	165.8	36417.0	1288.0
WE7	8.93	9.3	219.4	48203.1	1704.8
WE8	8.47	8.52	235.4	51721.1	1829.3
WE9	11.78	13.47	158.4	34801.7	1230.9
WE10	7.79	8.89	239.8	52682.4	1863.3

9.2 APPENDIX B – STRUCTURAL PERFORMANCE INVESTIGATION RESULTS

Evolution Paving Distress Survey

Surveyor: Will Goede Reference: ASTM D6433 Date Surveyed: 5/19/09

NOTE: Panels are divided into 9 equal subsections for PCI calculations

Panel ID: EG202106 **Panel #:** 02 **Loaded Trucks?** YES

Aggregate: 5/8" → 1 1/4" CR w/ 25% 3/8" RR **Depth:** 10" **Phase #:** 2

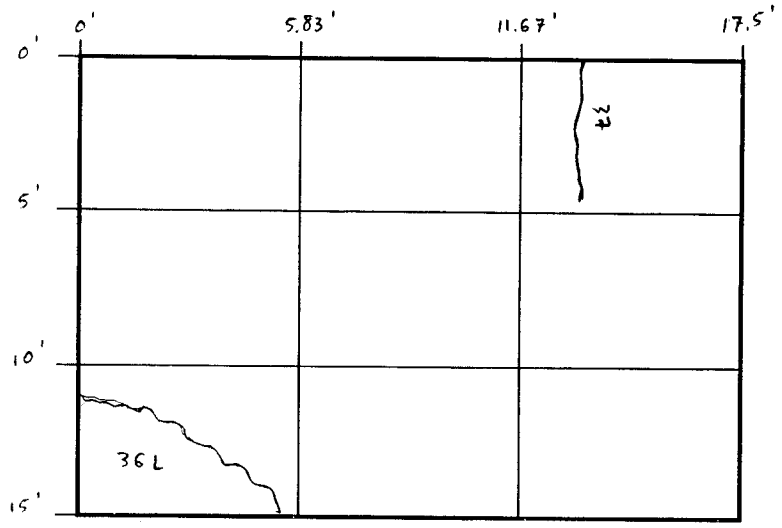

Panel ID: EG101075R **Panel #:** 01 **Loaded Trucks?** NO

Aggregate: 3/8" RR **Depth:** 07.5" **Phase #:** 1

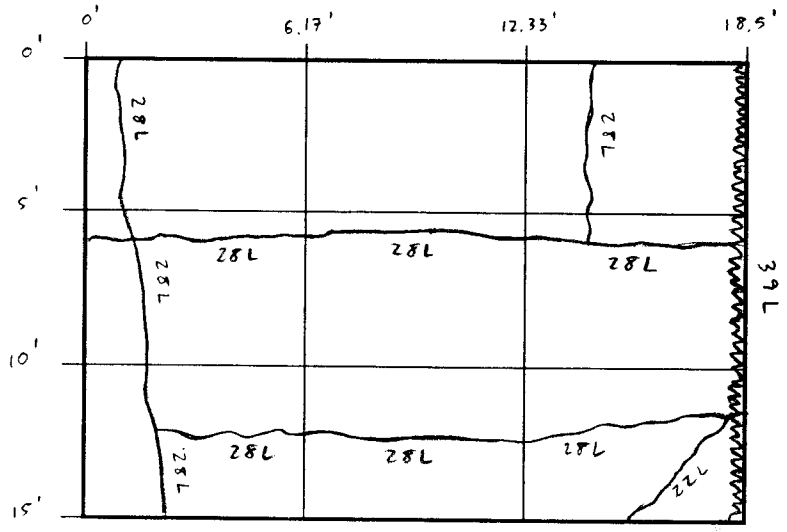

*measurements are an average of dimensions @ both ends of the panel

Evolution Paving Distress Survey

Surveyor: Will Goede Reference: ASTM D6433 Date Surveyed: 5/19/09

NOTE: Panels are divided into 9 equal subsections for PCI calculations

Panel ID: EG20407C **Panel #:** 04 **Loaded Trucks?** YES

Aggregate: 5/8" → 1/4" CR w/ 25% 3/8" RR **Depth:** 07" **Phase #:** 2

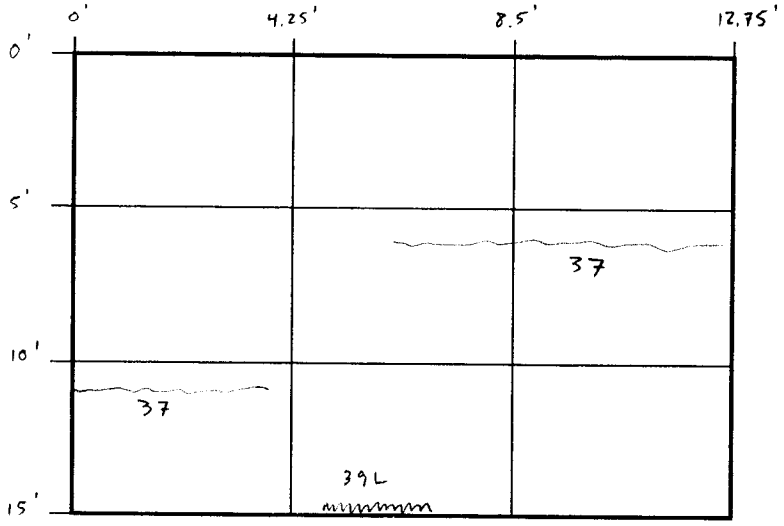

Panel ID: EG10310C **Panel #:** 03 **Loaded Trucks?** NO

Aggregate: 5/8" → 1/4" CR w/ 25% 3/8" RR **Depth:** 10" **Phase #:** 1

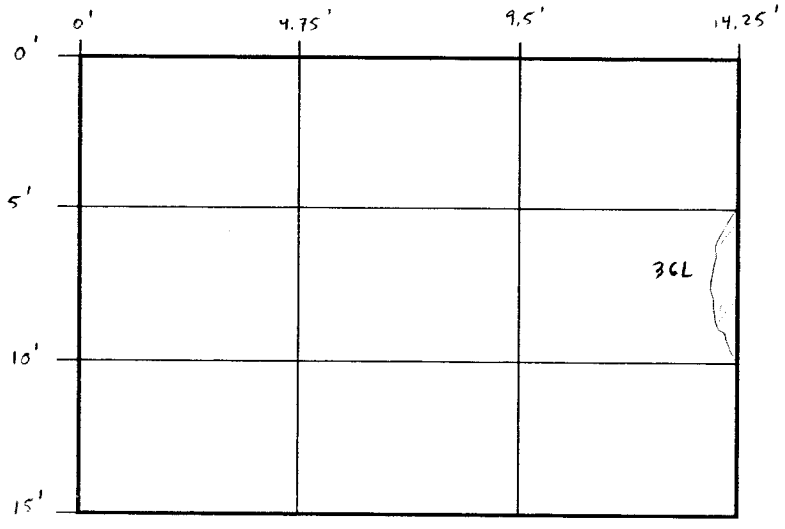

Evolution Paving Distress Survey

Surveyor: Will Goede Reference: ASTM D6433 Date Surveyed: 5/19/09

NOTE: Panels are divided into 9 equal subsections for PCI calculations

Panel ID: EG2 0605 C **Panel #:** 06 **Loaded Trucks?** YES

Aggregate: 1/2" → 1/4" CR **Depth:** 05" **Phase #:** 2

w/ 25% 1/4-10 CR

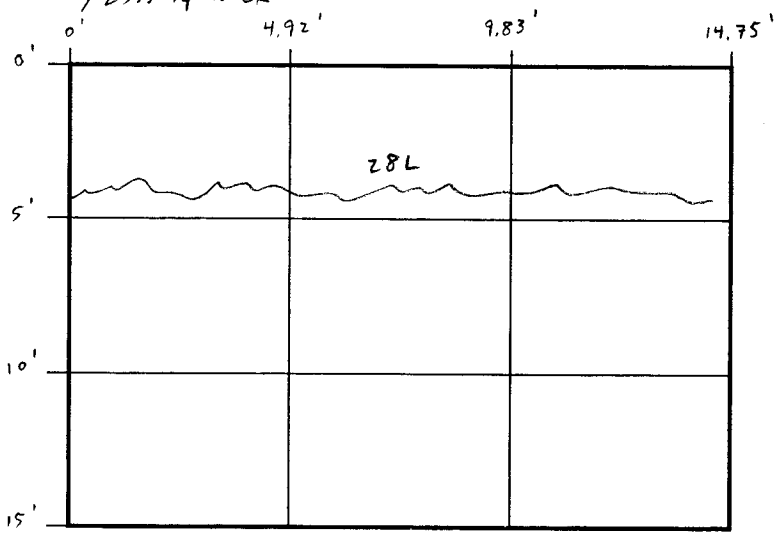

Panel ID: EG1 0508 C **Panel #:** 05 **Loaded Trucks?** NO

Aggregate: 5/8" → 1/4" CR **Depth:** 08" **Phase #:** 1

w/ 25% 3/8" RR

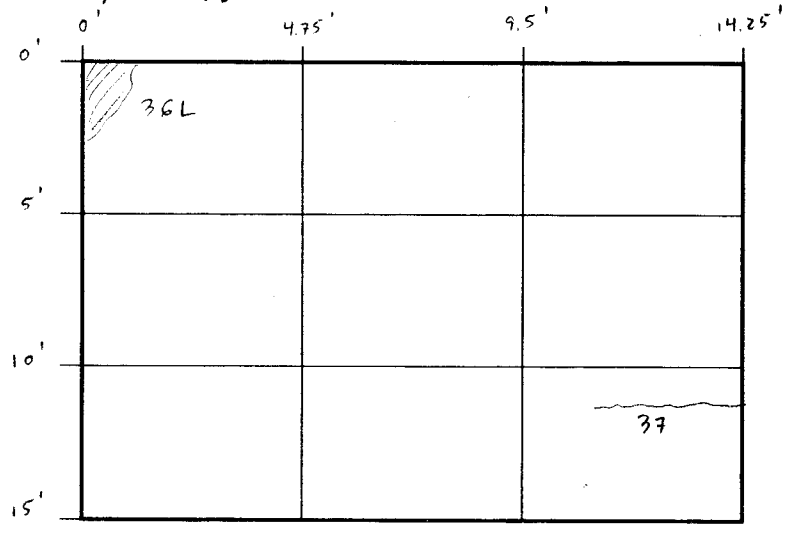

Evolution Paving Distress Survey

Surveyor: Will Goede Reference: ASTM D6433 Date Surveyed: 5/19/09

NOTE: Panels are divided into 9 equal subsections for PCI calculations

Panel ID: EGZ0805R **Panel #:** 08 **Loaded Trucks?** YES

Aggregate: 3/8" RR **Depth:** 05" **Phase #:** 2

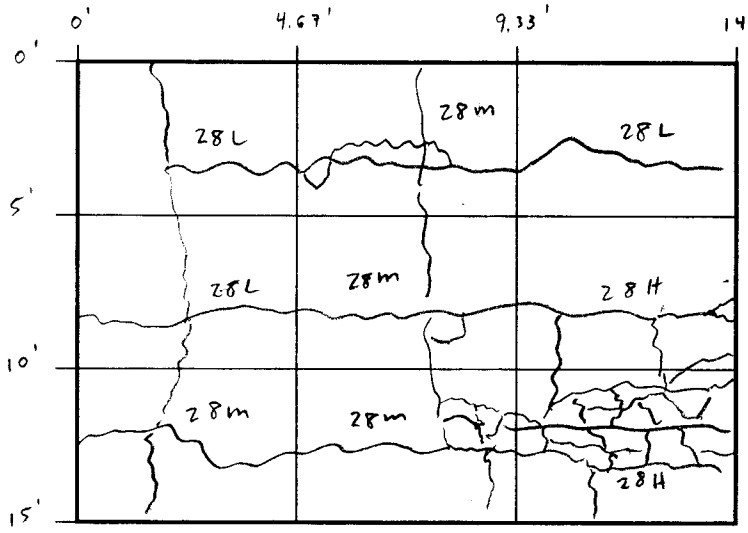

23H

Panel ID: EG10706C **Panel #:** 07 **Loaded Trucks?** NO

Aggregate: 5/8" → 1/4" CR w/ 25% 3/8" RR **Depth:** 06" **Phase #:** 1

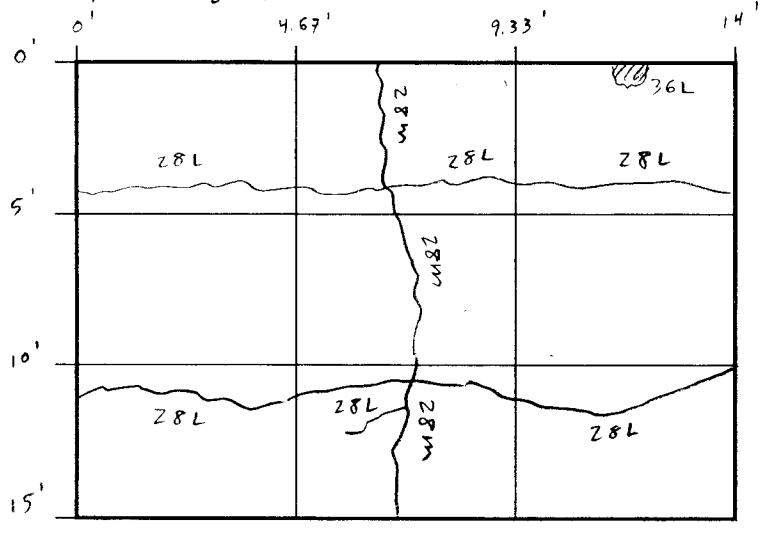

23m

Evolution Paving Distress Survey

Surveyor: Will Goede Reference: ASTM D6433 Date Surveyed: 5/19/09

NOTE: Panels are divided into 9 equal subsections for PCI calculations

Panel ID: EG210 04 E **Panel #:** 10 **Loaded Trucks?** YES

Aggregate: 3/8" RR **Depth:** 04" **Phase #:** 2

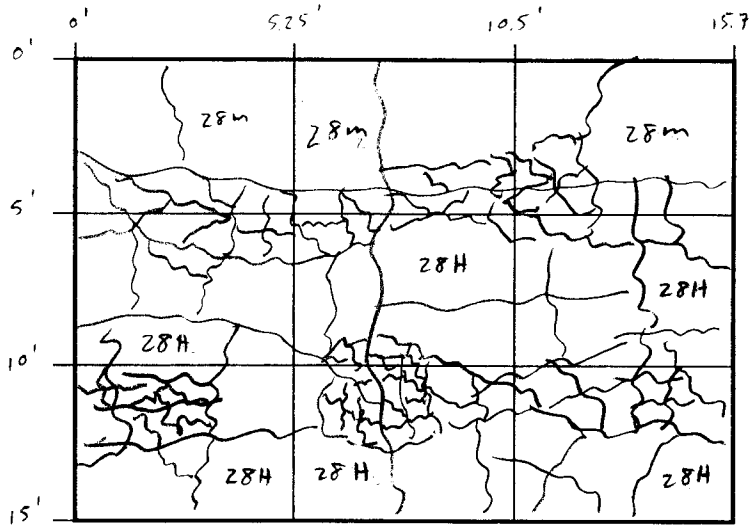

23 H

Panel ID: EG1 09 04 C **Panel #:** 09 **Loaded Trucks?** NO

Aggregate: 5/8" → 1/4" CR w/ 25% 3/8" RR **Depth:** 04" **Phase #:** 1

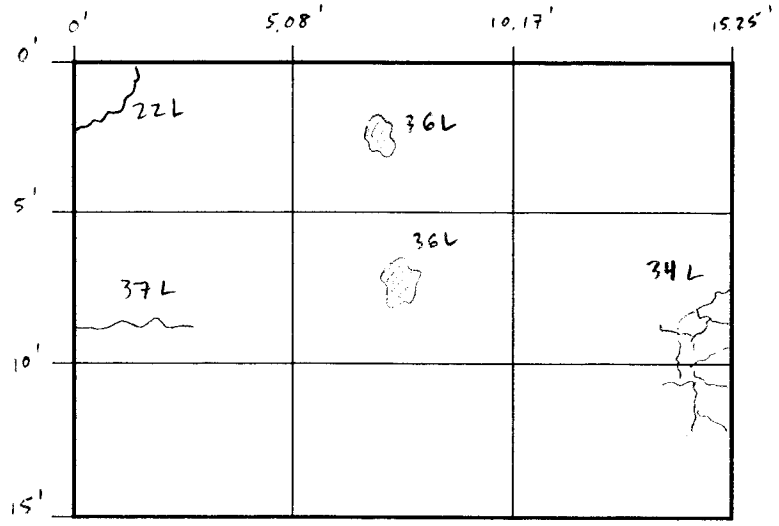

Evolution Paving Distress Survey

Surveyor: Will Goede Reference: ASTM D6433 Date Surveyed: 5/19/09

NOTE: Panels are divided into 9 equal subsections for PCI calculations

Panel ID: EG212.04R **Panel #:** 12 **Loaded Trucks?** YES

Aggregate: 3/8" RR **Depth:** 4.5" Compacted to 4" **Phase #:** 2

(1st generation pervious)

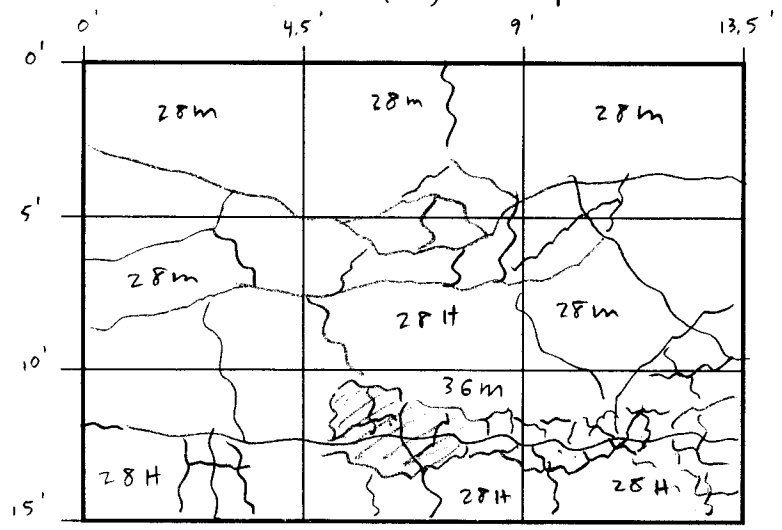

23 H

Panel ID: EG1104R **Panel #:** 11 **Loaded Trucks?** NO

Aggregate: 3/8" RR **Depth:** 04" **Phase #:** 1

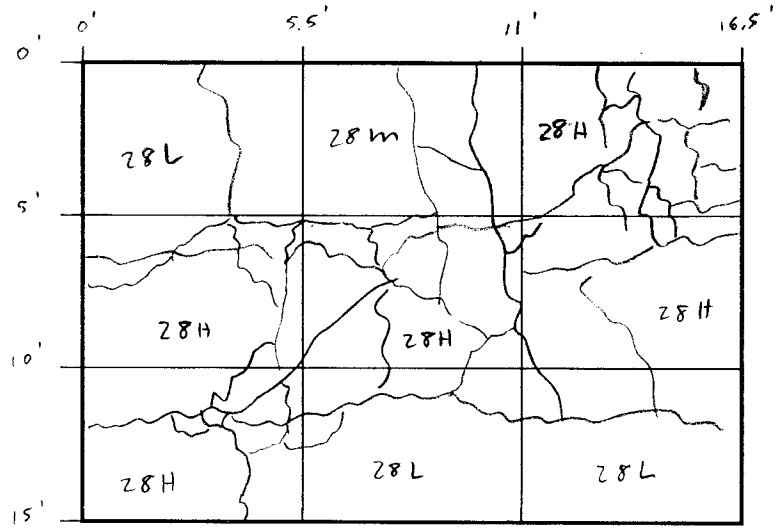

23 H

Evolution Paving Distress Survey

Surveyor: Will Goede Reference: ASTM D6433 Date Surveyed: 5/19/09

NOTE: Panels are divided into 9 equal subsections for PCI calculations

Panel ID: EG1 14 06 R **Panel #:** 14 **Loaded Trucks?** YES
Aggregate: 3/8" RR **Depth:** 06" **Phase #:** 1

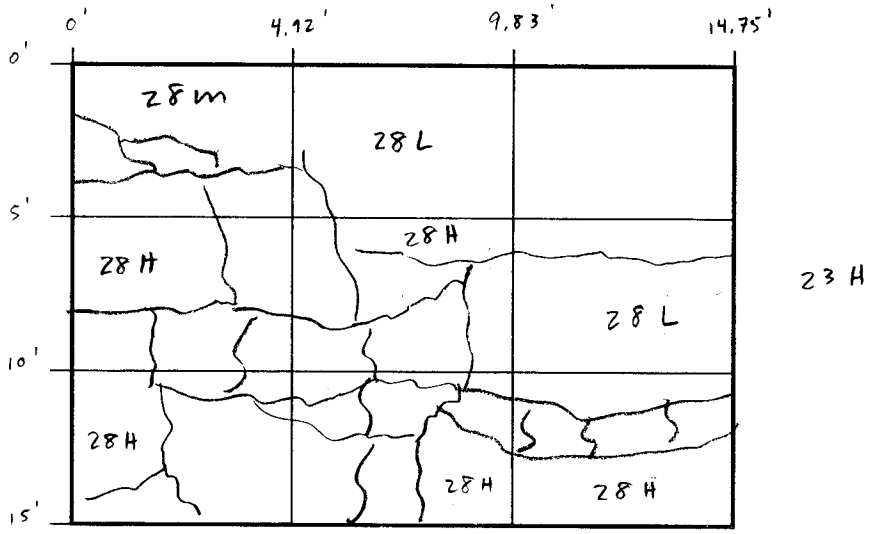

Panel ID: EG1 13 06 R **Panel #:** 13 **Loaded Trucks?** NO
Aggregate: 3/8" RR **Depth:** 06" **Phase #:** 1

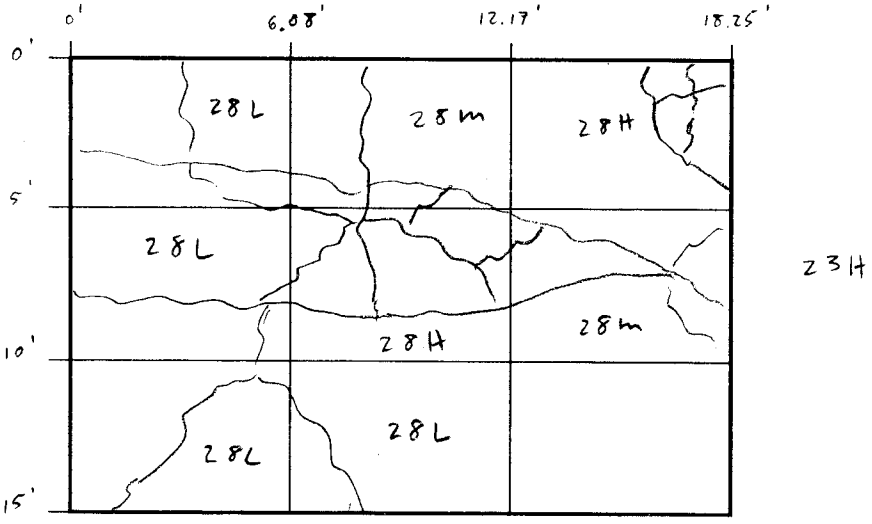

Evolution Paving Distress Survey

Surveyor: Will Goede Reference: ASTM D6433 Date Surveyed: 5/19/09

NOTE: Panels are divided into 9 equal subsections for PCI calculations

Panel ID: EG1608F **Panel #:** 16 **Loaded Trucks?** YES
Aggregate: 3/8" RR **Depth:** 08" **Phase #:** 1

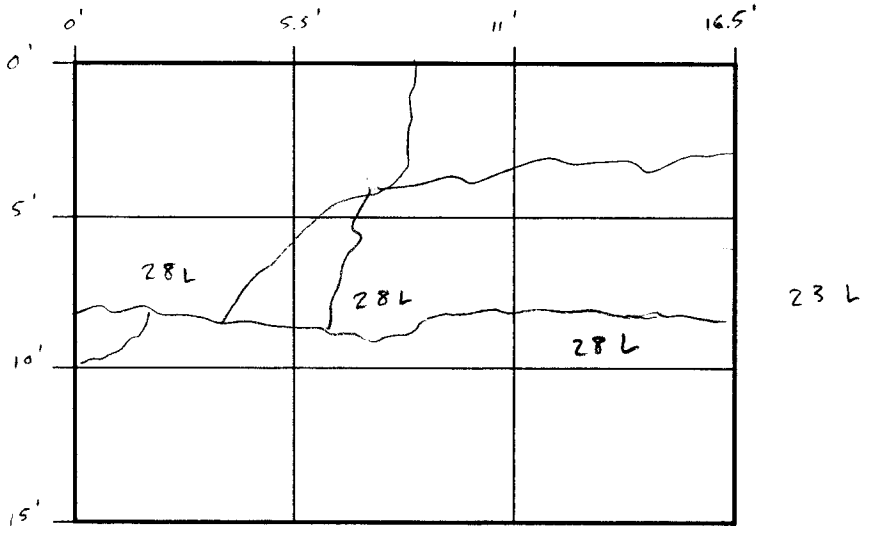

Panel ID: EG1508F **Panel #:** 15 **Loaded Trucks?** NO
Aggregate: 3/8" RR **Depth:** 08" **Phase #:** 1

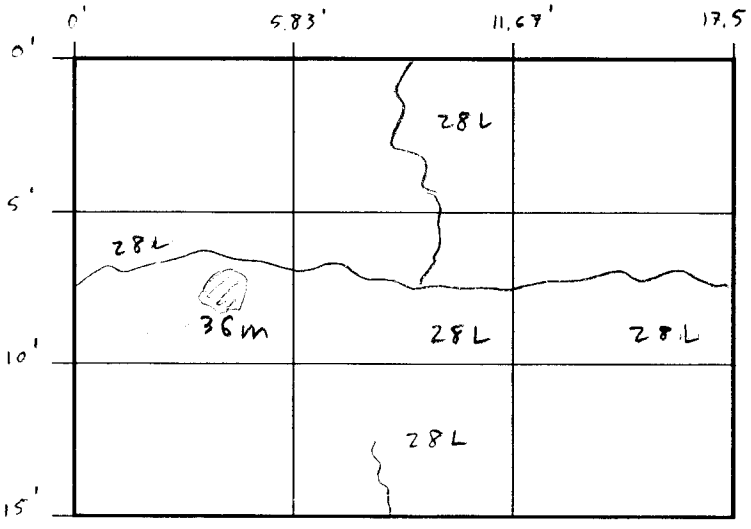

EVOLUTION PAVING D 6433 – 03

CONCRETE SURFACED ROADS AND PARKING LOTS
CONDITION SURVEY DATA SHEET FOR SAMPLE UNIT

BRANCH _____ SECTION 01 SAMPLE UNIT EG10107.5R
SURVEYED BY W.H DATE 5/19/09 SAMPLE AREA 1 Slab

Distress Types

21. Blow up/Buckling
22. Corner Break
23. Divided Slab
24. Durability Crack
25. Faulting
26. Joint Seal
27. Lane/Shoulder
28. Linear Cracking
29. Patching (Large)
30. Patching (Small)
31. Polished Aggregate
32. Popouts
33. Pumping
34. Punchout
35. Railroad Crossing
36. Scaling
37. Shrinkage
38. Spalling Corner
39. Spalling Joint

DIST TYPE	SEV	NO. SLABS	DENSITY %	DEDUCT VALUE
23	L	1	100	50
39	L	1	100	12

SKETCH:

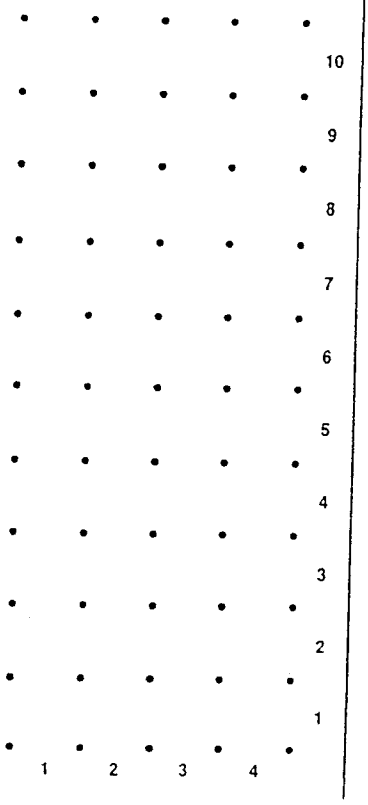

#	Deduct Values								Total	q	CDV
1	50	12							62	2	46
2	50	2							52	1	52
3											
4											
5											
6											
7											
8											

Max CDV = 52
PCI = 100 - Max CDV = 48
Rating = POOR

EVOLUTION PAVING D 6433 – 03

CONCRETE SURFACED ROADS AND PARKING LOTS
CONDITION SURVEY DATA SHEET FOR SAMPLE UNIT

BRANCH _____ SECTION 02 SAMPLE UNIT EG 02 10 C
SURVEYED BY W.H DATE 5/19/09 SAMPLE AREA 1 Slab

Distress Types

21. Blow up/Buckling
22. Corner Break
23. Divided Slab
24. Durability Crack
25. Faulting
26. Joint Seal
27. Lane/Shoulder
28. Linear Cracking
29. Patching (Large)
30. Patching (Small)
31. Polished Aggregate
32. Popouts
33. Pumping
34. Punchout
35. Railroad Crossing
36. Scaling
37. Shrinkage
38. Spalling Corner
39. Spalling Joint

DIST TYPE	SEV	NO. SLABS	DENSITY %	DEDUCT VALUE
37		1	100	4
36	L	1	100	11

SKETCH:

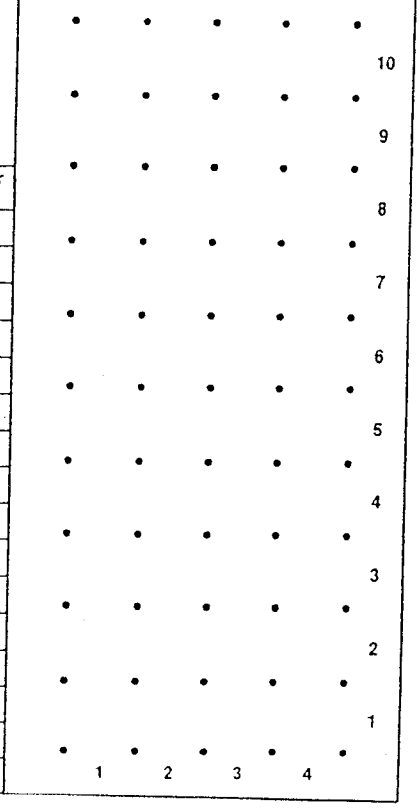

m = 8

#	Deduct Values								Total	q	CDV
1	11	4							15	2	12
2	11	2							13	1	13
3											
4											
5											
6											
7											
8											

Max CDV = 13
PCI = 100 - Max CDV = 87
Rating = Good

EVOLUTION PAVING D 6433 – 03

CONCRETE SURFACED ROADS AND PARKING LOTS
CONDITION SURVEY DATA SHEET FOR SAMPLE UNIT

BRANCH _____ SECTION 03 SAMPLE UNIT EG10310C
SURVEYED BY W.H DATE 5/19/09 SAMPLE AREA 1 Slab

Distress Types

21. Blow up/Buckling
22. Corner Break
23. Divided Slab
24. Durability Crack
25. Faulting
26. Joint Seal
27. Lane/Shoulder
28. Linear Cracking
29. Patching (Large)
30. Patching (Small)
31. Polished Aggregate
32. Popouts
33. Pumping
34. Punchout
35. Railroad Crossing
36. Scaling
37. Shrinkage
38. Spalling Corner
39. Spalling Joint

SKETCH:

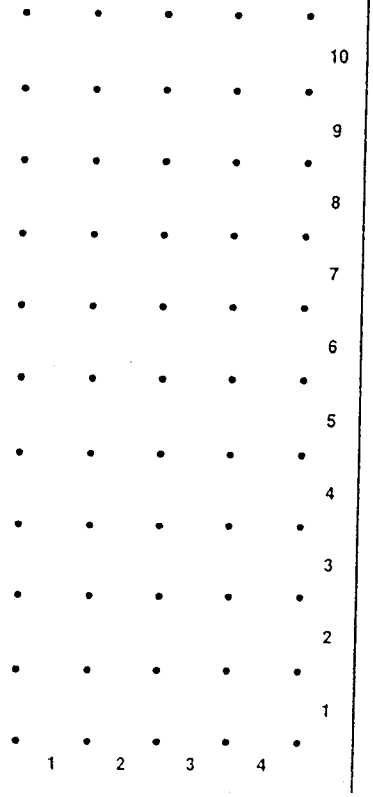

DIST TYPE	SEV	NO. SLABS	DENSITY %	DEDUCT VALUE
36	L	1	100	11

#	Deduct Values								Total	q	CDV
1	11								11	1	11
2											
3											
4											
5											
6											
7											
8											

Max CDV = 11
PCI = 100 - Max CDV = 89
Rating = GOOD

EVOLUTION PAVING D 6433 – 03

CONCRETE SURFACED ROADS AND PARKING LOTS
CONDITION SURVEY DATA SHEET FOR SAMPLE UNIT

BRANCH _____ SECTION 04 SAMPLE UNIT EG20407C
SURVEYED BY W.H DATE 5/19/09 SAMPLE AREA 1 Slab

Distress Types

21. Blow up/Buckling
22. Corner Break
23. Divided Slab
24. Durability Crack
25. Faulting
26. Joint Seal
27. Lane/Shoulder
28. Linear Cracking
29. Patching (Large)
30. Patching (Small)
31. Polished Aggregate
32. Popouts
33. Pumping
34. Punchout
35. Railroad Crossing
36. Scaling
37. Shrinkage
38. Spalling Corner
39. Spalling Joint

DIST TYPE	SEV	NO. SLABS	DENSITY %	DEDUCT VALUE
37	-	1	100	4
39	L	1	100	12

SKETCH:

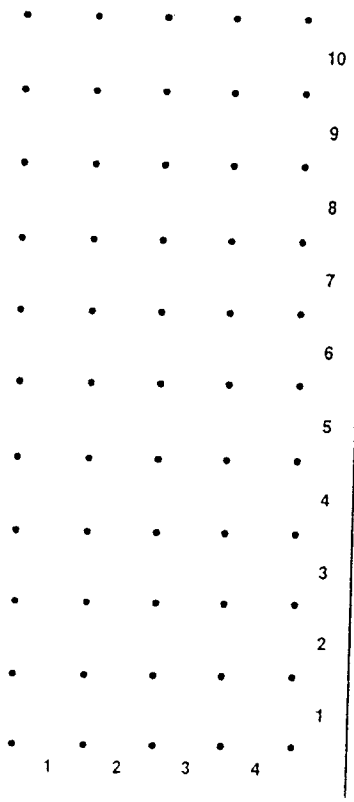

#	Deduct Values								Total	q	CDV
1	12	4							16	2	13
2	12	2							14	1	14
3											
4											
5											
6											
7											
8											

Max CDV = 14
PCI = 100 - Max CDV = 86
Rating = GOOD

EVOLUTION PAVING D 6433 – 03

CONCRETE SURFACED ROADS AND PARKING LOTS
CONDITION SURVEY DATA SHEET FOR SAMPLE UNIT

BRANCH _____ SECTION 05 SAMPLE UNIT EG105 08C
SURVEYED BY W.H DATE 5/19/09 SAMPLE AREA 1 Slab

Distress Types

21. Blow up/Buckling
22. Corner Break
23. Divided Slab
24. Durability Crack
25. Faulting
26. Joint Seal
27. Lane/Shoulder
28. Linear Cracking
29. Patching (Large)
30. Patching (Small)
31. Polished Aggregate
32. Popouts
33. Pumping
34. Punchout
35. Railroad Crossing
36. Scaling
37. Shrinkage
38. Spalling Corner
39. Spalling Joint

DIST TYPE	SEV	NO. SLABS	DENSITY %	DEDUCT VALUE
37	-	1	100	4
36	L	1	100	11

SKETCH:

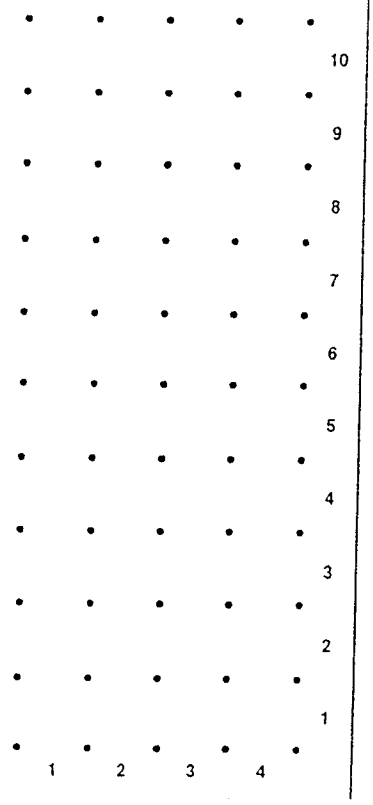

#	Deduct Values								Total	q	CDV
1	11	4							15	2	13
2	11	2							13	1	13
3											
4											
5											
6											
7											
8											

Max CDV = 13
PCI = 100 - Max CDV = 87
Rating = GOOD

EVOLUTION PAVING D 6433 – 03

CONCRETE SURFACED ROADS AND PARKING LOTS
CONDITION SURVEY DATA SHEET FOR SAMPLE UNIT

BRANCH _____ SECTION 06 SAMPLE UNIT EG20605C
SURVEYED BY W.H DATE 5/19/09 SAMPLE AREA 1 Slab

Distress Types

21. Blow up/Buckling
22. Corner Break
23. Divided Slab
24. Durability Crack
25. Faulting
26. Joint Seal
27. Lane/Shoulder
28. Linear Cracking
29. Patching (Large)
30. Patching (Small)
31. Polished Aggregate
32. Popouts
33. Pumping
34. Punchout
35. Railroad Crossing
36. Scaling
37. Shrinkage
38. Spalling Corner
39. Spalling Joint

DIST TYPE	SEV	NO. SLABS	DENSITY %	DEDUCT VALUE
28	L	1	100	23

SKETCH:

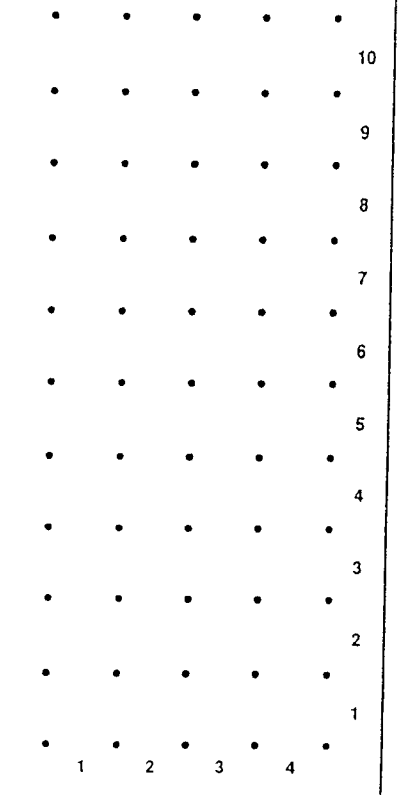

#	Deduct Values								Total	q	CDV
1	23								23	1	23
2											
3											
4											
5											
6											
7											
8											

Max CDV = 23
PCI = 100 - Max CDV = 77
Rating = SATISFACTORY

EVOLUTION PAVING D 6433 – 03

CONCRETE SURFACED ROADS AND PARKING LOTS
CONDITION SURVEY DATA SHEET FOR SAMPLE UNIT

BRANCH _____ SECTION 07 SAMPLE UNIT EG107060
SURVEYED BY Will DATE 5/19/09 SAMPLE AREA 1 Slab

Distress Types

21. Blow up/Buckling
22. Corner Break
23. Divided Slab
24. Durability Crack
25. Faulting
26. Joint Seal
27. Lane/Shoulder
28. Linear Cracking
29. Patching (Large)
30. Patching (Small)
31. Polished Aggregate
32. Popouts
33. Pumping
34. Punchout
35. Railroad Crossing
36. Scaling
37. Shrinkage
38. Spalling Corner
39. Spalling Joint

DIST TYPE	SEV	NO. SLABS	DENSITY %	DEDUCT VALUE
23	M	1	100	74

SKETCH:

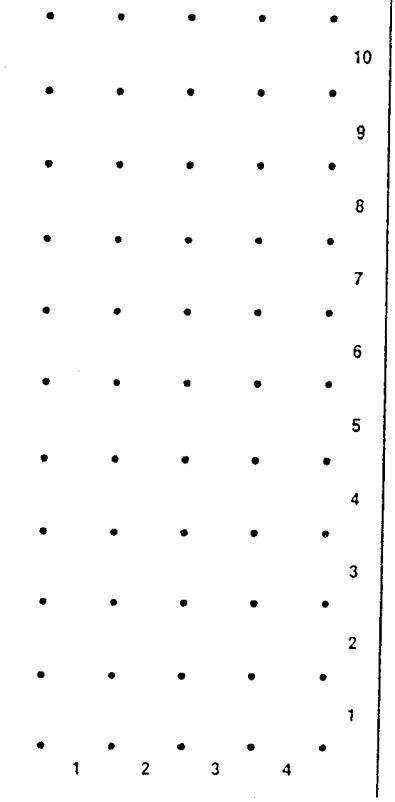

#	Deduct Values								Total	q	CDV
1	74								74	1	74
2											
3											
4											
5											
6											
7											
8											

Max CDV = 74
PCI = 100 - Max CDV = 26
Rating = VERY POOR

EVOLUTION PAVING D 6433 – 03

CONCRETE SURFACED ROADS AND PARKING LOTS
CONDITION SURVEY DATA SHEET FOR SAMPLE UNIT

BRANCH _____ SECTION 08 SAMPLE UNIT EG20805R
SURVEYED BY W.H DATE 5/19/09 SAMPLE AREA 1 Slab

Distress Types

21. Blow up/Buckling
22. Corner Break
23. Divided Slab
24. Durability Crack
25. Faulting
26. Joint Seal
27. Lane/Shoulder
28. Linear Cracking
29. Patching (Large)
30. Patching (Small)
31. Polished Aggregate
32. Popouts
33. Pumping
34. Punchout
35. Railroad Crossing
36. Scaling
37. Shrinkage
38. Spalling Corner
39. Spalling Joint

DIST TYPE	SEV	NO. SLABS	DENSITY %	DEDUCT VALUE
23	H	1	100	92

SKETCH:

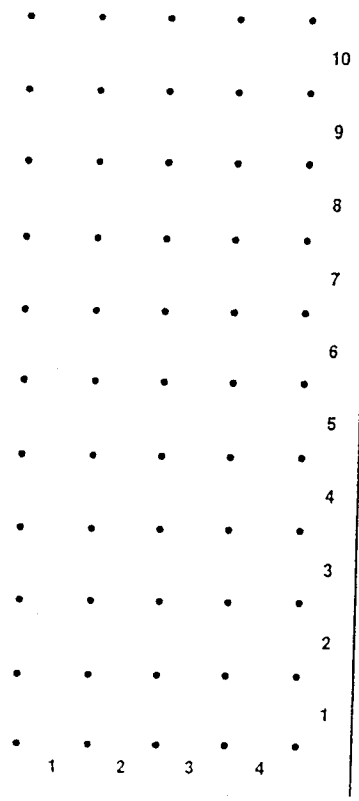

#	Deduct Values								Total	q	CDV
1	92								92	1	92
2											
3											
4											
5											
6											
7											
8											

Max CDV = 92
PCI = 100 - Max CDV = 8
Rating = FAILED

EVOLUTION PAVING D 6433 – 03

CONCRETE SURFACED ROADS AND PARKING LOTS
CONDITION SURVEY DATA SHEET FOR SAMPLE UNIT

BRANCH _____ SECTION 09 SAMPLE UNIT EG109 04 C
SURVEYED BY W.H DATE 5/19/09 SAMPLE AREA 1 Slab

Distress Types

21. Blow up/Buckling
22. Corner Break
23. Divided Slab
24. Durability Crack
25. Faulting
26. Joint Seal
27. Lane/Shoulder
28. Linear Cracking
29. Patching (Large)
30. Patching (Small)
31. Polished Aggregate
32. Popouts
33. Pumping
34. Punchout
35. Railroad Crossing
36. Scaling
37. Shrinkage
38. Spalling Corner
39. Spalling Joint

DIST TYPE	SEV	NO. SLABS	DENSITY %	DEDUCT VALUE
37	L	1	100	4
22	L	1	100	50
34	L	1	100	54

SKETCH:

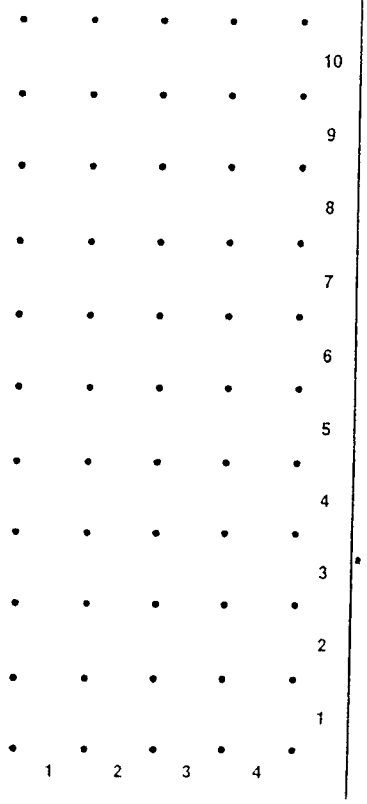

#	Deduct Values								Total	q	CDV
1	54	50	4						108	3	68
2	54	50	2						106	2	73
3	54	2	2						58	1	58
4											
5											
6											
7											
8											

Max CDV = 73
PCI = 100 - Max CDV = 27
Rating = VERY POOR

EVOLUTION PAVING D 6433 – 03

CONCRETE SURFACED ROADS AND PARKING LOTS
CONDITION SURVEY DATA SHEET FOR SAMPLE UNIT

BRANCH _____ SECTION 10 SAMPLE UNIT EG21004R
SURVEYED BY W.H DATE 5/19/09 SAMPLE AREA 1 Slab

Distress Types

21. Blow up/Buckling
22. Corner Break
23. Divided Slab
24. Durability Crack
25. Faulting
26. Joint Seal
27. Lane/Shoulder
28. Linear Cracking
29. Patching (Large)
30. Patching (Small)
31. Polished Aggregate
32. Popouts
33. Pumping
34. Punchout
35. Railroad Crossing
36. Scaling
37. Shrinkage
38. Spalling Corner
39. Spalling Joint

DIST TYPE	SEV	NO. SLABS	DENSITY %	DEDUCT VALUE
23	H	1	100	92

SKETCH:

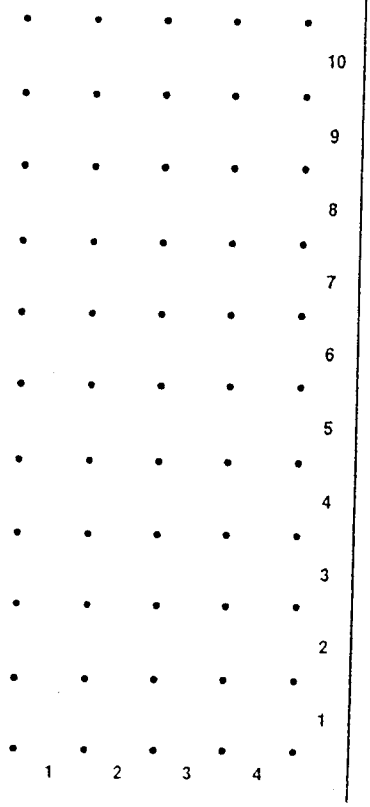

#	Deduct Values								Total	q	CDV
1	92								92	1	92
2											
3											
4											
5											
6											
7											
8											

Max CDV = 92
PCI = 100 - Max CDV = 8
Rating = FAILED

EVOLUTION PAVING D 6433 – 03

CONCRETE SURFACED ROADS AND PARKING LOTS
CONDITION SURVEY DATA SHEET FOR SAMPLE UNIT

BRANCH _____ SECTION 11 SAMPLE UNIT EG1104R
SURVEYED BY W.H DATE 5/19/09 SAMPLE AREA 1 Slab

Distress Types

21. Blow up/Buckling
22. Corner Break
23. Divided Slab
24. Durability Crack
25. Faulting
26. Joint Seal
27. Lane/Shoulder
28. Linear Cracking
29. Patching (Large)
30. Patching (Small)
31. Polished Aggregate
32. Popouts
33. Pumping
34. Punchout
35. Railroad Crossing
36. Scaling
37. Shrinkage
38. Spalling Corner
39. Spalling Joint

SKETCH:

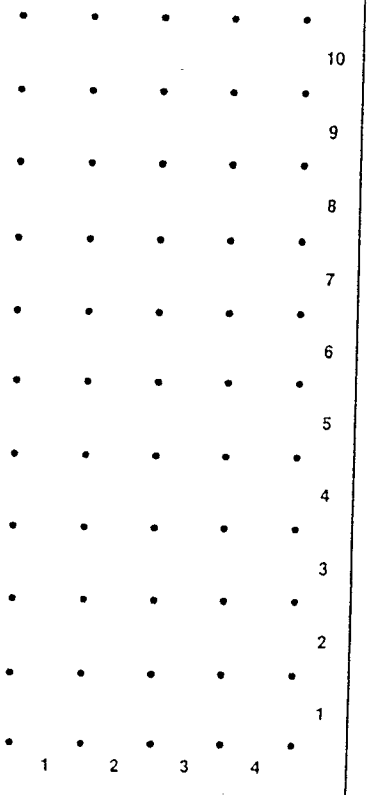

DIST TYPE	SEV	NO. SLABS	DENSITY %	DEDUCT VALUE
23	H	1	100	92

#	Deduct Values								Total	q	CDV
1	92								92	1	92
2											
3											
4											
5											
6											
7											
8											

Max CDV = 92
PCI = 100 - Max CDV = 8
Rating = FAILED

EVOLUTION PAVING D 6433 – 03

CONCRETE SURFACED ROADS AND PARKING LOTS
CONDITION SURVEY DATA SHEET FOR SAMPLE UNIT

BRANCH _____ SECTION 12 SAMPLE UNIT EG212 04R
SURVEYED BY W.H DATE 5/19/09 SAMPLE AREA 1 Slab

Distress Types

21. Blow up/Buckling
22. Corner Break
23. Divided Slab
24. Durability Crack
25. Faulting
26. Joint Seal
27. Lane/Shoulder
28. Linear Cracking
29. Patching (Large)
30. Patching (Small)
31. Polished Aggregate
32. Popouts
33. Pumping
34. Punchout
35. Railroad Crossing
36. Scaling
37. Shrinkage
38. Spalling Corner
39. Spalling Joint

DIST TYPE	SEV	NO. SLABS	DENSITY %	DEDUCT VALUE
23	H	1	100	92

SKETCH:

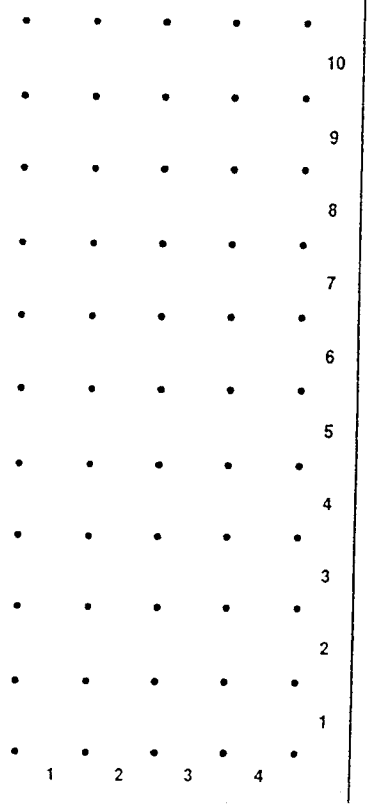

#	Deduct Values								Total	q	CDV
1	92								92	1	92
2											
3											
4											
5											
6											
7											
8											

Max CDV = 92
PCI = 100 - Max CDV = 8
Rating = FAILED

EVOLUTION PAVING D 6433 – 03

CONCRETE SURFACED ROADS AND PARKING LOTS
CONDITION SURVEY DATA SHEET FOR SAMPLE UNIT

BRANCH _____ SECTION 13 SAMPLE UNIT EG11306R
SURVEYED BY W.H DATE 5/19/09 SAMPLE AREA 1 Slab

Distress Types

21. Blow up/Buckling
22. Corner Break
23. Divided Slab
24. Durability Crack
25. Faulting
26. Joint Seal
27. Lane/Shoulder
28. Linear Cracking
29. Patching (Large)
30. Patching (Small)
31. Polished Aggregate
32. Popouts
33. Pumping
34. Punchout
35. Railroad Crossing
36. Scaling
37. Shrinkage
38. Spalling Corner
39. Spalling Joint

DIST TYPE	SEV	NO. SLABS	DENSITY %	DEDUCT VALUE
23	H	1	100	92

SKETCH:

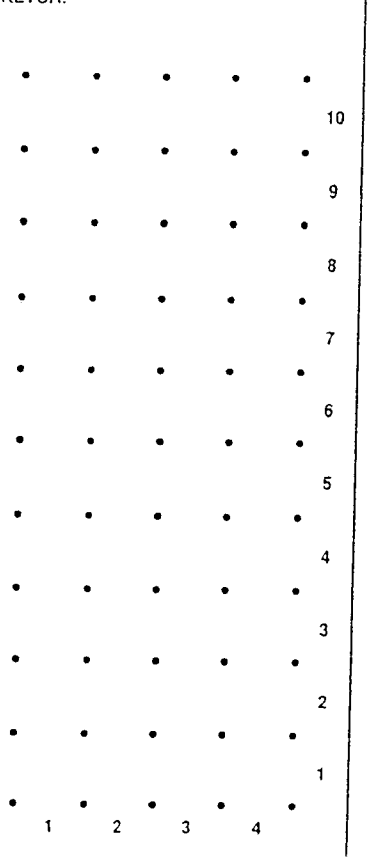

#	Deduct Values								Total	q	CDV
1	92								92	1	92
2											
3											
4											
5											
6											
7											
8											

Max CDV = 92
PCI = 100 - Max CDV = 8
Rating = FAILED

EVOLUTION PAVING D 6433 – 03

CONCRETE SURFACED ROADS AND PARKING LOTS
CONDITION SURVEY DATA SHEET FOR SAMPLE UNIT

BRANCH _____ SECTION 14 SAMPLE UNIT EG11406R
SURVEYED BY W.H DATE 5/19/09 SAMPLE AREA 1 Slab

Distress Types

21. Blow up/Buckling
22. Corner Break
23. Divided Slab
24. Durability Crack
25. Faulting
26. Joint Seal
27. Lane/Shoulder
28. Linear Cracking
29. Patching (Large)
30. Patching (Small)
31. Polished Aggregate
32. Popouts
33. Pumping
34. Punchout
35. Railroad Crossing
36. Scaling
37. Shrinkage
38. Spalling Corner
39. Spalling Joint

DIST TYPE	SEV	NO. SLABS	DENSITY %	DEDUCT VALUE
23	H	1	100	92

SKETCH:

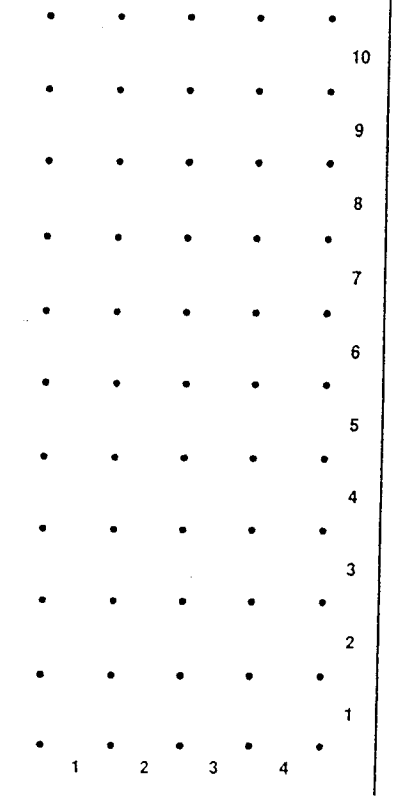

#	Deduct Values								Total	q	CDV
1	92								92	1	92
2											
3											
4											
5											
6											
7											
8											

Max CDV = 92
PCI = 100 - Max CDV = 8
Rating = FAILED

EVOLUTION PAVING D 6433 – 03

CONCRETE SURFACED ROADS AND PARKING LOTS
CONDITION SURVEY DATA SHEET FOR SAMPLE UNIT

BRANCH _____ SECTION 15 SAMPLE UNIT EG11508R
SURVEYED BY Will DATE 5/19/09 SAMPLE AREA 1 Slab

Distress Types

21. Blow up/Buckling
22. Corner Break
23. Divided Slab
24. Durability Crack
25. Faulting
26. Joint Seal
27. Lane/Shoulder
28. Linear Cracking
29. Patching (Large)
30. Patching (Small)
31. Polished Aggregate
32. Popouts
33. Pumping
34. Punchout
35. Railroad Crossing
36. Scaling
37. Shrinkage
38. Spalling Corner
39. Spalling Joint

DIST TYPE	SEV	NO. SLABS	DENSITY %	DEDUCT VALUE
28	M	1	100	38
36	L	1	100	11

SKETCH:

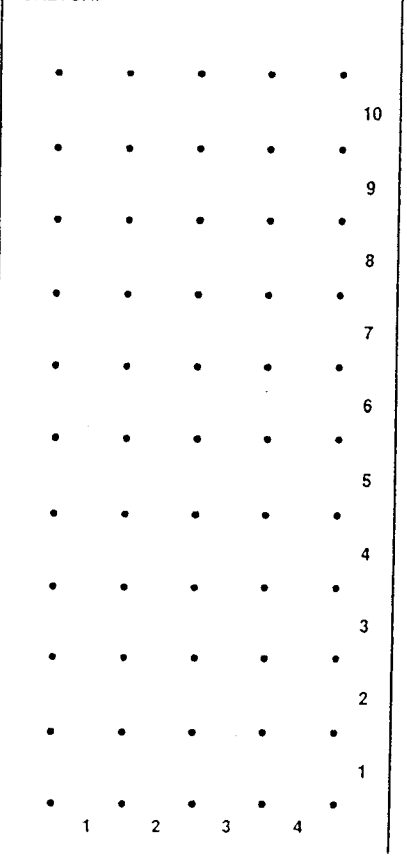

#	Deduct Values								Total	q	CDV
1	38	11							49	2	40
2	38	2							40	1	40
3											
4											
5											
6											
7											
8											

Max CDV = 40
PCI = 100 - Max CDV = 60
Rating = FAIR

EVOLUTION PAVING D 6433 – 03

CONCRETE SURFACED ROADS AND PARKING LOTS
CONDITION SURVEY DATA SHEET FOR SAMPLE UNIT

BRANCH _____ SECTION 16 SAMPLE UNIT EG11608R
SURVEYED BY W.H DATE 5/19/09 SAMPLE AREA 1 Slab

Distress Types

21. Blow up/Buckling
22. Corner Break
23. Divided Slab
24. Durability Crack
25. Faulting
26. Joint Seal
27. Lane/Shoulder
28. Linear Cracking
29. Patching (Large)
30. Patching (Small)
31. Polished Aggregate
32. Popouts
33. Pumping
34. Punchout
35. Railroad Crossing
36. Scaling
37. Shrinkage
38. Spalling Corner
39. Spalling Joint

DIST TYPE	SEV	NO. SLABS	DENSITY %	DEDUCT VALUE
23	L	1	100	50

SKETCH:

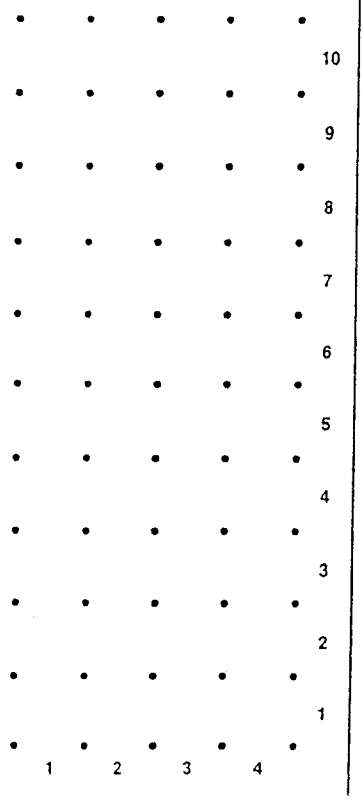

#	Deduct Values								Total	q	CDV
1	50								50	1	50
2											
3											
4											
5											
6											
7											
8											

Max CDV = 50
PCI = 100 - Max CDV = 50
Rating = POOR

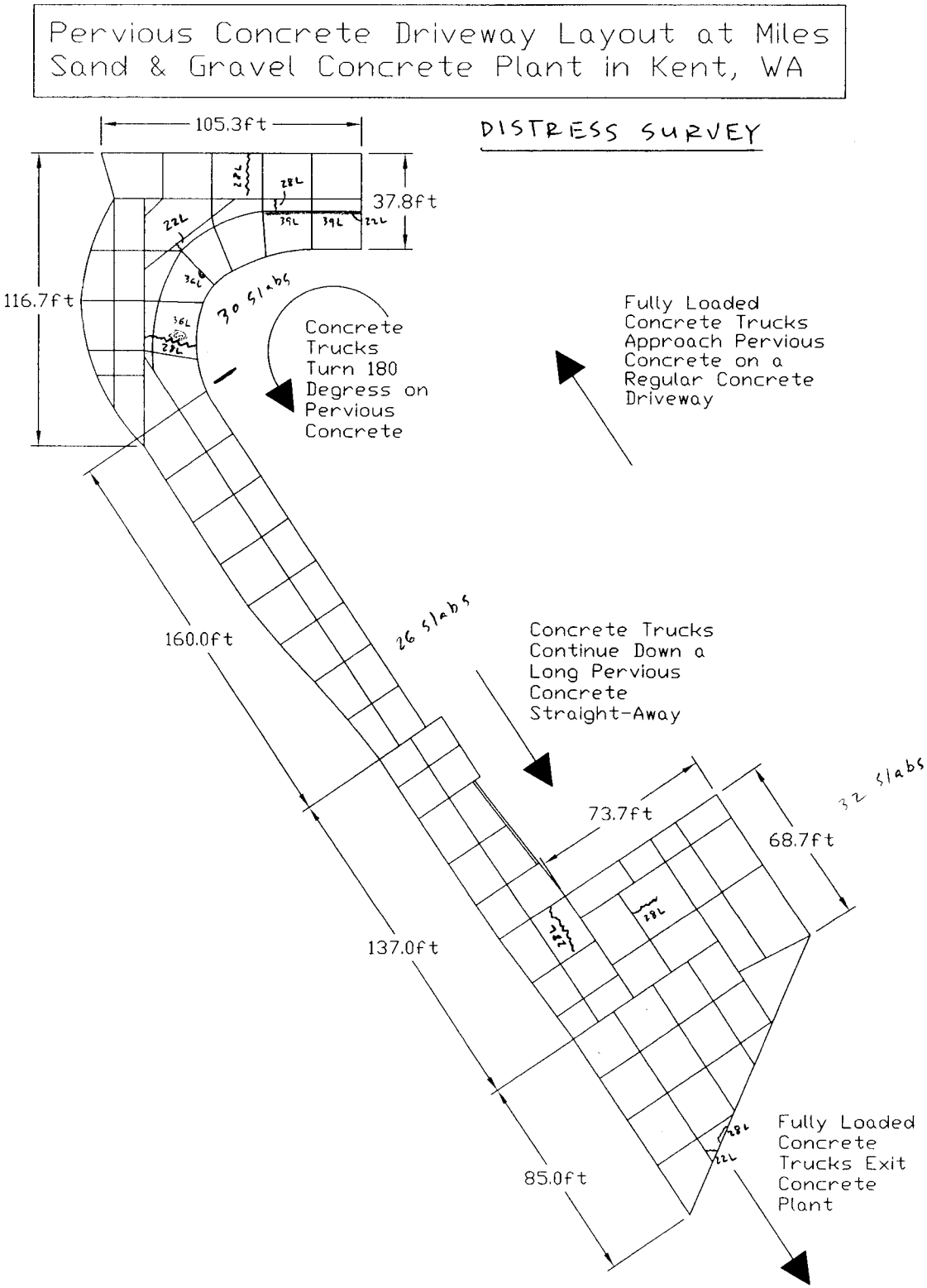
Pervious Concrete Driveway Layout at Miles Sand & Gravel Concrete Plant in Kent, WA
105.3ft
DISTRESS SURVEY
37.8ft
116.7ft
30 slabs
Concrete Trucks Turn 180 Degress on Pervious Concrete
Fully Loaded Concrete Trucks Approach Pervious Concrete on a Regular Concrete Driveway
160.0ft
26 slabs
Concrete Trucks Continue Down a Long Pervious Concrete Straight-Away
73.7ft
68.7ft
32 slabs
137.0ft
85.0ft
Fully Loaded Concrete Trucks Exit Concrete Plant

MILES SAND & GRAVEL

D 6433 – 03

CONCRETE SURFACED ROADS AND PARKING LOTS
CONDITION SURVEY DATA SHEET FOR SAMPLE UNIT

BRANCH _____ SECTION 180° Turn SAMPLE UNIT _____
SURVEYED BY W.H DATE 8/17/09 SAMPLE AREA 30 Slabs

Distress Types

21. Blow up/Buckling
22. Corner Break
23. Divided Slab
24. Durability Crack
25. Faulting
26. Joint Seal
27. Lane/Shoulder
28. Linear Cracking
29. Patching (Large)
30. Patching (Small)
31. Polished Aggregate
32. Popouts
33. Pumping
34. Punchout
35. Railroad Crossing
36. Scaling
37. Shrinkage
38. Spalling Corner
39. Spalling Joint

DIST TYPE	SEV	NO. SLABS	DENSITY %	DEDUCT VALUE
22	L	2	6.67	5
28	L	3	10.0	6
39	L	2	6.67	2
36	L	2	6.67	2

SKETCH:

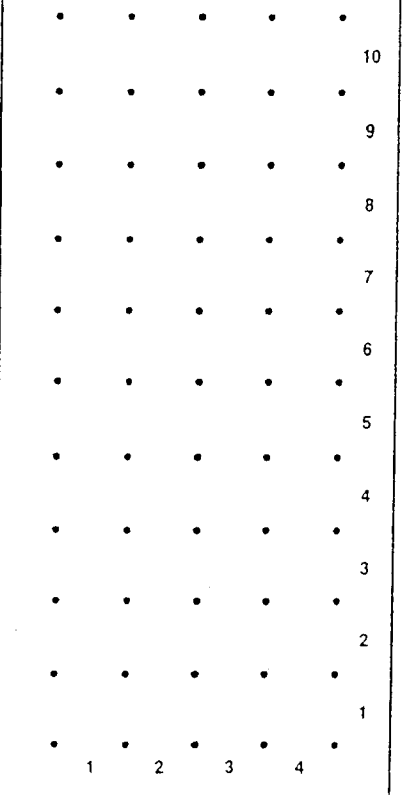

#	Deduct Values								Total	q	CDV
1	6	5	2	2					15	2	12
2	6	2	2	2					12	1	12
3											
4											
5											
6											
7											
8											

Max CDV = 12
PCI = 100 - Max CDV = 88
Rating = Good

MILES SAND & GRAVEL

D 6433 – 03

CONCRETE SURFACED ROADS AND PARKING LOTS
CONDITION SURVEY DATA SHEET FOR SAMPLE UNIT

BRANCH _____ SECTION Straight-away SAMPLE UNIT _____
SURVEYED BY W.H DATE 8/17/04 SAMPLE AREA 26 Slabs

Distress Types

21. Blow up/Buckling
22. Corner Break
23. Divided Slab
24. Durability Crack
25. Faulting
26. Joint Seal
27. Lane/Shoulder
28. Linear Cracking
29. Patching (Large)
30. Patching (Small)
31. Polished Aggregate
32. Popouts
33. Pumping
34. Punchout
35. Railroad Crossing
36. Scaling
37. Shrinkage
38. Spalling Corner
39. Spalling Joint

DIST TYPE	SEV	NO. SLABS	DENSITY %	DEDUCT VALUE
-	-	-	-	-

SKETCH:

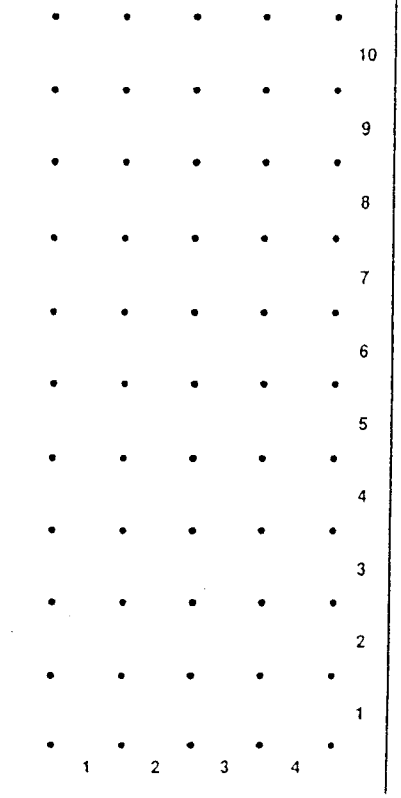

#	Deduct Values								Total	q	CDV
1											0
2											
3											
4											
5											
6											
7											
8											

Max CDV = 0
PCI = 100 - Max CDV = 100
Rating = GOOD

16

MILES SAND & GRAVEL

D 6433 – 03

CONCRETE SURFACED ROADS AND PARKING LOTS
CONDITION SURVEY DATA SHEET FOR SAMPLE UNIT

BRANCH _____ SECTION Exit Pad SAMPLE UNIT _____

SURVEYED BY W.H DATE 8/17/09 SAMPLE AREA 32 Slabs

Distress Types

21. Blow up/Buckling
22. Corner Break
23. Divided Slab
24. Durability Crack
25. Faulting
26. Joint Seal
27. Lane/Shoulder
28. Linear Cracking
29. Patching (Large)
30. Patching (Small)
31. Polished Aggregate
32. Popouts
33. Pumping
34. Punchout
35. Railroad Crossing
36. Scaling
37. Shrinkage
38. Spalling Corner
39. Spalling Joint

DIST TYPE	SEV	NO. SLABS	DENSITY %	DEDUCT VALUE
22	L	1	3.13	3
28	L	3	9.38	6

SKETCH:

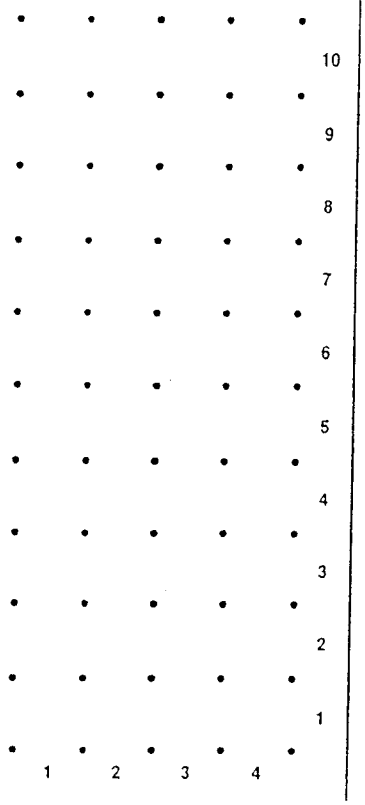

#	Deduct Values								Total	q	CDV
1	6	3							9	2	6
2	6	2							8	1	8
3											
4											
5											
6											
7											
8											

Max CDV = 8

PCI = 100 - Max CDV = 92

Rating = Good

16

MILES SAND & GRAVEL

D 6433 – 03

CONCRETE SURFACED ROADS AND PARKING LOTS
CONDITION SURVEY DATA SHEET FOR SAMPLE UNIT

BRANCH _____ SECTION Entire Driveway SAMPLE UNIT _____

SURVEYED BY W.H DATE 8/17/09 SAMPLE AREA 88 Slabs

Distress Types

21. Blow up/Buckling
22. Corner Break
23. Divided Slab
24. Durability Crack
25. Faulting
26. Joint Seal
27. Lane/Shoulder
28. Linear Cracking
29. Patching (Large)
30. Patching (Small)
31. Polished Aggregate
32. Popouts
33. Pumping
34. Punchout
35. Railroad Crossing
36. Scaling
37. Shrinkage
38. Spalling Corner
39. Spalling Joint

DIST TYPE	SEV	NO. SLABS	DENSITY %	DEDUCT VALUE
22	L	3	3.41	3
28	L	6	6.82	4
36	L	2	2.27	0
39	L	2	2.27	0

SKETCH:

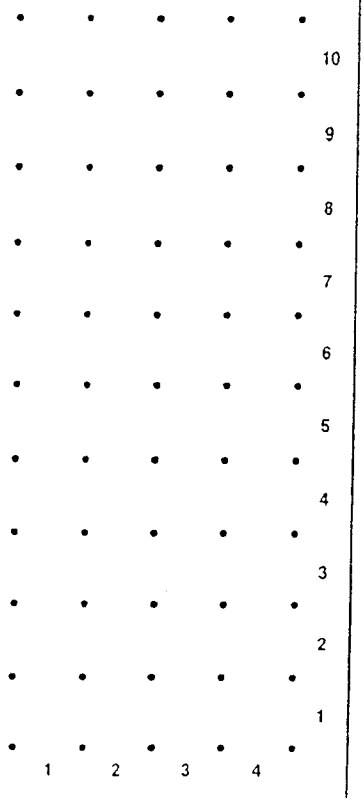

#	Deduct Values								Total	q	CDV
1	4	3	0	0					7	2	5
2	4	2	0	0					6	1	6
3											
4											
5											
6											
7											
8											

Max CDV = 6

PCI = 100 - Max CDV = 94

Rating = GOOD

16

9.3 APPENDIX C – THICKNESS DESIGN CALCULATIONS

Subgrade Modulus Calculations				
	# of blows	Accumulative Penetration (in)	Pentration Index (mm/blow)	Resilient Modulus M_r (MPa)
DCP-1	0	0		
	10	2.5	6.35	93
	10	6.125	9.2075	84
	10	7.325	3.048	104
	10	8.5	2.9845	104
	20	10.5	2.54	106
DCP-2	0	0		
	10	8.5	21.59	43
	10	15	16.51	60
	10	17	5.08	97
DCP-3	0	0		
	10	6	15.24	64
	10	10.5	11.43	77
	10	16.5	15.24	64
	10	21.5	12.7	72
DCP-4	0	0		
	10	5	12.7	72
	10	9	10.16	81
	10	12	7.62	89
	20	13.5	1.905	108
DCP-5	0	0		
	10	4.5	11.43	77
	10	7	6.35	93
	10	9	5.08	97
	20	11	2.54	106
DCP-6	0	0		
	10	4	10.16	81
	10	7.75	9.525	83
	10	12	10.795	79

Average	9.14	84

NOTE: Number of blows and accumulative penetration data was taken from a geotechnical report completed by Robert J. Slyh of Willamette Engineering and Earth Sciences on October 22, 2004

Name: *Will Goede* | **Class:** *Research - Pervious Concrete*

Reference: AASTHO (1993) design method

= adjustable values

= outputs of interest

Problem Statement:

Use AASHTO (1993) Method to calculate required thickness of pervious concrete panels at Evolution Paving using material characterization results and observed number of loads to first cracking.

Solution:

Material Characterization Results

Panel #	Depth (in)	Loaded Trucks?	Unit Weight (pcf)	Avg Flexural Strength (psi)	Avg Compressive Strength (psi)	Avg In-Situ Porosity	PCI	2007 ASTM Rating
1	7.5	no	122.1	297	3517	13.7%	48	Poor
2	10	yes	111.1		1780	21.4%	87	Good
3	10	no	126.7		5031	11.0%	89	Good
4	7	yes	117.3	284	2937	17.8%	86	Good
5	8	no	118.2	329	2904	17.0%	87	Good
6	5	yes	112.1	206	2261	22.2%	77	Satisfactory
7	6	no					26	Very Poor
8	5	yes	113.5	275	2836	20.7%	8	Failed
9	4	no					27	Very Poor
10	4	yes					8	Failed
11	4	no	109.0		2518	27.1%	8	Failed
12	4	yes	116.5		2729	19.9%	8	Failed
13	6	no	119.8	260	2884	19.1%	8	Failed
14	6	yes	122.3		4200	12.9%	8	Failed
15	8	no					60	Fair
16	8	yes	123.7	407	3473	11.9%	50	Poor

**The procedure for determining the thickness of pervious concrete is the same as AASHTO rigid pavement design,

Standard Deviation $S_o := 0.39$ Recommeded by Huang, 2004 for rigid pavements

Reliability $Rel := 85$ *for urban freeway reccomended values are 85-99.9 (ref Slide 8 in Handout received 9/1/09)*

Standard Normal Deviate $Z_R := -1.037$ *ref Slide 11 in Handout received 9/1/09*

Terminal Serviceability Index $p_t := 3.0$ *ref Slide 12 in Handout received 9/1/09*

Change in Serviceability Index $\Delta PSI := 4.5 - p_t$ $\Delta PSI = 1.5$

PANEL 2 DESIGN

panel number $i := 2$

Total Life ESALS

Calculated EALF for full concrete truck $EALF := 2 \cdot .082 + 1.92$ $EALF = 2.08$

Number of Loads at 1st Cracking $n := 65000$

Total Design Life ESALS $W_{18} := n \cdot EALF$ $W_{18} = 135460$

Subgrade Properties

From Geotech Report at Evolution Paving $PI_{avg} := 9.14 \frac{mm}{blow}$ *see excel sheet for calculations*

NOTE: Dynamic Cone Penetration Test was performed

Soil Resilient Modulus $M_r := \left(-3279 \cdot PI_{avg} + 114100\right) \cdot kPa$

$M_r = 84.13 \cdot MPa$ $M_r = 12202\ psi$ *Ref Dynamic Cone Penetration Test for Subgrade Assessment by Salgado & Yoon*

Assume subbase resilient modulus $E_{SB} := 20000 psi$

Subbase Thickness $D_{SB} := 14in - h_i$ $D_{SB} = 4 \cdot in$

Composite Subgrade Reaction $k := 600 pci$ $k = 162.87 \cdot \frac{MPa}{m}$ *Ref Fig 3.3 in AASHTO (1993)*

Corrected K Value for Potential Loss of Support $LS := 2.5$ *Ref Table 2.7 in AASTHO (1993)*

NOTE: Assumed fine-grained or natural subgrade materials $k := 28\ pci$ *Ref Figure 3.6 in AASTHO (1993)*

Pervious Concrete Properties

Compressive Strength $f'_{c_i} = 1780.46\ psi$ *from my graduate research*

Modulus of Rupture $S'_{c_i} := 5.3 \cdot \sqrt{f'_{c_i} \cdot psi}$ $S'_{c_i} = 223.6\ psi$ *from my graduate research*

NOTE: Since Flexural Test was unable to be performed on any samples from this panel, I use relationship between MOR and f`c developed from experiemental results

Modulus of Elasticity $E_{c_i} := 39.1 \cdot \left(w_{pc_i} \div pcf\right)^{1.5} \cdot \sqrt{f'_{c_i} \cdot psi}$ $E_{c_i} = 1932 \cdot ksi$ *from my graduate research*

Drainage Coefficient

$C_d := 1.1$ *Ref Table 12.20 in Pavement Analysis and Design by Huang*

NOTE: with proper drainage the structure should not be exposed to saturation moisture levels often

Load Transfer Coefficient

$J := 3.8$ NOTE: Pervous concrete is not tied *Ref Table 2.6 AASHTO (1993)*

Find Minimum Thickness

Given $D_i := 12$ *Ref Eqn 12.21 in Pavement Analysis and Design by Huang*

$$\log\left(W_{18}\right) = Z_R \cdot S_o + 7.35 \cdot \log\left(D_i + 1\right) - .06 + \frac{\log\left(\frac{\Delta PSI}{4.5 - 1.5}\right)}{1 + \frac{1.624 \cdot 10^7}{\left(D_i + 1\right)^{8.46}}} + \left(4.22 - .32 p_t\right) \cdot \log\left[\frac{\frac{S'_{c_i}}{psi} \cdot C_d \cdot \left[\left(D_i\right)^{0.75} - 1.132\right]}{215.63 \cdot J \cdot \left[\left(D_i\right)^{0.75} - \frac{18.42}{\left(\frac{E_{c_i}}{k \cdot psi}\right)^{.25}}\right]}\right]$$

Minimum Thickness of Pervious Concrete from AASHTO $D := Find(D)$ $D_i = 9.78$ in

Actual Pervious Concrete Depth at Evolution Paving $h_i = 10 \cdot in$

PANEL 4 DESIGN

panel number $i := 4$

Total Life ESALS

Calculated EALF for full concrete truck $EALF := 2 \cdot .082 + 1.92$ $EALF = 2.08$

Number of Loads at 1st Cracking $n := 50780$

Total Design Life ESALS $W_{18} := n \cdot EALF$ $W_{18} = 105825.52$

Subgrade Properties

From Geotech Report at Evolution Paving $PI_{avg} := 9.14 \frac{mm}{blow}$ *see excel sheet for calculations*

NOTE: Dynamic Cone Penetration Test was performed

Soil Resilient Modulus $M_r := \left(-3279 \cdot PI_{avg} + 114100\right) \cdot kPa$ $M_r = 84.13 \cdot MPa$ $M_r = 12202\ psi$ *Ref Dynamic Cone Penetration Test for Subgrade Assessment by Salgado & Yoon*

Assume subbase resilient modulus $E_{SB} := 20000 psi$

Subbase Thickness $D_{SB} := 14in - h_i$ $D_{SB} = 7 \cdot in$

Composite Subgrade Reaction $k := 600 pci$ $k = 162.87 \cdot \frac{MPa}{m}$ *Ref Fig 3.3 in AASHTO (1993)*

Corrected K Value for Potential Loss of Support $LS := 2.5$ *Ref Table 2.7 in AASTHO (1993)*

NOTE: Assumed fine-grained or natural subgrade materials $k := 28\ pci$ *Ref Figure 3.6 in AASTHO (1993)*

Pervious Concrete Properties

Compressive Strength $f'_{c_i} = 2936.97\ psi$ *from my graduate research*

Modulus of Rupture $S'_{c_i} := MOR_i$ $S'_{c_i} = 283.8\ psi$ *from my graduate research*

Modulus of Elasticity $E_{c_i} := 39.1 \cdot \left(w_{pc_i} \div pcf\right)^{1.5} \cdot \sqrt{f'_{c_i} \cdot psi}$ $E_{c_i} = 2693 \cdot ksi$ *from my graduate research*

Drainage Coefficient

$C_d := 1.1$ *Ref Table 12.20 in Pavement Analysis and Design by Huang*

NOTE: with proper drainage the structure should not be exposed to saturation moisture levels often

Load Transfer Coefficient

$J := 3.8$ NOTE: Pervous concrete is not tied *Ref Table 2.6 AASHTO (1993)*

Find Minimum Thickness

Given $D_i := 12$ *Ref Eqn 12.21 in Pavement Analysis & Design by Huang*

$$\log\left(W_{18}\right) = Z_R \cdot S_o + 7.35 \cdot \log\left(D_i + 1\right) - .06 + \frac{\log\left(\frac{\Delta PSI}{4.5 - 1.5}\right)}{1 + \frac{1.624 \cdot 10^7}{\left(D_i + 1\right)^{8.46}}} + \left(4.22 - .32 p_t\right) \cdot \log\left[\frac{\frac{S'_{c_i}}{psi} \cdot C_d \cdot \left[\left(D_i\right)^{0.75} - 1.132\right]}{215.63 \cdot J \cdot \left[\left(D_i\right)^{0.75} - \frac{18.42}{\left(\frac{E_{c_i}}{k \cdot psi}\right)^{.25}}\right]}\right]$$

Minimum Thickness of Pervious Concrete from AASHTO $D := \text{Find}(D)$ $D_i = 8.43$ in

Actual Pervious Concrete Depth at Evolution Paving $h_i = 7 \cdot in$

PANEL 6 DESIGN

panel number $i := 6$

Total Life ESALS

Calculated EALF for full concrete truck $EALF := 2 \cdot .082 + 1.92$ $EALF = 2.08$

Number of Loads at 1st Cracking $n := 27000$

Total Design Life ESALS $W_{18} := n \cdot EALF$ $W_{18} = 56268$

Subgrade Properties

From Geotech Report at Evolution Paving $PI_{avg} := 9.14 \frac{mm}{blow}$ *see excel sheet for calculations*

NOTE: Dynamic Cone Penetration Test was performed

Soil Resilient Modulus $M_r := \left(-3279 \cdot PI_{avg} + 114100\right) \cdot kPa$ $M_r = 84.13 \cdot MPa$ $M_r = 12202\ psi$ *Ref Dynamic Cone Penetration Test for Subgrade Assessment by Salgado & Yoon*

Assume subbase resilient modulus $E_{SB} := 20000 psi$

Subbase Thickness $D_{SB} := 14in - h_i$ $D_{SB} = 9 \cdot in$

Composite Subgrade Reaction $k := 600 pci$ $k = 162.87 \cdot \frac{MPa}{m}$ *Ref Fig 3.3 in AASHTO (1993)*

Corrected K Value for Potential Loss of Support $LS := 2.5$ *Ref Table 2.7 in AASTHO (1993)*

NOTE: Assumed fine-grained or natural subgrade materials $k := 28\ pci$ *Ref Figure 3.6 in AASTHO (1993)*

Pervious Concrete Properties

Compressive Strength $f'_{c_i} = 2260.52\ psi$ *from my graduate research*

Modulus of Rupture $S'_{c_i} := MOR_i$ $S'_{c_i} = 206.1\ psi$ *from my graduate research*

Modulus of Elasticity $E_{c_i} := 39.1 \cdot \left(w_{pc_i} \div pcf\right)^{1.5} \cdot \sqrt{f'_{c_i} \cdot psi}$ $E_{c_i} = 2205 \cdot ksi$ *from my graduate research*

Drainage Coefficient

$C_d := 1.1$ *Ref Table 12.20 in Pavement Analysis and Design by Huang*

NOTE: with proper drainage the structure should not be exposed to saturation moisture levels often

Load Transfer Coefficient

$J := 3.8$ NOTE: Pervous concrete is not tied *Ref Table 2.6 AASHTO (1993)*

Find Minimum Thickness

Given $D_i := 12$ *Ref Eqn 12.21 in Pavement Analysis & Design by Huang*

$$\log\left(W_{18}\right) = Z_R \cdot S_o + 7.35 \cdot \log\left(D_i + 1\right) - .06 + \frac{\log\left(\frac{\Delta PSI}{4.5 - 1.5}\right)}{1 + \frac{1.624 \cdot 10^7}{\left(D_i + 1\right)^{8.46}}} + \left(4.22 - .32 p_t\right) \cdot \log\left[\frac{\frac{S'_{c_i}}{psi} \cdot C_d \cdot \left[\left(D_i\right)^{0.75} - 1.132\right]}{215.63 \cdot J \cdot \left[\left(D_i\right)^{0.75} - \frac{18.42}{\left(\frac{E_{c_i}}{k \cdot psi}\right)^{.25}}\right]}\right]$$

Minimum Thickness of Pervious Concrete from AASHTO $D := Find(D)$ $D_i = 8.936\ in$

Actual Pervious Concrete Depth at Evolution Paving $h_i = 5 \cdot in$

PANEL 8 DESIGN

panel number $i := 8$

Total Life ESALS

Calculated EALF for full concrete truck $EALF := 2 \cdot .082 + 1.92$ $EALF = 2.08$

Number of Loads at 1st Cracking $n := 10000$

Total Design Life ESALS $W_{18} := n \cdot EALF$ $W_{18} = 20840$

Subgrade Properties

From Geotech Report at Evolution Paving $PI_{avg} := 9.14 \frac{mm}{blow}$ *see excel sheet for calculations*

NOTE: Dynamic Cone Penetration Test was performed

Soil Resilient Modulus $M_r := \left(-3279 \cdot PI_{avg} + 114100\right) \cdot kPa$ *Ref Dynamic Cone Penetration Test for Subgrade Assessment by Salgado & Yoon*

$M_r = 84.13 \cdot MPa$ $M_r = 12202\ psi$

Assume subbase resilient modulus $E_{SB} := 20000psi$

Subbase Thickness $D_{SB} := 14in - h_i$ $D_{SB} = 9 \cdot in$

Composite Subgrade Reaction $k := 600pci$ $k = 162.87 \cdot \frac{MPa}{m}$ *Ref Fig 3.3 in AASHTO (1993)*

Corrected K Value for Potential Loss of Support $LS := 2.5$ *Ref Table 2.7 in AASTHO (1993)*

NOTE: Assumed fine-grained or natural subgrade materials $k := 28\ pci$ *Ref Figure 3.6 in AASTHO (1993)*

Pervious Concrete Properties

Compressive Strength $f'_{c_i} = 2835.53\ psi$ *from my graduate research*

Modulus of Rupture $S'_{c_i} := MOR_i$ $S'_{c_i} = 275\ psi$ *from my graduate research*

Modulus of Elasticity $E_{c_i} := 39.1 \cdot \left(w_{pc_i} \div pcf\right)^{1.5} \cdot \sqrt{f'_{c_i} \cdot psi}$ $E_{c_i} = 2517 \cdot ksi$ *from my graduate research*

Drainage Coefficient

$C_d := 1.1$ *Ref Table 12.20 in Pavement Analysis and Design by Huang*

NOTE: with proper drainage the structure should not be exposed to saturation moisture levels often

Load Transfer Coefficient

$J := 3.8$ NOTE: Pervous concrete is not tied *Ref Table 2.6 AASHTO (1993)*

Find Minimum Thickness

Given $D_i := 12$ *Ref Eqn 12.21 in Pavement Analysis & Design by Huang*

$$\log\left(W_{18}\right) = Z_R \cdot S_o + 7.35 \cdot \log\left(D_i + 1\right) - .06 + \frac{\log\left(\frac{\Delta PSI}{4.5 - 1.5}\right)}{1 + \frac{1.624 \cdot 10^7}{\left(D_i + 1\right)^{8.46}}} + \left(4.22 - .32 p_t\right) \cdot \log\left[\frac{\frac{S'_{c_i}}{psi} \cdot C_d \cdot \left[\left(D_i\right)^{0.75} - 1.132\right]}{215.63 \cdot J \cdot \left[\left(D_i\right)^{0.75} - \frac{18.42}{\left(\frac{E_{c_i}}{k \cdot psi}\right)^{.25}}\right]}\right]$$

Minimum Thickness of Pervious Concrete from AASHTO $D := Find(D)$ $D_i = 6.44$ in

Actual Pervious Concrete Depth at Evolution Paving $h_i = 5 \cdot in$

PANEL 12 DESIGN panel number $i := 12$

Total Life ESALS

Calculated EALF for full concrete truck $EALF := 2 \cdot .082 + 1.92$ $EALF = 2.08$

Number of Loads at 1st Cracking $n := 375$

Total Design Life ESALS $W_{18} := n \cdot EALF$ $W_{18} = 781.5$

Subgrade Properties

From Geotech Report at Evolution Paving $PI_{avg} := 9.14 \frac{mm}{blow}$ *see excel sheet for calculations*

NOTE: Dynamic Cone Penetration Test was performed

Soil Resilient Modulus $M_r := \left(-3279 \cdot PI_{avg} + 114100\right) \cdot kPa$ *Ref Dynamic Cone Penetration Test for Subgrade Assessment by Salgado & Yoon*

$M_r = 84.13 \cdot MPa$ $M_r = 12202\ psi$

Assume subbase resilient modulus $E_{SB} := 20000 psi$

Subbase Thickness $D_{SB} := 14in - h_i$ $D_{SB} = 10 \cdot in$

Composite Subgrade Reaction $k := 600 pci$ $k = 162.87 \cdot \frac{MPa}{m}$ *Ref Fig 3.3 in AASHTO (1993)*

Corrected K Value for Potential Loss of Support $LS := 2.5$ *Ref Table 2.7 in AASTHO (1993)*

NOTE: Assumed fine-grained or natural subgrade materials $k := 28\ pci$ *Ref Figure 3.6 in AASTHO (1993)*

Pervious Concrete Properties

Compressive Strength $f'_{c_i} = 2729.09\ psi$ *from my graduate research*

Modulus of Rupture $S'_{c_i} := 5.3 \cdot \sqrt{f'_{c_i} \cdot psi}$ $S'_{c_i} = 276.9\ psi$ *from my graduate research*

NOTE: Since Flexural Test was unable to be performed on any samples from this panel, I use relationship between MOR and f`c developed from experiemental results

Modulus of Elasticity $E_{c_i} := 39.1 \cdot \left(w_{pc_i} \div pcf\right)^{1.5} \cdot \sqrt{f'_{c_i} \cdot psi}$ $E_{c_i} = 2568 \cdot ksi$ *from my graduate research*

Drainage Coefficient

$C_d := 1.1$ *Ref Table 12.20 in Pavement Analysis and Design by Huang*

NOTE: with proper drainage the structure should not be exposed to saturation moisture levels often

Load Transfer Coefficient

$J := 3.8$ NOTE: Pervous concrete is not tied *Ref Table 2.6 AASHTO (1993)*

Find Minimum Thickness

Given $D_i := 12$ *Ref Eqn 12.21 in Pavement Analysis & Design by Huang*

$$\log\left(W_{18}\right) = Z_R \cdot S_o + 7.35 \cdot \log\left(D_i + 1\right) - .06 + \frac{\log\left(\frac{\Delta PSI}{4.5 - 1.5}\right)}{1 + \frac{1.624 \cdot 10^7}{\left(D_i + 1\right)^{8.46}}} + \left(4.22 - .32 p_t\right) \cdot \log\left[\frac{\frac{S'_{c_i}}{psi} \cdot C_d \cdot \left[\left(D_i\right)^{0.75} - 1.132\right]}{215.63 \cdot J \cdot \left[\left(D_i\right)^{0.75} - \frac{18.42}{\left(\frac{E_{c_i}}{k \cdot psi}\right)^{.25}}\right]}\right]$$

Minimum Thickness of Pervious Concrete from AASHTO $D := \text{Find}(D)$ $D_i = 3.55$ in

Actual Pervious Concrete Depth at Evolution Paving $h_i = 4 \cdot in$

PANEL 14 DESIGN panel number $i := 14$

Total Life ESALS

Calculated EALF for full concrete truck $EALF := 2 \cdot .082 + 1.92$ $EALF = 2.08$

Number of Loads at 1st Cracking $n := 12500$

Total Design Life ESALS $W_{18} := n \cdot EALF$ $W_{18} = 26050$

Subgrade Properties

From Geotech Report at Evolution Paving $PI_{avg} := 9.14 \frac{mm}{blow}$ *see excel sheet for calculations*

NOTE: Dynamic Cone Penetration Test was performed

Soil Resilient Modulus $M_r := \left(-3279 \cdot PI_{avg} + 114100\right) \cdot kPa$ *Ref Dynamic Cone Penetration Test for Subgrade Assessment by Salgado & Yoon*

$M_r = 84.13 \cdot MPa$ $M_r = 12202\ psi$

Assume subbase resilient modulus $E_{SB} := 20000 psi$

Subbase Thickness $D_{SB} := 14in - h_i$ $D_{SB} = 8 \cdot in$

Composite Subgrade Reaction $k := 600 pci$ $k = 162.87 \cdot \frac{MPa}{m}$ *Ref Fig 3.3 in AASHTO (1993)*

Corrected K Value for Potential Loss of Support $LS := 2.5$ *Ref Table 2.7 in AASTHO (1993)*

NOTE: Assumed fine-grained or natural subgrade materials $k := 28\ pci$ *Ref Figure 3.6 in AASTHO (1993)*

Pervious Concrete Properties

Compressive Strength $f'_{c_i} = 4199.8\ psi$ *from my graduate research*

Modulus of Rupture $S'_{c_i} := 5.3 \cdot \sqrt{f'_{c_i} \cdot psi}$ $S'_{c_i} = 343.5\ psi$ *from my graduate research*

NOTE: Since Flexural Test was unable to be performed on any samples from this panel, I use relationship between MOR and f`c developed from experiemental results

Modulus of Elasticity $E_{c_i} := 39.1 \cdot \left(w_{pc_i} \div pcf\right)^{1.5} \cdot \sqrt{f'_{c_i} \cdot psi}$ $E_{c_i} = 3426 \cdot ksi$ *from my graduate research*

Drainage Coefficient

$C_d := 1.1$ *Ref Table 12.20 in Pavement Analysis and Design by Huang*

NOTE: with proper drainage the structure should not be exposed to saturation moisture levels often

Load Transfer Coefficient

$J := 3.8$ NOTE: Pervous concrete is not tied *Ref Table 2.6 AASHTO (1993)*

Find Minimum Thickness

Given $D_i := 12$ *Ref Eqn 12.21 in Pavement Analysis & Design by Huang*

$$\log\left(W_{18}\right) = Z_R \cdot S_o + 7.35 \cdot \log\left(D_i + 1\right) - .06 + \frac{\log\left(\frac{\Delta PSI}{4.5 - 1.5}\right)}{1 + \frac{1.624 \cdot 10^7}{\left(D_i + 1\right)^{8.46}}} + \left(4.22 - .32 p_t\right) \cdot \log\left[\frac{\frac{S'_{c_i}}{psi} \cdot C_d \cdot \left[\left(D_i\right)^{0.75} - 1.132\right]}{215.63 \cdot J \cdot \left[\left(D_i\right)^{0.75} - \frac{18.42}{\left(\frac{E_{c_i}}{k \cdot psi}\right)^{.25}}\right]}\right]$$

Minimum Thickness of Pervious Concrete from AASHTO $D := \text{Find}(D)$ $D_i = 5.95$ in

Actual Pervious Concrete Depth at Evolution Paving $h_i = 6 \cdot in$

PANEL 16 DESIGN panel number $i := 16$

Total Life ESALS

Calculated EALF for full concrete truck $EALF := 2 \cdot .082 + 1.92$ $EALF = 2.08$

Number of Loads at 1st Cracking $n := 13990$

Total Design Life ESALS $W_{18} := n \cdot EALF$ $W_{18} = 29155.16$

Subgrade Properties

From Geotech Report at Evolution Paving $PI_{avg} := 9.14 \frac{mm}{blow}$ *see excel sheet for calculations*

NOTE: Dynamic Cone Penetration Test was performed

Soil Resilient Modulus $M_r := \left(-3279 \cdot PI_{avg} + 114100\right) \cdot kPa$ *Ref Dynamic Cone Penetration Test for Subgrade Assessment by Salgado & Yoon*

$M_r = 84.13 \cdot MPa$ $M_r = 12202\ psi$

Assume subbase resilient modulus $E_{SB} := 20000 psi$

Subbase Thickness $D_{SB} := 14in - h_i$ $D_{SB} = 6 \cdot in$

Composite Subgrade Reaction $k := 600 pci$ $k = 162.87 \cdot \frac{MPa}{m}$ *Ref Fig 3.3 in AASHTO (1993)*

Corrected K Value for Potential Loss of Support $LS := 2.5$ *Ref Table 2.7 in AASTHO (1993)*

NOTE: Assumed fine-grained or natural subgrade materials $k := 28\ pci$ *Ref Figure 3.6 in AASTHO (1993)*

Pervious Concrete Properties

Compressive Strength $f'_{c_i} = 3472.83\ psi$ *from my graduate research*

Modulus of Rupture $S'_{c_i} := MOR_i$ $S'_{c_i} = 406.7\ psi$ *from my graduate research*

Modulus of Elasticity $E_{c_i} := 39.1 \cdot \left(w_{pc_i} \div pcf\right)^{1.5} \cdot \sqrt{f'_{c_i} \cdot psi}$ $E_{c_i} = 3172 \cdot ksi$ *from my graduate research*

Drainage Coefficient

$C_d := 1.1$ *Ref Table 12.20 in Pavement Analysis and Design by Huang*

NOTE: with proper drainage the structure should not be exposed to saturation moisture levels often

Load Transfer Coefficient

$J := 3.8$ NOTE: Pervous concrete is not tied *Ref Table 2.6 AASHTO (1993)*

Find Minimum Thickness

Given $D_i := 12$ *Ref Eqn 12.21 in Pavement Analysis & Design by Huang*

$$\log\left(W_{18}\right) = Z_R \cdot S_o + 7.35 \cdot \log\left(D_i + 1\right) - .06 + \frac{\log\left(\frac{\Delta PSI}{4.5 - 1.5}\right)}{1 + \frac{1.624 \cdot 10^7}{\left(D_i + 1\right)^{8.46}}} + \left(4.22 - .32 p_t\right) \cdot \log\left[\frac{\frac{S'_{c_i}}{psi} \cdot C_d \cdot \left[\left(D_i\right)^{0.75} - 1.132\right]}{215.63 \cdot J \cdot \left[\left(D_i\right)^{0.75} - \frac{18.42}{\left(\frac{E_{c_i}}{k \cdot psi}\right)^{.25}}\right]}\right]$$

Minimum Thickness of Pervious Concrete from AASHTO $D := Find(D)$ $D_i = 5.45$ in

Actual Pervious Concrete Depth at Evolution Paving $h_i = 8 \cdot in$

Name: *Will Goede* | **Class:** *Research - Pervious Concrete*

Reference: AASTHO (1993) design method

= adjustable values

= outputs of interest

Problem Statement:

Use AASHTO (1993) Method to calculate number of ESALs to failure for Evolution Paving pervious concrete panels using material characterization results and actual pavement depths.

Solution:

Material Characterization Results

Panel #	Depth (in)	Loaded Trucks?	Unit Weight (pcf)	Avg Flexural Strength (psi)	Avg Compressive Strength (psi)	Avg In-Situ Porosity	PCI	2007 ASTM Rating
1	7.5	no	122.1	297	3517	13.7%	48	Poor
2	10	yes	111.1		1780	21.4%	87	Good
3	10	no	126.7		5031	11.0%	89	Good
4	7	yes	117.3	284	2937	17.8%	86	Good
5	8	no	118.2	329	2904	17.0%	87	Good
6	5	yes	112.1	206	2261	22.2%	77	Satisfactory
7	6	no					26	Very Poor
8	5	yes	113.5	275	2836	20.7%	8	Failed
9	4	no					27	Very Poor
10	4	yes					8	Failed
11	4	no	109.0		2518	27.1%	8	Failed
12	4	yes	116.5		2729	19.9%	8	Failed
13	6	no	119.8	260	2884	19.1%	8	Failed
14	6	yes	122.3		4200	12.9%	8	Failed
15	8	no					60	Fair
16	8	yes	123.7	407	3473	11.9%	50	Poor

**The procedure for determining the thickness of pervious concrete is the same as AASHTO rigid pavement design,

Standard Deviation $S_o := 0.39$ Recommeded by Huang, 2004 for rigid pavements

Reliability $Rel := 85$ *for urban freeway reccomended values are 85-99.9 (ref Slide 8 in Handout received 9/1/09)*

Standard Normal Deviate $Z_R := -1.037$ *ref Slide 11 in Handout received 9/1/09*

Terminal Serviceability Index $p_t := 3.0$ *ref Slide 12 in Handout received 9/1/09*

Change in Serviceability Index $\Delta PSI := 4.5 - p_t$ $\Delta PSI = 1.5$

PANEL 2 DESIGN

panel number $i := 2$

Total Life ESALS

Calculated EALF for full concrete truck $EALF := 2 \cdot .082 + 1.92$ $EALF = 2.08$

Number of Loads at 1st Cracking $n := 65000$

Total Design Life ESALS $N_i := n \cdot EALF$ $N_i = 135460$

Subgrade Properties

From Geotech Report at Evolution Paving $PI_{avg} := 9.14 \frac{mm}{blow}$ *see excel sheet for calculations*

NOTE: Dynamic Cone Penetration Test was performed

Soil Resilient Modulus $M_r := \left(-3279 \cdot PI_{avg} + 114100\right) \cdot kPa$ $M_r = 84.13 \cdot MPa$ $M_r = 12202\ psi$ *Ref Dynamic Cone Penetration Test for Subgrade Assessment by Salgado & Yoon*

Assume subbase resilient modulus $E_{SB} := 20000 psi$

Subbase Thickness $D_{SB} := 14in - h_i$ $D_{SB} = 4 \cdot in$

Composite Subgrade Reaction $k := 1000 pci$ $k = 271.45 \cdot \frac{MPa}{m}$ *Ref Fig 3.3 in AASHTO (1993)*

Corrected K Value for Potential Loss of Support $LS := 2.5$ *Ref Table 2.7 in AASTHO (1993)*

NOTE: Assumed fine-grained or natural subgrade materials $k := 38\ pci$ *Ref Figure 3.6 in AASTHO (1993)*

Pervious Concrete Properties

Compressive Strength $f'_{c_i} = 1780.46\ psi$ *from my graduate research*

Modulus of Rupture $S'_{c_i} := 5.3 \cdot \sqrt{f'_{c_i} \cdot psi}$ $S'_{c_i} = 223.6\ psi$ *from my graduate research*

NOTE: Since Flexural Test was unable to be performed on any samples from this panel, I use relationship between MOR and f`c developed from experiemental results

Modulus of Elasticity $E_{c_i} := 39.1 \cdot \left(w_{pc_i} \div pcf\right)^{1.5} \cdot \sqrt{f'_{c_i} \cdot psi}$ $E_{c_i} = 1932 \cdot ksi$ *from my graduate research*

Drainage Coefficient

$C_d := 1.1$ *Ref Table 12.20 in Pavement Analysis and Design by Huang*

NOTE: with proper drainage the structure should not be exposed to saturation moisture levels often

Load Transfer Coefficient

$J := 3.8$ NOTE: Pervous concrete is not tied *Ref Table 2.6 AASHTO (1993)*

Find Minimum Thickness

Given $D_i := h_i \div in$ $W_{18_i} := 1000$ *Ref Eqn 12.21 in Pavement Analysis &Design by Huang*

$$\log\left(W_{18_i}\right) = Z_R \cdot S_o + 7.35 \cdot \log\left(D_i + 1\right) - .06 + \frac{\log\left(\frac{\Delta PSI}{4.5 - 1.5}\right)}{1 + \frac{1.624 \cdot 10^7}{\left(D_i + 1\right)^{8.46}}} + \left(4.22 - .32 p_t\right) \cdot \log\left[\frac{\frac{S'_{c_i}}{psi} \cdot C_d \cdot \left[\left(D_i\right)^{0.75} - 1.132\right]}{215.63 \cdot J \cdot \left[\left(D_i\right)^{0.75} - \frac{18.42}{\left(\frac{E_{c_i}}{k \cdot psi}\right)^{.25}}\right]}\right]$$

Estimated Number of ESALS to failure $W_{18} := \text{Find}\left(W_{18}\right)$ $W_{18_i} = 167027$

Actual Number of ESALS to 1st Cracking $N_i = 135460$

PANEL 4 DESIGN

panel number $i := 4$

Total Life ESALS

Calculated EALF for full concrete truck $EALF := 2 \cdot .082 + 1.92$ $EALF = 2.08$

Number of Loads at 1st Cracking $n := 50780$

Total Design Life ESALS $N_i := n \cdot EALF$ $N_i = 105826$

Subgrade Properties

From Geotech Report at Evolution Paving $PI_{avg} := 9.14 \frac{mm}{blow}$ *see excel sheet for calculations*

NOTE: Dynamic Cone Penetration Test was performed

Soil Resilient Modulus $M_r := \left(-3279 \cdot PI_{avg} + 114100\right) \cdot kPa$

$M_r = 84.13 \cdot MPa$ $M_r = 12202\ psi$

Ref Dynamic Cone Penetration Test for Subgrade Assessment by Salgado & Yoon

Assume subbase resilient modulus $E_{SB} := 20000 psi$

Subbase Thickness $D_{SB} := 14in - h_i$ $D_{SB} = 7 \cdot in$

Composite Subgrade Reaction $k := 500 pci$ $k = 135.72 \cdot \frac{MPa}{m}$ *Ref Fig 3.3 in AASHTO (1993)*

Corrected K Value for Potential Loss of Support $LS := 2.5$ *Ref Table 2.7 in AASTHO (1993)*

NOTE: Assumed fine-grained or natural subgrade materials $k := 26\ pci$ *Ref Figure 3.6 in AASTHO (1993)*

Pervious Concrete Properties

Compressive Strength $f'_{c_i} = 2936.97\ psi$ *from my graduate research*

Modulus of Rupture $S'_{c_i} := MOR_i$ $S'_{c_i} = 283.8\ psi$ *from my graduate research*

Modulus of Elasticity $E_{c_i} := 39.1 \cdot \left(w_{pc_i} \div pcf\right)^{1.5} \cdot \sqrt{f'_{c_i} \cdot psi}$ $E_{c_i} = 2693 \cdot ksi$ *from my graduate research*

Drainage Coefficient

$C_d := 1.1$ *Ref Table 12.20 in Pavement Analysis and Design by Huang*

NOTE: with proper drainage the structure should not be exposed to saturation moisture levels often

Load Transfer Coefficient

$J := 3.8$ NOTE: Pervous concrete is not tied *Ref Table 2.6 AASHTO (1993)*

Find Minimum Thickness

Given $D_i := h_i \div in$ $W_{18_i} := 1000$ *Ref Eqn 12.21 in Pavement Analysis &Design by Huang*

$$\log\left(W_{18_i}\right) = Z_R \cdot S_o + 7.35 \cdot \log\left(D_i + 1\right) - .06 + \frac{\log\left(\frac{\Delta PSI}{4.5 - 1.5}\right)}{1 + \frac{1.624 \cdot 10^7}{\left(D_i + 1\right)^{8.46}}} + \left(4.22 - .32 p_t\right) \cdot \log\left[\frac{\frac{S'_{c_i}}{psi} \cdot C_d \cdot \left[\left(D_i\right)^{0.75} - 1.132\right]}{215.63 \cdot J \cdot \left[\left(D_i\right)^{0.75} - \frac{18.42}{\left(\frac{E_{c_i}}{k \cdot psi}\right)^{.25}}\right]}\right]$$

Estimated Number of ESALS to failure $W_{18} := \text{Find}\left(W_{18}\right)$ $W_{18_i} = 34806$

Actual Number of ESALS to 1st Cracking $N_i = 105826$

PANEL 6 DESIGN panel number $i := 6$

Total Life ESALS

Calculated EALF for full concrete truck $EALF := 2 \cdot .082 + 1.92$ $EALF = 2.08$

Number of Loads at 1st Cracking $n := 27000$

Total Design Life ESALS $N_i := n \cdot EALF$ $N_i = 56268$

Subgrade Properties

From Geotech Report at Evolution Paving $PI_{avg} := 9.14 \frac{mm}{blow}$ *see excel sheet for calculations*

NOTE: Dynamic Cone Penetration Test was performed

Soil Resilient Modulus $M_r := \left(-3279 \cdot PI_{avg} + 114100\right) \cdot kPa$ $M_r = 84.13 \cdot MPa$ $M_r = 12202\ psi$ *Ref Dynamic Cone Penetration Test for Subgrade Assessment by Salgado & Yoon*

Assume subbase resilient modulus $E_{SB} := 20000 psi$

Subbase Thickness $D_{SB} := 14in - h_i$ $D_{SB} = 9 \cdot in$

Composite Subgrade Reaction $k := 380 pci$ $k = 103.15 \cdot \frac{MPa}{m}$ *Ref Fig 3.3 in AASHTO (1993)*

Corrected K Value for Potential Loss of Support $LS := 2.5$ *Ref Table 2.7 in AASTHO (1993)*

NOTE: Assumed fine-grained or natural subgrade materials $k := 21\ pci$ *Ref Figure 3.6 in AASTHO (1993)*

Pervious Concrete Properties

Compressive Strength $f'_{c_i} = 2260.52\ psi$ *from my graduate research*

Modulus of Rupture $S'_{c_i} := MOR_i$ $S'_{c_i} = 206.1\ psi$ *from my graduate research*

Modulus of Elasticity $E_{c_i} := 39.1 \cdot \left(w_{pc_i} \div pcf\right)^{1.5} \cdot \sqrt{f'_{c_i} \cdot psi}$ $E_{c_i} = 2205 \cdot ksi$ *from my graduate research*

Drainage Coefficient

$C_d := 1.1$ *Ref Table 12.20 in Pavement Analysis and Design by Huang*

NOTE: with proper drainage the structure should not be exposed to saturation moisture levels often

Load Transfer Coefficient

$J := 3.8$ NOTE: Pervous concrete is not tied *Ref Table 2.6 AASHTO (1993)*

Find Minimum Thickness

Given $D_i := h_i \div in$ $W_{18_i} := 1000$ *Ref Eqn 12.21 in Pavement Analysis &Design by Huang*

$$\log\left(W_{18_i}\right) = Z_R \cdot S_o + 7.35 \cdot \log\left(D_i + 1\right) - .06 + \frac{\log\left(\frac{\Delta PSI}{4.5 - 1.5}\right)}{1 + \frac{1.624 \cdot 10^7}{\left(D_i + 1\right)^{8.46}}} + \left(4.22 - .32 p_t\right) \cdot \log\left[\frac{\frac{S'_{c_i}}{psi} \cdot C_d \cdot \left[\left(D_i\right)^{0.75} - 1.132\right]}{215.63 \cdot J \cdot \left[\left(D_i\right)^{0.75} - \frac{18.42}{\left(\frac{E_{c_i}}{k \cdot psi}\right)^{.25}}\right]}\right]$$

Estimated Number of ESALS to failure $W_{18} := \text{Find}\left(W_{18}\right)$ $W_{18_i} = 2043$

Actual Number of ESALS to 1st Cracking $N_i = 56268$

PANEL 8 DESIGN panel number $i := 8$

Total Life ESALS

Calculated EALF for full concrete truck $EALF := 2 \cdot .082 + 1.92$ $EALF = 2.08$

Number of Loads at 1st Cracking $n := 10000$

Total Design Life ESALS $N_i := n \cdot EALF$ $N_i = 20840$

Subgrade Properties

From Geotech Report at Evolution Paving $PI_{avg} := 9.14 \frac{mm}{blow}$ *see excel sheet for calculations*

NOTE: Dynamic Cone Penetration Test was performed

Soil Resilient Modulus $M_r := \left(-3279 \cdot PI_{avg} + 114100\right) \cdot kPa$ *Ref Dynamic Cone Penetration Test for Subgrade Assessment by Salgado & Yoon*

$M_r = 84.13 \cdot MPa$ $M_r = 12202\ psi$

Assume subbase resilient modulus $E_{SB} := 20000 psi$

Subbase Thickness $D_{SB} := 14in - h_i$ $D_{SB} = 9 \cdot in$

Composite Subgrade Reaction $k := 380 pci$ $k = 103.15 \cdot \frac{MPa}{m}$ *Ref Fig 3.3 in AASHTO (1993)*

Corrected K Value for Potential Loss of Support $LS := 2.5$ *Ref Table 2.7 in AASTHO (1993)*

NOTE: Assumed fine-grained or natural subgrade materials $k := 21\ pci$ *Ref Figure 3.6 in AASTHO (1993)*

Pervious Concrete Properties

Compressive Strength $f'_{c_i} = 2835.53\ psi$ *from my graduate research*

Modulus of Rupture $S'_{c_i} := MOR_i$ $S'_{c_i} = 275\ psi$ *from my graduate research*

Modulus of Elasticity $E_{c_i} := 39.1 \cdot \left(w_{pc_i} \div pcf\right)^{1.5} \cdot \sqrt{f'_{c_i} \cdot psi}$ $E_{c_i} = 2517 \cdot ksi$ *from my graduate research*

Drainage Coefficient

$C_d := 1.1$ *Ref Table 12.20 in Pavement Analysis and Design by Huang*

NOTE: with proper drainage the structure should not be exposed to saturation moisture levels often

Load Transfer Coefficient

$J := 3.8$ NOTE: Pervous concrete is not tied *Ref Table 2.6 AASHTO (1993)*

Find Minimum Thickness

Given $D_i := h_i \div in$ $W_{18_i} := 1000$ *Ref Eqn 12.21 in Pavement Analysis &Design by Huang*

$$\log\left(W_{18_i}\right) = Z_R \cdot S_o + 7.35 \cdot \log\left(D_i + 1\right) - .06 + \frac{\log\left(\frac{\Delta PSI}{4.5 - 1.5}\right)}{1 + \frac{1.624 \cdot 10^7}{\left(D_i + 1\right)^{8.46}}} + \left(4.22 - .32 p_t\right) \cdot \log\left[\frac{\frac{S'_{c_i}}{psi} \cdot C_d \cdot \left[\left(D_i\right)^{0.75} - 1.132\right]}{215.63 \cdot J \cdot \left[\left(D_i\right)^{0.75} - \frac{18.42}{\left(\frac{E_{c_i}}{k \cdot psi}\right)^{.25}}\right]}\right]$$

Estimated Number of ESALS to failure $W_{18} := \text{Find}\left(W_{18}\right)$ $W_{18_i} = 4994$

Actual Number of ESALS to 1st Cracking $N_i = 20840$

PANEL 12 DESIGN panel number $i := 12$

Total Life ESALS

Calculated EALF for full concrete truck $EALF := 2 \cdot .082 + 1.92$ $EALF = 2.08$

Number of Loads at 1st Cracking $n := 375$

Total Design Life ESALS $N_i := n \cdot EALF$ $N_i = 782$

Subgrade Properties

From Geotech Report at Evolution Paving $PI_{avg} := 9.14 \frac{mm}{blow}$ *see excel sheet for calculations*

NOTE: Dynamic Cone Penetration Test was performed

Soil Resilient Modulus $M_r := \left(-3279 \cdot PI_{avg} + 114100\right) \cdot kPa$ *Ref Dynamic Cone Penetration Test for Subgrade Assessment by Salgado & Yoon*

$M_r = 84.13 \cdot MPa$ $M_r = 12202\ psi$

Assume subbase resilient modulus $E_{SB} := 20000 psi$

Subbase Thickness $D_{SB} := 14in - h_i$ $D_{SB} = 10 \cdot in$

Composite Subgrade Reaction $k := 350 pci$ $k = 95.01 \cdot \frac{MPa}{m}$ *Ref Fig 3.3 in AASHTO (1993)*

Corrected K Value for Potential Loss of Support $LS := 2.5$ *Ref Table 2.7 in AASTHO (1993)*

NOTE: Assumed fine-grained or natural subgrade materials $k := 20\ pci$ *Ref Figure 3.6 in AASTHO (1993)*

Pervious Concrete Properties

Compressive Strength $f'_{c_i} = 2729.09\ psi$ *from my graduate research*

Modulus of Rupture $S'_{c_i} := 5.3 \cdot \sqrt{f'_{c_i} \cdot psi}$ $S'_{c_i} = 276.9\ psi$ *from my graduate research*

NOTE: Since Flexural Test was unable to be performed on any samples from this panel, I use relationship between MOR and f`c developed from experiemental results

Modulus of Elasticity $E_{c_i} := 39.1 \cdot \left(w_{pc_i} \div pcf\right)^{1.5} \cdot \sqrt{f'_{c_i} \cdot psi}$ $E_{c_i} = 2568 \cdot ksi$ *from my graduate research*

Drainage Coefficient $C_d := 1.1$ *Ref Table 12.20 in Pavement Analysis and Design by Huang*

NOTE: with proper drainage the structure should not be exposed to saturation moisture levels often

Load Transfer Coefficient $J := 3.8$ NOTE: Pervous concrete is not tied *Ref Table 2.6 AASHTO (1993)*

Find Minimum Thickness Given $D_i := h_i \div in$ $W_{18_i} := 1000$ *Ref Eqn 12.21 in Pavement Analysis &Design by Huang*

$$\log\left(W_{18_i}\right) = Z_R \cdot S_o + 7.35 \cdot \log\left(D_i + 1\right) - .06 + \frac{\log\left(\frac{\Delta PSI}{4.5 - 1.5}\right)}{1 + \frac{1.624 \cdot 10^7}{\left(D_i + 1\right)^{8.46}}} + \left(4.22 - .32 p_t\right) \cdot \log\left[\frac{\frac{S'_{c_i}}{psi} \cdot C_d \cdot \left[\left(D_i\right)^{0.75} - 1.132\right]}{215.63 \cdot J \cdot \left[\left(D_i\right)^{0.75} - \frac{18.42}{\left(\frac{E_{c_i}}{k \cdot psi}\right)^{.25}}\right]}\right]$$

Estimated Number of ESALS to failure $W_{18} := \text{Find}\left(W_{18}\right)$ $W_{18_i} = 1351$

Actual Number of ESALS to 1st Cracking $N_i = 782$

PANEL 14 DESIGN panel number $i := 14$

Total Life ESALS

Calculated EALF for full concrete truck $EALF := 2 \cdot .082 + 1.92$ $EALF = 2.08$

Number of Loads at 1st Cracking $n := 12500$

Total Design Life ESALS $N_i := n \cdot EALF$ $N_i = 26050$

Subgrade Properties

From Geotech Report at Evolution Paving $PI_{avg} := 9.14 \frac{mm}{blow}$ *see excel sheet for calculations*

NOTE: Dynamic Cone Penetration Test was performed

Soil Resilient Modulus $M_r := \left(-3279 \cdot PI_{avg} + 114100\right) \cdot kPa$ *Ref Dynamic Cone Penetration Test for Subgrade Assessment by Salgado & Yoon*

$M_r = 84.13 \cdot MPa$ $M_r = 12202\ psi$

Assume subbase resilient modulus $E_{SB} := 20000 psi$

Subbase Thickness $D_{SB} := 14in - h_i$ $D_{SB} = 8 \cdot in$

Composite Subgrade Reaction $k := 450 pci$ $k = 122.15 \cdot \frac{MPa}{m}$ *Ref Fig 3.3 in AASHTO (1993)*

Corrected K Value for Potential Loss of Support $LS := 2.5$ *Ref Table 2.7 in AASTHO (1993)*

NOTE: Assumed fine-grained or natural subgrade materials $k := 24\ pci$ *Ref Figure 3.6 in AASTHO (1993)*

Pervious Concrete Properties

Compressive Strength $f'_{c_i} = 4199.8\ psi$ *from my graduate research*

Modulus of Rupture $S'_{c_i} := 5.3 \cdot \sqrt{f'_{c_i} \cdot psi}$ $S'_{c_i} = 343.5\ psi$ *from my graduate research*

NOTE: Since Flexural Test was unable to be performed on any samples from this panel, I use relationship between MOR and f`c developed from experiemental results

Modulus of Elasticity $E_{c_i} := 39.1 \cdot \left(w_{pc_i} \div pcf\right)^{1.5} \cdot \sqrt{f'_{c_i} \cdot psi}$ $E_{c_i} = 3426 \cdot ksi$ *from my graduate research*

Drainage Coefficient

$C_d := 1.1$ *Ref Table 12.20 in Pavement Analysis and Design by Huang*

NOTE: with proper drainage the structure should not be exposed to saturation moisture levels often

Load Transfer Coefficient

$J := 3.8$ NOTE: Pervous concrete is not tied *Ref Table 2.6 AASHTO (1993)*

Find Minimum Thickness

Given $D_i := h_i \div in$ $W_{18_i} := 1000$ *Ref Eqn 12.21 in Pavement Analysis &Design by Huang*

$$\log\left(W_{18_i}\right) = Z_R \cdot S_o + 7.35 \cdot \log\left(D_i + 1\right) - .06 + \frac{\log\left(\frac{\Delta PSI}{4.5 - 1.5}\right)}{1 + \frac{1.624 \cdot 10^7}{\left(D_i + 1\right)^{8.46}}} + \left(4.22 - .32 p_t\right) \cdot \log\left[\frac{\frac{S'_{c_i}}{psi} \cdot C_d \cdot \left[\left(D_i\right)^{0.75} - 1.132\right]}{215.63 \cdot J \cdot \left[\left(D_i\right)^{0.75} - \frac{18.42}{\left(\frac{E_{c_i}}{k \cdot psi}\right)^{.25}}\right]}\right]$$

Estimated Number of ESALS to failure $W_{18} := \text{Find}\left(W_{18}\right)$ $W_{18_i} = 26157$

Actual Number of ESALS to 1st Cracking $N_i = 26050$

PANEL 16 DESIGN panel number $i := 16$

Total Life ESALS

Calculated EALF for full concrete truck $EALF := 2 \cdot .082 + 1.92$ $EALF = 2.08$

Number of Loads at 1st Cracking $n := 13990$

Total Design Life ESALS $N_i := n \cdot EALF$ $N_i = 29155$

Subgrade Properties

From Geotech Report at Evolution Paving $PI_{avg} := 9.14 \frac{mm}{blow}$ *see excel sheet for calculations*

NOTE: Dynamic Cone Penetration Test was performed

Soil Resilient Modulus $M_r := \left(-3279 \cdot PI_{avg} + 114100\right) \cdot kPa$ $M_r = 84.13 \cdot MPa$ $M_r = 12202\ psi$ *Ref Dynamic Cone Penetration Test for Subgrade Assessment by Salgado & Yoon*

Assume subbase resilient modulus $E_{SB} := 20000 psi$

Subbase Thickness $D_{SB} := 14in - h_i$ $D_{SB} = 6 \cdot in$

Composite Subgrade Reaction $k := 600 pci$ $k = 162.87 \cdot \frac{MPa}{m}$ *Ref Fig 3.3 in AASHTO (1993)*

Corrected K Value for Potential Loss of Support $LS := 2.5$ *Ref Table 2.7 in AASTHO (1993)*

NOTE: Assumed fine-grained or natural subgrade materials $k := 28\ pci$ *Ref Figure 3.6 in AASTHO (1993)*

Pervious Concrete Properties

Compressive Strength $f'_{c_i} = 3472.83\ psi$ *from my graduate research*

Modulus of Rupture $S'_{c_i} := MOR_i$ $S'_{c_i} = 406.7\ psi$ *from my graduate research*

Modulus of Elasticity $E_{c_i} := 39.1 \cdot \left(w_{pc_i} \div pcf\right)^{1.5} \cdot \sqrt{f'_{c_i} \cdot psi}$ $E_{c_i} = 3172 \cdot ksi$ *from my graduate research*

Drainage Coefficient

$C_d := 1.1$ *Ref Table 12.20 in Pavement Analysis and Design by Huang*

NOTE: with proper drainage the structure should not be exposed to saturation moisture levels often

Load Transfer Coefficient

$J := 3.8$ NOTE: Pervous concrete is not tied *Ref Table 2.6 AASHTO (1993)*

Find Minimum Thickness

Given $D_i := h_i \div in$ $W18_i := 1000$ *Ref Eqn 12.21 in Pavement Analysis &Design by Huang*

$$\log\left(W18_i\right) = Z_R \cdot S_o + 7.35 \cdot \log\left(D_i + 1\right) - .06 + \frac{\log\left(\frac{\Delta PSI}{4.5 - 1.5}\right)}{1 + \frac{1.624 \cdot 10^7}{\left(D_i + 1\right)^{8.46}}} + \left(4.22 - .32 p_t\right) \cdot \log\left[\frac{\frac{S'_{c_i}}{psi} \cdot C_d \cdot \left[\left(D_i\right)^{0.75} - 1.132\right]}{215.63 \cdot J \cdot \left[\left(D_i\right)^{0.75} - \frac{18.42}{\left(\frac{E_{c_i}}{k \cdot psi}\right)^{.25}}\right]}\right]$$

Estimated Number of ESALS to failure $W18 := \text{Find}\left(W18_i\right)$ $W18_i = 239050$

Actual Number of ESALS to 1st Cracking $N_i = 29155$

Name: *Will Goede* | **Class:** *Research - Pervious Concrete*

Reference: PCA (1984) design method

= adjustable values

= outputs of interest

Problem Statement:

Use PCA (1984) FATIGUE ANALYSIS to calculate required thickness of pervious concrete panels at Evolution Paving using material characterization results and observed number of loads to first cracking.

Solution:

Material Characterization Results

Panel #	Depth (in)	Loaded Trucks?	Unit Weight (pcf)	Avg Flexural Strength (psi)	Avg Compressive Strength (psi)	Avg In-Situ Porosity	PCI	2007 ASTM Rating
1	7.5	no	122.1	297	3517	13.7%	48	Poor
2	10	yes	111.1		1780	21.4%	87	Good
3	10	no	126.7		5031	11.0%	89	Good
4	7	yes	117.3	284	2937	17.8%	86	Good
5	8	no	118.2	329	2904	17.0%	87	Good
6	5	yes	112.1	206	2261	22.2%	77	Satisfactory
7	6	no					26	Very Poor
8	5	yes	113.5	275	2836	20.7%	8	Failed
9	4	no					27	Very Poor
10	4	yes					8	Failed
11	4	no	109.0		2518	27.1%	8	Failed
12	4	yes	116.5		2729	19.9%	8	Failed
13	6	no	119.8	260	2884	19.1%	8	Failed
14	6	yes	122.3		4200	12.9%	8	Failed
15	8	no					60	Fair
16	8	yes	123.7	407	3473	11.9%	50	Poor

Safety Factor $LSF := 1.1$

PANEL 2 DESIGN

panel number $i := 2$

Total Life ESALS

Number of Loads at 1st Cracking $n := 65000$ $n := n \cdot LSF$

Number of 10kip singles axles applied $n_1 := n \cdot 2$ $n_1 = 143000$

Number of 45kip tridem axles applied $n_3 := n$ $n_3 = 71500$

NOTE: Similarly to AASHTO design, assume that tridem axle holds 45kip and front and back booster axle hold 10kip

Subgrade Properties

From Geotech Report at Evolution Paving $PI_{avg} := 9.1 \frac{mm}{blow}$ *see excel sheet for calculations*

NOTE: Dynamic Cone Penetration Test was performed

Subbase Thickness $D_{SB} := 14in - h_i$ $D_{SB} = 4 \cdot in$

Soil Resilient Modulus $M_r := \left(-3279 \cdot PI_{avg} + 114100\right) \cdot kPa$ $M_r = 84.13 \cdot MPa$ $M_r = 12202\ psi$ *Ref Dynamic Cone Penetration Test for Subgrade Assessment by Salgado & Yoon*

Subgrade Reaction $CBR := 15$ *Ref Fig 7.10 in Huang's text* $k := 230 \frac{psi}{in}$ *Ref Fig 7.36: Pavement Analysis & Design by Huang*

Composite Subgrade Reaction $k := 250pci$ $k = 67.86 \cdot \frac{MPa}{m}$ *Ref Table 1 in PCA (1984)*

Pervious Concrete Properties

Compressive Strength $f'_{c_i} = 1780.46\ psi$ *from my graduate research*

Modulus of Rupture $S_{c_i} := 5.3 \cdot \sqrt{f'_{c_i} \cdot psi}$ $S_{c_i} = 223.6\ psi$ *from my graduate research*

NOTE: Since Flexural Test was unable to be performed on any samples from this panel, I use relationship between MOR and f`c developed from experiemental results

Equivalent Stress for Slabs without Shoulders

Trial Thickness $D := 8.8in$ Actual thickness $h_i = 10 \cdot in$

	10kip Single Axle		45kip Tridem Axle	
Equivalent Stress	$\sigma_1 := 206psi$	*Ref Table 6a in PCA (1984)*	$\sigma_3 := 133.5psi$	*Ref Table C1 in PCA (1984)*

NOTE: Equivalent stress for slabs without concrete shoulders was used

Stress Ratio Factor	$SR_1 := \frac{\sigma_1}{S_{c_i}}$	$SR_1 = 0.92$	$SR_3 := \frac{\sigma_3}{S_{c_i}}$	$SR_3 = 0.6$
Allowable Load Repetitions	$n_{1all} := 160 \cdot 10^3$ *Ref Figure 5 in PCA (1984)*		$n_{3all} := 450 \cdot 10^3$ *Ref Figure 5 in PCA (1984)*	

NOTE: When finding allowable load repetitions for tridem axle, use scale for single axle in Figure 12.12 and divide tridem axle load by 3. (*Ref p. 567 in Pavement Analysis and Design by Huang)*

Fatigue Percent	$\%_{f1} := \frac{n_1}{n_{1all}}$	$\%_{f1} = 89.375 \cdot \%$	$\%_{f3} := \frac{n_3}{n_{3all}}$	$\%_{f3} = 15.889 \cdot \%$

Total Fatigue $Fatigue := \%_{f1} + \%_{f3}$ $Fatigue = 105.3 \cdot \%$ For $D = 8.8 \cdot in$

PANEL 4 DESIGN

panel number $i := 4$

Total Life ESALS

Number of Loads at 1st Cracking $n := 50780$ $n := n \cdot LSF$

Number of 10kip singles axles applied $n_1 := n \cdot 2$ $n_1 = 111716$

Number of 45kip tridem axles applied $n_3 := n$ $n_3 = 55858$

NOTE: Similarly to AASHTO design, assume that tridem axle holds 45kip and front and back booster axle hold 10kip

Subgrade Properties

From Geotech Report at Evolution Paving $PI_{avg} := 9.1 \frac{mm}{blow}$ *see excel sheet for calculations*

NOTE: Dynamic Cone Penetration Test was performed

Subbase Thickness $D_{SB} := 14in - h_i$ $D_{SB} = 7 \cdot in$

Soil Resilient Modulus $M_r := \left(-3279 \cdot PI_{avg} + 114100\right) \cdot kPa$ $M_r = 84.13 \cdot MPa$ $M_r = 12202\ psi$ *Ref Dynamic Cone Penetration Test for Subgrade Assessment by Salgado & Yoon*

Subgrade Reaction $CBR := 15$ *Ref Fig 7.10 in Huang's text* $k := 230 \frac{psi}{in}$ *Ref Fig 7.36: Pavement Analysis & Design by Huang*

Composite Subgrade Reaction $k := 273pci$ $k = 74.11 \cdot \frac{MPa}{m}$ *Ref Table 1 in PCA (1984)*

Pervious Concrete Properties

Compressive Strength $f'_{c_i} = 2936.97\ psi$ *from my graduate research*

Modulus of Rupture $S_{c_i} := MOR_i$ $S_{c_i} = 283.8\ psi$ *from my graduate research*

Equivalent Stress for Slabs without Shoulders

Trial Thickness $D := 7.2in$ Actual thickness $h_i = 7 \cdot in$

	10kip Single Axle		45kip Tridem Axle	
Equivalent Stress	$\sigma_1 := 265psi$	*Ref Table 6a in PCA (1984)*	$\sigma_3 := 166psi$	*Ref Table C1 in PCA (1984)*

NOTE: Equivalent stress for slabs without concrete shoulders was used

Stress Ratio Factor	$SR_1 := \frac{\sigma_1}{S_{c_i}}$	$SR_1 = 0.93$	$SR_3 := \frac{\sigma_3}{S_{c_i}}$	$SR_3 = 0.58$
Allowable Load Repetitions	$n_{1all} := 120 \cdot 10^3$ *Ref Figure 5 in PCA (1984)*		$n_{3all} := 1000 \cdot 10^3$ *Ref Figure 5 in PCA (1984)*	

NOTE: When finding allowable load repetitions for tridem axle, use scale for single axle in Figure 12.12 and divide tridem axle load by 3. (*Ref p. 567 in Pavement Analysis and Design by Huang)*

Fatigue Percent	$\%_{f1} := \frac{n_1}{n_{1all}}$	$\%_{f1} = 93.097 \cdot \%$	$\%_{f3} := \frac{n_3}{n_{3all}}$	$\%_{f3} = 5.586 \cdot \%$

Total Fatigue $Fatigue := \%_{f1} + \%_{f3}$ $Fatigue = 98.7 \cdot \%$ For $D = 7.2 \cdot in$

PANEL 6 DESIGN

panel number $i := 6$

Total Life ESALS

Number of Loads at 1st Cracking $n := 27000$ $n := n \cdot LSF$

Number of 10kip singles axles applied $n_1 := n \cdot 2$ $n_1 = 59400$

Number of 45kip tridem axles applied $n_3 := n$ $n_3 = 29700$

NOTE: Similarly to AASHTO design, assume that tridem axle holds 45kip and front and back booster axle hold 10kip

Subgrade Properties

From Geotech Report at Evolution Paving $PI_{avg} := 9.1 \frac{mm}{blow}$ *see excel sheet for calculations*

NOTE: Dynamic Cone Penetration Test was performed

Subbase Thickness $D_{SB} := 14in - h_i$ $D_{SB} = 9 \cdot in$

Soil Resilient Modulus $M_r := \left(-3279 \cdot PI_{avg} + 114100\right) \cdot kPa$ $M_r = 84.13 \cdot MPa$ $M_r = 12202\ psi$ *Ref Dynamic Cone Penetration Test for Subgrade Assessment by Salgado & Yoon*

Subgrade Reaction $CBR := 15$ *Ref Fig 7.10 in Huang's text* $k := 230 \frac{psi}{in}$ *Ref Fig 7.36: Pavement Analysis & Design by Huang*

Composite Subgrade Reaction $k := 300pci$ $k = 81.43 \cdot \frac{MPa}{m}$ *Ref Table 1 in PCA (1984)*

Pervious Concrete Properties

Compressive Strength $f'_{c_i} = 2260.52\ psi$ *from my graduate research*

Modulus of Rupture $S_{c_i} := MOR_i$ $S_{c_i} = 206.1\ psi$ *from my graduate research*

Equivalent Stress for Slabs without Shoulders

Trial Thickness $D := 8.7in$ Actual thickness $h_i = 5 \cdot in$

	10kip Single Axle		45kip Tridem Axle	
Equivalent Stress	$\sigma_1 := 200psi$	*Ref Table 6a in PCA (1984)*	$\sigma_3 := 127psi$	*Ref Table C1 in PCA (1984)*

NOTE: Equivalent stress for slabs without concrete shoulders was used

Stress Ratio Factor $SR_1 := \frac{\sigma_1}{S_{c_i}}$ $SR_1 = 0.97$ $SR_3 := \frac{\sigma_3}{S_{c_i}}$ $SR_3 = 0.62$

Allowable Load Repetitions $n_{1all} := 65 \cdot 10^3$ *Ref Figure 5 in PCA (1984)* $n_{3all} := 300 \cdot 10^3$ *Ref Figure 5 in PCA (1984)*

NOTE: When finding allowable load repetitions for tridem axle, use scale for single axle in Figure 12.12 and divide tridem axle load by 3. (*Ref p. 567 in Pavement Analysis and Design by Huang)*

Fatigue Percent $\%_{f1} := \frac{n_1}{n_{1all}}$ $\%_{f1} = 91.385 \cdot \%$ $\%_{f3} := \frac{n_3}{n_{3all}}$ $\%_{f3} = 9.9 \cdot \%$

Total Fatigue $Fatigue := \%_{f1} + \%_{f3}$ $Fatigue = 101.3 \cdot \%$ For $D = 8.7 \cdot in$

PANEL 8 DESIGN

panel number $i := 8$

Total Life ESALS

Number of Loads at 1st Cracking $n := 10000$ $n := n \cdot LSF$

Number of 10kip singles axles applied $n_1 := n \cdot 2$ $n_1 = 22000$

Number of 45kip tridem axles applied $n_3 := n$ $n_3 = 11000$

NOTE: Similarly to AASHTO design, assume that tridem axle holds 45kip and front and back booster axle hold 10kip

Subgrade Properties

From Geotech Report at Evolution Paving $PI_{avg} := 9.1 \frac{mm}{blow}$ *see excel sheet for calculations*

NOTE: Dynamic Cone Penetration Test was performed

Subbase Thickness $D_{SB} := 14in - h_i$ $D_{SB} = 9 \cdot in$

Soil Resilient Modulus $M_r := \left(-3279 \cdot PI_{avg} + 114100\right) \cdot kPa$ $M_r = 84.13 \cdot MPa$ $M_r = 12202\ psi$ *Ref Dynamic Cone Penetration Test for Subgrade Assessment by Salgado & Yoon*

Subgrade Reaction $CBR := 15$ *Ref Fig 7.10 in Huang's text* $k := 230 \frac{psi}{in}$ *Ref Fig 7.36: Pavement Analysis & Design by Huang*

Composite Subgrade Reaction $k := 300pci$ $k = 81.43 \cdot \frac{MPa}{m}$ *Ref Table 1 in PCA (1984)*

Pervious Concrete Properties

Compressive Strength $f'_{c_i} = 2835.53\ psi$ *from my graduate research*

Modulus of Rupture $S_{c_i} := MOR_i$ $S_{c_i} = 275\ psi$ *from my graduate research*

Equivalent Stress for Slabs without Shoulders

Trial Thickness $D := 6.7in$ Actual thickness $h_i = 5 \cdot in$

	10kip Single Axle		45kip Tridem Axle	
Equivalent Stress	$\sigma_1 := 288psi$	*Ref Table 6a in PCA (1984)*	$\sigma_3 := 178.4psi$	*Ref Table C1 in PCA (1984)*

NOTE: Equivalent stress for slabs without concrete shoulders was used

Stress Ratio Factor $SR_1 := \frac{\sigma_1}{S_{c_i}}$ $SR_1 = 1.05$ $SR_3 := \frac{\sigma_3}{S_{c_i}}$ $SR_3 = 0.65$

Allowable Load Repetitions $n_{1all} := 23 \cdot 10^3$ *Ref Figure 5 in PCA (1984)* $n_{3all} := 110 \cdot 10^3$ *Ref Figure 5 in PCA (1984)*

NOTE: When finding allowable load repetitions for tridem axle, use scale for single axle in Figure 12.12 and divide tridem axle load by 3. (*Ref p. 567 in Pavement Analysis and Design by Huang)*

Fatigue Percent $\%_{f1} := \frac{n_1}{n_{1all}}$ $\%_{f1} = 95.652 \cdot \%$ $\%_{f3} := \frac{n_3}{n_{3all}}$ $\%_{f3} = 10 \cdot \%$

Total Fatigue $Fatigue := \%_{f1} + \%_{f3}$ $Fatigue = 105.7 \cdot \%$ For $D = 6.7 \cdot in$

PANEL 12 DESIGN panel number $i := 12$

Total Life ESALS

Number of Loads at 1st Cracking $n := 375$ $n := n \cdot LSF$

Number of 10kip singles axles applied $n_1 := n \cdot 2$ $n_1 = 825$

Number of 45kip tridem axles applied $n_3 := n$ $n_3 = 412.5$

NOTE: Similarly to AASHTO design, assume that tridem axle holds 45kip and front and back booster axle hold 10kip

Subgrade Properties

From Geotech Report at Evolution Paving $PI_{avg} := 9.1 \frac{mm}{blow}$ *see excel sheet for calculations*

NOTE: Dynamic Cone Penetration Test was performed

Subbase Thickness $D_{SB} := 14in - h_i$ $D_{SB} = 10 \cdot in$

Soil Resilient Modulus $M_r := (-3279 \cdot PI_{avg} + 114100) \cdot kPa$ $M_r = 84.13 \cdot MPa$ $M_r = 12202\ psi$ *Ref Dynamic Cone Penetration Test for Subgrade Assessment by Salgado & Yoon*

Subgrade Reaction $CBR := 15$ *Ref Fig 7.10 in Huang's text* $k := 230 \frac{psi}{in}$ *Ref Fig 7.36: Pavement Analysis & Design by Huang*

Composite Subgrade Reaction $k := 317pci$ $k = 86.05 \cdot \frac{MPa}{m}$ *Ref Table 1 in PCA (1984)*

Pervious Concrete Properties

Compressive Strength $f'_{c_i} = 2729.09\ psi$ *from my graduate research*

Modulus of Rupture $S_{c_i} := 5.3 \cdot \sqrt{f'_{c_i} \cdot psi}$ $S_{c_i} = 276.9\ psi$ *from my graduate research*

NOTE: Since Flexural Test was unable to be performed on any samples from this panel, I use relationship between MOR and f`c developed from experiemental results

Equivalent Stress for Slabs without Shoulders

Trial Thickness $D := 5.8in$ Actual thickness $h_i = 4 \cdot in$

	10kip Single Axle		45kip Tridem Axle	
Equivalent Stress	$\sigma_1 := 350psi$	*Ref Table 6a in PCA (1984)*	$\sigma_3 := 221psi$	*Ref Table C1 in PCA (1984)*

NOTE: Equivalent stress for slabs without concrete shoulders was used

Stress Ratio Factor	$SR_1 := \frac{\sigma_1}{S_{c_i}}$	$SR_1 = 1.26$	$SR_3 := \frac{\sigma_3}{S_{c_i}}$	$SR_3 = 0.8$
Allowable Load Repetitions	$n_{1all} := 900$ *Ref Figure 5 in PCA (1984)*		$n_{3all} := 3200$ *Ref Figure 5 in PCA (1984)*	

NOTE: When finding allowable load repetitions for tridem axle, use scale for single axle in Figure 12.12 and divide tridem axle load by 3. (*Ref p. 567 in Pavement Analysis and Design by Huang)*

Fatigue Percent	$\%_{f1} := \frac{n_1}{n_{1all}}$	$\%_{f1} = 91.667 \cdot \%$	$\%_{f3} := \frac{n_3}{n_{3all}}$	$\%_{f3} = 12.891 \cdot \%$

Total Fatigue $Fatigue := \%_{f1} + \%_{f3}$ $Fatigue = 104.6 \cdot \%$ For $D = 5.8 \cdot in$

PANEL 14 DESIGN panel number $i := 14$

Total Life ESALS

Number of Loads at 1st Cracking $n := 12500$ $n := n \cdot LSF$

Number of 10kip singles axles applied $n_1 := n \cdot 2$ $n_1 = 27500$

Number of 45kip tridem axles applied $n_3 := n$ $n_3 = 13750$

NOTE: Similarly to AASHTO design, assume that tridem axle holds 45kip and front and back booster axle hold 10kip

Subgrade Properties

From Geotech Report at Evolution Paving $PI_{avg} := 9.14 \frac{mm}{blow}$ *see excel sheet for calculations*

NOTE: Dynamic Cone Penetration Test was performed

Subbase Thickness $D_{SB} := 14in - h_i$ $D_{SB} = 8 \cdot in$

Soil Resilient Modulus $M_r := \left(-3279 \cdot PI_{avg} + 114100\right) \cdot kPa$ $M_r = 84.13 \cdot MPa$ $M_r = 12202\ psi$ *Ref Dynamic Cone Penetration Test for Subgrade Assessment by Salgado & Yoon*

Subgrade Reaction $CBR := 15$ *Ref Fig 7.10 in Huang's text* $k := 230 \frac{psi}{in}$ *Ref Fig 7.36: Pavement Analysis & Design by Huang*

Composite Subgrade Reaction $k := 287pci$ $k = 77.91 \cdot \frac{MPa}{m}$ *Ref Table 1 in PCA (1984)*

Pervious Concrete Properties

Compressive Strength $f'_{c_i} = 4199.8\ psi$ *from my graduate research*

Modulus of Rupture $S_{c_i} := 5.3 \cdot \sqrt{f'_{c_i} \cdot psi}$ $S_{c_i} = 343.5\ psi$ *from my graduate research*

NOTE: Since Flexural Test was unable to be performed on any samples from this panel, I use relationship between MOR and f`c developed from experiemental results

Equivalent Stress for Slabs without Shoulders

Trial Thickness $D := 5.8in$ Actual thickness $h_i = 6 \cdot in$

	10kip Single Axle		45kip Tridem Axle	
Equivalent Stress	$\sigma_1 := 355psi$	*Ref Table 6a in PCA (1984)*	$\sigma_3 := 223psi$	*Ref Table C1 in PCA (1984)*

NOTE: Equivalent stress for slabs without concrete shoulders was used

Stress Ratio Factor $SR_1 := \frac{\sigma_1}{S_{c_i}}$ $SR_1 = 1.03$ $SR_3 := \frac{\sigma_3}{S_{c_i}}$ $SR_3 = 0.65$

Allowable Load Repetition $n_{1all} := 30 \cdot 10^3$ *Ref Figure 5 in PCA (1984)* $n_{3all} := 120 \cdot 10^3$ *Ref Figure 5 in PCA (1984)*

NOTE: When finding allowable load repetitions for tridem axle, use scale for single axle in Figure 12.12 and divide tridem axle load by 3 *(Ref p. 567 in Pavement Analysis and Design by Huang)*

Fatigue Percent $\%_{f1} := \frac{n_1}{n_{1all}}$ $\%_{f1} = 91.667 \cdot \%$ $\%_{f3} := \frac{n_3}{n_{3all}}$ $\%_{f3} = 11.458 \cdot \%$

Total Fatigue $Fatigue := \%_{f1} + \%_{f3}$ $Fatigue = 103.1 \cdot \%$ For $D = 5.8 \cdot in$

PANEL 16 DESIGN panel number $i := 16$

Total Life ESALS

Number of Loads at 1st Cracking $n := 13990$ $n := n \cdot LSF$

Number of 10kip singles axles applied $n_1 := n \cdot 2$ $n_1 = 30778$

Number of 45kip tridem axles applied $n_3 := n$ $n_3 = 15389$

NOTE: Similarly to AASHTO design, assume that tridem axle holds 45kip and front and back booster axle hold 10kip

Subgrade Properties

From Geotech Report at Evolution Paving $PI_{avg} := 9.1 \frac{mm}{blow}$ *see excel sheet for calculations*

NOTE: Dynamic Cone Penetration Test was performed

Subbase Thickness $D_{SB} := 14in - h_i$ $D_{SB} = 6 \cdot in$

Soil Resilient Modulus $M_r := \left(-3279 \cdot PI_{avg} + 114100\right) \cdot kPa$ $M_r = 84.13 \cdot MPa$ $M_r = 12202\ psi$ *Ref Dynamic Cone Penetration Test for Subgrade Assessment by Salgado & Yoon*

Subgrade Reaction $CBR := 15$ *Ref Fig 7.10 in Huang's text* $k := 230 \frac{psi}{in}$ *Ref Fig 7.36: Pavement Analysis & Design by Huang*

Composite Subgrade Reaction $k := 260pci$ $k = 70.58 \cdot \frac{MPa}{m}$ *Ref Table 1 in PCA (1984)*

Pervious Concrete Properties

Compressive Strength $f'_{c_i} = 3472.83\ psi$ *from my graduate research*

Modulus of Rupture $S_{c_i} := MOR_i$ $S_{c_i} = 406.7\ psi$ *from my graduate research*

Equivalent Stress for Slabs without Shoulders

Trial Thickness $D := 5.3in$ Actual thickness $h_i = 8 \cdot in$

	10kip Single Axle		45kip Tridem Axle	
Equivalent Stress	$\sigma_1 := 413psi$	*Ref Table 6a in PCA (1984)*	$\sigma_3 := 262psi$	*Ref Table C1 in PCA (1984)*

NOTE: Equivalent stress for slabs without concrete shoulders was used

Stress Ratio Factor $SR_1 := \frac{\sigma_1}{S_{c_i}}$ $SR_1 = 1.02$ $SR_3 := \frac{\sigma_3}{S_{c_i}}$ $SR_3 = 0.64$

Allowable Load Repetitions $n_{1all} := 34 \cdot 10^3$ *Ref Figure 5 in PCA (1984)* $n_{3all} := 150 \cdot 10^3$ *Ref Figure 5 in PCA (1984)*

NOTE: When finding allowable load repetitions for tridem axle, use scale for single axle in Figure 12.12 and divide tridem axle load by 3. (*Ref p. 567 in Pavement Analysis and Design by Huang)*

Fatigue Percent $\%_{f1} := \frac{n_1}{n_{1all}}$ $\%_{f1} = 90.524 \cdot \%$ $\%_{f3} := \frac{n_3}{n_{3all}}$ $\%_{f3} = 10.259 \cdot \%$

Total Fatigue $Fatigue := \%_{f1} + \%_{f3}$ $Fatigue = 100.8 \cdot \%$ For $D = 5.3 \cdot in$

Name: *Will Goede* | **Class:** *Research - Pervious Concrete*

Reference: PCA (1984) design method

= adjustable values

= outputs of interest

Problem Statement:

Use PCA (1984) EROSION ANALYSIS to calculate required thickness of pervious concrete panels at Evolution Paving using material characterization results and observed number of loads to first cracking.

Solution:

Material Characterization Results

Panel #	Depth (in)	Loaded Trucks?	Unit Weight (pcf)	Avg Flexural Strength (psi)	Avg Compressive Strength (psi)	Avg In-Situ Porosity	PCI	2007 ASTM Rating
1	7.5	no	122.1	297	3517	13.7%	48	Poor
2	10	yes	111.1		1780	21.4%	87	Good
3	10	no	126.7		5031	11.0%	89	Good
4	7	yes	117.3	284	2937	17.8%	86	Good
5	8	no	118.2	329	2904	17.0%	87	Good
6	5	yes	112.1	206	2261	22.2%	77	Satisfactory
7	6	no					26	Very Poor
8	5	yes	113.5	275	2836	20.7%	8	Failed
9	4	no					27	Very Poor
10	4	yes					8	Failed
11	4	no	109.0		2518	27.1%	8	Failed
12	4	yes	116.5		2729	19.9%	8	Failed
13	6	no	119.8	260	2884	19.1%	8	Failed
14	6	yes	122.3		4200	12.9%	8	Failed
15	8	no					60	Fair
16	8	yes	123.7	407	3473	11.9%	50	Poor

Safety Factor $LSF := 1.1$ For moderate volumes of truck traffic *Ref PCA (1984)*

PANEL 2 DESIGN

panel number $i := 2$

Total Life ESALS

Number of Loads at 1st Cracking $n := 65000$ $n := n \cdot LSF$

Number of 10kip singles axles applied $n_1 := n \cdot 2$ $n_1 = 143000$

Number of 45kip tridem axles applied $n_3 := n$ $n_3 = 71500$

NOTE: Similarly to AASHTO design, assume that tridem axle holds 45kip and front and back booster axle hold 10kip

Subgrade Properties

From Geotech Report at Evolution Paving $PI_{avg} := 9.1 \frac{mm}{blow}$ *see excel sheet for calculations*

NOTE: Dynamic Cone Penetration Test was performed

Subbase Thickness $D_{SB} := 14in - h_i$ $D_{SB} = 4 \cdot in$

Soil Resilient Modulus $M_r := \left(-3279 \cdot PI_{avg} + 114100\right) \cdot kPa$ $M_r = 84.13 \cdot MPa$ $M_r = 12202\ psi$ *Ref Dynamic Cone Penetration Test for Subgrade Assessment by Salgado & Yoon*

Subgrade Reaction $CBR := 15$ *Ref Fig 7.10 in Huang's text* $k := 230 \frac{psi}{in}$ *Ref Fig 7.36: Pavement Analysis & Design by Huang*

Composite Subgrade Reaction $k := 250pci$ $k = 67.86 \cdot \frac{MPa}{m}$ *Ref Table 1 in PCA (1984)*

Erosion Factor for Slabs without Shoulders

Trial Thickness $D := 4.2in$ Actual thickness $h_i = 10 \cdot in$

	10kip Single Axle		45kip Tridem Axle	
Erosion Factor	$f_{e1} := 3.82psi$	*Ref Table 7b in PCA (1984)*	$f_{e3} := 3.8psi$	*Ref Table C3 in PCA (1984)*

NOTE: Erosion Factor for slabs without concrete shoulders was used

Allowable Load Repetitions	$n_{1all} := 650 \cdot 10^3$	*Ref Figure 6a in PCa (1984)*	$n_{3all} := 80 \cdot 10^3$	*Ref Figure 6a in PCA (1984)*

NOTE: When finding allowable load repetitions for tridem axle, use scale for single axle in Figure 12.13 and divide tridem axle load by 3. (*Ref p. 567 in Pavement Analysis and Design by Huang)*

Percent Erosion Damage $\%_{f1} := \frac{n_1}{n_{1all}}$ $\%_{f1} = 22 \cdot \%$ $\%_{f3} := \frac{n_3}{n_{3all}}$ $\%_{f3} = 89.375 \cdot \%$

Total % Erosion Damage $Erosion := \%_{f1} + \%_{f3}$ $Erosion = 111.4 \cdot \%$ For $D = 4.2 \cdot in$

PANEL 4 DESIGN

panel number $i := 4$

Total Life ESALS

Number of Loads at 1st Cracking $n := 50780$ $n := n \cdot LSF$

Number of 10kip singles axles applied $n_1 := n \cdot 2$ $n_1 = 111716$

Number of 45kip tridem axles applied $n_3 := n$ $n_3 = 55858$

NOTE: Similarly to AASHTO design, assume that tridem axle holds 45kip and front and back booster axle hold 10kip

Subgrade Properties

From Geotech Report at Evolution Paving $PI_{avg} := 9.1 \frac{mm}{blow}$ *see excel sheet for calculations*

NOTE: Dynamic Cone Penetration Test was performed

Subbase Thickness $D_{SB} := 14in - h_i$ $D_{SB} = 7 \cdot in$

Soil Resilient Modulus $M_r := (-3279 \cdot PI_{avg} + 114100) \cdot kPa$ $M_r = 84.13 \cdot MPa$ $M_r = 12202\ psi$ *Ref Dynamic Cone Penetration Test for Subgrade Assessment by Salgado & Yoon*

Subgrade Reaction $CBR := 15$ *Ref Fig 7.10 in Huang's text* $k := 230 \frac{psi}{in}$ *Ref Fig 7.36: Pavement Analysis & Design by Huang*

Composite Subgrade Reaction $k := 273pci$ $k = 74.11 \cdot \frac{MPa}{m}$ *Ref Table 1 in PCA (1984)*

Erosion Factor for Slabs without Shoulders

Trial Thickness $D := 4.1in$ Actual thickness $h_i = 7 \cdot in$

	10kip Single Axle		45kip Tridem Axle	
Erosion Factor	$f_{e1} := 3.84psi$	*Ref Table 7b in PCA (1984)*	$f_{e3} := 3.81psi$	*Ref Table C3 in PCA (1984)*

NOTE: Erosion Factor for slabs without concrete shoulders was used

Allowable Load Repetitions	$n_{1all} := 550 \cdot 10^3$	*Ref Figure 6a in PCa (1984)*	$n_{3all} := 70 \cdot 10^3$	*Ref Figure 6a in PCA (1984)*

NOTE: When finding allowable load repetitions for tridem axle, use scale for single axle in Figure 12.13 and divide tridem axle load by 3. (*Ref p. 567 in Pavement Analysis and Design by Huang)*

Percent Erosion Damage $\%_{f1} := \frac{n_1}{n_{1all}}$ $\%_{f1} = 20.312 \cdot \%$ $\%_{f3} := \frac{n_3}{n_{3all}}$ $\%_{f3} = 79.797 \cdot \%$

Total % Erosion Damage $Erosion := \%_{f1} + \%_{f3}$ $Erosion = 100.1 \cdot \%$ For $D = 4.1 \cdot in$

PANEL 6 DESIGN

panel number $i := 6$

Total Life ESALS

Number of Loads at 1st Cracking $n := 27000$ $n := n \cdot LSF$

Number of 10kip singles axles applied $n_1 := n \cdot 2$ $n_1 = 59400$

Number of 45kip tridem axles applied $n_3 := n$ $n_3 = 29700$

NOTE: Similarly to AASHTO design, assume that tridem axle holds 45kip and front and back booster axle hold 10kip

Subgrade Properties

From Geotech Report at Evolution Paving $PI_{avg} := 9.1 \frac{mm}{blow}$ *see excel sheet for calculations*

NOTE: Dynamic Cone Penetration Test was performed

Subbase Thickness $D_{SB} := 14in - h_i$ $D_{SB} = 9 \cdot in$

Soil Resilient Modulus $M_r := \left(-3279 \cdot PI_{avg} + 114100\right) \cdot kPa$ $M_r = 84.13 \cdot MPa$ $M_r = 12202\ psi$ *Ref Dynamic Cone Penetration Test for Subgrade Assessment by Salgado & Yoon*

Subgrade Reaction $CBR := 15$ *Ref Fig 7.10 in Huang's text* $k := 230 \frac{psi}{in}$ *Ref Fig 7.36: Pavement Analysis & Design by Huang*

Composite Subgrade Reaction $k := 300pci$ $k = 81.43 \cdot \frac{MPa}{m}$ *Ref Table 1 in PCA (1984)*

Erosion Factor for Slabs without Shoulders

Trial Thickness $D := 4.0in$ Actual thickness $h_i = 5 \cdot in$

	10kip Single Axle		45kip Tridem Axle	
Erosion Factor	$f_{e1} := 3.86psi$	*Ref Table 7b in PCA (1984)*	$f_{e3} := 3.82psi$	*Ref Table C3 in PCA (1984)*

NOTE: Erosion Factor for slabs without concrete shoulders was used

Allowable Load Repetitions	$n_{1all} := 500 \cdot 10^3$	*Ref Figure 6a in PCA (1984)*	$n_{3all} := 65 \cdot 10^3$	*Ref Figure 6a in PCA (1984)*

NOTE: When finding allowable load repetitions for tridem axle, use scale for single axle in Figure 12.13 and divide tridem axle load by 3. (*Ref p. 567 in Pavement Analysis and Design by Huang)*

Percent Erosion Damage $\%_{f1} := \frac{n_1}{n_{1all}}$ $\%_{f1} = 11.88 \cdot \%$ $\%_{f3} := \frac{n_3}{n_{3all}}$ $\%_{f3} = 45.692 \cdot \%$

Total % Erosion Damage $Erosion := \%_{f1} + \%_{f3}$ $Erosion = 57.6 \cdot \%$ For $D = 4 \cdot in$

Design Tables do not show values for slabs < 4 in. thick

PANEL 8 DESIGN

panel number $i := 8$

Total Life ESALS

Number of Loads at 1st Cracking $n := 10000$ $n := n \cdot LSF$

Number of 10kip singles axles applied $n_1 := n \cdot 2$ $n_1 = 22000$

Number of 45kip tridem axles applied $n_3 := n$ $n_3 = 11000$

NOTE: Similarly to AASHTO design, assume that tridem axle holds 45kip and front and back booster axle hold 10kip

Subgrade Properties

From Geotech Report at Evolution Paving $PI_{avg} := 9.1 \frac{mm}{blow}$ *see excel sheet for calculations*

NOTE: Dynamic Cone Penetration Test was performed

Subbase Thickness $D_{SB} := 14in - h_i$ $D_{SB} = 9 \cdot in$

Soil Resilient Modulus $M_r := (-3279 \cdot PI_{avg} + 114100) \cdot kPa$ $M_r = 84.13 \cdot MPa$ $M_r = 12202\ psi$ *Ref Dynamic Cone Penetration Test for Subgrade Assessment by Salgado & Yoon*

Subgrade Reaction $CBR := 15$ *Ref Fig 7.10 in Huang's text* $k := 230 \frac{psi}{in}$ *Ref Fig 7.36: Pavement Analysis & Design by Huang*

Composite Subgrade Reaction $k := 300pci$ $k = 81.43 \cdot \frac{MPa}{m}$ *Ref Table 1 in PCA (1984)*

Erosion Factor for Slabs without Shoulders

Trial Thickness $D := 4.0in$ Actual thickness $h_i = 5 \cdot in$

	10kip Single Axle		45kip Tridem Axle	
Erosion Factor	$f_{e1} := 3.86psi$	*Ref Table 7b in PCA (1984)*	$f_{e3} := 3.82psi$	*Ref Table C3 in PCA (1984)*
Allowable Load Repetitions	$n_{1all} := 500 \cdot 10^3$	*Ref Figure 6a in PCa (1984)*	$n_{3all} := 65 \cdot 10^3$	*Ref Figure 6a in PCA (1984)*

NOTE: When finding allowable load repetitions for tridem axle, use scale for single axle in Figure 12.13 and divide tridem axle load by 3. (*Ref p. 567 in Pavement Analysis and Design by Huang)*

Percent Erosion Damage $\%_{f1} := \frac{n_1}{n_{1all}}$ $\%_{f1} = 4.4 \cdot \%$ $\%_{f3} := \frac{n_3}{n_{3all}}$ $\%_{f3} = 16.923 \cdot \%$

Total % Erosion Damage $Erosion := \%_{f1} + \%_{f3}$ $Erosion = 21.3 \cdot \%$ For $D = 4 \cdot in$

Design Tables do not show values for slabs < 4 in. thick

PANEL 12 DESIGN panel number $i := 12$

Total Life ESALS

Number of Loads at 1st Cracking $n := 375$ $n := n \cdot LSF$

Number of 10kip singles axles applied $n_1 := n \cdot 2$ $n_1 = 825$

Number of 45kip tridem axles applied $n_3 := n$ $n_3 = 412.5$

NOTE: Similarly to AASHTO design, assume that tridem axle holds 45kip and front and back booster axle hold 10kip

Subgrade Properties

From Geotech Report at Evolution Paving $PI_{avg} := 9.1 \frac{mm}{blow}$ *see excel sheet for calculations*

NOTE: Dynamic Cone Penetration Test was performed

Subbase Thickness $D_{SB} := 14in - h_i$ $D_{SB} = 10 \cdot in$

Soil Resilient Modulus $M_r := (-3279 \cdot PI_{avg} + 114100) \cdot kPa$ $M_r = 84.13 \cdot MPa$ $M_r = 12202\ psi$ *Ref Dynamic Cone Penetration Test for Subgrade Assessment by Salgado & Yoon*

Subgrade Reaction $CBR := 15$ *Ref Fig 7.10 in Huang's text* $k := 230 \frac{psi}{in}$ *Ref Fig 7.36: Pavement Analysis & Design by Huang*

Composite Subgrade Reaction $k := 317pci$ $k = 86.05 \cdot \frac{MPa}{m}$ *Ref Table 1 in PCA (1984)*

Erosion Factor for Slabs without Shoulders

Trial Thickness $D := 4.0in$ Actual thickness $h_i = 4 \cdot in$

	10kip Single Axle		45kip Tridem Axle	
Erosion Factor	$f_{e1} := 3.85psi$	*Ref Table 7b in PCA (1984)*	$f_{e3} := 3.80psi$	*Ref Table C3 in PCA (1984)*

NOTE: Erosion Factor for slabs without concrete shoulders was used

Allowable Load Repetitions	$n_{1all} := 500 \cdot 10^3$	*Ref Figure 6a in PCa (1984)*	$n_{3all} := 70 \cdot 10^3$	*Ref Figure 6a in PCA (1984)*

NOTE: When finding allowable load repetitions for tridem axle, use scale for single axle in Figure 12.13 and divide tridem axle load by 3. (*Ref p. 567 in Pavement Analysis and Design by Huang)*

Percent Erosion Damage $\%_{f1} := \frac{n_1}{n_{1all}}$ $\%_{f1} = 0.165 \cdot \%$ $\%_{f3} := \frac{n_3}{n_{3all}}$ $\%_{f3} = 0.589 \cdot \%$

Total % Erosion Damage $Erosion := \%_{f1} + \%_{f3}$ $Erosion = 0.8 \cdot \%$ For $D = 4 \cdot in$

Design Tables do not show values for slabs < 4 in. thick

PANEL 14 DESIGN panel number $i := 14$

Total Life ESALS

Number of Loads at 1st Cracking $n := 12500$ $n := n \cdot LSF$

Number of 10kip singles axles applied $n_1 := n \cdot 2$ $n_1 = 27500$

Number of 45kip tridem axles applied $n_3 := n$ $n_3 = 13750$

NOTE: Similarly to AASHTO design, assume that tridem axle holds 45kip and front and back booster axle hold 10kip

Subgrade Properties

From Geotech Report at Evolution Paving $PI_{avg} := 9.1 \frac{mm}{blow}$ *see excel sheet for calculations*

NOTE: Dynamic Cone Penetration Test was performed

Subbase Thickness $D_{SB} := 14in - h_i$ $D_{SB} = 8 \cdot in$

Soil Resilient Modulus $M_r := (-3279 \cdot PI_{avg} + 114100) \cdot kPa$ $M_r = 84.13 \cdot MPa$ $M_r = 12202\ psi$ *Ref Dynamic Cone Penetration Test for Subgrade Assessment by Salgado & Yoon*

Subgrade Reaction $CBR := 15$ *Ref Fig 7.10 in Huang's text* $k := 230 \frac{psi}{in}$ *Ref Fig 7.36: Pavement Analysis & Design by Huang*

Composite Subgrade Reaction $k := 287pci$ $k = 77.91 \cdot \frac{MPa}{m}$ *Ref Table 1 in PCA (1984)*

Erosion Factor for Slabs without Shoulders

Trial Thickness $D := 4.0in$ Actual thickness $h_i = 6 \cdot in$

	10kip Single Axle		45kip Tridem Axle	
Erosion Factor	$f_{e1} := 3.86psi$	*Ref Table 7b in PCA (1984)*	$f_{e3} := 3.82psi$	*Ref Table C3 in PCA (1984)*

NOTE: Erosion Factor for slabs without concrete shoulders was used

Allowable Load Repetitions	$n_{1all} := 500 \cdot 10^3$	*Ref Figure 6a in PCa (1984)*	$n_{3all} := 65 \cdot 10^3$	*Ref Figure 6a in PCA (1984)*

NOTE: When finding allowable load repetitions for tridem axle, use scale for single axle in Figure 12.13 and divide tridem axle load by 3. (*Ref p. 567 in Pavement Analysis and Design by Huang)*

Percent Erosion Damage $\%_{f1} := \frac{n_1}{n_{1all}}$ $\%_{f1} = 5.5 \cdot \%$ $\%_{f3} := \frac{n_3}{n_{3all}}$ $\%_{f3} = 21.154 \cdot \%$

Total % Erosion Damage $Erosion := \%_{f1} + \%_{f3}$ $Erosion = 26.7 \cdot \%$ For $D = 4 \cdot in$

Design Tables do not show values for slabs < 4 in. thick

PANEL 16 DESIGN panel number $i := 16$

Total Life ESALS

Number of Loads at 1st Cracking $n := 13990$ $n := n \cdot LSF$

Number of 10kip singles axles applied $n_1 := n \cdot 2$ $n_1 = 30778$

Number of 45kip tridem axles applied $n_3 := n$ $n_3 = 15389$

NOTE: Similarly to AASHTO design, assume that tridem axle holds 45kip and front and back booster axle hold 10kip

Subgrade Properties

From Geotech Report at Evolution Paving $PI_{avg} := 9.1 \frac{mm}{blow}$ *see excel sheet for calculations*

NOTE: Dynamic Cone Penetration Test was performed

Subbase Thickness $D_{SB} := 14in - h_i$ $D_{SB} = 6 \cdot in$

Soil Resilient Modulus $M_r := (-3279 \cdot PI_{avg} + 114100) \cdot kPa$ $M_r = 84.13 \cdot MPa$ $M_r = 12202\ psi$ *Ref Dynamic Cone Penetration Test for Subgrade Assessment by Salgado & Yoon*

Subgrade Reaction $CBR := 15$ *Ref Fig 7.10 in Huang's text* $k := 230 \frac{psi}{in}$ *Ref Fig 7.36: Pavement Analysis & Design by Huang*

Composite Subgrade Reaction $k := 260pci$ $k = 70.58 \cdot \frac{MPa}{m}$ *Ref Table 1 in PCA (1984)*

Erosion Factor for Slabs without Shoulders

Trial Thickness $D := 4.0in$ Actual thickness $h_i = 8 \cdot in$

	10kip Single Axle		45kip Tridem Axle	
Erosion Factor	$f_{e1} := 3.87psi$	*Ref Table 7b in PCA (1984)*	$f_{e3} := 3.84psi$	*Ref Table C3 in PCA (1984)*

NOTE: Erosion Factor for slabs without concrete shoulders was used

Allowable Load Repetitions	$n_{1all} := 450 \cdot 10^3$	*Ref Figure 6a in PCa (1984)*	$n_{3all} := 60 \cdot 10^3$	*Ref Figure 6a in PCA (1984)*

NOTE: When finding allowable load repetitions for tridem axle, use scale for single axle in Figure 12.13 and divide tridem axle load by 3. (*Ref p. 567 in Pavement Analysis and Design by Huang)*

Percent Erosion Damage $\%_{f1} := \frac{n_1}{n_{1all}}$ $\%_{f1} = 6.84 \cdot \%$ $\%_{f3} := \frac{n_3}{n_{3all}}$ $\%_{f3} = 25.648 \cdot \%$

Total % Erosion Damage $Erosion := \%_{f1} + \%_{f3}$ $Erosion = 32.5 \cdot \%$ For $D = 4 \cdot in$

Design Tables do not show values for slabs < 4 in. thick